School of Applied Geology

PETROLOGY OF JURASSIC COAL, HILL RIVER AREA, PERTH BASIN, WESTERN AUSTRALIA

Nana Suwarna

This thesis is presented as part of the
requirements for the award of
Degree of Doctor of Philosophy
of
Curtin University of Technology

December 1993

ABSTRACT

The Early Jurassic coal samples for the study were obtained from CRA Exploration Pty Ltd. (CRAE), drilled in the Gairdner and Mintaja Blocks, Gairdner Range of the Hill River Area, northern Perth Basin, Western Australia. The area is located approximately 280 km north of Perth. The coal measures subcrop in a half- graben bounded by the Lesueur-Peron Fault in the west, and the Warradarge Fault in the east. The coal occurs within the shallow sequence of the Cattamarra Member which is also described as the Cattamarra Coal Measures of the Cockleshell Gully Formation.

Six sub-seams of seam G, namely G1 to G6, from the six drill cores, were examined for petrological and geochemical investigation. The coal predominantly comprises of banded, dull banded, and dull lithotypes, with minor bright banded, bright and fusainous types. Based on maceral analyses, the dominant maceral groups are vitrinite and inertinite, whilst the exinite and mineral matter are in minor contents. The vitrinite content has a range between 47.2 % to 73.0 %, and it is composed mainly of telocollinite and desmocollinite. The inertinite is dominated by semifusinite, fusinite, and inertodetrinite, and it has a range from 10.4 % to 24.8 %. The exinite group varies between 7.2 % to 20.8 % in content, and it is represented by sporinite, cutinite, alginite and resinite. The mineral matter dominated by clays and pyrite, ranges between 4.5 % to 20.6 %. The microlithotype analyses shows that the vitrite plus clarite content varies from 47.0 % to 70.0 %, intermediates between 8.0% to 26.0 %, whilst inertite plus durite content is relatively low, varying from 6.55 % to 14.0 %. The maximum reflectance of vitrinite has a value between 0.47 % and 0.53 %, which represents rank at sub-bituminous level based on the Australian rank values and corresponding to the sub-bituminous A and B rank of the ASTM classification and to the metalignitous type of the Pareek classification. On the

basis of carbon and hydrogen content, the coal is categorised as per-hydrous meta- to ortho-lignitous type. The trace elements As, B, Be, Cd, Co, Cr, Cu, Ga, Mn, Mo, Ni, Pb, Sr, Th, U, V, Y, Zn, and Zr, are spectrographically analysed in the coal ash. The B content in the coal supports the presence of marine influence during peat deposition in the basin.

On the basis of lithotype, maceral, microlithotype, trace element distribution, pyrite and total sulphur in the coal, the depositional environment for coal and the coal measures, is interpreted as an upper to lower delta type within a regressive phase of marine transgression.

ACKNOWLEDGMENTS

This study was undertaken for the degree of Doctor of Philosophy at Curtin University of Technology, whilst I was in receipt of a scholarship from the Australian International Development Assistance Bureau (AIDAB) under the Indonesian-Australian Geological Mapping Project (IAGMP) scheme. The financial support from AIDAB is gratefully acknowledged. I also express my sincere thanks to the Director of the Geological Research and Development Centre (GRDC), Department of Mines and Energy, Indonesia, for the support and advice in continuing my study at Curtin University of Technology, Perth, Australia.

The study was undertaken from 1990 to 1993 at the Coal Research Laboratory, School of Applied Geology, Curtin University of Technology, and supervised by Associate Professor Krishna K. Sappal of the School and the Deputy Director, University Development. I am indebted to Associate Professor Sappal for suggesting the topic for the thesis, and for his continued supervision and guidance throughout the study. My special thanks are due to Associate supervisor Dr. L.B. Collins, Senior Lecturer School of Applied Geology, and Mr. S. Kristensen, Principal Geologist CRA Exploration Pty Ltd. (CRAE). I am also grateful to Mr. S. Kristensen for fruitful discussions and support in obtaining the coal samples for this study.

I wish to acknowledge the facilities provided by Associate Professor S. Wilde, Head School of Applied Geology, and I also thank the support staff of the School of Applied Geology for their encouragement during my study.

This acknowledgment would not be complete without expressing my special thanks to Mrs. Sue Woods, Director of Centre for International English (ELICOS), Curtin

University of Technology , for her support, friendship, humour and help during my stay in Perth.

Last but not least, appreciation and thanks go to my wife Iis Riswati, my children Mima, Rizal, Rozaly, and Reza, and also my mother Rukayah Priatin, for their encouragement, patience and understanding during my study and writing of the thesis.

This thesis consists of original research work carried out by the author, except where indicated. This work has not previously been submitted for a higher degree to any other university or such institution.

N. Suwarna

TABLE OF CONTENTS

LIST OF TABLES

LIST OF FIGURES

Addendum:

Author: Suwarna, Nana
Title: Petrology of Jurassic coal, Hill River area, Perth Basin, Western Australia
Degree: PhD
Date: 1993

Page 1 of Chapter 1 is missing from the final published version of the above thesis in both the paper and electronic versions.

Despite its best endeavors, the University has been unable to source the missing page.

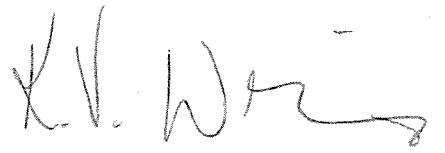

Prof Kate Wright,
Associate Deputy Vice-Chancellor, Research Training
Graduate Research School, Curtin University.

18 December 2015

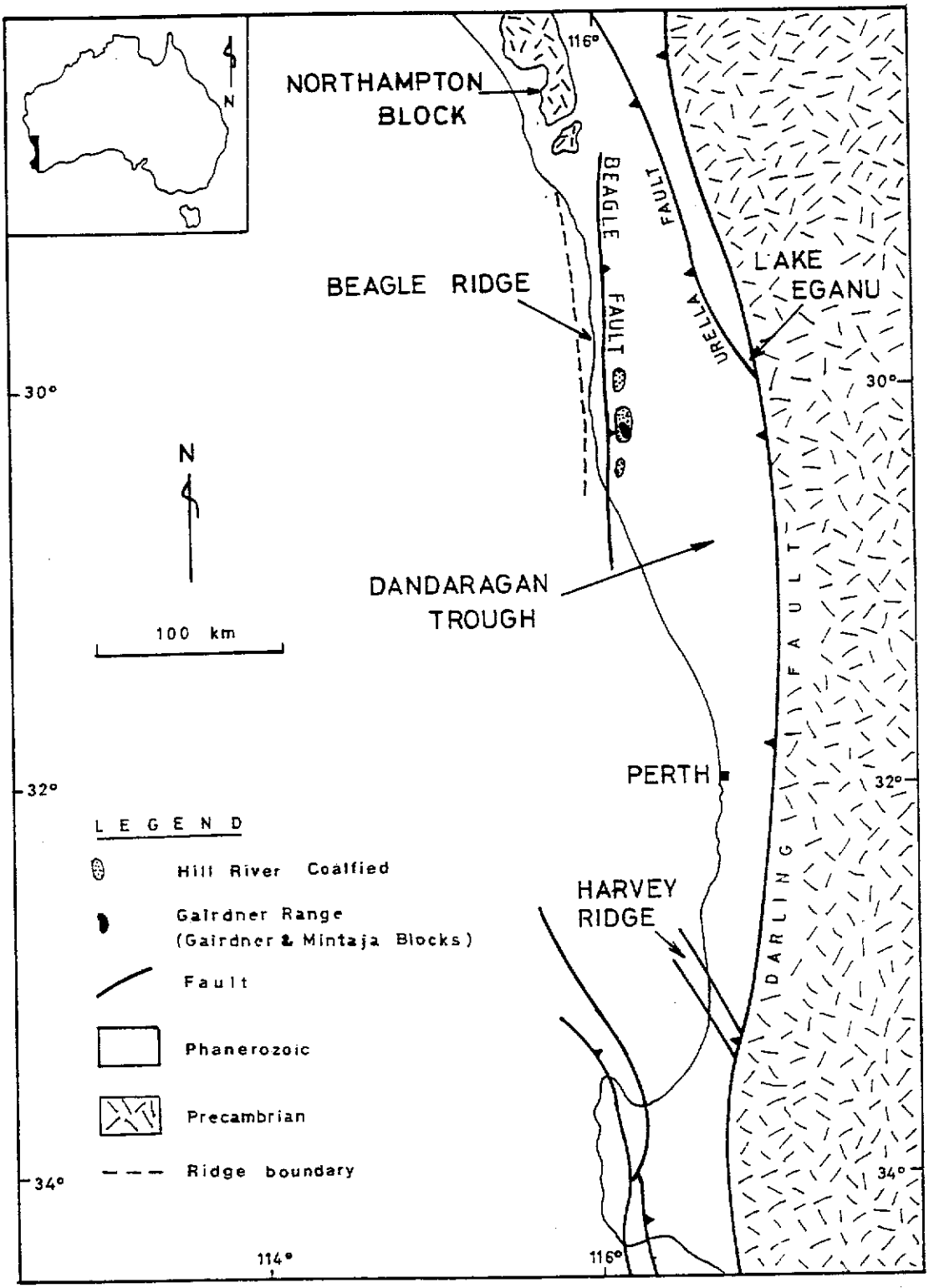

Figure 1.1. Regional setting and locality, Hill River Coalfield, Western Australia.

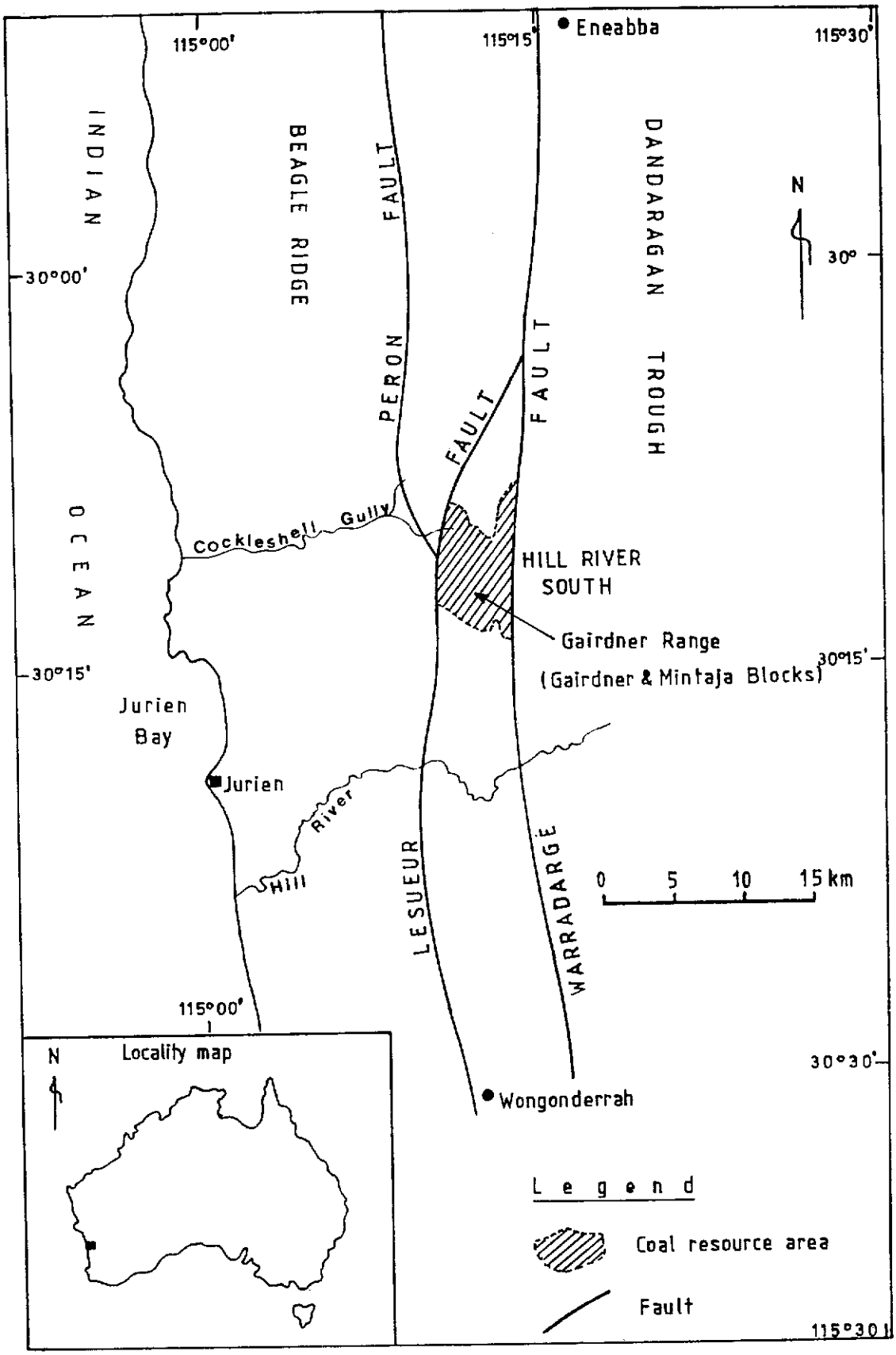

Figure 1.2. Structural setting of the Gairdner Range, Perth Basin, Western Australia (after Kristensen, 1989).

lower part of the Early Jurassic Coal Measures. This seam is composed of six sub-seams or splits, named as G1, G2, G3, G4, G5, and G6, from top to bottom respectively .

A number of recent publications in coal petrology show that the petrographic data on coal are extremely useful in its utilisation for coking and power generation. Permian coals of Eastern Australia have been investigated for maceral and microlithotype composition in relation to their depositional environment by Shibaoka (1972), Shibaoka and Smyth (1975), Marchioni (1980), Smyth and Cameron (1982), Smyth (1984, 1989) and Diessel (1982 and 1986). Sappal (1986) undertook detailed petrographic investigation of Permian coal, Collie Basin, Western Australia. In 1991, Glikson and Fielding reported a petrographic study of the Triassic coal of the Callide Coal Measures, Queensland, and its application to the environment of deposition. Organic petrology of Lower Jurassic sediments in the Eromanga Basin, South Australia has been undertaken by Smyth and Cameron (1982). Leblang, Rayment and Smyth (1981), McLean-Hodgson and Kempton (1981), Salehy (1986), and Fielding (1993) reported coal petrographic study and facies analysis of Jurassic coal of Queensland. In addition, Miao, Qian and Zhang (1989) studied the Jurassic coal basin in China, whereas, Petersen (1993) reported on facies analysis of Lower to Middle Jurassic coal of Denmark. The first preliminary petrographic data on the Early Jurassic coal of Western Australia is reported by Suwarna and Sappal (1991).

However, there is a lack of published data on the petrography of Jurassic coal from Western Australia. Due to the economic significance of the Jurassic Hill River coal, a petrographic study was undertaken by the author from 1990 to 1993, as a requirement of the PhD thesis. The laboratory preparations and petrological investigations were completed in the Coal Research Laboratory, School of Applied Geology, Curtin University of Technology, Perth, Western Australia.

Additional data collected from CRAE, namely proximate analyses and ultimate analyses are used in coal classification and interpretation of depositional environment. The palynological data of Sappal and Islam (1990) is also used in the interpretation of the depositional environment of the coal measures.

The techniques and methods carried out in the examination of the Jurassic Hill River coal of Western Australia will be equally applicable in assessing Indonesian coal for its utilisation and dispersed organic matter in sediments for exploration of hydrocarbons.

The author is responsible for all the preparations of polished sections and the SEM samples for the study. The prepared samples are housed in the School of Applied Geology, Curtin University of Technology. The list of specimens and their locations is given in Table 3.1 and Figure 3.1.

1.3. Structure of the Thesis

The thesis consists of eight chapters, and the contents of the individual chapter are :

Chapter 1 describes the introduction to the thesis. It includes the location of the samples and drill cores, aims of the project and the structure of the thesis.

Chapter 2 consists of the geological setting of the Hill River Area. The description is focused on published and unpublished reports regarding the stratigraphy, structure and depositional history of the area. In addition, the geomorphology, climate, and vegetation of the Gairdner Range are also described in this chapter.

Chapter 3 deals with methods, techniques, terminology, and nomenclature used in the present study. The classification of coal and mineral matter, and the basis of the interpretation of the coal depositional environment are also described in this chapter. The analytical procedures and petrographic nomenclature are emphasised in this chapter.

Chapter 4 covers the petrographic analyses of the Mintaja and Gairdner Blocks coal. The analyses include petrographic composition in terms of lithotypes, macerals, and microlithotypes of the coal. Rank variation and classification of the coal based on the vitrinite reflectance are also included in this chapter.

Chapter 5 focuses on the nature and distribution of mineral matter in the coal. A description of the minerals identified under the microscope and SEM is also included in this chapter

Chapter 6 includes information on the proximate, ultimate and trace element analyses of the coal. Affinity between trace elements and organic or inorganic matter in the coal is interpreted. In addition, coal rank and classification based on the proximate and ultimate analyses are also presented in this chapter.

In Chapter 7, discussion on the coal forming environment based on macerals, microlithotypes, and mineral matter content in the coal is given . It is supported by sulphur and trace element distribution in the coal and also by sedimentary structures recognised in the interseam sediments.

The final chapter, Chapter 8, presents the conclusions of the study inclusive of brief geological setting, petrography, geochemistry, and depositional environment.

CHAPTER 2. GEOLOGY OF THE HILL RIVER AREA

2.1. Introduction

A preliminary geological investigation of the Jurassic coal in the Perth Basin was carried out in 1961 (Johnstone, 1964), and the coals were intersected between 1,943 and 1,963 m in the Eneabba No. 1 well, northern Perth Basin. Discovery of coals was subsequently made during the course of drilling for water and in the seismic shot holes at a number of localities in the northern Perth Basin. These discoveries encouraged prospecting for coal in areas other than the Collie Basin. Serious exploration for coal commenced in 1964 by Western Australia Petroleum (WAPET) to evaluate coal intersections from 22 boreholes in the Perth Basin, Western Australia.

The investigations of coal conducted by Western Australia Petroleum (WAPET) between 1962 and 1977 have been regional in scope and have involved definition of bulk compositional characteristics, such as an estimated coal resource. From 1969 to 1971, Goldfield Exploration Pty Ltd. was active in exploring the Hill River area. However, it produced insufficient coal data.

Since 1982, the CRA Exploration (CRAE) Pty Ltd. has been active in exploration in the Hill River area. The exploration has been directed mainly towards evaluating its potential for mining and use in power generation. This involved mapping, exploratory drilling, coal resource estimation, palynostratigraphy, coal quality analysis, and evaluation of selected coal petrography data. In 1990 CRAE submitted a tender to supply coal based power to the State Energy Commission of Western Australia based on Hill River coal with a capacity of 600 Megawatts.

2.2. Location and Access

The coal samples for this study were obtained from the bore holes drilled in the Gairdner and Mintaja Blocks of the Gairdner Range , which is located 225 km north of Perth. These blocks, occupying the proposed southern mining area of CRA Exploration, are accessible by Banovich Road from the Brand Highway. The location of the Gairdner and Mintaja Blocks is shown in Figure 2.1.

2.3. Geomorphology

According to Playford, Cockbain and Low (1976), the Gairdner Range is located within the geomorphological unit known as the Arrowsmith Region (Figure 2.2). The western boundary of the Arrowsmith Region is delineated by the Gingin Scarp followed by the physiographic units of Eneabba Plain, Bassendean Dunes, and the Swan Coastal Plain (Figures 2.2 and 2.3). The eastern limit of the region is marked by the Dandaragan Scarp (Figures 2.2 and 2.4), and the physiographic units of Dandaragan Plateau, and the Yarra Yarra Region . The Arrowsmith Region is an eroded remnant of the tertiary land surface, Burbridge, Hopper and van Leeuwen (1990) . It is a residual laterite and sand covered upland with mainly mature valley forms incised into it, although those containing the headwaters of the Cockleshell Gully are youthful. This type of land surface is an *Incipient* (Lateritic) *Etch plain* , according to Finkl (1979).

The Arrowsmith Region can be divided into the following five units, as shown in Figure 2.5, namely Peron Slopes, Lesueur Dissected Upland, Gairdner Dissected Upland, Bitter Pool Rises, and Banovich Upland. The headwaters of the drainage systems of the Arrowsmith Region are located in the Gairdner Range.

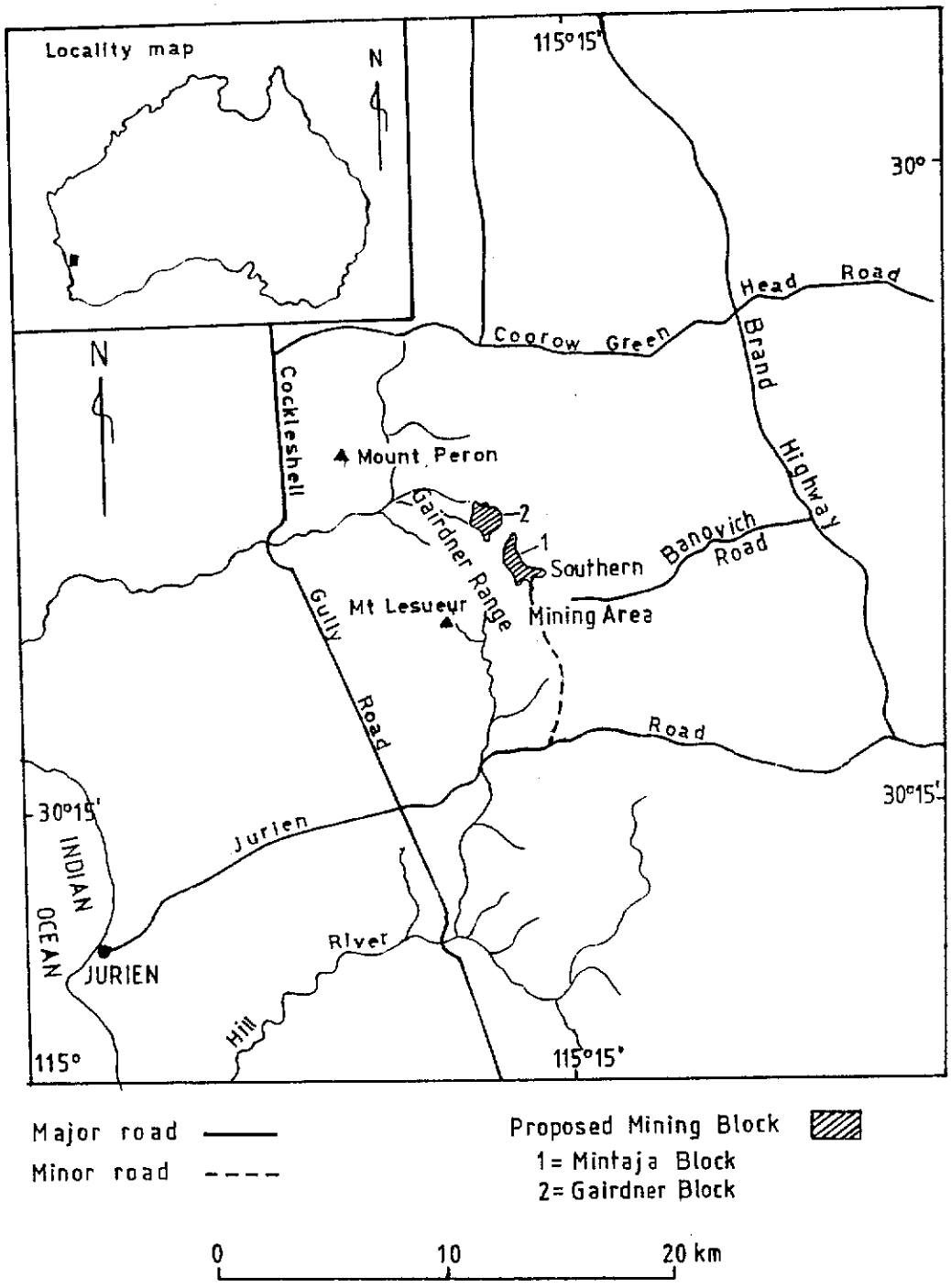

Figure 2.1 Location and access map of the proposed Hill River Mining area (modified from Burbridge, Hopper and van Leeuwen, 1990).

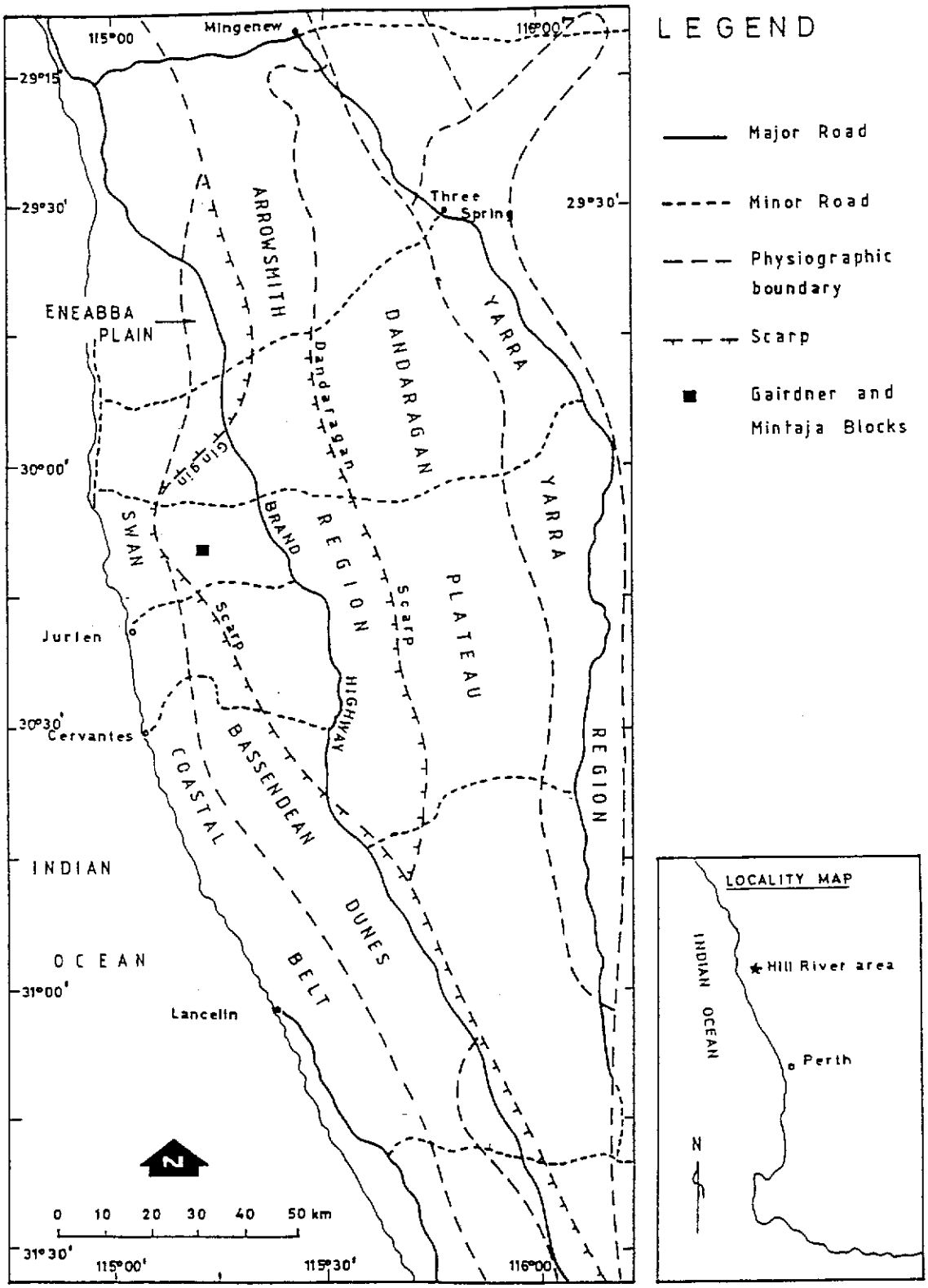

Figure 2.2. Physiographic Regions of the northern Perth Basin (after Burbridge, Hopper and van Leeuwen, 1990).

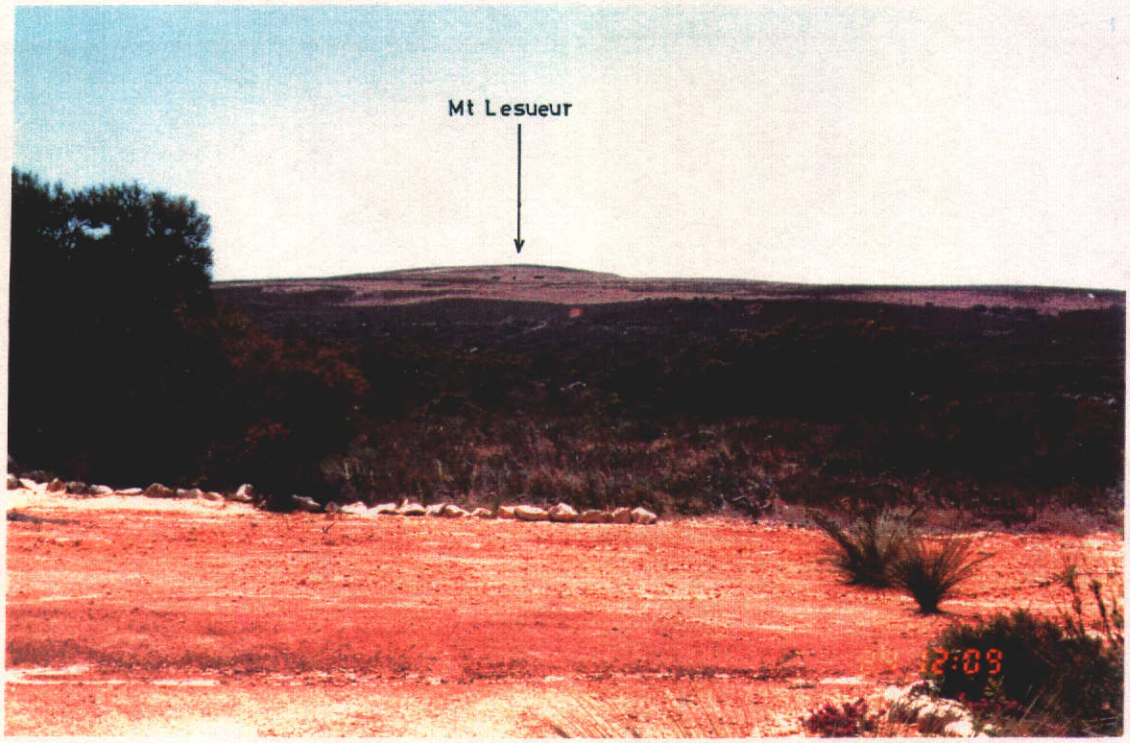

Figure 2.3. Western boundary of Arrowsmith Region, Hill River Area (view looking west from the Mintaja Block.

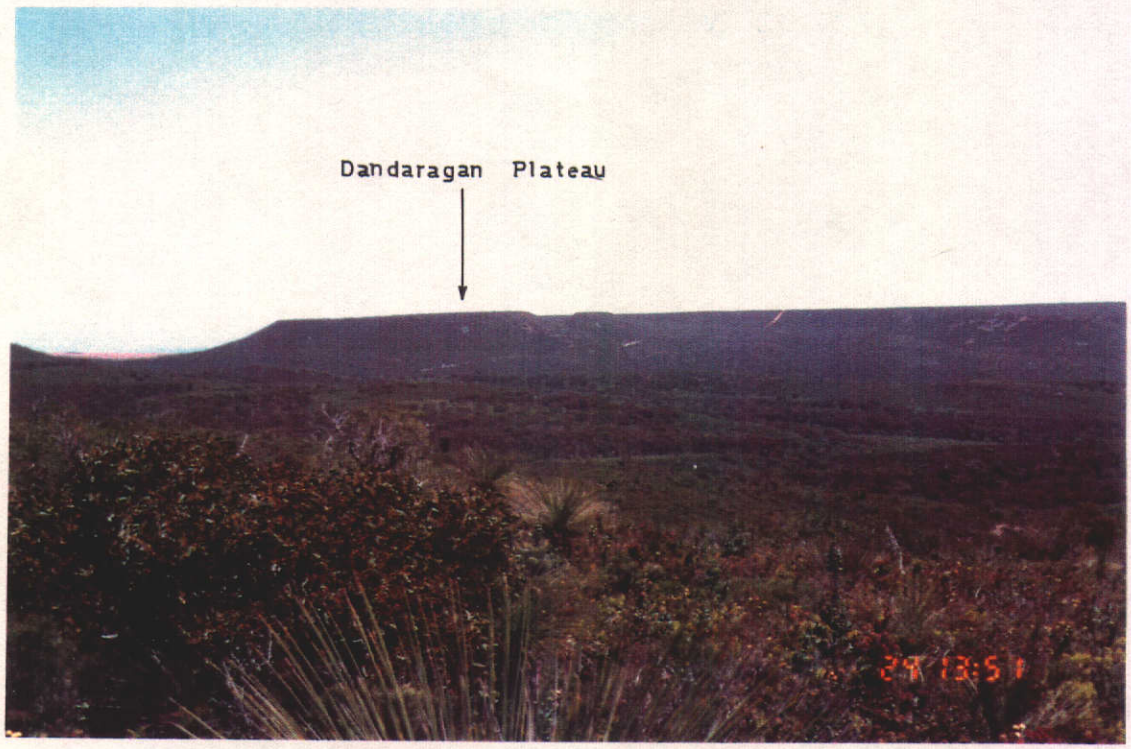

Figure 2.4. View of the eastern limit of the Arrowsmith region marked by the Dandaragan Scarp and Plateau looking east from the Mintaja Block.

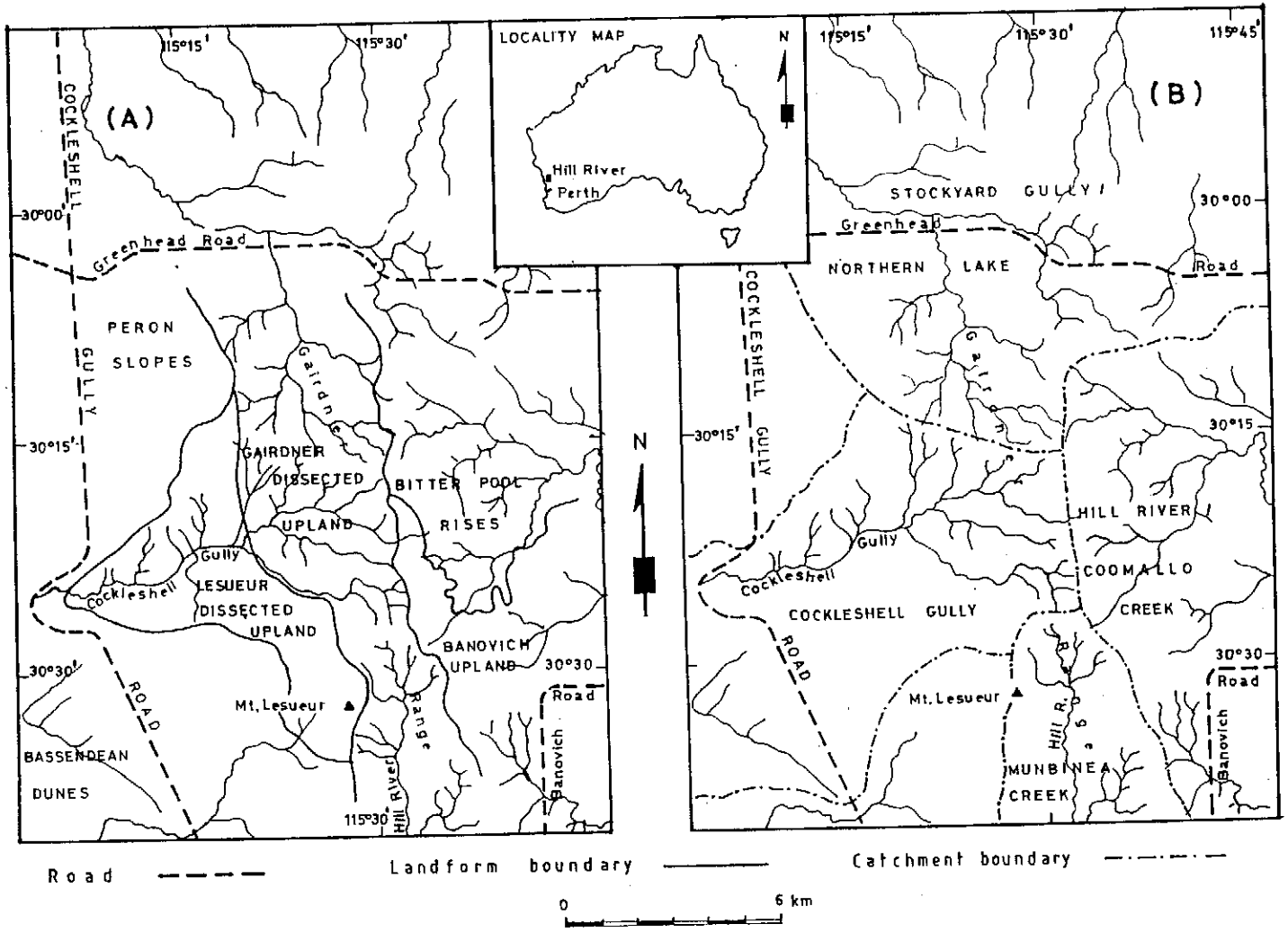

Figure 2.5. Sub-division of landform (A), and drainage and catchments (B) of the Arrowsmith Region, Hill River Area (modified from Burbridge, Hopper, and van Leeuwen, 1990)

2.4. Climate, Soil, and Vegetation

The description of climate, soil and vegetation of the Arrowsmith Region, is summarised from Burbridge, Hopper and van Leeuwen (1990). The climate is a mediterranean type with hot and dry summers, and cool and wet winters with moderately reliable rainfall. The mean maximum temperature for the hottest month varies from 30.5° to 32.5° C, while the mean minimum for the coldest month varies from 9° to 10° C. The average potential evaporation of the region is approximately 1,780 mm.

The soils in the Hill River area are variable and they range from sands to clays. Mostly, the soils are shallow, with a total thickness of only a few centimetres, and are underlain by rock or hard duricrust. A number of soil associations have been recognised, which have been found to be closely related to both the topography and the principal vegetation type, Northcote *et al.* (1967). The soils of the Arrowsmith Region are shown in Figure 2.6, and these are :

- Gairdner Associations which are an extremely complex mixture of siliceous sands, lateritic gravels, yellow duplexes, yellow massive earth, and brown mottled cracking clays.
- Banovich Associations, predominantly consisting of lateritic gravelly soils, with minor colluvial quartz sands.
- Bitter Pool Associations, which are composed of gravelly yellow duplex soils, yellow massive earths, and brown structured cracking clays.

A relationship between the main types of vegetation, soils and topography has been recognised in the Gairdner Dissected- and the Banovich Uplands by Burbridge, Hopper and van Leeuwen (1990). The landform of these two uplands is occupied by various types of soils, and it contains a wide range of vegetation types and the vegetation consists mainly of shrublands and woodlands interspersed in a complex

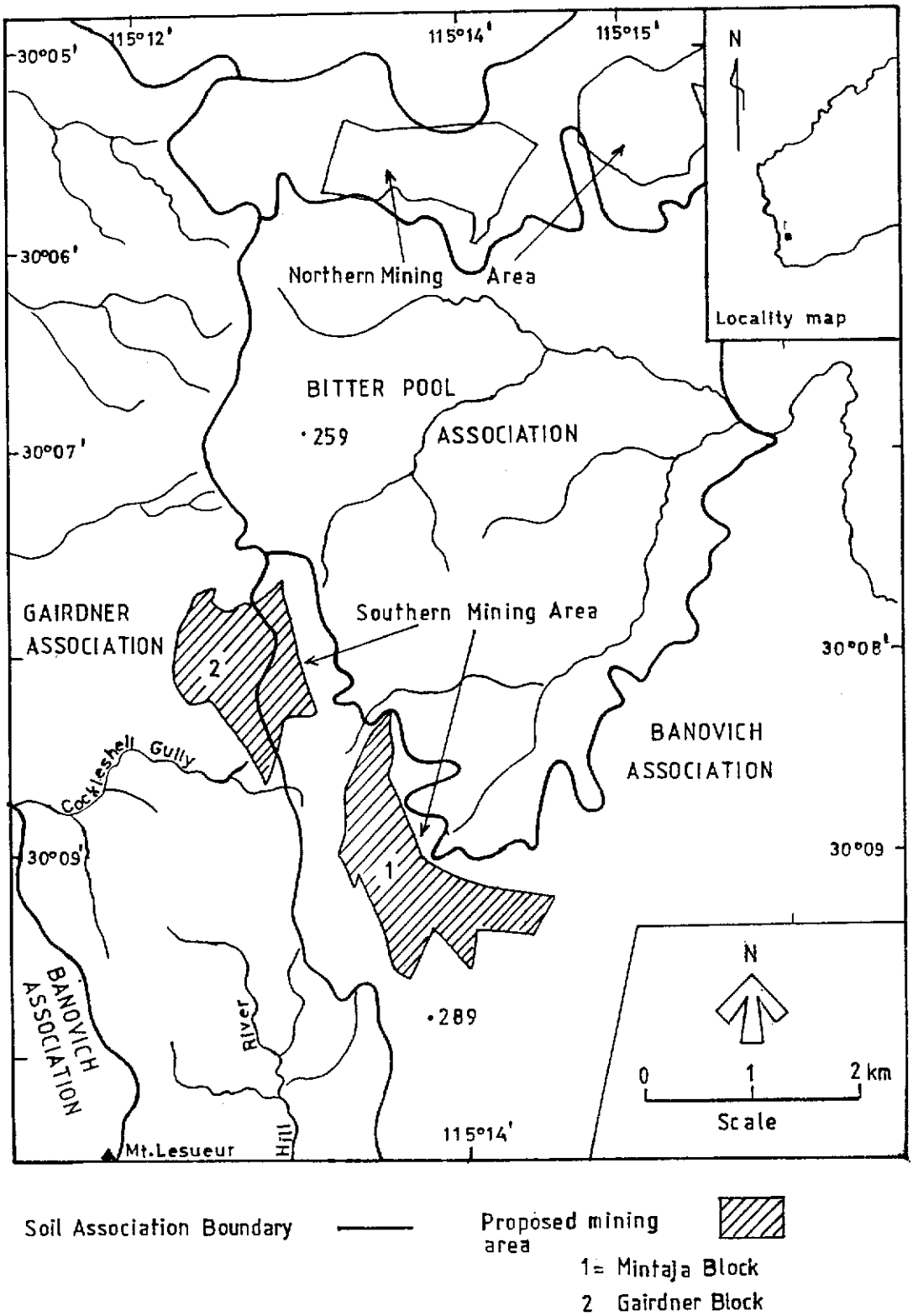

Figure 2.6. Soil classification on the proposed CRAE's mining area (modified from Burbridge, Hopper and van Leeuwen, 1990).

fine-scale mosaic of abruptly changing vegetation. The great diversity of communities reflects the complexity of the underlying geology. The Gairdner Dissected Uplands landform has the largest area of *Eucalyptus wandoo* woodlands, which occupy yellow duplex soils. On flatter slopes, where stony shallow brown siliceous sand, shallow gravelly sands, and bleached sand occur, different wandoo woodland types dominated by *Melaleuca undulata*, *Melaleuca uncinata*, *Thomasia foliosa* or sometimes *Baeckea camphorosmae,* have understoreyed. In some places *Eucalyptus drummondii* accompanying *Banksia tricuspis*, forms scrub heath on the bare sandstone.

2.5. Geological Setting

2.5.1. Perth Basin

The Hill River area is located in the northern part of the Perth Basin, shown in Figure 2.7). The name Perth Basin was first used by Andrews (1938). The basin forms a deep linear trough, an epicontinental wedge, extending from north of the Murchison River to the south coast over a distance of nearly 1,000 km. The eastern boundary of the basin is marked by a major tectonic feature named the Darling Fault with a continental slope to the west.

According to Cockbain (1990), the basin is polycyclic, and a Silurian to Early Neocomian sequence was deposited in an interior-fracture setting, whereas a Late Neocomian to Quaternary sequence was laid down in a marginal-sag basin. The Permian to Jurassic stratigraphy in the Dandaragan Trough of the Perth Basin is given in Figure 2.8.

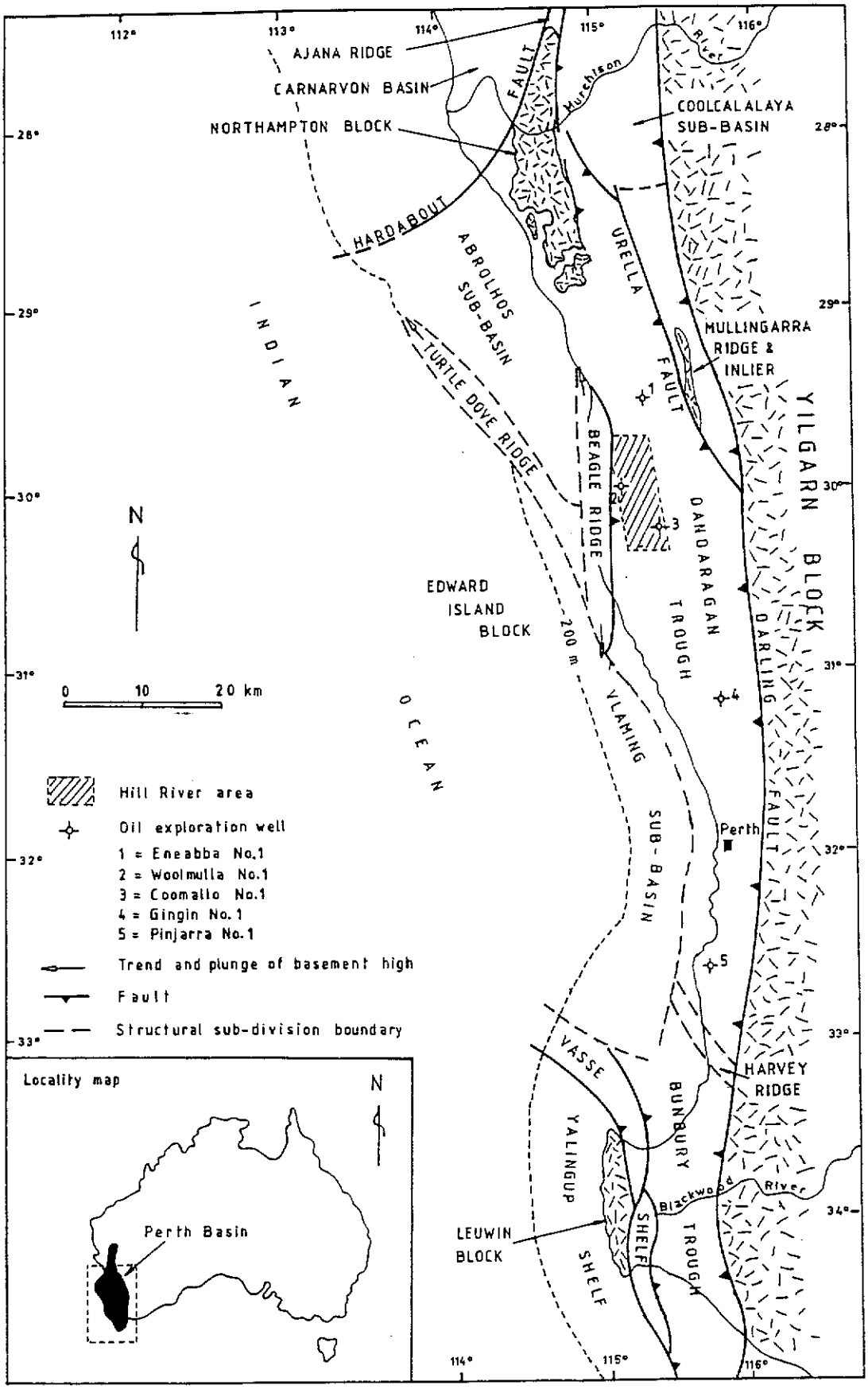

Figure 2.7. Location map and structural sub-division of the Perth Basin (after Playford, Cockbain and Low 1976).

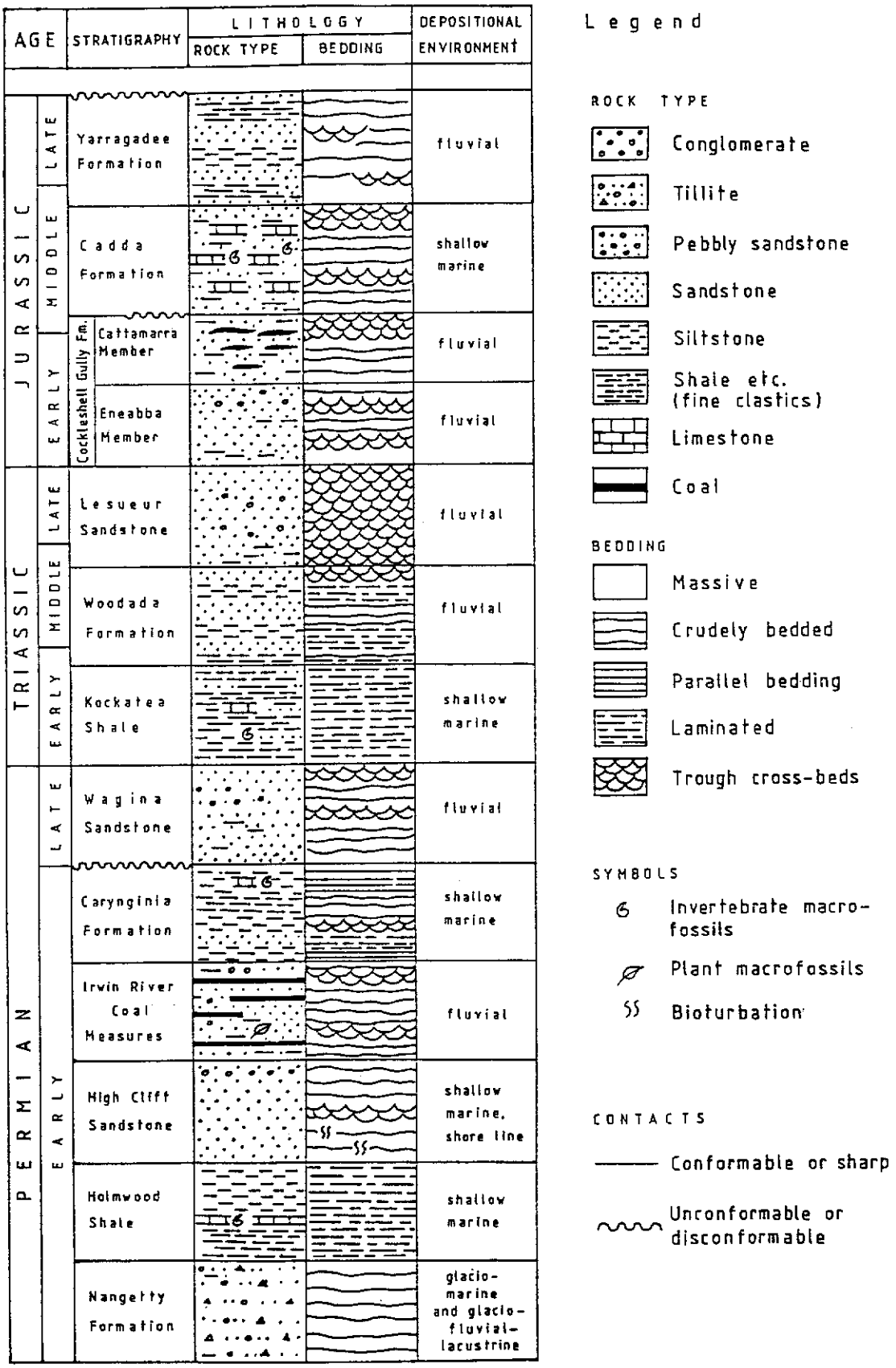

Figure 2.8. Permian - Jurassic lithostratigraphic sequence of the Dandaragan Trough, Perth Basin (modified from Cockbain, 1990).

The basin is intensely faulted. Generally, the faults are in a northwest direction, and are thrown down to the east; whilst some are thrown down to the west. In some areas of the basin, the draping of sediments over fault blocks leads to folding.

The graben structure of the Perth Basin was first recognised by Maitland (1907). The basin has been divided into eight sub-basins and six intra-basin structural highs (Figure 2.7). The sub-basins, which are separated by intra-basinal structural highs, are the Dandaragan and Bunbury Troughs in the south, and the Coolcalalaya, Abrolhos and Vlaming sub-basins, and the Vasse and Yallingup Shelves. The intra-basinal structural highs include the Beagle, Turtle Dove, Ajana, Harvey and Mullingarra Ridge and Inlier, and the Edward's Island Block.

2.5.2. Dandaragan Trough

The Dandaragan Trough, where the Gairdner Range is situated, is a half graben. It represents the deepest part of the Perth Basin, being filled with approximately 15,000 m of predominantly Permian to Mesozoic (with minor Tertiary) clastic sediments and associated coals. The sediments were deposited in marine and/or terrestrial environments (Figures 2.8).

The Dandaragan Trough is elongated in an approximately north-northwest to south-southeast direction, which is parallel to and bounded by the Darling-Urella Faults in the east and the Beagle-Turtle Dove Ridges to the west. To the north the terrain is bounded by the Northampton Block and Coolcalalaya Sub-basins, and to the south by the Harvey Ridge (Figure 2.7).

The Dandaragan Trough is occupied by the Permian to Mesozoic clastic sediments and coals (Figure 2.8), which were deposited in marine and/or terrestrial

environments, Playford, Cockbain and Low (1976) and Cockbain, (1990). A series of approximately north-south trending normal faults has distorted the deposits, as shown in the cross section of Figure 2.9.

The Permian sedimentary rocks in the Dandaragan Trough occur subsurfacially, with a total thickness exceeding 2,600 m. The succession ranges in age from Early to Late Permian, unconformably overlain by the Triassic sediments described as the Kockatea Shale, Woodada Formation, and Lesueur Sandstone, respectively. The Jurassic sequence is conformable on the Triassic sequence, and is described as Cockleshell Gully Formation, Cadda Formation and the Yarragadee Formation. A brief description of the stratigraphy of the Hill River which contains the coalfield follows.

2.5.3. Hill River Area

The geology and coal measures of the Hill River area, Perth Basin, Western Australia, were first described by Willmott (1964), followed by a comprehensive review by Kristensen (1989) and Smith (1990). The regional geology of the Hill River area is described by Cockbain (1990).

The Hill River Area and the coalfield occupy the Hill River Shelf of the North Perth Basin, Kristensen (1989). This shelf is located at the western flank of the Dandaragan Trough and the area is bounded by the Lesueur-Peron Faults in the west and the Warradarge Fault in the east (Figures 2.9 and 2.10).

The Hill River Coalfield was discovered in 1961 following the intersection of coal in the Cattamarra Member of the Cockleshell Gully Formation during a search for petroleum by West Australian Petroleum (WAPET) Pty . The Cockleshell Gully

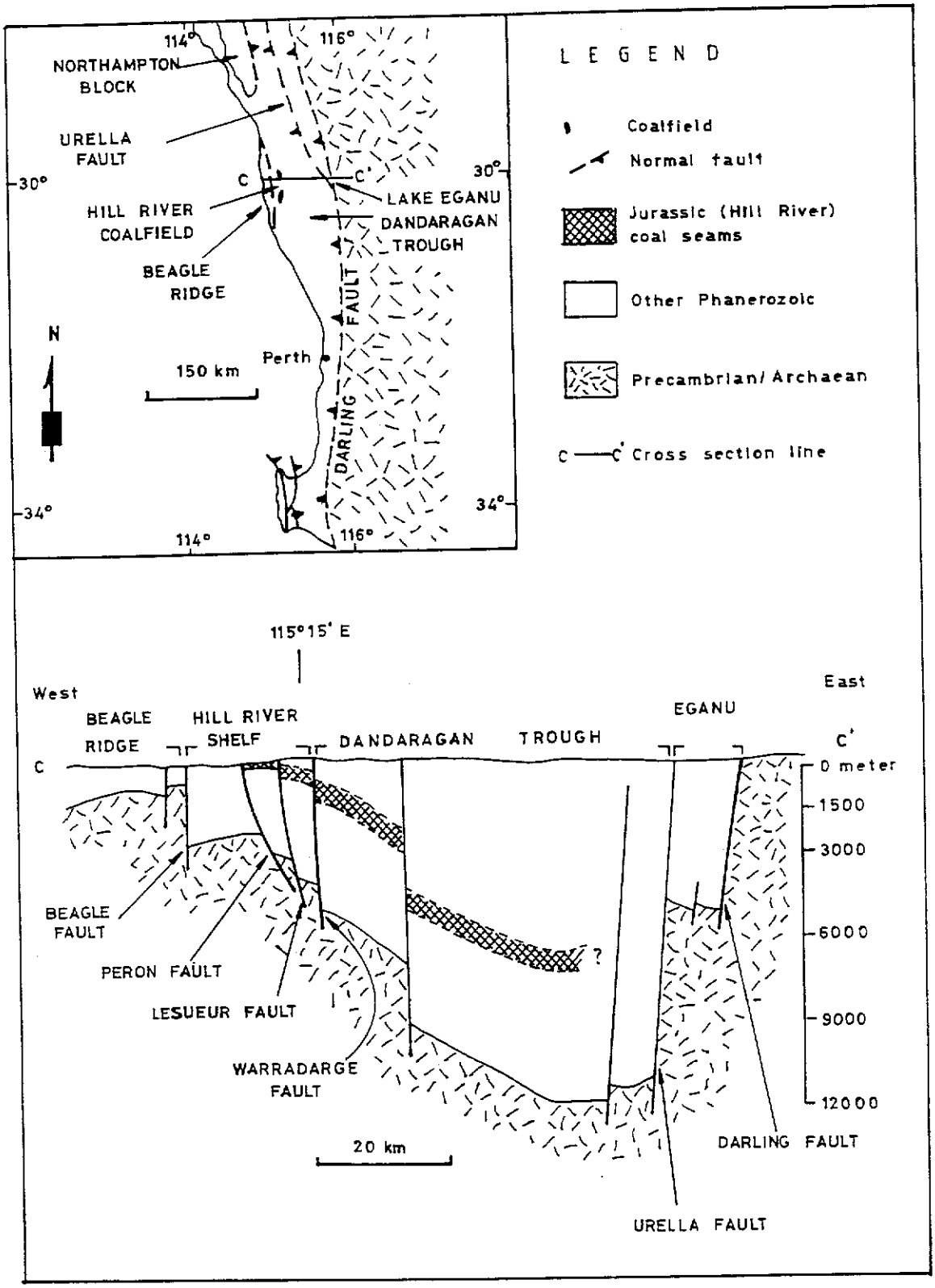

Figure 2.9. Location map and cross section of Hill River Area (modified from Playford, 1976, and Smith, 1990).

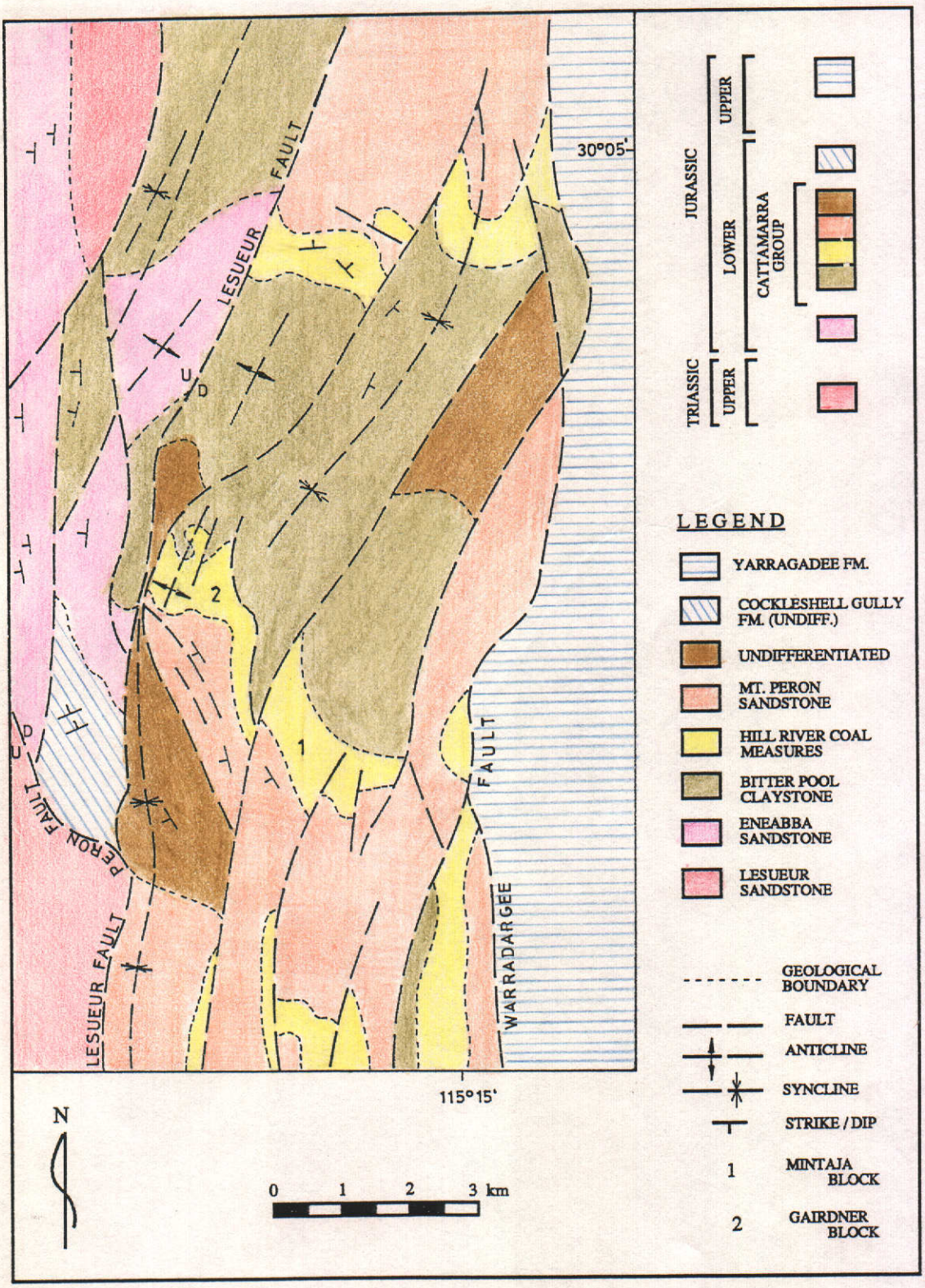

Figure 2.10. Geological map of the Hill River Shelf, North Perth Basin (after Kristensen, 1989).

Formation has been assigned Lower Jurassic to Middle Jurassic age and consists of two member namely Eneabba Member and the Cattamarra Member (Table 2.1).

The shallow sequence of the Cattamarra Member, also described as the Cattamarra Coal Measures, outcrops and subcrops on the fault block, with a width of 5-10 km and a length of 80 km, extending from Eneabba to Wongonderrah Spring (Figure 1.2).

According to the CRAE Nomenclature given in Table 2.1, the Cattamarra Coal Measures are defined as a group, consisting of two units, namely, the lower Bitter Pool Claystone and the upper Hill River Coal Measures. This is the nomenclature adopted by the author in this study.

The Upper Triassic and Jurassic geology of the Hill River Shelf is shown in Figure 2.10, and the brief stratigraphy of the units, structure and the depositional history follows:

Lesueur Sandstone

The Lesueur Sandstone of Upper Triassic age predominantly consists of fluviatile coarse- to very coarse-grained felspathic and kaolinitic sandstone, with large-scale cross-bedding; and conglomerate with minor siltstone beds. The type section of the Lesueur Sandstone is identified in the Woolmulla No. 1 well and the additional reference section is in the Eneabba No. 1 well. The sandstone thickness increases from north to south of the area, as shown in Figure 2.11 (A). According to Playford, Cockbain and Low (1976), the unit also continues in the southern Perth Basin. The contact of the formation with the overlying Eneabba Formation/Sandstone is

Table 2.1. Upper Triassic - Jurassic stratigraphy of the Hill River Coalfield (modified from Kristensen, 1989).

<table>
<tr><th>AGE</th><th colspan="2">EXISTING NOMENCLATURE</th><th>CRAE NOMENCLATURE</th></tr>
<tr><td>Upper Jurassic</td><td colspan="2">Yarragadee Formation</td><td>Mt. Peron Sandstone</td></tr>
<tr><td>Middle Jurassic</td><td>Cadda Formation</td><td rowspan="2">Cattamarra Coal Measures (Member)</td><td rowspan="2">Hill River Coal Measures
Cattamarra Group
Bitter Pool Claystone</td></tr>
<tr><td>Lower Jurassic</td><td>Cockleshell Gully Formation</td></tr>
<tr><td></td><td></td><td>Eneabba Member</td><td>Eneabba Formation</td></tr>
<tr><td>Middle - Upper Triassic</td><td colspan="2">Lesueur Sandstone</td><td>Lesueur Sandstone</td></tr>
</table>

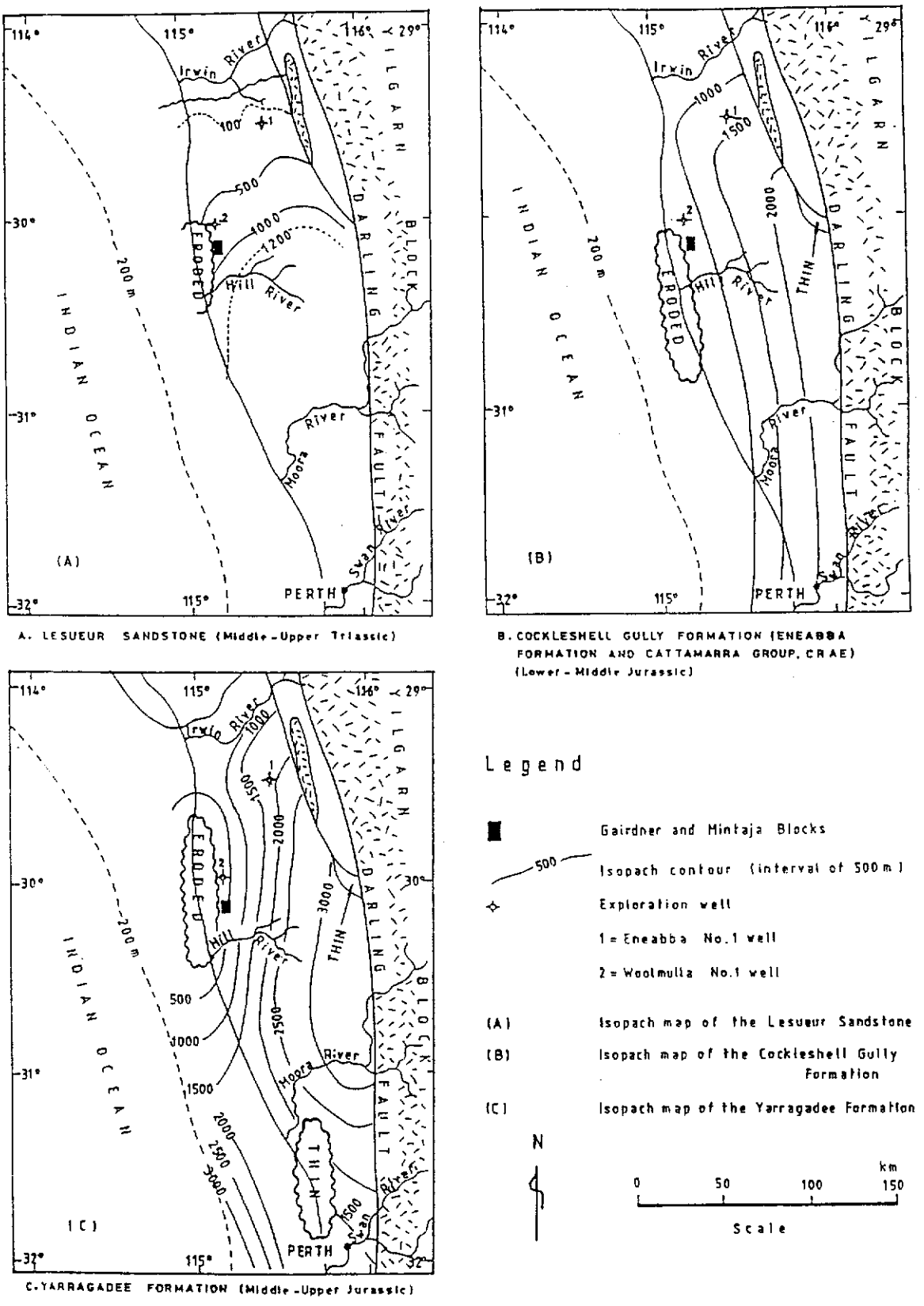

Figure 2.11. Isopach maps of the Upper Triassic to Upper Jurassic formations in the Dandaragan Trough (modified from Playford, Cockbain and Low, 1976).

transitional or conformable, and the sandstone is presumed to be a fluviatile deposit, Playford, Cockbain and Low (1976). The age of the unit assigned by Balme (1969) on the basis of palynology is Middle to Late Jurassic.

Eneabba Formation

The overlying Eneabba Formation was originally reported as the "Multicolour Member", because of its multicoloured appearance. This formation is composed of interbedded mottled and multicoloured claystone with some fine-grained sandstone, mottled siltstone, and conglomerate. Tabular cross-beds are present in the formation.

Based on the palynological dating, the age of the formation is Early Jurassic, Balme (1964). The type section is located in the Eneabba No. 1 well (Figure 2.11 B) with a total thickness of 676 m. The depositional environment is marine or paralic, supported by the occurrence of microplanktons in some sections. However, most of the formation is presumed to be of a high energy, braided stream, flood plain type setting.

Cattamarra Group

The Cattamarra Group conformably overlying the Eneabba Formation consists of two formations, namely the Bitter Pool Claystone and the Hill River Coal Measures.

The Bitter Pool Claystone is composed of claystone (Figure 2.12) with a thickness of probably more than 500 m. In the northern Perth Basin, this unit was intersected only in limited geophysical logging holes. An interdistributary, marginal or shallow marine environment has been presumed for the unit.

Figure 2.12. Parallel laminated claystone of Bitter Pool Claystone outcropping in the Mintaja Block, Hill River Area.

The Hill River Coal Measures consist of a cyclical series of sandstones, fining-upward into interbedded mudstone (and/or shale) and coal. The sand/shale ratio gradually increases towards the base. The unit is dominated by fine-grained sandstone with some zones of marine and brackish-water microfossils and shell beds , Sappal and Islam (1992). Rip-up clasts of underlying coal and mudstone are commonly recognised within the sandstone. The sequence grades upward into strongly bioturbated flaser-bedded and ripple cross-laminated sandstone (Figures 2.13, 2.14 and 2.15), and are capped by a coal zone (Figures 2.16). An erosively based fluvial sandstone overlies the main coal seam. Four zones of coal are developed in the coal measures with a cumulative thickness of 16 m. The type section of the Hill River Coal Measures of the Cattamarra Group is situated in the Eneabba No. 1 well (Figure 2.11 B). Apparently, it is continuos, but in fact, to the west side of the basin it is very lenticular. An isopach map of the Cockleshell Gully Formation (Cattamarra Group of the CRAE nomenclature) is shown in Figure 2.11 B, which shows that the formation thickens from the west towards the Darling Fault in the east of the Perth Basin.

Mt. Peron Sandstone

The Mt. Peron Sandstone rests conformably on the Hill River Coal Measures. The unit has similar lithologies to the underlying formation, but it contains thicker and coarser sandstone units. Higher energy, fluviatile conditions prevailed during its deposition, which were less favourable for coal formation. The Mt.Peron Sandstone is believed to be equivalent to the basal part of the Yarragadee Formation of Upper Jurassic age. The formation consists of interfingering sandstone and siltstone, with lesser amounts of shale, claystone and conglomerate. The sandstone generally is poorly sorted, fine- to very coarse-grained, and usually poorly bedded with local cross-bedding. The siltstone is for the most part thin bedded to fissile. Mottled red,

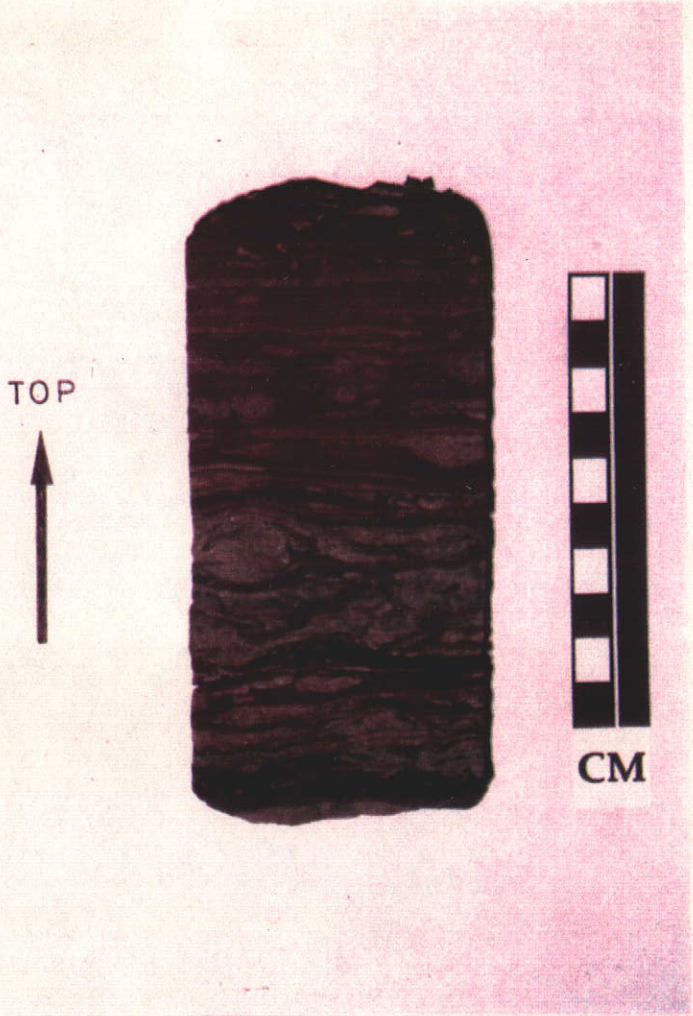

Figure 2.13. Flaser-bedded sandstone recognised in the drill core CPCH 1, Hill River Coal Measures, Mintaja Block.

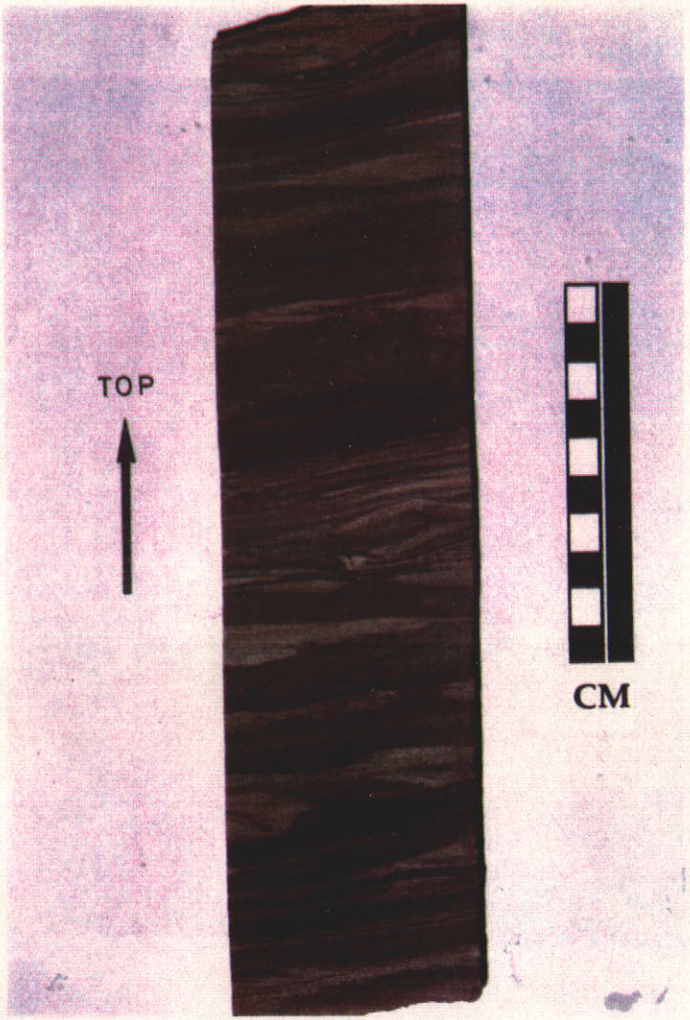

Figure 2.14. Ripple cross-laminated and parallel-laminated sandstone in the drill core CPCH 1, Hill River Coal Measures, Mintaja Block.

Figure 2.15. Cross-bedded sandstone outcropping in the Hill River Coal Measures, Mintaja Block.

Figure 2.16. Coal sub-seam G1 outcropping in the Girdner Block, Hill River Area.

yellow, and white colouring is a characteristic feature at the surface of the siltstone, while subsurficially, it is light to dark grey, with some white and brown beds. The type section is located 2.4 km south-southeast of Yarragadee homestead within a coordinate of 29 05'48" S and 115 24'50" E. Individual exposures are rarely thicker than 30 m . However, in Gingin No. 1 well, the thickness of the unit exceeds 2,965 m. Overall thickness of the Yarragadee Formation increases from the west towards the Darling Fault in the east (Figure 2.11 C). Microflora of the formation belong to the *Dampieri* and *Microcachryidites* assemblage of Balme (1964) which indicates Middle to Late Jurassic (?Tithonian to Aptian ages). The lower Yarragadee Formation is presumed to be of fluviatile origin, while the upper part of the unit was deposited in shallow-marine, paralic, and continental environments, Playford, Cockbain and Low (1976).

2.5.4. Structure

The dominant structure element of the northern Perth basin is faulting (Figures 2.7 and 2.9), and these faults are of normal type. In the basin, the prevalent faults are in the north-northeast direction, with a few in the north-northwest direction. The conspicuous folds in the Hill River Shelf are associated with faults (Figure 2.10).

The Cockleshell Gully Anticline present in the Hill River Area, is highly faulted (Figures 2.9 and 2.10) and consists of a series of blocks, which step down to the east. The highly distorted dome-like structure is present, which is flanked by two faults with displacements exceeding 1,000 m.

The normal faults which bound the area from the west to the east are the Beagle, the Lesueur-Peron and the Warradarge Faults (Figures 2.9 and 2.10), respectively. The structural pattern is complicated by a second series of faults as the result of strike-slip

movements along the curvilinear Lesueur-Peron and Warradarge Faults. Conjugate sets of faults and joints striking north - northeast and north - northwest are due to these movements. Cockbain (1990) stated that folding has been due to drag on faults or incompetent flexuring over them, although differential compaction probably has produced some folds.

2.5.5. Depositional History

The depositional history of the sediments in the Hill River Shelf, commenced in the late Middle Triassic, when the Lesueur Sandstone was deposited. The sandstone, predominantly consists of poorly sorted, continental sandstone, and was deposited in a series of fans along the fault scarp, Cockbain (1990), with the source area located in the Yilgarn Block. It is the main rock unit laid down as a result of late Middle to Late Triassic tectonism.

The unit's thickness increases from north to south with a maximum thickness of 1200 m, north of the Hill River area (Figure 2.11 A), and thus during the deposition of the Lesueur Sandstone, the depth of the basin (trough) increased gently towards the southern part of the basin.

The fluvial conditions which occurred in the late Middle to Late Triassic age, were followed by more quiescent ones without interruption into the Early Jurassic age, while active faulting took place. These relatively stable tectonic conditions provided the deposition of the multicoloured Eneabba Formation, which was succeeded by the Cattamarra Group composed of a continental sequence of coal-bearing clastic sediments with a few marine influxes, and the coal swamps were widespread throughout the area. The source terrane of sediments was more mature than before, demonstrated by the occurrence of finer-grained and better sorted clastic sediments.

A marine incursion initiated deposition of the Cadda Formation, which is equivalent to the upper part of the Cattamarra Group, Cockbain (1990).

Isopach map in Figure 2.11 B, shows that the isopach lines are parallel to the Darling Fault. This indicates that the depth of the basin, from the northern edge to the southern edge area, increased constantly towards the Darling Fault bounding the basin in the east. Fluvial conditions returned in the late Middle to Late Jurassic, and flooded the Lower Jurassic extensive coal swamps of the Cattamarra Group. A renewed movement took place along the Darling and the Urella Faults, and the deposition of the Yarragadee Formation took place. The thickness of the Yarragadee Formation increases constantly from the west towards the east , as shown in the isopach map on Figure 2.11 C, indicating the increase in the depth of the Dandaragan Trough, towards the east during the Late Jurassic time.

During the Early Cretaceous, the sedimentary deposition was interrupted by a major tectonic pulse centred in the Beagle Ridge, Thomas (1979) and the western flank of the Dandaragan Trough was uplifted and truncated. This activity produced the present structures which occur in the Hill River Shelf.

CHAPTER 3. SAMPLING OF COAL, METHODS, TECHNIQUES, TERMINOLOGY AND NOMENCLATURE

3.1 Introduction

The samples of coal for this study were collected from the drill holes, drilled in the Gairdner and Mintaja Blocks of the Hill River area, Perth Basin, Western Australia. The core samples were obtained during the study from CRA Exploration Pty Ltd. Samples of six drill cores were obtained for detailed petrographic and trace-element analyses. Of these, one is a full core of 8 cm in diameter, while the remainders are coarse to medium grained particulate coal. The location of the six drill holes is shown in Figure 3.1 and Table 3.1.

The selection of core locations was made by the author based on information from outcrops and borehole records around the Southern Mining area of CRA Exploration Pty. Ltd. The drilling indicates the existence of four seams, of which the seam G consists of six sub-seams, named G1 to G 6 . The seam G is best developed for proposed open cut mining at the Hill River area.

To enable detailed examination of the megascopic and microscopic aspects of coal type variation within each drilled core sample, a series of polished sections were prepared. For hole CPCH 1, it was possible to prepare a complete set of polished blocks and polished particulate pellets/briquettes. A total of 175 polished sections were prepared, covering a total 14 metres of seam G from the six boreholes.

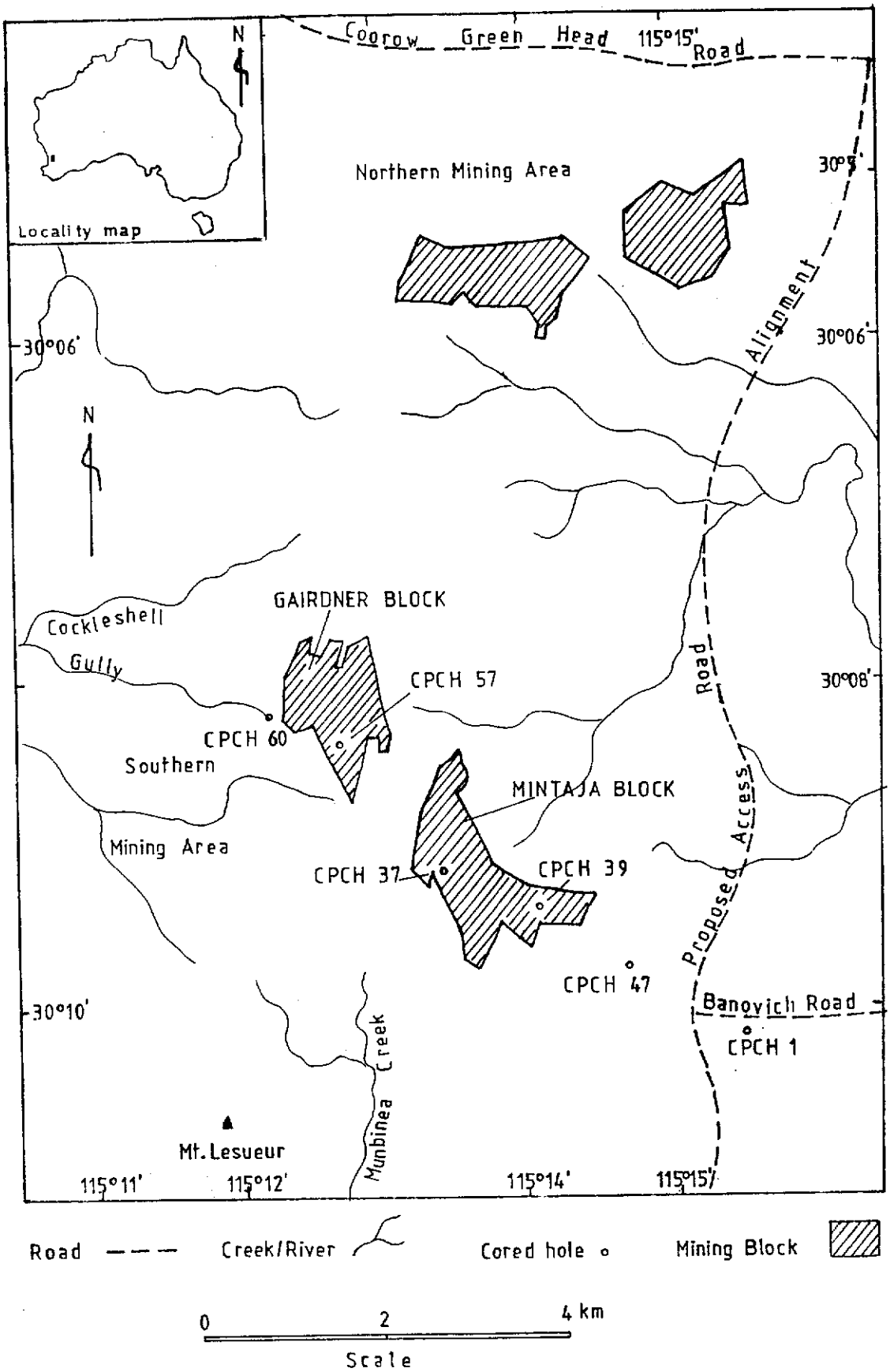

Figure 3.1. Location map of drilled holes (CPCH 1. 37, 39, 47, 57 and 60) in the Hill River Area.

Table 3.1. Location of studied drill holes in the Mintaja and Gairdner Blocks, Gairdner Range, Hill River Area.

Drill holes	Longitude	Latitude	Blocks
CPCH 1	115°15'06"	30°10'43"	Mintaja
CPCH 37	115°13'26"	30°09'12"	
CPCH 39	115°14'01"	30°09'24"	
CPCH 47	115°14'34"	30°09'45"	
CPCH 57	115°12'55"	30°08'41"	Gairdner
CPCH 60	115°12'23"	30°08'19"	

3.2. Methods And Techniques

The methods used in the petrological study of the Hill River coal, include the polished section preparations, macroscopic and microscopic examinations, and the Scanning Electron Microscopy (SEM) examination of selected polished sections.

The procedures adopted for the preparations and the analytical techniques in this study are according to the Australian Standards described in Table 3.2. A flow chart of sample preparation for petrographic analysis is given in Figure 3.2.

3.2.1. Sample preparations

Drill core of CPCH 1 was logged, for both coal lithotypes and lithology (Figure 3.3 and 3.4). On the basis of lithotype characteristics and distinct shale partings, the profile was subdivided into 11 sub-sections (Figure 3.4), in order to assess the vertical variations in petrography of coal, ash yields, and trace-elements. A maximum length of approximately ~~half a meter~~ 0.5 m was used for each sub-section to gain convenience in crushing. The individual lithotype samples in each sub-section were mixed together to form a sub-section sample for crushing.

Selected samples from the drill core were sliced in halves and polished to study sedimentary structures.

For reflected light and fluorescence examination, coal samples were prepared as polished briquettes of particulates and polished blocks of selected lithotypes from the cores.

Table 3.2. Australian Standard Association Code in Coal Petrology.

AS	2061	Code of practice for preparation of hard coal samples for microscopical examination by reflected light.
AS	K 183	Graphical representation of coal seams.
AS	K 149	Glossary of terms for coal and coke
AS	2418	(parts 5) Terms relating to the petrographic analysis of bituminous coal and anthracite (hard coal).
AS	2515	Determination of maceral group composition of bituminous coal and anthracite (hard coal).
AS	2486	Microscopical determination of the reflectance of coal macerals.

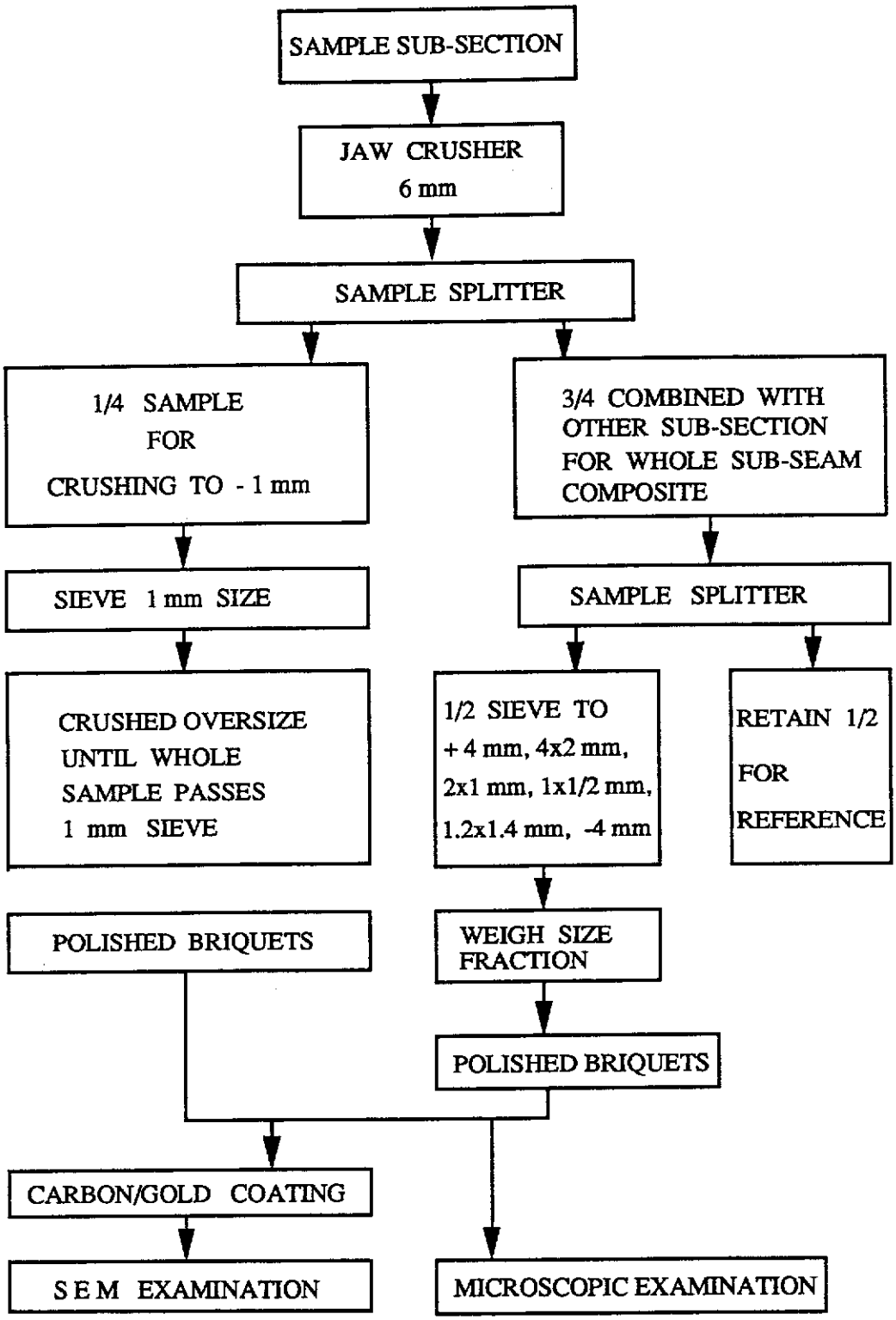

Figure 3.2. Flowchart of polished specimen preparation carried out in the present study (modified from Sappal, 1986).

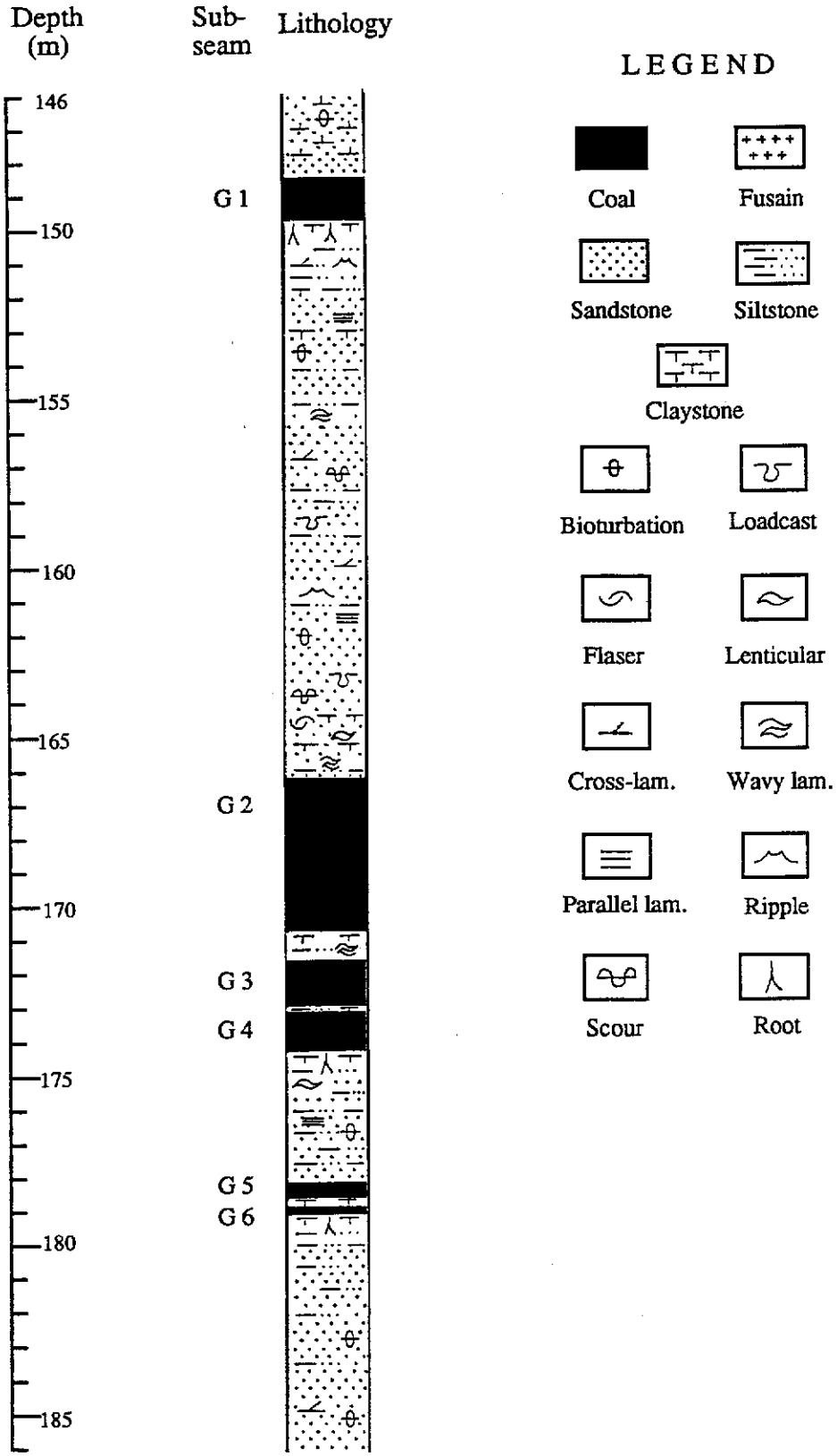

Figure 3.3. Lithology and sedimentary structures log of drill core CPCH 1 located south of Banovich Road, Hill River Area.

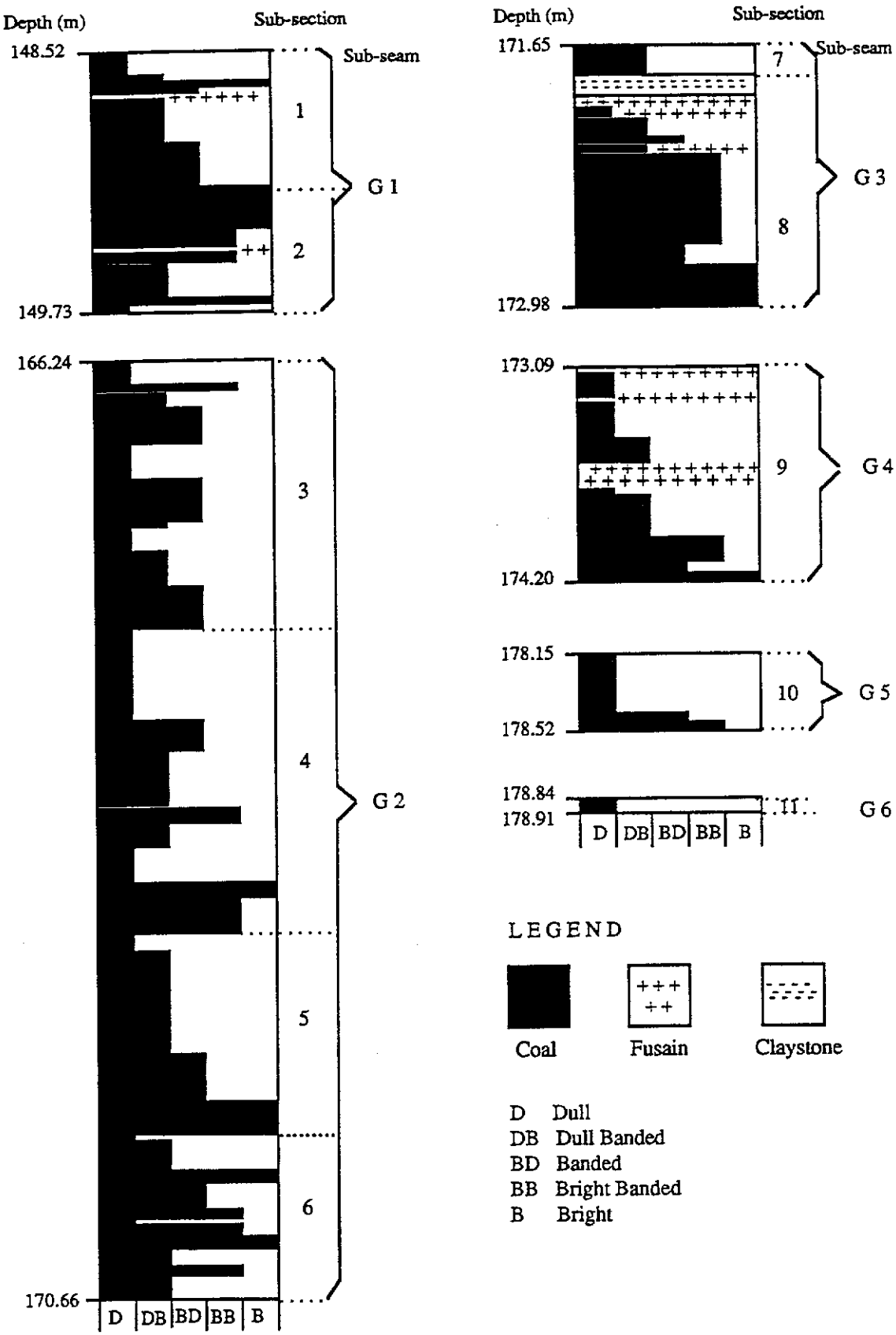

Figure 3.4 . Lithotype profile and sub-divisions of coal representing seam G (sub-seam G 1 - G 6) of drill hole CPCH 1, Hill River Area.

3.2.1.1. Polished sections

Polished sections of coal for petrographic analysis were prepared as polished briquettes and polished blocks (Figure 3.5). The polished briquettes were made of crushed samples representing coal sub seams, G1 to G6, and the individual sub sections 1 to 11. Stages in preparation of polished sections are:

Crushing

The coal from each sub-section or sub-seam was first crushed in a jaw crusher or a mortar, so that all coal would pass through a standard 4 mm screen/sieve. For each coal sample of different sub-section/sub-seam, the crusher was thoroughly cleaned to avoid contamination of the subsequent sub-section/sub-seam. The crushed coal sample of approximately 4 mm in size, was crushed in a coffee mill (Figure 3.6) to gain 1 mm size of coal for preparation of polished briquettes. The polished briquettes were prepared for representative samples of <1 mm size fractions, and also for the size fractions of > 4 mm, 4x2 mm, 2x1 mm, 1x1/2 mm, 1/2x1/4 mm and < 1/4 mm. The flow chart for crushing and sieving of coal samples is shown in Figure 3.2.

Embedding

Sample splitters were used to obtain a representative sample of each size fraction. For each of the < 1 mm, 1x1/2 mm, 1/2x1/4 mm, and < 1/4 mm size fractions, approximately 20 grams or 3/4 vial volume of coal was required, whilst, approximately 120 grams of coals was required for the > 4 mm and 4x2 mm size fractions. 40 grams of coal was required for the 2x1 mm size fractions. Every

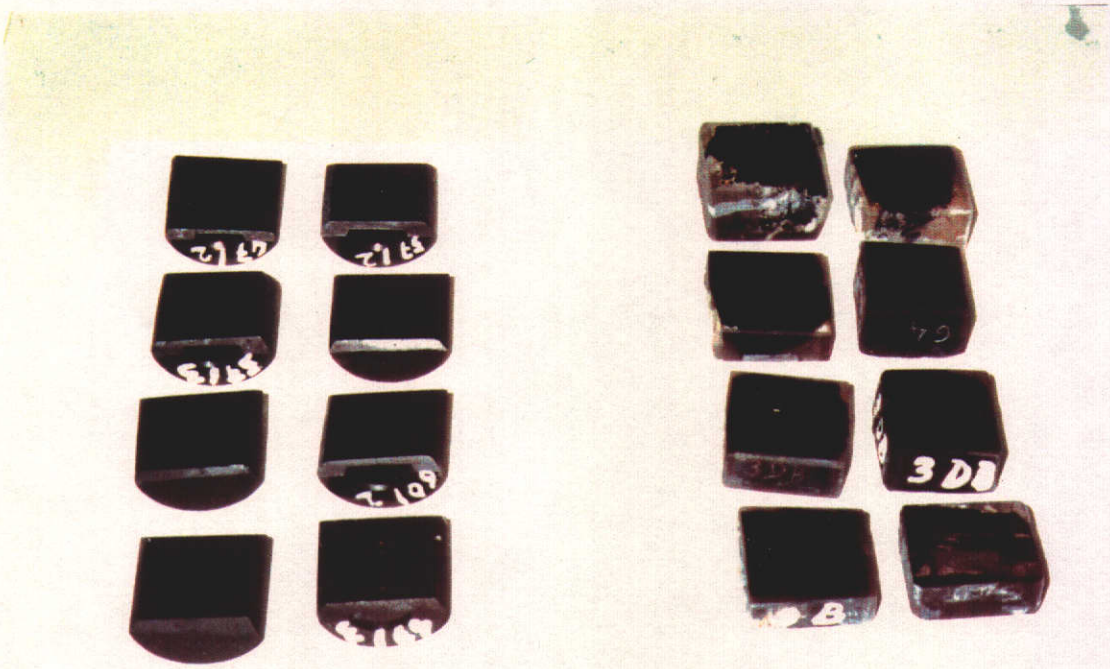

Figure 3.5. Polished briquettes (left side) and polished blocks (right side) of coal.

Figure 3.6. Equipment used in the preparation of coal samples.

20 grams of individual sample was placed into labelled vials of 2.5 cm in diameter (Figure 3.7), and embedded in a coal- setting polyester resin.

The embedding medium used was an epoxy resin, that is a mixture of Epibond 1184 and hardener. Araldite was also used as an embedding medium for polished samples. The formation of cracks and blisters was avoided as they were detrimental to the polishing and reflectance measurement.

The mixtures of coal and embedding resin were stirred to a fairly thick paste, in order to prevent the grains sinking during hardening, as well as obtaining a uniform portion of grains in the block. These mixtures were evacuated in a vacuum chamber (Figure 3.6) to avoid the formation of bubbles for about 1 to 2 hours. Then the samples were left overnight in a fume cupboard to set (Figure 3.7).

Grinding

After setting, the plastic vials filled with the mixture of coal and embedding medium were cut into halves vertically by a diamond saw (Figure 3.6). After the halves had been removed from the plastic vials, the blocks were labelled. One block was prepared for petrographic analysis, while the other was kept either for reference or SEM analysis.

The individual block was ground on wet durite papers of grades 150, 200, 400, 600, 800 followed by 1200 grits successively . After each stage of grinding, the specimen was thoroughly rinsed in a stream of water to remove grit and grinding residues. Then, the block was cleaned in an ultrasonic bath (Figure 3.8) for 30 minutes, prior to polishing.

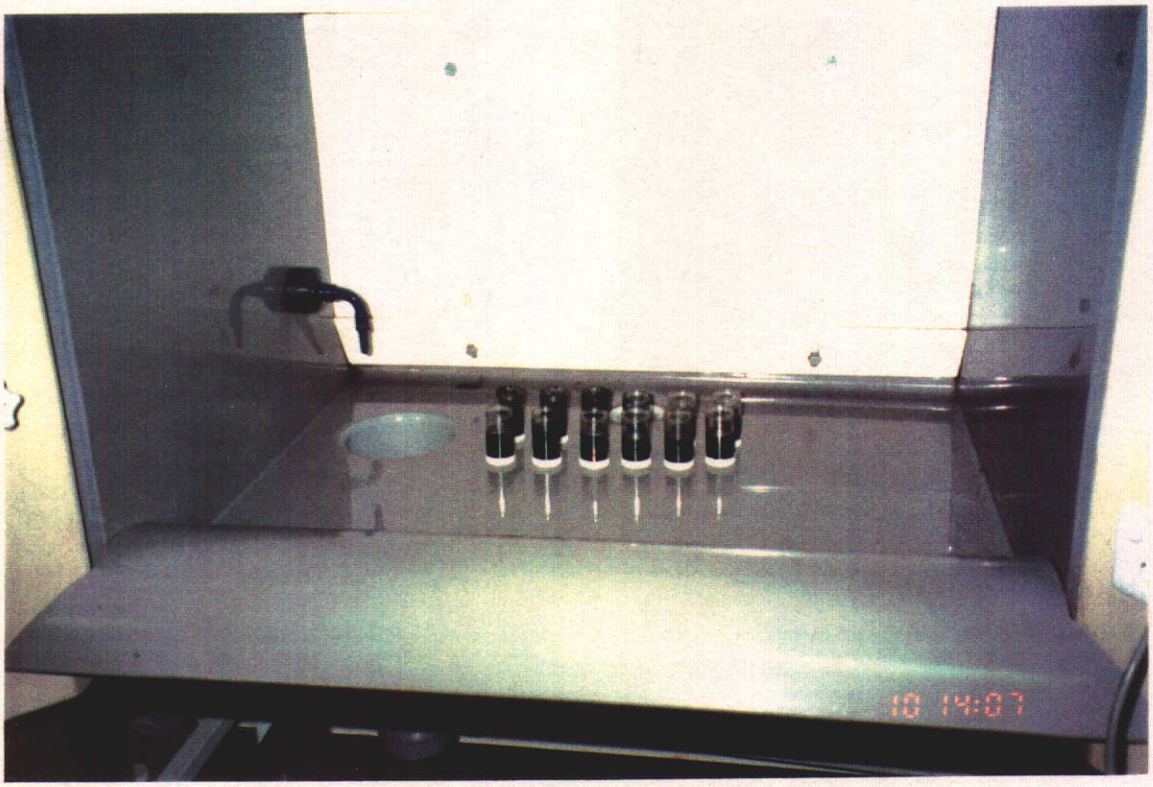

Figure 3.7. Fume cupboard with vials of coal sample embedded in the polyester resin.

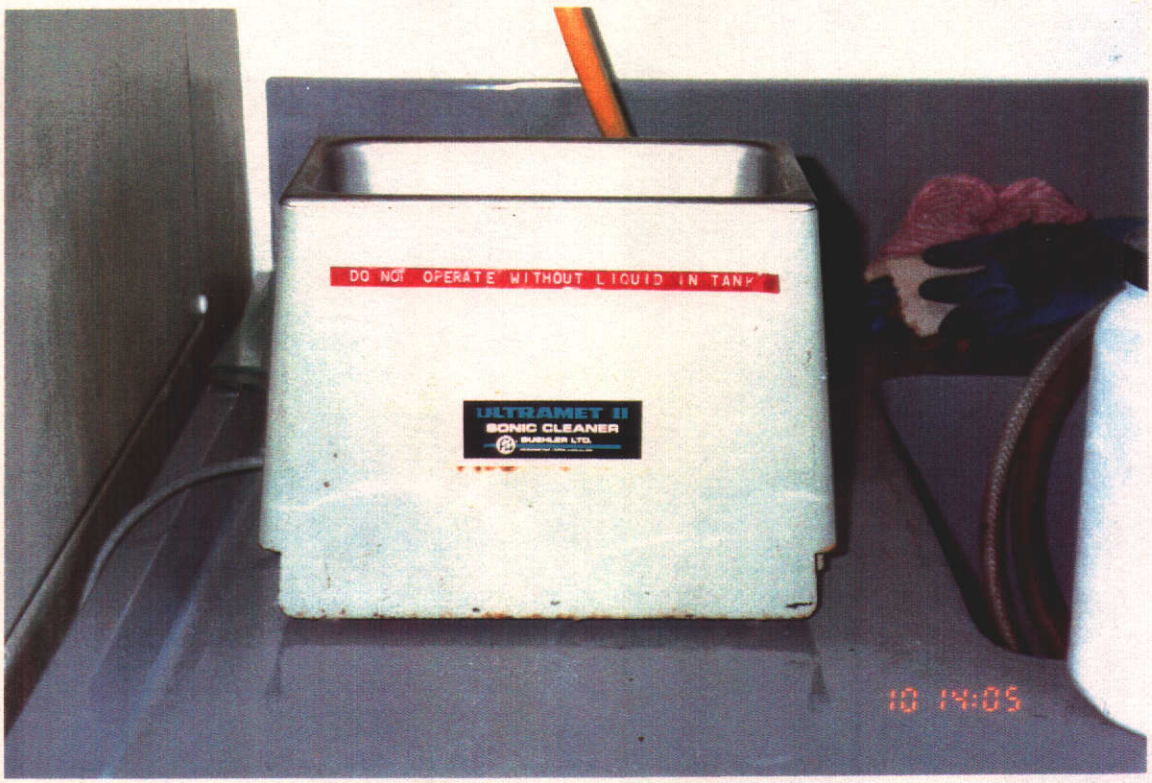

Figure 3.8. Ultrasonic bath used in polished section preparation.

Polishing

Polishing was done in two stages using either alumina powder slurry or colloidal silica polishing suspension , on a rotating disc covered with a synthetic silk cloth (Figure 3.9). The first stage was coarse polishing done by a 1 micron alpha alumina slurry at speed of 250 rpm for 15 minutes. The second one was the fine polishing using 0.05 micron gamma alumina slurry for 10 to 15 minutes. This was followed by polishing, using distilled water for 20 to 30 minutes. Finally , the block was thoroughly washed under a stream of water.

The washed polished block of particulate coal was placed in an ultrasonic bath to remove dirt for a period of 25 to 30 minutes. Finally, it was rinsed with distilled water, and dried in a fume cupboard for petrographic analysis. The advantage of using colloidal silica polishing liquid in the preference to alumina is that there is relatively no relief formed in the surface of polished block. The specimens used for measurement of reflectance were prepared using colloidal silica.

Polished blocks

The procedure was to cut small blocks of suitable coal from the individual lithotypes in each sub-seam of a cored sample, using a diamond saw. These individual blocks were labelled as to their stratigraphic position and orientation in the coal seam. For the brittle and also highly fractured coals, embedding in an epoxy resin mixture was necessary prior to cutting into smaller blocks.

A block with cross-sectional surface area about 3x3 cm was adequate for the preparation and was primarily prepared for microscopic examination. This size fits into the rectangular holder of the polishing machine. The block was then placed

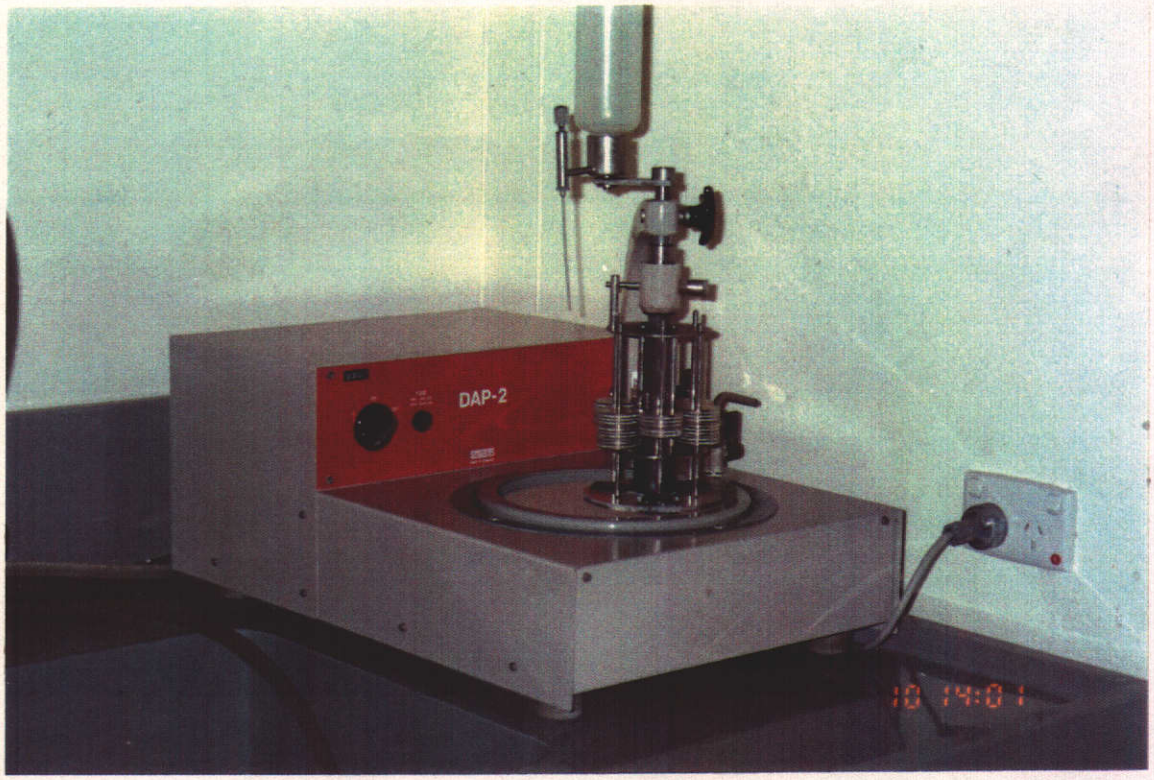

Figure 3.9. Polishing machine with rotating-disc covered by a synthetic silk cloth.

in rectangular moulds made of aluminium foil with the surface to be polished placed face down.

The mould was then filled with an epoxy resin mixture. Afterwards, the sample was left overnight to cure it, ready for cutting, grinding, and polishing. The procedures for grinding and polishing which were carried out, were the same as used for the polished briquettes.

3.2.2. Analytical Techniques

3.2.2.1. Lithotype examination

The G1 to G6 coal sub-seams of CPCH 1 borehole were logged macroscopically in order to prepare a lithotype profile (Figure 3.3). Prior to the lithotype logging, the core was split lengthwise to obtain fresh surfaces for visual determination.

Lithotype profile of the sub-seams was compiled and logged using the lithotype classification proposed by Diessel (1965) (Table 3.3). Quantitatively, the exact proportions of each lithotype were determined by "calculating the aggregate thickness of each lithotype as a *percentage* of the total seam thickness *excluding clastic bands*". This classification is based on the lustre or brightness (bright versus dull), fracture pattern, type of stratification, and macroscopic bands of coal. A minimum band thickness of 5 mm is used for classification. Following six coal lithotypes used for the profiles are:

- Bright Coal (B) 90% - 100% bright coal.
- Bright Banded Coal (BB) 60% - 90% bright coal.
- Banded Coal (BD) 40% - 60% bright coal.
- Dull Banded Coal (DB) 10% - 40% bright coal.

Table 3.3 . Lithotype nomenclature used in the present study.

Stopes 1919	Present study (after Diessel, 1965)	Description
vitrain	bright coal	subvitreous to vitreous lustre, conchoidal fracture, less than 10% dull coal laminae.
	bright banded coal	predominantly bright coal with 10% to 40% dull coal laminae.
clarain	banded coal	bright and dull coal interlaminated in approximately equal proportion.
	banded dull coal	dull coal with 10% to 40% bright coal laminae.
durain	dull coal	matt lustre, uneven fracture, less than 10% bright coal laminae.
fusain	fibrous coal	satin lustre, very friable.

- Dull Coal (D)	0% - 10% bright coal.
- Fusain	Fibrous coal

Very thin bands of fusain associated with the above lithotype have been logged as Fusain (F), and their presence is recorded on the lithotype profile of the individual seam. In addition, shaly coal, coaly shale, and carbonaceous shale is recorded in the log. Shaly coal is an intimate mixture of coal and clay minerals (20%-60%), with dull appearance, brown streak colour, showing alternatively laminae of coal and shale. Coaly shale is shale containing < 40% thin coal bands, while carbonaceous shale consists of shale containing < 40% finely disseminated carbonaceous matter. A lithological log of clastic sediments , especially the immediate roof and floor materials, and any non-coal bands/partings within the sub-seam, using features such as lithology and sedimentary structures is shown in Figure 3.3.

A standard graphical profile was drawn for the section which enabled sub-sections for subsequent testing to be selected. The core was sub-divided, to separate sub-seams and sub-sections for analytical work (Figure 3.4).

3.2.2.2. Microscopic Examination (Macerals and Microlithotypes)

Microscopic examination of polished sections was carried out in reflected white light and also in a fluorescence mode. A Leitz Orthoplan reflected light microscope fitted with a 75 W tungsten lamp and oil immersion objectives of X32 and X50, and 10X eyepiece, was used for all examinations of polished sections (Figure 3.10). The microscope was connected to Swift Point Counting device for quantitative work. Fluorescence-mode observations were carried out in conjunction with reflected white light , using the same microscope with the aid of a 100 W mercury lamp , and ultra violet light excitation. A filter system comprising a 3-mm BG 3 excitation filter, a TK

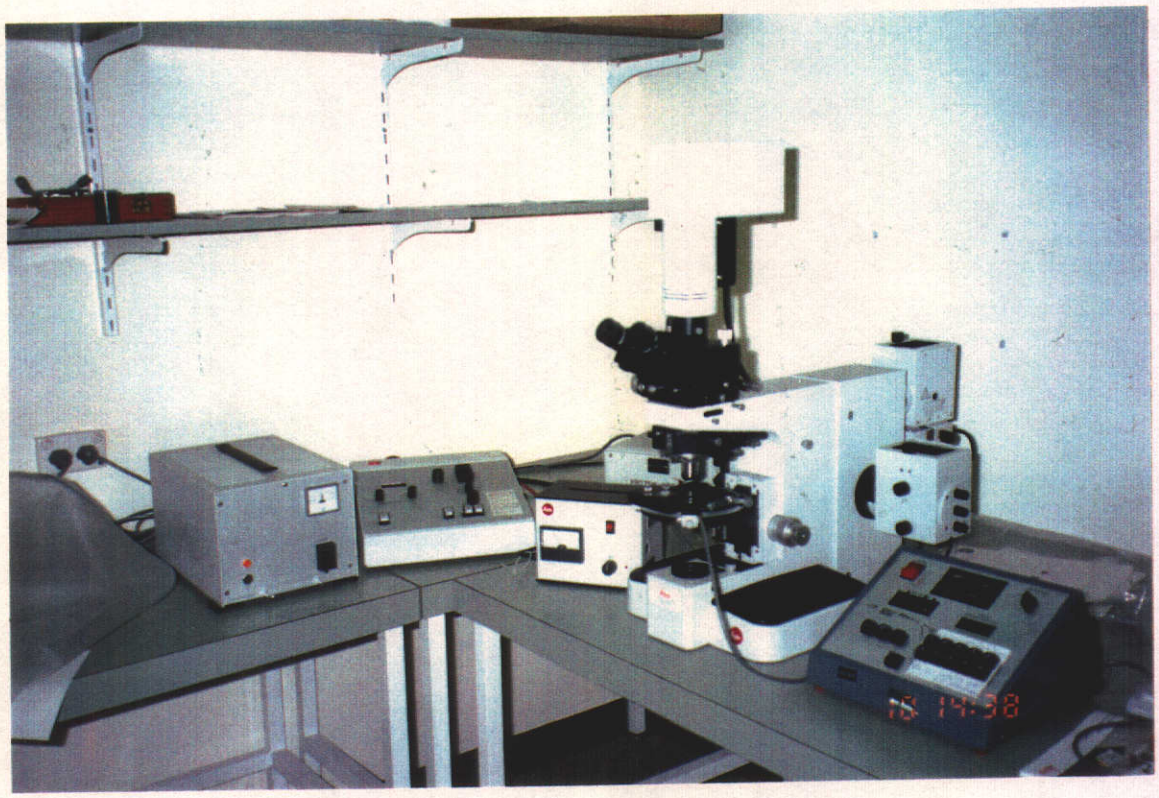

Figure 3.10. Equipment used for petrographic analysis.

400 dichroic beam-splitting mirror, and a K 470 or K 490 suppression (barrier) filter were used. A dichroic beam splitter was placed in the vertical illuminator of the microscope and a suppression (barrier) filter was used for cutting excitation light during visual observation. The fluorescence mode was used as an aid to distinguish between exinite macerals and clay minerals.

The observations of the relative abundances of macerals are based on normal point counting techniques. Within each traverse of view, the maceral under each cross-hair of the eyepiece reticule is identified and counted. The required number of points is 500, using the Swift automatic point counter Model-E. The traverses are made from top to bottom of the polished sections, rather than across it, in terms of the orientation of coal particles set in plastic. The step length (traverse spacing) is changed relative to particle sizes of the specimens, to gain representative counts. It is half the maximum particle size of coal, which is 0.5 mm for a sample with a particle size of approximately 1 mm, and 2 mm for a sample with a particle size of 4 mm. Approximately 90 % of the surface of each block is counted.

The standard error of estimation is calculated by formula: $s = \sqrt{P(100-P)/N}$, where P is the estimated percentage of a component and N is the total number of points in the sample counted (Australian Standard 2486 - 1981).

For polished blocks of the size fractions - 1 mm, 1X1/2 mm, 1/2X1/4 mm, and -1/4 mm, one block each was required for microscopic examination, while six blocks each were required for the size fractions of + 4 mm, 4X2 mm, and 2X1 mm.

The proportions of maceral and mineral matter content are recorded for each block. Vitrinite A and B is distinguished according to the definition of Brown *et al.* (1984) and Cook and Kantsler (1983). Vitrinite A is dominated by telocollinite with rare

telinite, while vitrinite B is dominated by desmocollinite with rare corpocollinite and very rare vitrodetrinite.

The volume percentages of the macerals obtained are recalculated on mineral matter free basis , using the following formula :

a). Mineral Matter Counted:

% Vitrinite + % Exinite + % Inertinite + % Mineral Matter = 100

b). Mineral Matter Free Basis (mmf):

% Vitrinite + % Exinite + % Inertinite = 100

Coloured photographs in both reflected white light and fluorescence mode were taken using a Leica WILD MPS 52 system fitted to the Leitz Orthoplan Microscope with the aid of a WILD MPS 46 Photoautomat (Figure 3.11).

The microlithotype analyses on polished blocks of selected lithotypes were performed in a similar manner to maceral analyses, but a suitable 20 point graticule or a square of 50 X 50 micrometer was used. The position of the graticule inter - sections or viewed squared area with respect to maceral composition of the microlithotypes is shown in Figure 3.12, and is described as follows:

- Monomaceral : all intersections cover a single maceral; eg. vitrinite -- vitrite, inertinite -- inertite.
- Bimaceral : at least two intersections on each of the two macerals of which the microlithotypes is made up; eg. vitrinite+exinite -- clarite, vitrinite + inertinite -- inertite
- Trimaceral : at least one intersection on each of the three macerals of which the microlithotype is comprised.

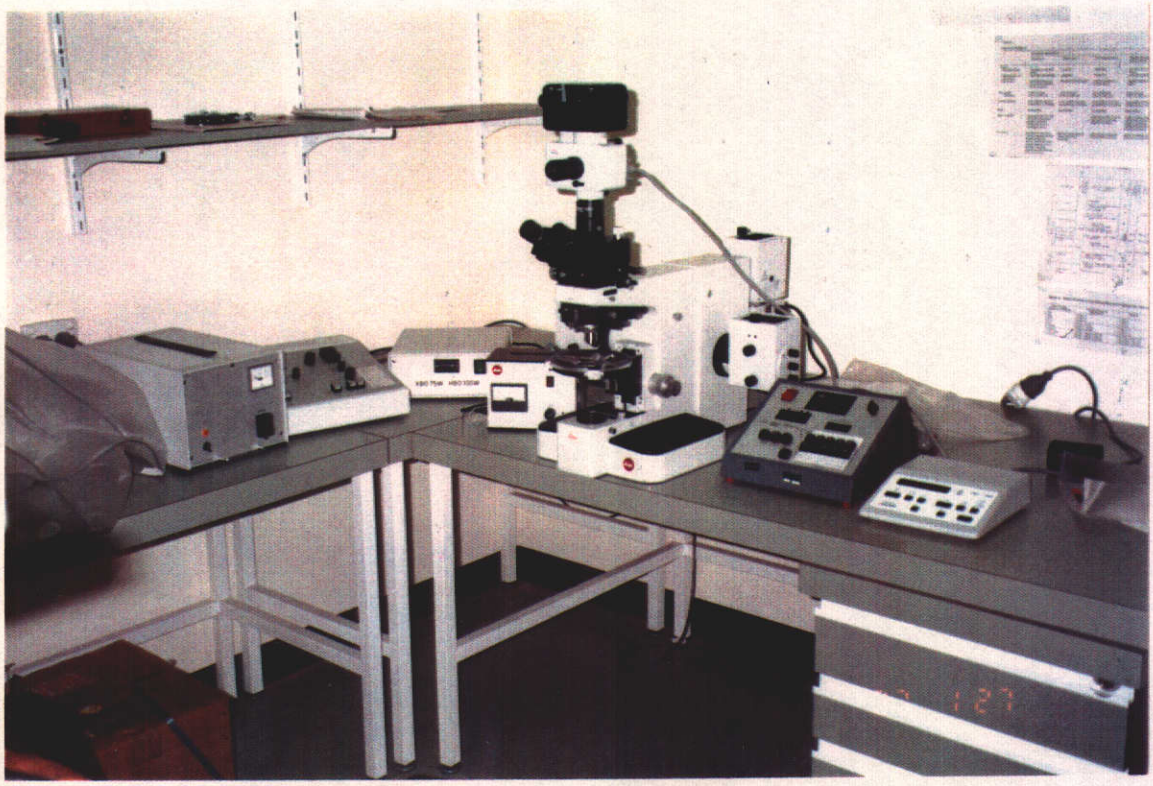

Figure 3.11. Photomicrographic equipment.

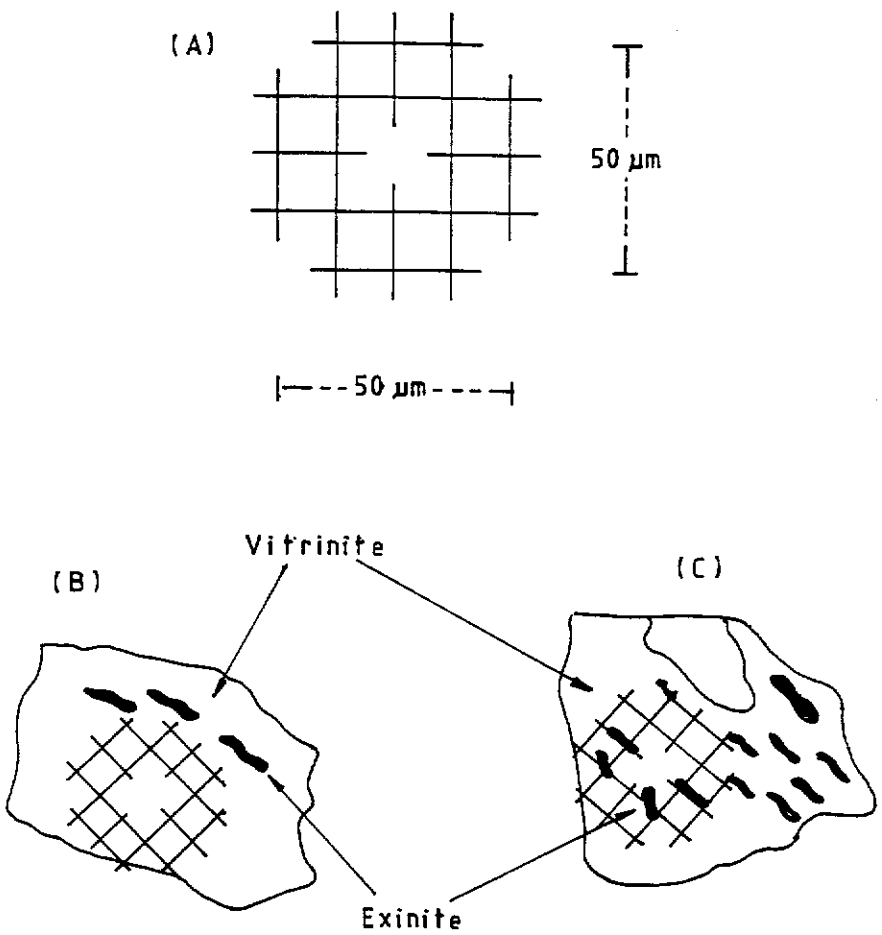

(A) 20-point graticule eye-piece

(B) Vitrite : all intersections cover a single maceral (vitrinite), ——→ monomaceral

(C) Clarite : intersections cover two maceral groups (vitrinite and exinite), each maceral 5% ——→ bimaceral

Figure 3.12. Position of 20-point graticule intersections with respect to macerals (modified from Stach *et al.* , 1982).

A complete microlithotype analysis with 500 areas have to be observed, including mineral observations. Carbominerite is identified when 4 to 12 intersections (5 - 60 %) coincide with minerals (Table 3.4).

The point counting technique of Stach *et al* . (1982) was used in the microlithotype observations. The microlithotypes were examined with plane polarised reflected light, as well as with fluorescence mode by using blue-light excitation. All microlithotypes determined are as per definitions of the International Committee on Coal Petrography, ICCP (1963 and 1971).

A whole sub-seam microlithotype composition was calculated by weighted percentages of microlithotype data, and plotted on a ternary diagram , illustrating three fields of composition, which are, vitrite+clarite, intermediates consisting of vitrinertite and trimacerite, and durite+fusite (Figure 3.13).

3.2.2.3. Reflectance Measurements

Reflectance measurements performed on vitrinite were carried out according to the Australian Standard AS 2486 - 1981 Microscopical Determination of the Reflectance of Coal Macerals.

Polished sections which contain vitrinite free from scratches and relief, were selected for measurement of vitrinite reflectance. The measurements were performed only on vitrinite A in accordance with Brown *et al.* (1961), and carried out using a Leitz MPV 1 micro photometer (Figure 3.10) fitted to a Leitz Orthoplan microscope with a 50X objective and 10X eyepiece lens. Oil immersion with a refractive index of 1.518 at 23°$\pm$ 1° C was used. A synthetic standard of 0.576 % reflectance was used for calibration. Random and maximum reflectance measurements were carried out using

Table 3.4. Summary of carbominerite composition (after Falcon and Snyman, 1983).

Association of coal with a specific mineral or mineral group	Composition	Collective term for imprecisely designated coal-mineral association
Carbargillite	Coal + 20-60 % clay minerals	Carbominerites
Carbosilicate	Coal + 20-60 % quartz	
Carbopyrite	Coal + 5-20 % sulphides	
Carbankerite	Coal + 20-60 % carbonates	
Carbopolyminerites	Coal + 20-60 % mineral matter	

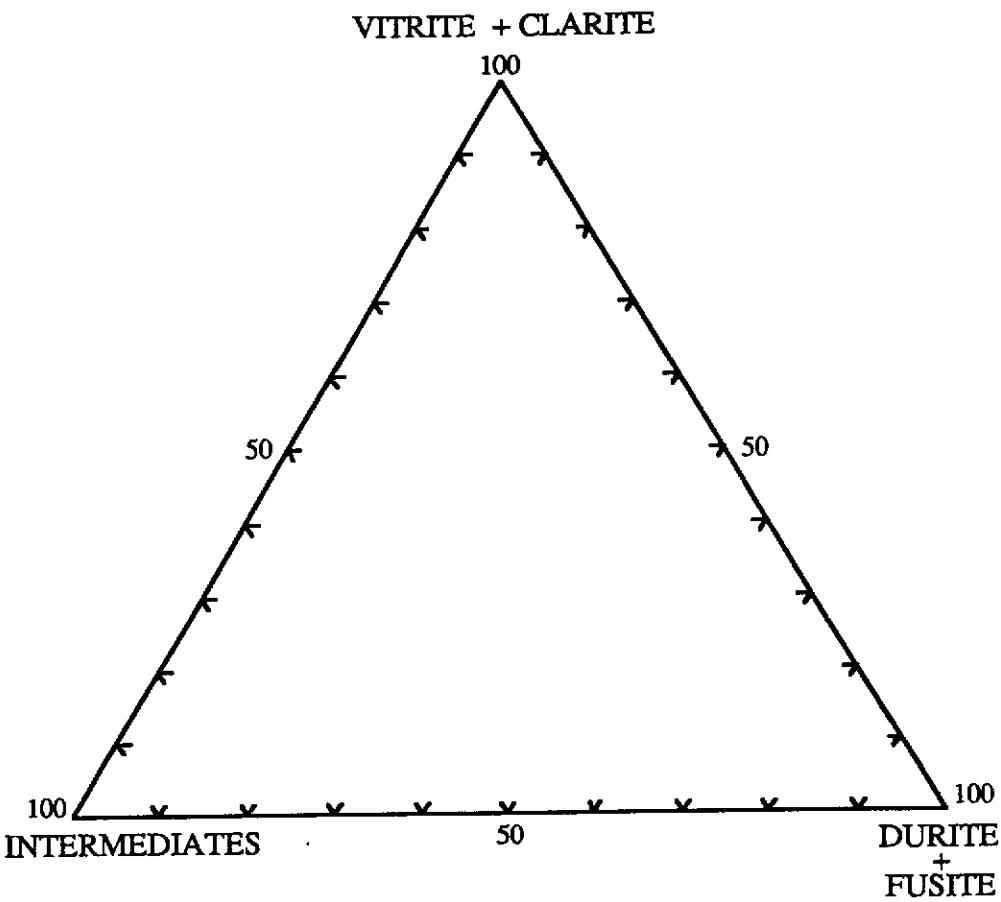

Intermediates = Trimacerites + Vitrinertite

Figure 3.13. Ternary diagram of microlithotype composition of the coal (after Smyth, 1979; Stach *et al.*, 1982).

reflected light, with an interference filter that had a pass band peak at 546 nm wavelength and was placed between the measuring diaphragm and photomultiplier. Random reflectance measurements were made using non-polarised light, whereas, the maximum reflectance measurements were carried out in polarised light. The polariser was set at 45 ° and a Berek prism was used.

Prior to the commencement of reflectance measurements, the photometer was turned on for half an hour to stabilise it. After that, the photometer readout was first adjusted to 0.00 and then the reflectance of the standard was calculated and read, by focusing the view accurately on the featureless surface of the standard.

Traverse along the first line on the surface of the specimen was continued until a grain of suitable vitrinite was seen and located in the eyepiece cross-hair. The surface of the vitrinite was focused sharply to avoid measuring errors. Reflected light is then turned aside from the photometer, and the eyepieces were blocked off against incoming light.

The value of random reflectance measurement was read immediately. For maximum reflectance measurement, the stage was rotated through 360 °, and the highest value was recorded. Two maxima and two minima were recognised. Traverse of the line was continued until another suitable vitrinite grain was found.

The standard calibration was checked every 20 to 30 minutes, and also at the end of observation, to avoid misreading or mis-measurement.

A maximum of 100 measurement pairs of random reflectance (Ro_{rnd}) and standard deviation (s) were made on each sample, while maximum reflectance (Ro_{max}) was taken at a total of 30 direct measurements. Calculation of the arithmetic mean of random reflectance used the following formula (Australian Standard 2486 - 1981) :

$$Ro_{rnd} = \frac{1}{N}\sum_{N} Rn$$

where Ro_{rnd} = mean reflectance (%)

R_n = the n^{th} observed reflectance value

N = total number of reflectance measurements

The mean maximum reflectance was also calculated using the formula of Diessel :

$$Ro_{max} = Ro_{rnd} \times 1.07 - 0.01$$

Ro_{max} = mean maximum reflectance in oil immersion.

Ro_{rnd} = mean random reflectance in oil immersion.

Standard deviation, s, was calculated from the following formula:

$$s = \sqrt{\left[\sum_{N} R_N^2 - N R_{rnd}^2\right] / (N-1)}$$

The repeatability for measurement was performed to avoid measurement errors, read during observation.

3.2.2.4. Mineral Matter Analysis

In the present study, the mineral matter was examined by reflected light microscopy with the aid of fluorescence mode, to distinguish between clay minerals and exinite macerals. Furthermore, the SEM mode was used to determine the mineral matter which could not be recognised by reflected light microscopy.

An assessment of the type of mineral matter present was included in a petrographic analysis of macerals. The analysis showed the proportions of species of mineral matter (eg. clay, quartz, pyrite) visible under the microscope. Many occurrences of

mineral matter in coal were not recognised by optical examination, due to their small size, low reflectance or intimate association with macerals, although it was aided by the use of fluorescence mode.

3.2.2.5. Ash, Trace Element, and Geochemical Analyses

Thirty two samples for ash content and sixteen samples of the coal for trace element analyses were prepared from six drill cores. The samples selected for analyses were then crushed in a coffee mill and sieved to obtain grains of - 60 mesh (< 250 micrometre) in size.

The determination of ash is empirical, because of the conditions of incineration that control the extent to which reaction occurs. The method used was a single furnace method as per the Australian Standard 1038, part-3, 1977. A representative of 2.5 to 5.0 mg of sample was used for the determination of the ash content. The representative sample was heated inside the furnace to 500° C for 30 minutes. The temperature was then increased to 815° C in 90 minutes. Finally, the temperature was kept at 815° C, until the mass was constant, which required three hours to obtain an incineration of the sample. The percentage (mass) of the ash was obtained by calculating the weight ratio of ash and the pre-incinerated sample. The percentage of the ash is calculated by the formula:

$$A = \frac{m3 - m4}{m2 - m1} X100\%$$

where : A = percentage of ash

m_1 = mass of dish plus cover, in grams

m_2 = mass of dish plus cover plus sample, in grams

m_3 = mass of dish plus cover plus ash, in grams

m_4 = mass of dish plus cover after ash has been brushed out, in grams

The result of ash determinations were reported to the nearest 0.1 %. Precision of the determination was obtained by repeating the analysis for three times.

Sixteen ashes of the samples were analysed for "diagnostic" trace element content, which are, B, Be, V, Cr, Mn, Co, Ni, Cu, Zn, Sr, Y, Zr, Mo, and Th. The coal samples were analysed by inductively couple plasma - optical emission spectroscopy using the G 1201 method (Perchloric, Hydrochloric and Hydrofluoric Acid Digestion); and Pb, Ga, and U using the G 1222 method (Perchloric, Hydrochloric Acid and Hydrofluoric Acid Digestion) of inductively coupled plasma - mass spectroscopy . As was detected by the GA 114 method (Perchloric Acid Digestion) of atomic absorption spectroscopy .The analyses were performed by ANALABS, in Perth, Western Australia.

Proximate and ultimate analyses of coal samples were obtained from CRAE Pty. Ltd., which were carried out as per the Australian Standards (AS 1038).

3.2.3. Scanning Electron Microscopy (SEM)

Polished section preparation for SEM examination was the same as that for the reflected light microscopy. Specimens were polished carefully with respect to the least surface relief. Strong topography affected the Back Scattered (BS) images at high magnification, so that too much relief was avoided. However, slight relief was useful for maceral identification in the Secondary Electron (SE) Image.

Carbon coating was used on each polished sample, so as to block the tendency of charging due to the interaction of the electron beam with the coal surface. The coating

of carbon was made as thin as possible, to obtain the best result with a solid state Back Scattered (BS) detector, so that the macerals were readily distinguished from mineral matter.

A gold coating was also used for some specimens, because it is ideal in the SE mode for highlighting the surface relief of the macerals. The carbon coating was done in accordance with Hamilton and Salehy (1986), who stated that carbon is the best coating material for BS work because of its low atomic number. Specimen sizes of up to 2.5 X 2.5 cm with 1 cm thick were used in the JEOL 6400 SEM instrument, with an attached computer set and the automatic camera .

The SEM analyses on selected polished sections were focused on qualitative and semi-quantitative mineral matter observations, with particular reference to pyrite and clay minerals, which could not be examined in detailed in optical microscopy. SEM with an energy dispersive X-ray analysis was carried out for the mineral matter determination and minor elements associated with the macerals.

Morphology indicated by relief or by contrasting grey level (Table 3.5), is best done by the SE mode. Exinite is darker than vitrinite, inertinite is brighter than vitrinite, while mineral matter is brighter than inertinite. Grey levels of some inertinites are equal to that of vitrinite, but these two macerals can still be distinguished by their structural differences. With the SE mode, lower accelerating voltages in the range of 15 - 20 KV were used to obtain better images of macerals and minerals.

In the BS mode, macerals were readily distinguished from mineral matter. Grey level (brightness) in the BS images of coal were used for the determination of maceral groups and mineral matter. With a higher voltage, the magnifications up to X 1000 were obtained during observations. Because shrinkage cracks can cause charging, freshly polished sections without cracks were used during examination.

Table 3.5 . Maceral and mineral matter characteristics in SEM examination (after Hamilton and Salehy, 1986).

Maceral Group	Morphology	BS Grey Level	Polishing Relief in SE Mode
Vitrinite	structureless groundmass or distinct layers	intermediate	low
Exinite	spore shapes, laminar or serriate, ovoid, elongated	low	high to low
Inertinite	cell structure	bright intermediate	very high
Mineral matter	varied	very high	moderate to very high

The specimens were not left under the strong electron beam for a long period, as the electron beam could damage the coal surface.

3.3. Terminology and Nomenclature

Petrographically, coal can be examined in terms of coal type and rank. Basically, coal type is related to the nature of peat-forming plants, which were transformed in geological time to macerals in favourable depositional environments. The coal type is expressed as lithotypes in macroscopic examination, and microlithotypes and macerals under microscopic examination. The coal rank is defined on the basis of vitrinite reflectance, which shows the position of coal in the coalification series: peat - brown coal - bituminous coal - anthracite.

The historical development of terminology and nomenclature in coal petrology are described, and the terminology and nomenclature used in the present study is emphasised.

3.3.1. Lithotypes

Macroscopic analysis is used to identify and classify the distinctive lithotypes which are present in coal. Valuable information in terms of coal composition, genesis, and physical properties can be gained from lithotype analysis. However, the macroscopic description of coal, which represents a gross indication of coal composition, cannot be used to substitute microscopic analysis, Cameron (1978). Due to the presence of finely disseminated mineral matter and fine laminations in Western Australian coal, several "dull" coals were recognised to be rich in vitrinite, Sappal (1986). Diessel (1982) reported that "dullness" in coal may be due to the content of "dry" or "wet"

type macerals and also mineral matter. The dry macerals are structured inertinites and groundmass macrinite, whereas, the wet ones include inertodetrinite, discrete macrinite, sporinite, and alginite.

Stopes (1919) and Thiessen (1920) first introduced the concept of lithologic classification of coal, on the basis of "the four visible ingredients" namely vitrain, clarain, durain and fusain. In 1954, Seyler introduced the term "lithotype" to designate the different macroscopically recognisable bands of humic coals. Lithotype nomenclature was modified by Schopf (1960), Diessel (1965), and Taylor (1967), based on relative brightness, to avoid confusion with maceral/microlithotype nomenclature. The nomenclature proposed by Diessel (1965) for Australian coal, used in this study, is given in Table 3.2.

3.3.2. Macerals

Coal is a heterogeneous substance, composed of both organic and inorganic constituents. The microscopic organic entities are described as macerals, derived from the Greek word "*macerare*". Cook and Kantsler (1982), Stach *et al.* (1982) and Roberts (1989) stated, that in general, macerals of coal vary widely in their chemical composition and physical properties. These properties depend on their precursor, that is peat, and the degree of coalification. Cohen (1973), Corvinus and Cohen (1984) and Raymond *et al.* (1986) stated that a combination of botanic and depositional factors controls petrographic composition of peat, the precursor of coal. ICCP (1963 and 1973) proposed the three main groups of macerals which are given in Table 3.6, on the basis of the Stopes and Heerlen system (1935). Based on the physical and chemical properties, macerals are described under three groups, namely vitrinite, exinite, and inertinite. Each of maceral groups is sub-divided into macerals, based primarily on optical properties , Stach *et al.* (1982). The maceral groups of the Hill

Table 3.6 . Maceral groups and their characteristics.

Group	Origin	Microscopic appearance
Vitrinite	Humified woody or cellulosic tissue	Medium grey in reflected light. In coals, generally forms groundmass for other components. Fluorescence very weak.
Exinite	Waxy or resinous material. Cuticles and spores and pollen exines. Algal bodies, phyto-plankton.	Dark grey in reflected light. Strong to intense autofluorescence in blue, violet, and ultra-violet light. Generally, as small isolated bodies.
Inertinite	Biochemically altered woody and other tissues. Chemically oxidised material-charcoal.	Pale grey, white or yellowish white in reflected light. Sometimes as isolated fragments or massive layers. More or less open cell-lumens. No fluorescence.

River coal shown in Figures 3.14 were recognised on the basis of shape, structure, colour, reflectance, and fluorescence.

Petrographic nomenclatures of ICCP (1963 and 1972), Stach *et al.*. (1982), Bustin *et al.* (1983) which defines the macerals, maceral groups, and microlithotypes, are used in this study. A compilation of this nomenclature in groups and macerals is shown in Table 3.7. A brief description of maceral groups and their macerals follows.

Vitrinite Group

The most common maceral group in most coals is vitrinite. It is derived partly from woody tissues and bark of trees, and partly from a product of the maceration of all vegetal substances during the successive stages of humification and gelification, Cook and Kantsler (1983) and Roberts (1989). Microscopically, cell structures are often recognised. The microscopic appearance is more closely linked with biochemical transformations taking place during coalification. The significant property of vitrinite is its ability to contribute to the rank parameter of coal. The vitrinite group consists of five macerals, namely telinite, telocollinite, desmocollinite, corpocollinite, and vitrodetrinite.

Brown *et al.* (1964) separated the structured vitrinite macerals from the unstructured or degraded vitrinites accordingly. Vitrinite A consists mainly of the macerals telinite and telocollinite, derived from xylem and cortex tissues. Vitrinite B, which is often associated intimately with other macerals, is composed mainly of desmocollinite, rare corpocollinite, and very rare vitrodetrinite. The reflectance of vitrinite A is higher than that of vitrinite B of the same coal.

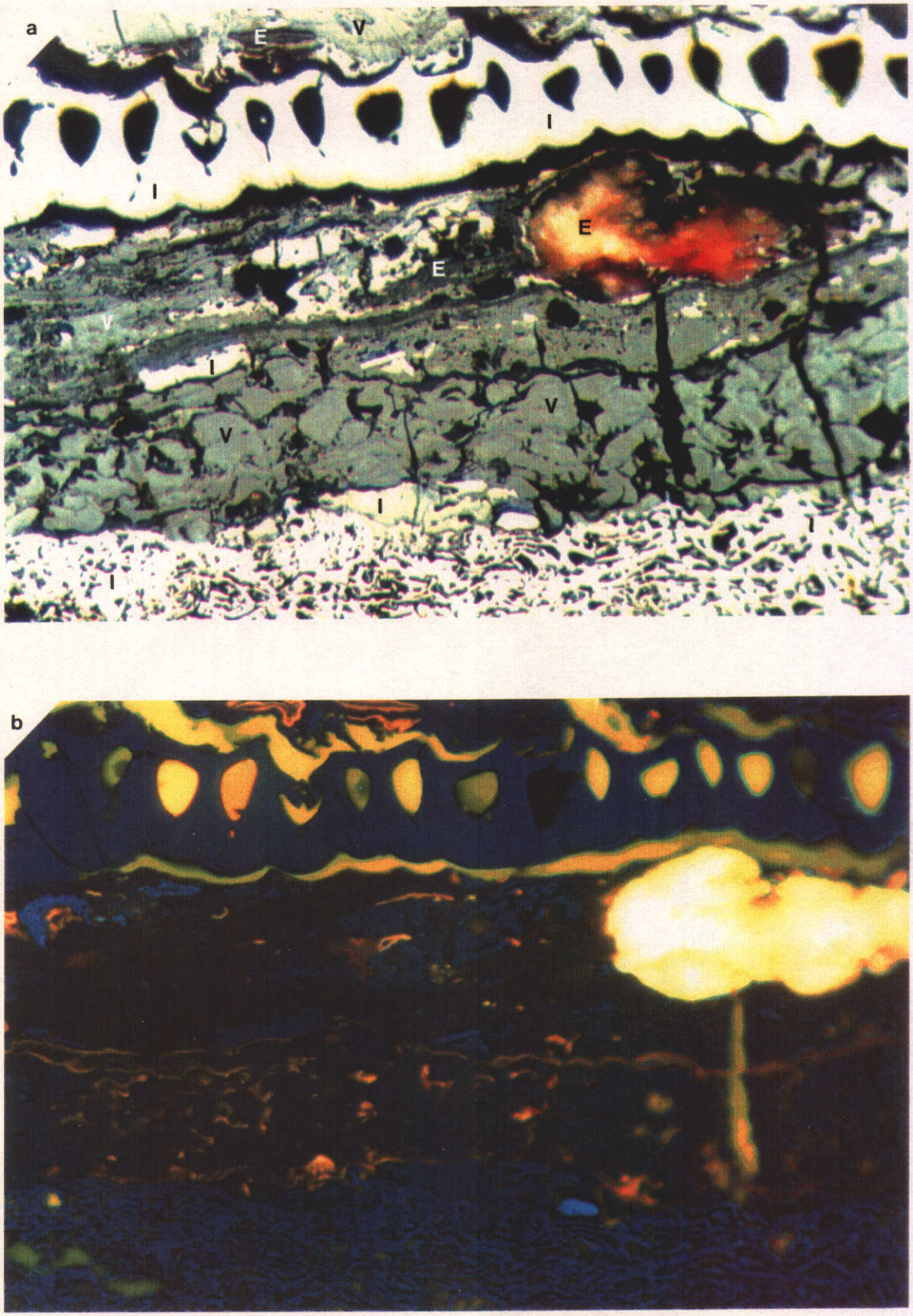

Figure 3.14. Maceral groups of sub-seam G2 of drill core CPCH 1, Hill River coal. Vitrinite (V), Inertinite (I), and Exinite (E).
(a) Reflected light (b) Fluorescence mode
(Oil immersion), X 320.

Table 3.7. Maceral groups & macerals and their characteristics.

Maceral group	Maceral	Characteristics
Vitrinite	Telinite	Well-preserved cellular structure
	Telocollinite	Homogeneous structureless
	Desmocollinite	Fragmentary groundmass forming thin layers of collinite
	Corpocollinite	Homogeneous detrital circular or oval bodies
	Vitrodetrinite	Fragmentary detrital angular pieces
Exinite	Resinite	Secondary cell-filling, layers or dispersed, often zonation and internal reflection
	Sporinite	Individual bodies or fossil form, with distinct cell walls, high relief
	Cutinite	Bands, which may have serrated edges, high relief
	Alginite	Individual bodies or colonies of fossil form, high relief
	Liptodetrinite	Fragmental/finely detrital nature of exinite
Inertinite	Semifusinite	Cellular structure, reflectance between vitrinite and fusinite, smaller cell lumina often closed, often cloudy appearance
	Fusinite	Empty or mineral filled cellular structure. Cell structure ususally well preserved; high reflectance, thin cell walls, "bogen structure"
	Macrinite	Amorphous bodies or irregular shape, high reflectance
	Sclerotinite	Cellular structure, fossil form
	Micrinite	Granular grounded grains, ca. <1 micron
	Inertodetrinite	Fragments of other inertinitic macerals (normally < 30 microns)
Mineral matter	Clay, pyrite and other minerals	

Telinite

Telinite shows the cellular network of various vegetal tissues. Telinite is partly derived from cellulosic tissues and moreover from parenchyma, with the regular geometry of rectangular cells. The cell lumens may be empty or filled with collinite, resinite and various exinites .

Telocollinite

Telocollinite is unstructured vitrinite, showing homogeneous substance in reflected light with uniform reflectance . According to Alpern (1971 a), some telocollinite is seen to be structured after irradiation by radioactive minerals or exposure to chemical substances.

Desmocollinite

Desmocollinite is present as clusters of fine vitrinitic particles in coal and is fairly homogeneous in reflected white light. Desmocollinite has a lower reflectance in comparison to telinite and telocollinite, because of the original composition which is richer in cellulose.

Corpocollinite

This maceral occurs as oval-shaped cellular-sized bodies which filled the vegetal cells, Roberts (1989). Its reflectance is similar to that of the telinitic walls enclosing it. This maceral originated either from (oxidised) resinites, or, more commonly, from secretions of tannins or phlobaphenes. Corpocollinite occurs mostly in roots or barks where tannins are located.

Vitrodetrinite

Vitrodetrinite is detritus of vitrinite occurring as fragments in coal. This maceral mostly originates from plants or humic - peat particles which were degraded at an early stage of coalification.

Exinite (Liptinite) Group

The term exinite was firstly used by Stopes (1935) for the coal constituents represented by the spore exines. Ammosov (1956) introduced the term liptinite as a substitute for exinite.

Strong fluorescence but weak reflectance relative to macerals of the vitrinite and inertinite groups, is the characteristic feature of the exinite group of macerals. In principle, all exinites display varying degrees of fluorescent colours, when they are irradiated with UV light. This characteristic can be used to distinguish exinite from other maceral groups, especially from low reflecting mineral matter such as clay minerals. The fluorescent colour changes with increasing rank, Roberts (1989), Cook and Kantsler (1982) and Stach *et al.* (1982).

The exinite derived from hydrogen-rich plant organs, algal and bacterial remains, is classified into three main sub-groups:

a). Macerals originate from "leaf" secretions or of secretions of various plant parts, essentially tissues from chlorophyllian parenchymes, such as cutinite.

b). Macerals correspond to vegetal reproductive organs, ie. resinite and sporinite.

c). Macerals originate from aliphatic-rich membranes of lower organisms, such as alginite

Brief description of individual macerals of the exinite group follows.

Cutinite

It forms a layer that protects superficial parenchymes of plants against desiccation. This maceral has a very characteristic morphology which mean it is easily recognised in any rank of coal. Cutinite is very resistant to chemical and biological attack, so that it sometimes form natural concentrations, following destruction of cellulose or other

tissue constituents. Cutin, a precursor of cutinite, is formed from glycerol esters and highly polymerised fatty acids. It is easily visible in fluorescence with green to yellow coloration in low ranks, and orange to yellow and red in higher rank of coal. The intense coloration emphasis its structure.

Resinite

This maceral corresponds to all the vegetal secretions. Its name is taken from *resin* , which is the product of a rather vascular metabolism, and more developed in the resinous gymnosperms than in angiosperms (Roberts, 1989). Its fluorescence is green to greenish yellow in the low rank coal, and changes to orange-yellow in sub bituminous coals.

According to Roberts (1989), resinite originated principally from two main types of vegetal wax secretions, and these are :

a). Gymnosperms .

b). Angiosperms.

Sporinite

Sporinite represents the reproductive elements of plants and especially of higher plants. This maceral is spherical in shape, and usually flattened, which is due to rapid disappearances of its cellulosic "intine" (inner wall) of spores. Only the outer wall "exine" is preserved. The fluorescence colour of sporinite varies between yellow to greenish and brownish yellow in coals of low to medium rank. On the basis of its size, sporinite may be divided into :

a). Megasporinite which is more than 0.2 mm in length, and is related to giant *Lepidodendron.*

b). Microsporinite of 10 to 200 micrometers in size. It includes cryptogam spores and phanerogam pollen grains. Based on the thickness of its wall, there are two types

of microsporinite, *tenuisporinite* (thin wall) and *crassisporinite* (thick wall) (Stach *et al.*, 1982).

Alginite

It originated from algal matter of non-vascular plants. In fluorescence mode, it shows yellowish -brownish colour. Hutton et al . (1980), Sherwood and Cook (1984) and Cook and Sherwood (1985) proposed the subdivision of alginite into two types:

a). Telalginite represents structured alginite, including the main genera of unicellular and colonial algae.

b). Lamalginite exists as structureless alginite and often occurs in lamellae.

Liptodetrinite

The maceral includes all constituents of the exinite group, which can no longer be accurately identified, because of the finely detrital nature. It occurs as small size particles. Liptodetrinite is easily identified in the fluorescence mode. This maceral originated from either mechanical disintegration of exinite, or chemical-microbiological decompositional fractions, Cook and Kantsler (1982). Liptodetrinites are abundant in subaquatic coals, such as sapropelic coals, certain clarites, durites and trimacerites, Teichmuller (1989).

Inertinite Group

Inertinite like vitrinite, is a significant component of most coals. It is characterised by its higher reflectance compared with other maceral groups and also by its inability ("inertia") to swell and melt in the coking process, Bustin *et al.* (1983). All inertinites are totally devoid of fluorescence in blue light excitation. On the basis of morphology, reflectance and origin, this maceral group is sub-divided into six macerals (Table 3.7).

The term inertinite is derived from the "lack of plasticity shown by the macerals when coals of bituminous rank are carbonised", Cook and Kantsler (1982). In other word, during carbonisation, inertinite does not soften. Most inertinite was formed by the alteration of humic matter during the peat stage, either by charring or biochemical activity (fungi and bacteria). However, some inertinite was of primary origin, such as fungal sclerotinite and primary fusinite.

The main maceral varieties of inertinite correspond to vegetal tissues, which, in the most part, have been submitted to a pre-burial aerobic alteration affecting their main properties. The cellular or vascular structures have been preserved quite well in fusinite and semifusinite.

Fusinite

Fusinite is the most conspicuous maceral, because of its clear cellular and vascular structures, often with very thin walls. The geometrical honeycomb shapes or the accumulation of fragments of cellular walls have a high reflectance (Ro) and white to yellow-white coloration in reflected white light microscopy. Four varieties of fusinite, according to their mode of generation are :

a). Primary fusinite directly generated by plants (sclerenchyma of some barks, plectenchyme of fungi).

b). Pyrofusinite which is a natural charcoal, originating from forest or peat-bog fires.

c). Degradofusinite or oxyfusinite which shows less thin structures. This is due to a biochemical shallow or deep degradation.

d). Rank fusinite, a transformation of some cellulosic cell walls preserved from sub aerial alteration by a natural lipidic protection (waxes, resins) during coalification.

Teichmüller (1989) recognised two types of inertinite based on cell structure :

a). Pyrofusinite and pyro-semifusinite which are partly formed by charring of plant material or peat, due to fires in coal swamp, and show preserved cell structures.

b). Degradofusinite and degrado-semifusinite which are characterised by poorly preserved cell structures. They are presumed to be a product of mouldering, oxidation and dehydration.

Semifusinite

This maceral is very similar to fusinite but its properties represent intermediate characters between those of vitrinite and fusinite. It is commonly related to the "degradofusinite" form due to its less well preserved structures.

Macrinite

This maceral occur as a homogeneous fraction of unstructured inertinites. Sometimes, it is the only representative of the group generally associated with exinite and semifusinite, Stach and Alpern (1966).

Inertodetrinite

Inertodetrinite is inertinite that cannot be classified with fusinite or semifusinite, Cook and Kantsler (1982), Roberts (1989), and Stach *et al* . (1982). Inertodetrinite is heterogeneous and made up of islands of small particles lacking cell structure, and considered to have been resulted from the breakage of any of inertinite macerals which were formed before burial stage. Its reflectance is similar to semifusinite.

Sclerotinite

This maceral is mostly of fungal origin with possibly two variations:

a). Exclusively derived from fungal remains which occur as a sub spherical sclerotic shape (reproductive organ) or tissue derived from the plectenchyme (hyphae, mycelium) of fungi, forming an irregular network.

b). Fungal remains of sclerotia and plectenchyme which are more frequently circular (spherical) in shape due to fusinisation or oxidation of small droplets of secretions,

resins, and tannins. The reflectance (Ro) is high in comparison to other macerals of inertinite group.

3.3.3. Macerals and Coal Classification

The type of coal may be determined by the proportions of the maceral groups and the term "coal type" was proposed firstly by White (1909); and was adopted subsequently by Thiessen (1931). Based on the maceral composition, van Krevelen (1954) proposed a scheme of coal classification and codification, and thus the petrographic analysis of coals is represented by a three-figure code number designating vitrinite, exinite and inertinite contents, while the coal rank is expressed as an index to the vitrinite code number.

Alpern (1979 a, b; 1981) proposed the usage of macerals, vitrinite reflectance and ash content for defining coal type, coal rank, and coal facies, respectively. Furthermore, Alpern *et al.* (1988) stated that the Alpern - ICCP classification could be used for qualifying Gondwana coals from various basins.

A new classification and codification system of coals, was proposed by Uribe and Perez (1985). It was based mainly on vitrinite and exinite contents, and reflectance of vitrinite obtained from petrographic study. This classification was supported by qualifying parameters obtained from volatile matter content for anthracitic coals, maximum dilatation for semi-anthracites and bituminous coals, and calorific value for sub-bituminous coals and lignites.

Sappal (1986) classified Permian Collie coal on the basis of vitrinite content and the maximum reflectance of vitrinite; eg. the "043" means the reflectance of vitrinite is

between 0.4 % and 0.5 %, and the value of vitrinite content lies between 30 % and 39 %. The maximum reflectance of vitrinite is plotted against the vitrinite content.

Sen (1992) proposed a classification of coal based on vitrinite and exinite contents (mineral matter free basis) of coal. Table 3.8 shows the detailed characteristics of the parameters used in the Sen's classification. A three-figure code for each coal can be expressed, ie. the "404" petrographic code number, shows that this coal contains a vitrinite content of group 4 (55.0 - 45.1 %), exinite content of group "0" (0 - 0.9 %), and a reflectance value of group 4 (RO max : 1.40 - 1.11 %). This classification and codification can be used for defining the coal category used in industrial application and usage. The coal classification developed by Sappal (1986) and Sen (1992) is used in the present study, to classify Hill River coal.

are these both the same ?

Macerals and depositional environment

The maceral compositions obtained from petrographic data have been used as a basis for the interpretation of depositional environment by a number of coal petrologists including Teichmüller (1962), Hacquebard (1969), Smyth (1974, 1984), Cook (1975, 1982), Diessel (1982, 1986), Hunt (1982), Stach *et al.* (1982),Bustin *et al.* (1983), Lamberson *et al.* (1989), Marchioni and Kalkreuth (1991), and Kalkreuth *et al.* (1991). In this study, petrographic indices, calculated from the diagnostic maceral compositions are used as parameters in interpretation of the depositional environment of coal. These petrographic indices include semifusinite ratio, wood ratio, inert ratio, gelification index, and tissue preservation index.

Diessel (1982) used diagnostic macerals as palaeoenvironment indicators and compared the diagnostic macerals to the remaining macerals. Macerals such as, telinite, telocollinite, semifusinite, fusinite, inertodetrinite, alginite, and sporinite are

Table 3.8. Characteristics of the parameters of Sen's coal classification (after Sen, 1992)

Group Number	Vitrinite		Exinite		Reflectance (% RO max)
	Type	Content (%)	Genera	Content (%)	
9	Per-vitrinous (A)	> 95 %			> 3.00
8	Per-vitrinous (B)	95.0 - 85.1			3.00 - 2.51
7	Meta-vitrinous (A)	85.0 - 75.1	Per-exinous (C)	> 25 %	2.50 - 2.11
6	Meta-vitrinous (B)	75.0 - 65.1	Per-exinous (B)	25.0 - 20.1	2.10 - 1.71
5	Ortho-vitrinous (A)	65.0 - 55.1	Per-exinous (A)	20.0 - 15.1	1.70 - 1.41
4	Ortho-vitrinous (B)	55.0 - 45.1	Ortho-exinous (B)	15.0 - 10.1	1.40 - 1.11
3	Para-vitrinous (A)	45.0 - 35.1	Ortho-exinous (A)	10.0 - 5.1	1.10 - 0.81
2	Para-vitrinous (B)	35.0 - 25.1	Para-exinous	5.0 - 2.6	0.80 - 0.51
1	Sub-vitrinous (A)	25.0 - 15.1	Sub-exinous	2.5 - 1.0	0.50 - 0.20
0	Sub-vitrinous (B)	15.0 - 5.1	Non-exinous	0.9 - 0.0	< 0.20

considered as facies diagnostics. Telinite and telocollinite are derived from partially gelified woody tissues, formed in relatively high moisture conditions. The structured inertinite macerals (fusinite and semifusinite) originate from woody vegetation, but under relatively dry oxidising conditions. Inertodetrinite is derived from the disintegration of structured inertinites, and has the same origin as fusinite and semifusinite. Sporinites transported to the limno-telmatic or limnic zones, were produced from several areas of the swamp, while alginite precursor, that is algae, occurred in a sub-aqueous environment.

Two separate ternary facies diagrams were used to compare the diagnostic macerals to the remaining ones, as shown in Figure 3.15. The first one (WDR triangle), is prepared by grouping the macerals as follows:

- W (woody) = Telinite + Telocollinite + Semifusinite + Fusinite
- D (dispersed) = Alginite + Sporinite + Inertodetrinite
- R (remainder) = Other macerals (principally desmocollinite)

Coal containing diagnostic macerals, W+D, < 50 % are referred to as a " mixed facies" type which have probably resulted from a rather mixed coal forming environment without a strong tendency towards either forest moor or limnic conditions. These are plotted on WDR triangle.

Coal with a diagnostic maceral(W+D) content of around or > 50.0 % is the plotted on the TFD triangle. The combination of the macerals are modified from the first ternary diagram, and the TFD triangle consists of the macerals expressed as follows:

- T (telinite) = Telinite + Telocollinite
- F (fusinite) = Fusinite + Semifusinite
- D (dispersed) = Alginite + Sporinite + Inertodetrinite

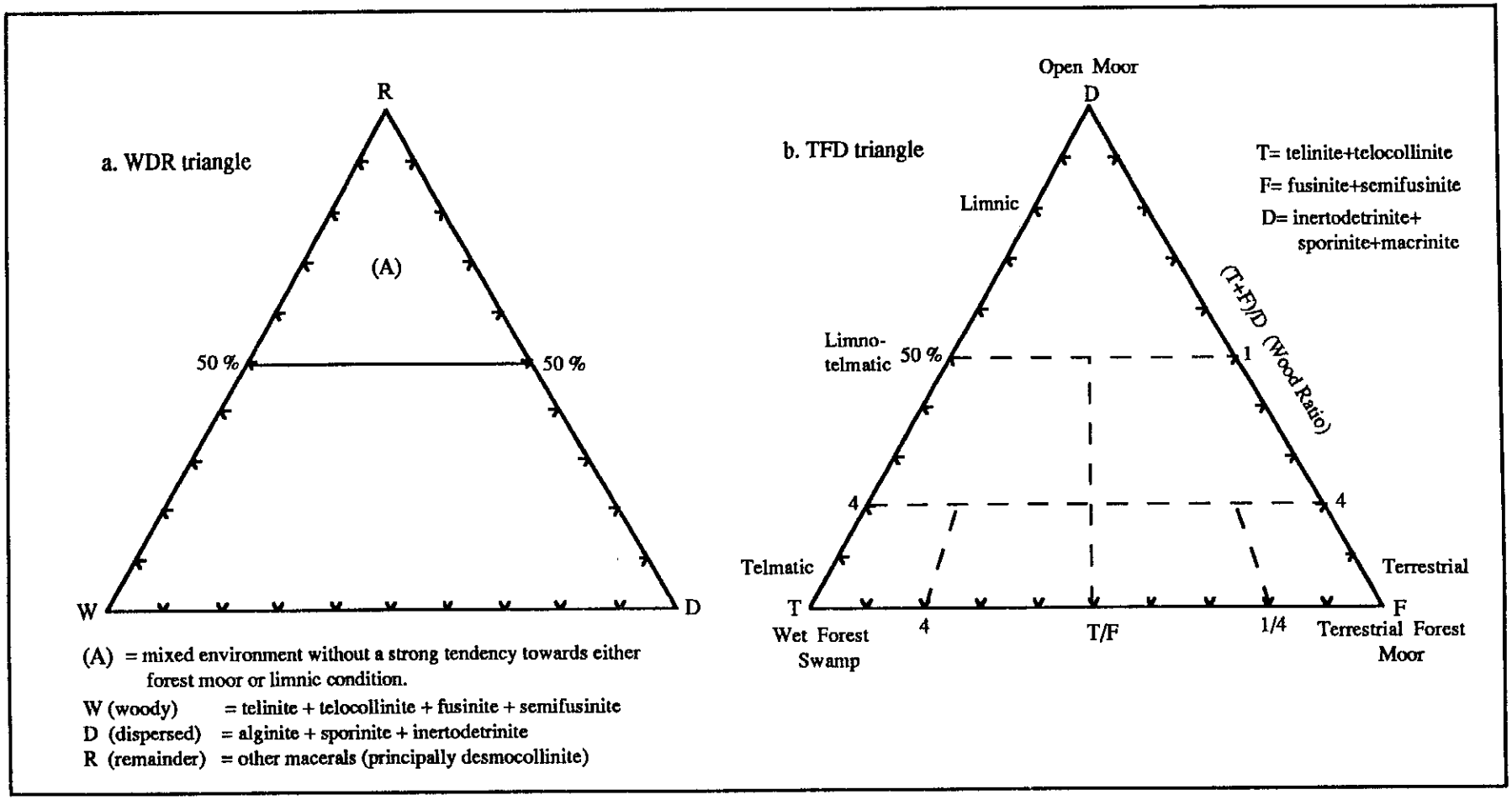

Figure 3.15. Ternary facies diagrams (WDR and TFD) of coal (after Diessel, 1982).

In this diagram, the ratio T+F/D is termed as the "wood ratio", which indicates the degree of rich-woody tissue substances which have contributed to the coal precursor. The wood ratio (T+F/D) < 1 indicates an open moor facies, while, T+F/D > 1 is a forest moor facies. Diessel (1982) suggested that the T/F ratio expressed the degree of gelification of the woody tissue, which demonstrates a wetness for forest moors. Hence, this parameter indicates a drying trend of depositional environment. If T/F << 1, it shows a drier environment. In the study, T+F/D and T/F ratios were significant in defining compositional differences between sub-seams.

Furthermore the coal facies is interpreted from the facies diagram proposed by Diessel (1986), which is based on two petrographic indices, namely the Gelification Index (GI) and the Tissue Preservation Index (TPI) as shown in Figure 3.16. It is a modification of Diessel's earlier approach to the coal facies. Using diagnostic maceral composition, a GI is plotted against TPI, to establish a correlation between coal facies indicators and the depositional environment of coal formation.

The GI is a measure of the persistence of wet conditions and is formulated as :

$$GI = \frac{\text{vitrinite} + \text{macrinite}}{\text{semifusinite} + \text{fusinite} + \text{inertodetrinite}}$$

A decrease in the GI indicates an increase in oxidation, so that the GI is an inverted oxidation index.

The TPI is a measure of the predominance of material with remnant cellular structure over that without cellular structure, and is expressed as :

$$TPI = \frac{\text{telinite} + \text{telocollinite} + \text{semifusinite} + \text{fusinite}}{\text{desmocollinite} + \text{corpocollinite} + \text{inertodetrinite} + \text{macrinite}}$$

Higher TPI values indicate the existence of more well preserved plant tissue, and is interpreted as an increase in the percentage of arboreal vegetation (lignified tissues),

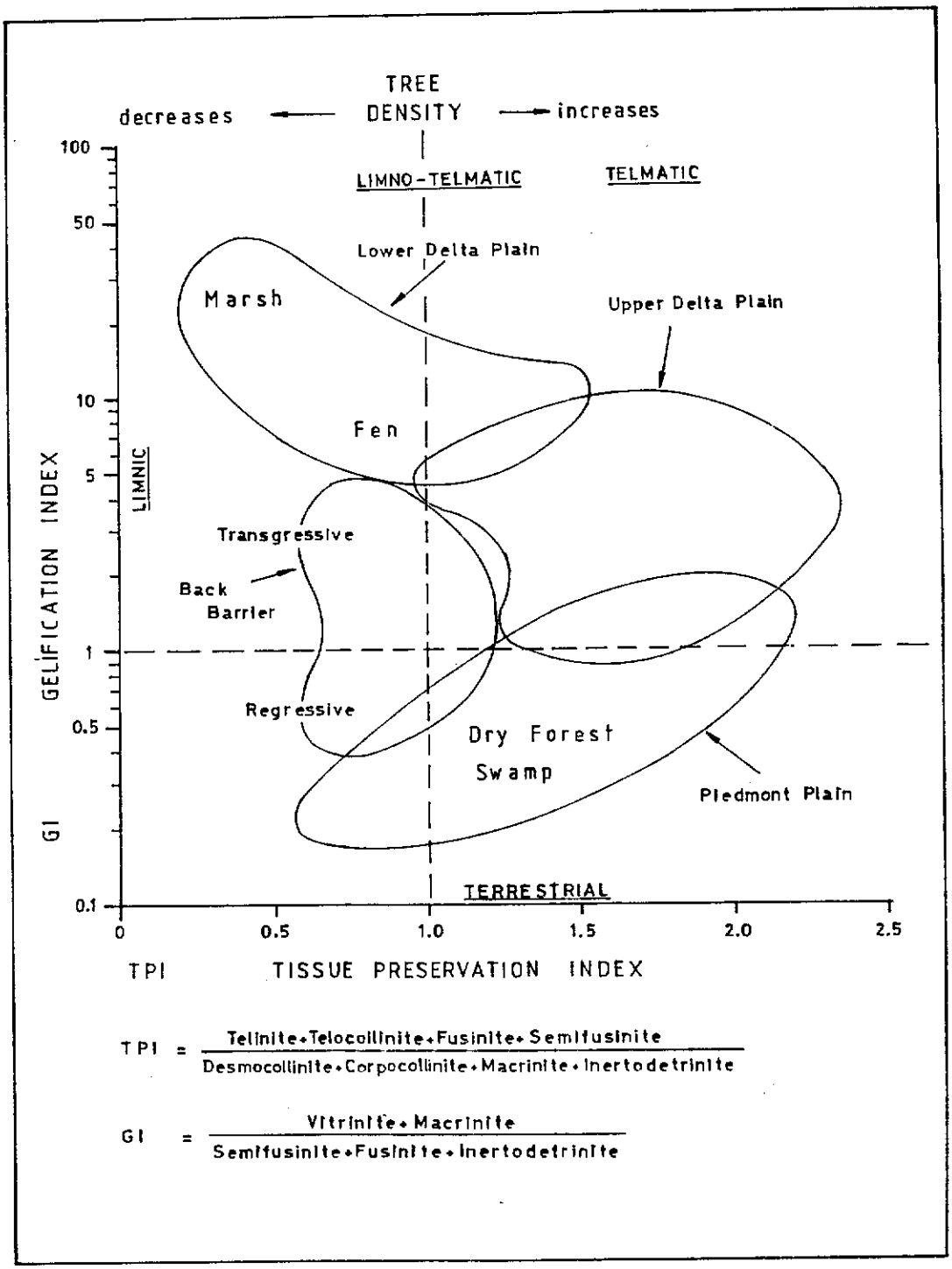

Figure 3.16. Facies diagram of coal based on GI and TPI (after Diessel, 1986 and 1992).

also the higher TPI demonstrates decomposition of peat by rapid oxidation (ie. burning conditions). Thus there is a relationship between coal facies indicator (GI and TPI) and the four main coal depositional environments, namely, lower delta plain, upper delta plain, alluvial valley, and piedmont plain (Figure 3.16). Diessel (1986) also differentiated between wet and dry forest swamps, which show an overall higher lignin/cellulose ratio (higher TPI ratio) than the marsh environments.

Facies diagrams of Diessel (1982, 1986, 1992) are used as major models in the interpretation of the depositional environment of Hill River coal, also supported by Kalkreuth (1991) to interpret mire palaeoenvironment.

3.3.4. Microlithotypes

Microlithotypes in humic coal, are defined as "typical associations of macerals with a minimum band width of 50 micrometers" , ICCP (1963). The term microlithotype was first introduced by Seyler (1954), based on characteristics of some typical association of macerals in humic coals. The suffix "-ite" is used, to distinguish microlithotype from maceral terms. Microlithotype group can be subdivided into individual microlithotypes by taking account of the maceral association. The microscopic examination of Hill River coals revealed the presence of all the microlithotype groups.

Microlithotypes demonstrate how macerals are associated with one another, Stach *et al.* (1982). Macerals in coal commonly occur in association with macerals of the same or other two maceral groups. Based on whether they contain representative macerals of one, two, or three of the maceral groups, three main groups of microlithotypes are designated as monomaceralic, bimaceralic and trimaceralic microlithotypes, Stach *et al.* (1975, 1982), Bustin *et al.* (1983), and Smyth (1990).

In addition, carbominerites comprising mixtures of various minerals and macerals are also identified.

The microlithotype classification used in this study is the one of Bustin *et al.* (1983), and Smyth (1990), expressed in Table 3.9 and Figure 3.17. During the microlithotype analysis, the so-called "5 % rule" applies, that is macerals of less than 5 % in an assemblage are neglected. A brief description of microlithotypes of coal follows.

Vitrite

This term was adopted by the I.C.C.P. in 1955 and first proposed by Potonie (1924). It consists of vitrinite occurring in bands of more than 50 microns in thickness.

Liptite

Liptite is a microlithotype, composed of exinite maceral group (sporite, cutite, algite, resite, and liptodetrite).

Inertite

The term "inertite" which is composed of inertinite maceral group, was adopted by the I.C.C.P. in 1964. In the present study, only fusite and macroite are recognised.

Clarite

It is a bimaceral microlithotype consisting of vitrinite and exinite maceral groups (Table 3.9). Macerals of both groups must account for more than 95 % of the total amount. It can be subdivided into exinite poor clarites termed as clarite-V and exinite rich clarite known as clarite-E.

Table 3.9. Microlithotype classification (after Bustin et al., 1983; Smyth, 1990).

Microlithotype	Maceral Group	Composition (mmf)	GROUP
Vitrite	Vitrinite (V)	> 95 % V	Mono-maceralic
Liptite (Sporite ((Cutite	Exinite (E)	> 95 % E	
Inertite (Fusite ((Macroite	Inertinite (I)	> 95 % I	
Clarite	Vitrinite + Exinite	> 95 % V + I	Bimaceralic
Durite	Inertinite + Exinite	> 95 % I + E	
Vitrinertite	Vitrinite + Inertinite	> 95 % V + E	
Duroclarite	Vitrinite+Exinite+Inertinite	V,E,I each>5%, VI,E	Trimaceralic
Vitrinertoliptite	Vitrinite+Exinite+Inertinite	V,E,I each>5%, EI,V	
Clarodurite	Vitrinite+Exinite+Inertinite	V,E,I each>5%, VE,I	

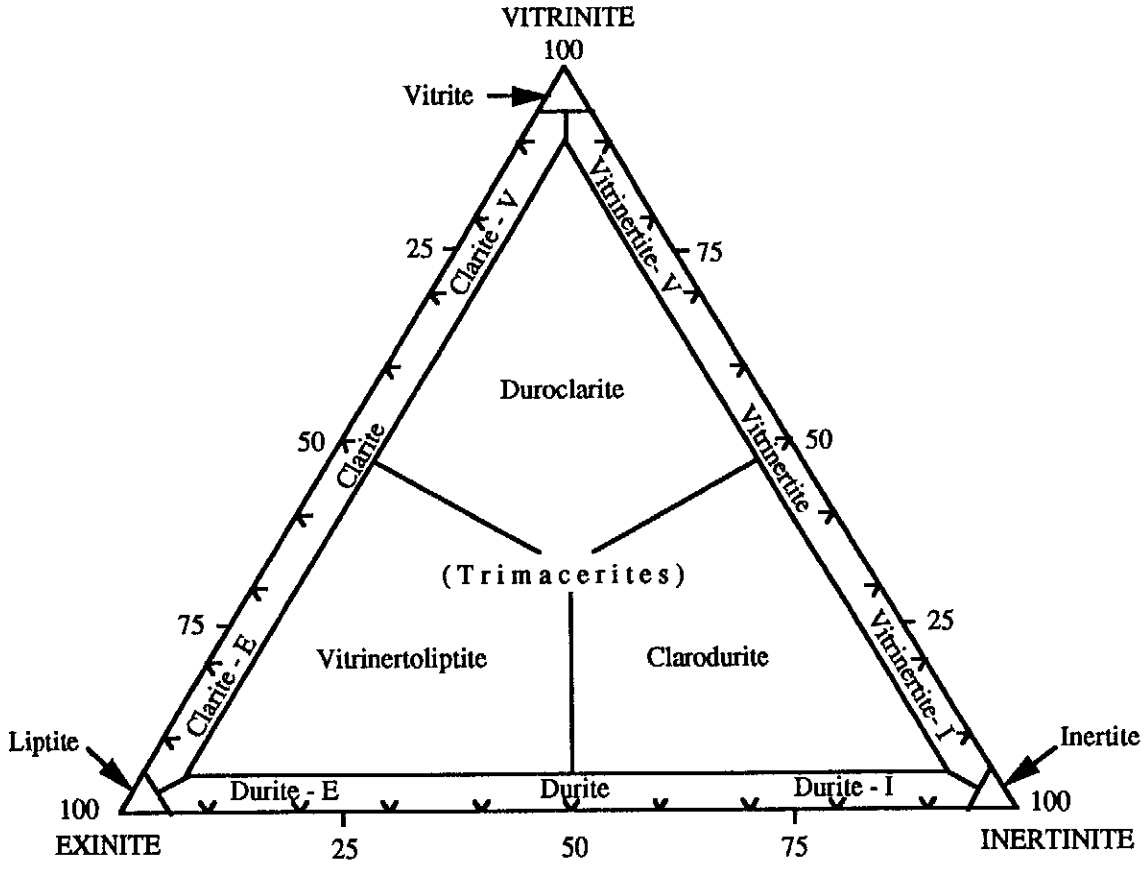

Figure 3.17. Diagrammatic classification of microlithotypes and maceral - microlithotype relationship (modified from (Bustin *et al.*, 1982).

Vitrinertite

It is derived from the term "vitrinertain" (Alpern, 1954), which was modified and adopted by the I.C.C.P. in 1955 as "vitrinertite". Microscopically, vitrinertite consists of 95 % vitrinite and inertite maceral groups. Furthermore, it can be subdivided into vitrinite-rich vitrinertite classified as vitrinertite-V and inertinite-rich vitrinertite as vitrinertite-I, (Figure 3.17).

Durite

Durite is a combination of exinite and inertinite maceral groups which together amount to at least 95 % of the total . Hill River coal shows that durite contains all macerals of the inertinite group, such as semifusinite, inertodetrinite, and fusinite. Durite containing thick-walled spores (crassisporinites) is termed as crassidurite.

Trimacerite

It was proposed by Mackowsky (1964) and accepted by the I.C.C.P. (1964), for the 50 micron band , composed of vitrinite, exinite, and inertinite maceral groups. Trimacerite contains more than 5.0 % from each of these three maceral groups. This microlithotype can be subdivided into duroclarite, clarodurite, and vitrinertoliptite, (Figure 3.17).

Duroclarite (Trimacerite-V)

It is characterised by the dominant amount of vitrinite and exinite other than inertinite. Each maceral group must be more than 5 %.

Clarodurite (Trimacerite-I)

It contains more than 5 % of each maceral group. The proportion of inertinite must exceed that of vitrinite and exinite.

Vitrinertoliptite (Trimacerite-E)

It has more exinite (liptinite) than vitrinite and inertinite. The amount of each maceral group is more than 5 %.

Carbominerite

This term was proposed by Mackowsky (1963) for the association of microlithotypes with the minerals. The mineral contents should consists of 5 - 60 % by volume. Based on the dominance of a particular mineral, five groups of carbominerite are recognised (Table 3.4).

Maceral and microlithotype analyses of a whole seam, show a relationship, which can be expressed in vitrinite and inertinite by the following formula (Smyth, 1979):

vitrinite % = vitrite %+ clarite %+ 0.5 (intermediate) %

inertinite % = inertite %+ durite % + 0.5 (intermediates) %

In 1970, Bennet and Taylor proposed a classification scheme of coal based on microlithotype analysis (vitrite % and clarite % + 0.5 intermediates %) and maximum reflectance of vitrinite in oil (Ro_{max}). They plotted the microlithotype per cent volume against the mean reflectance of vitrinite. The point which falls in the diagram, shows the category of classification. It is expressed as a three digit nomogram, ie. 084. The first two digits (08) indicate that the mean maximum reflectance of vitrinite is between 0.80 % and 0.89 %. The third digit (4) shows the proportion of (vitrite+clarite+0.5 intermediates) or of vitrinite, which lies between 40.00 % and 49.00 %.

Microlithotypes and depositional environment

Stach *et al.* (1975, 1982) used microlithotypes to interpret the depositional

environment of coal, as shown in Table 3.10. Smyth (1979) schemed a relationship between the microlithotype compositions and environmental types of coal formation, which is displayed graphically in a ternary diagram in Figure 3.18, and divided the microlithotype compositions of coal seams into the degree of oxidation before burial of the organic matter. By neglecting the small amount of exinite, she paid attention to vitrinite and inertinite maceral groups. The 50 %-vitrinite-line represents the equal proportion of vitrinite (vitrite+clarite) to inertinite (inertite+durite) amounts, or in other words, the amount of unoxidised organic matter to oxidised organic matter. The ratio of vitrinite (vitrite+clarite) to inertinite (inertite+durite) may be used as an oxidation indicator.

Coal types from different seams are concentrated in particular parts of the triangle. These concentrations suggest that the coal type is related to the environment where each seam occurs. Lakes and lower delta plains are dominated by durite+inertite -rich coals, whereas, in upper deltaic fluvial and lagoonal environments, vitrite+clarite-rich coals predominate. On the basis of microlithotype analysis, the following environmental types are interpreted:

- lacustrine (A) = lower coastal plain, plus area dominated by coal swamp
- fluvial (B)
- lagoonal (C) = channel belt plus large lake
- upper deltaic (D) = upper coastal plain
- lower deltaic (E) = area dominated by channel deposits, plus (minor) upper coastal plain

Several microlithotypes defined by the ICCP (1963, 1971) were also used in the ternary facies diagram by Marchioni (1980), and the facies diagram is similar to that of Hacquebard and Donaldson (1969), with the modified components as shown in Figure 3.19. The upper triangle represents relatively dry conditions (increasingly dry

Table 3.10. Microlithotypes and coal depositional environment (after Stach et al., 1982).

Microlithotype	Origin	Depositional environment
Vitrite	Derived from woody tissues, like stems, branches, and roots.	A forest swamp
Clarite	Decomposed forest litter (wood, bark). reeds and non-arborescent vegetation.	A forest moor
Durite	Ooze deposits	Sub-aquatic, or above water table, where extensive oxidation (and fires) occur.
Trimacerites		A forest swamp, sub-aquatic or areas of low water table and increased oxidation.

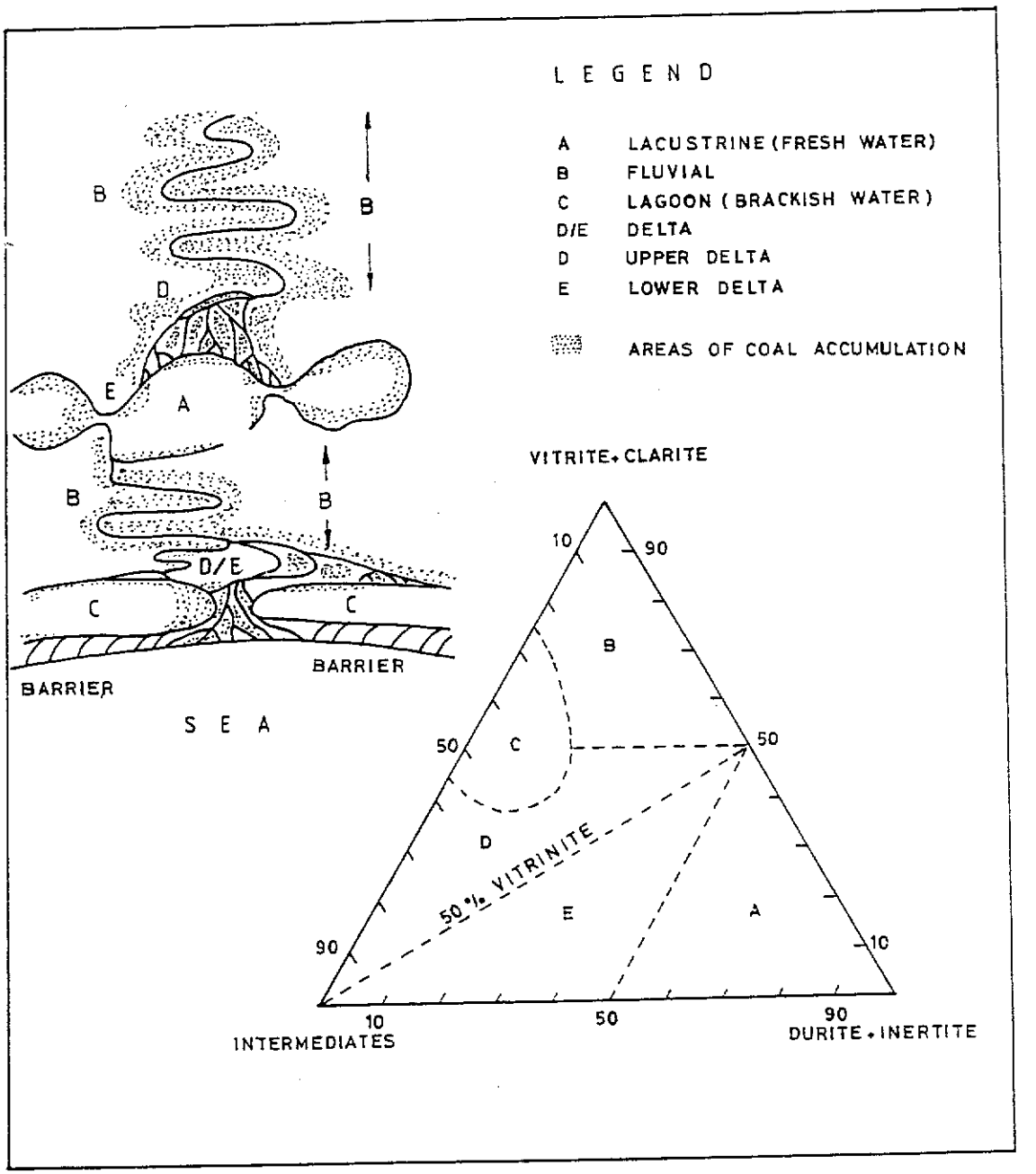

Figure 3.18. Ternary diagram of coal depositional environment, interpreted from microlithotype composition (after Smyth, 1979).

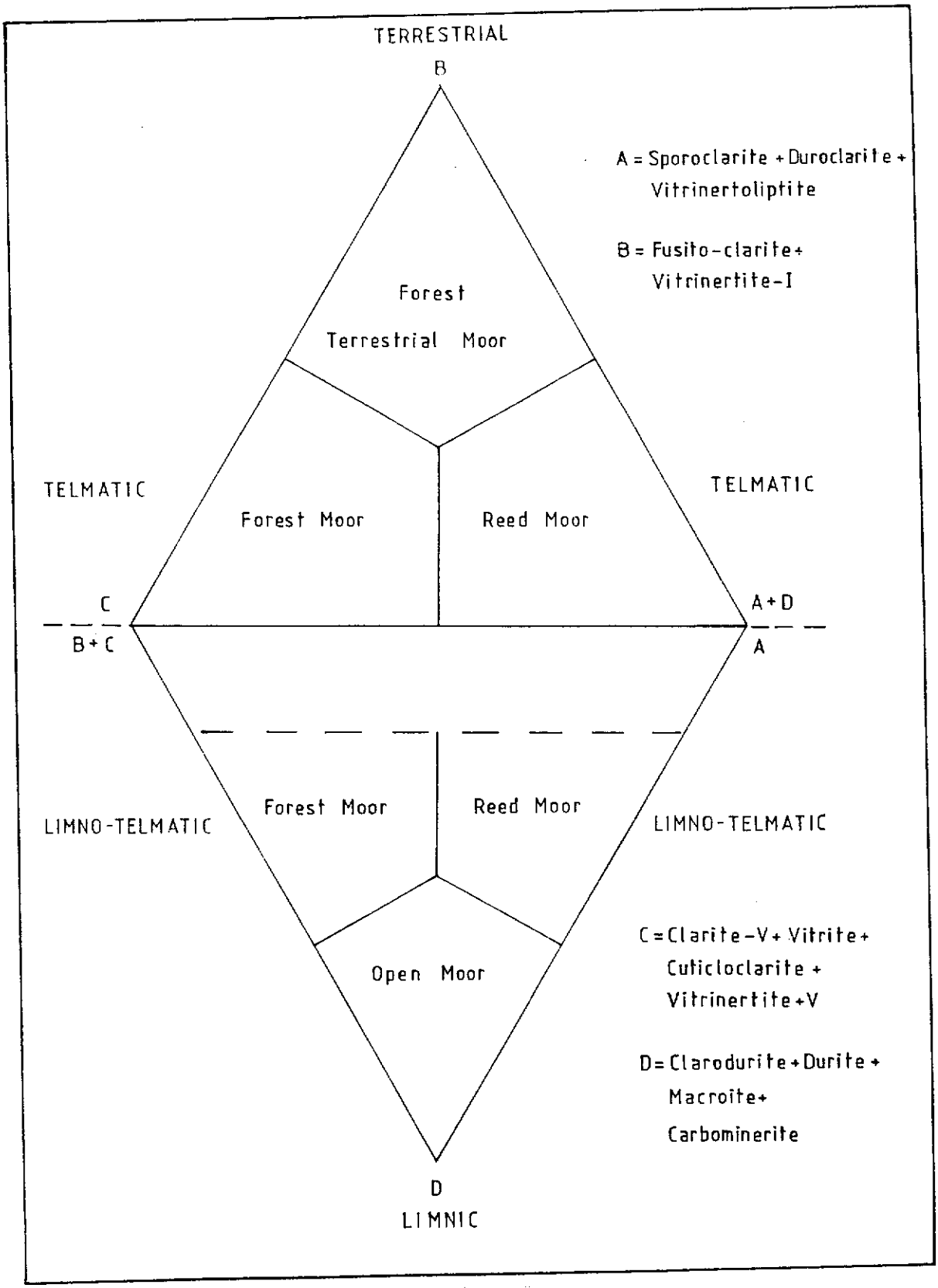

Figure 3.19. Ternary facies diagram of coal, based on microlithotype composition (after Marchioni, 1980).

towards the "terrestrial" apex), while, the lower triangle is a representative of relatively wet conditions.

In the present study, the depositional model of Smyth (1979) and Marchioni (1980) is used to interpret the depositional environment of Hill River coal based on microlithotype analysis.

3.3.5. Coal rank

"Coal rank" is a measure of coal maturity, McCartney and Teichmüller (1972), Cook and Kantsler (1982), and Bustin *et al.* (1983) which is normally assessed in terms of reflectance of vitrinite, moisture content, carbon content, volatile matter content, and specific energy. Standard systems for classification of coals by rank observations are intended mainly as guides for utilisation parameters, Jones *et al.* (1984). Rank variable is one of the more important bases of coal classification as shown in Table 3.11 and it is normally used in commercial utilisation of coal.

In the present study, vitrinite reflectance (Ro max) is used to define the coal rank, because the vitrinite reflectance method has a high degree of accuracy and precision, and can be done rapidly and inexpensively, so it is the most practical method for assessing the coal rank. In addition, moisture content, volatile matter, specific energy, and carbon content are also used to define the coal rank. McCartney and Teichmüller (1972) reported that the reflectance of vitrinite in bituminous coals with less than 30% of volatile matter, was the best single criterion of rank. According to Castano and Sparks (1974), Bustin *et al.* (1977) and Marchioni (1980), vitrinite reflectance can also be used as a rank parameter in lignite coals, but with careful selection of the vitrinite component used for measurement.

Table 3.11. Rank / classification of coal based on the maximum reflectance of vitrinite (after Cook and Kantsler, 1982).

Rank Stages	% Ro max Vitrinite	AUSTRALIA (AS) Coal class	GERMANY DIN	USA ASTM	USSR
Peat	0.2		Peat	Peat	
Brown Coal	0.3		Brown Coal: Soft	Lignite	B 1
			Brown Coal: Mat	Sub-Bituminous C	B 2
	0.4			Sub-Bituminous B	B 3
Sub-Bituminous	0.5	9		Sub-Bituminous A / High Volatile Bituminous C	D
	0.6	8	Hard Coal: Flame	High Volatile Bituminous B	G
High Volatile Bituminous	0.7	7	Hard Coal: Gas-Flame	High Volatile Bituminous A	
	0.8	6			
	0.9				
	1.0	5	Hard Coal: Gas		J
Medium Volatile Bituminous	1.2	4 B		Medium Volatile Bituminous	K
	1.5	4 A	Hard Coal: Fat		
Low Volatile Bituminous		3	Hard Coal: Ess	Low Volatile Bituminous	OS
	2.0	2	Hard Coal: Lean	Semi Anthracite	T
Semi-Anthracite	2.5				
Anthracite	3.0	1	Anthracite	Anthracite	PA
	5.0		Meta Anthracite	Meta Anthracite	A
Meta Anthracite					

CHAPTER 4. PETROGRAPHY OF COAL

4.1. Introduction

In coal petrography organic constituents of coal are described in terms of lithotypes, microlithotypes and macerals according to the International Classification of Coal, ICCP (1963). The petrographic characterisation of Hill River coal is established on cored samples from the drill cores CPCH 1, CPCH 37, CPCH 39 and CPCH 47, from the Mintaja Block and its surrounds, and also from the drill cores CPCH 57 and CPCH 60 located in the Gairdner Block, (Figure 4.1).

The coal samples from the drill hole CPCH 1 located in the Mintaja Block represent the entire core and the lithotype, microlithotype and maceral analyses were undertaken on the entire core. The samples from other holes represent only fractions of different sub-seams, and thus only maceral and microlithotype analyses had been undertaken. The lithotype, maceral and microlithotype analyses of the coal is described in this chapter. The minerals identified and their association with maceral groups is described in detail in chapter 5. Detailed discussion on the petrographic data for the interpretation of the depositional environment of the coal is presented in chapter 7.

4.2. Lithotypes (CPCH 1)

Lithotype analysis of the coal seam G and its sub-seams, Gl, G2, G3, G4, G5, and G6 from the drill hole CPCH 1, Hill River area, was completed to establish the vertical variability within the sub-seams. The coal was logged in terms of lithotypes, parting of clastic bands, and their lithology. For each sub-seam, a lithotype profile

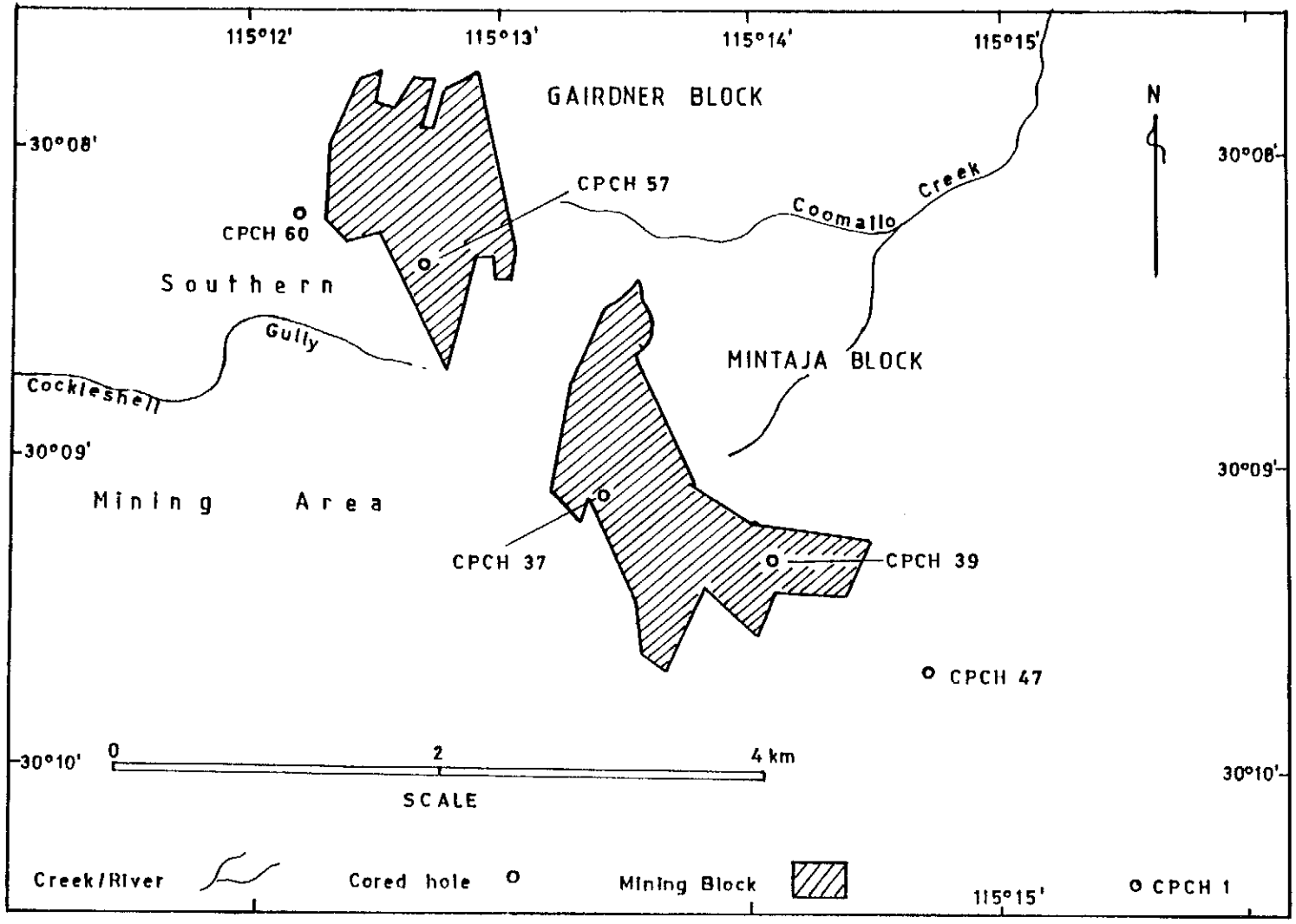

Figure 4.1. Location of drilled holes, Mintaja and Gairdner Blocks, Hill River Area.

(Figures 3.3 and 4.2) was prepared from the lithotype log. The lithotype log for the whole seam G and its sub-seams is given in Appendix 1.

Detailed macroscopic examination of coal from drill hole CPCH 1, shows that the coal is finely banded and is of intermediate lustre. Based on the terminology of Stopes (1919), the dominant proportion of coal is regarded as clarain and durain, with minor amounts of vitrain and fusain. However, according to the terminology adopted for this thesis (Table 3.3), the graphic lithotype profile shows a predominance of dull banded, banded, and dull lithotypes (Figures 3.4 and 4.2). The bright and bright banded lithotypes occur as minor components. Thin bands of fusain (fibrous coal) which are less than 1 cm thick are recognised in a relatively minor proportion in the sub-seams. However, 11 cm thick fusainous layer is recorded in the sub-seam G4.

4.2.1. Lithotype Log and Lithotype Profile

The six sub-seams of CPCH 1 are divided into 11 sub-sections (Figure 4.2), which show different trends of lithotype sequences. Dull coal type occurs in close association with a clastic band, sub-seam G3. The sub-seam G1 is subdivided into two sub-sections 1 and 2 based on lithotypes and the relatively brighter sub-section 2 grades into the duller sub-section 1. The sub-seam G2 is subdivided into four sub-sections namely 3, 4, 5, and 6. In these sub-sections the brighter lithotype grades upward into the duller ones.

The above upward grading of brighter lithotypes into duller lithotypes is also represented in the sub-seam G3 and G4 and their respective sub-sections 8 and 9. A similar trend is also indicative within the sub-section 10 of the sub-seam G5. Sub-

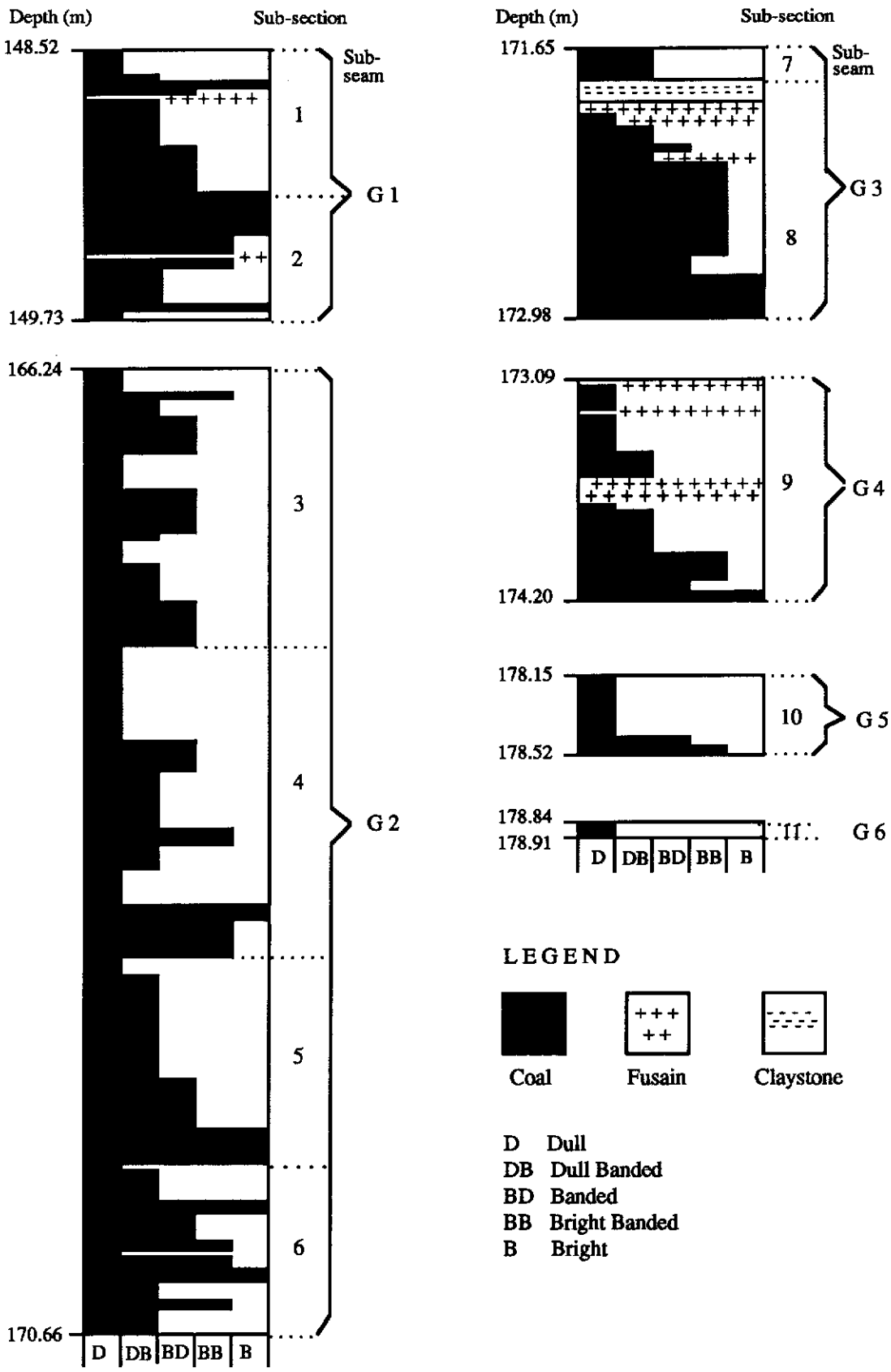

Figure 4.2. Lithotype profile of sub-seams G1 - G6, drill hole CPCH 1.

section 11 of the sub-seam G6 is relatively thin and consists only of the dull lithotype.

Tiny specks of pyrite with less than 0.5 mm dimension are present in the coal. In sub-seam G3, clastic parting of 8 cm thick claystone-siltstone is present. The lowest coal sub-seam (G6) tends to become brittle and friable with dull lustre. The coal from sub-seams G1, G2, G3, and G4, breaks with sub-conchoidal to conchoidal fracture with greasy lustre.

The upward grading of duller lithotypes from brighter ones in the profile indicate that changes in the water table had occurred during the deposition of peat, as different rates of subsidence of a mire and peat growth lead to the formation of lithotypes. Bright and bright banded types are formed due to flooding in the mire, at a relatively shallow depth. Dull coal is generally formed under somewhat deeper water, while fusain is formed under shallow water with frequent access to air at low rates of subsidence showing driest conditions and combined with fires. Based on the depth of water required for coal formation, Tasch (1960) arranged the lithotype sequence as follows:

Dry Fusain
Bright and bright banded coals
Banded coal
Dull banded and dull coals
Carbonaceous shale
Wet Inorganic sediments

The type variation in coal is associated with frequency of changes in the water table during the peat formation, as observed from the lithotype profile. A relative duration of emergence or submergence of the peat is reflected by the thickness of individual

lithotypes. However, this also depends on other factors like tectonic events, differential compaction and the rate of sedimentation.

4.2.2. Lithotype Variation

The proportions of lithotypes vary from sub-seam to sub-seam, and are given in Table 4.1 which includes the percentages of the aggregate thickness of each lithotype and clastic parting in an individual sub-seam, calculated on the basis of their proportions. The lithotype content of the individual sub-seams is also plotted in Figures 4.3 to 4.8.

The sub-seam G1 is dominated by dull banded type (Figure 4.3) consisting of rather thick coal bands, which represents 38.84 % of the sub-seam. The bright type is 19.83 % and it is the second dominant lithotype, followed by 16.53 % of the banded type. The bright banded and dull lithotypes have a similar amount of 11.57 % each. The fusainous type occurs as a very thin layer of 1 cm in thickness in the sub-seam G1. The sub-seam G2 with a total thickness of 4.42 m, has a low amount of bright coal (6.1 %), and absence of fibrous (fusain) coal, (Figure 4.4). In this sub-seam, duller lithotype predominates, and 57 % of the lithotype profile is made up of dull and dull banded types, and the bottom part of the sub-seam is sheared. The sub-seam G3 contains an 8 cm thick clastic layer, and the sub-seam is dominated by the brighter type, with 46 % being bright and bright banded lithotypes, fusainous type and clastic layer amount to 6.02 %, (Figure 4.5). In contrast, the sub-seam G4 is characterised by a high amount of fibrous fusain coal (29.69 %), (Figure 4.6). This sub-seam is dominated by the duller type, with only 11 % of the profile composed of bright and bright banded lithotypes. Dull coal predominates in sub-seam G5, with only 5.41 % made up of banded bright type. Bright, dull banded, and fusainous

Table 4.1 . Lithotype content (linear %) of the sub-seams of the drill core CPCH 1.

Sub-Seam	Thickness (m)	Bright %	Bright Banded %	Banded %	Dull Banded %	Dull %	Fusain %	Clastics %
G 1	1.21	19.83	11.57	16.53	38.84	11.57	1.66	0.00
G 2	4.42	6.10	7.92	22.40	34.61	28.97	0.00	0.00
G 3	1.33	13.53	32.33	10.52	28.57	3.01	6.02	6.02
G4	1.13	2.42	8.48	2.42	24.85	21.21	29.69	0.00
G 5	0.37	0.00	5.41	10.82	0.00	83.77	0.00	0.00
G 6	0.07	0.00	0.00	0.00	0.00	100.00	0.00	0.00

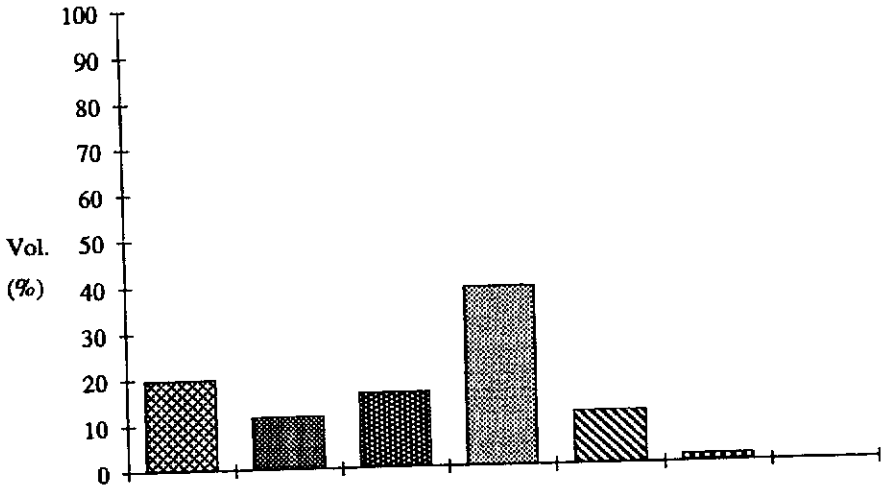

Figure 4.3. Lithotype distribution of sub-seam G 1, drill hole CPCH 1.

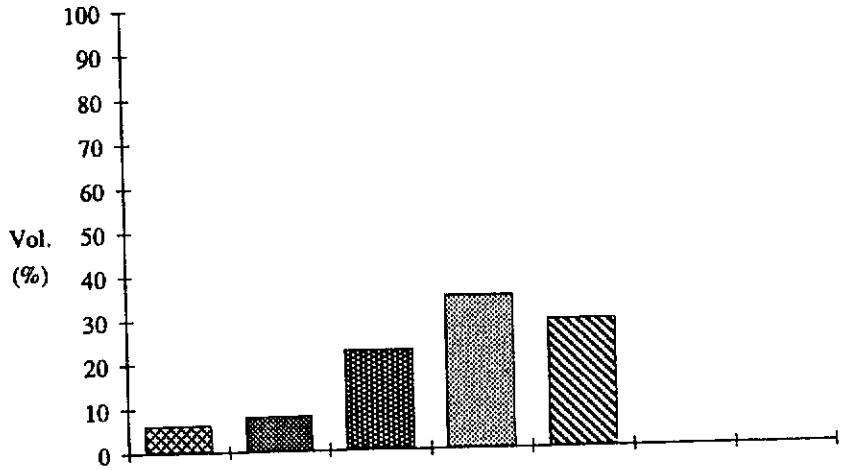

Figure 4.4. Lithotype distribution of sub-seam G 2, drill hole CPCH 1.

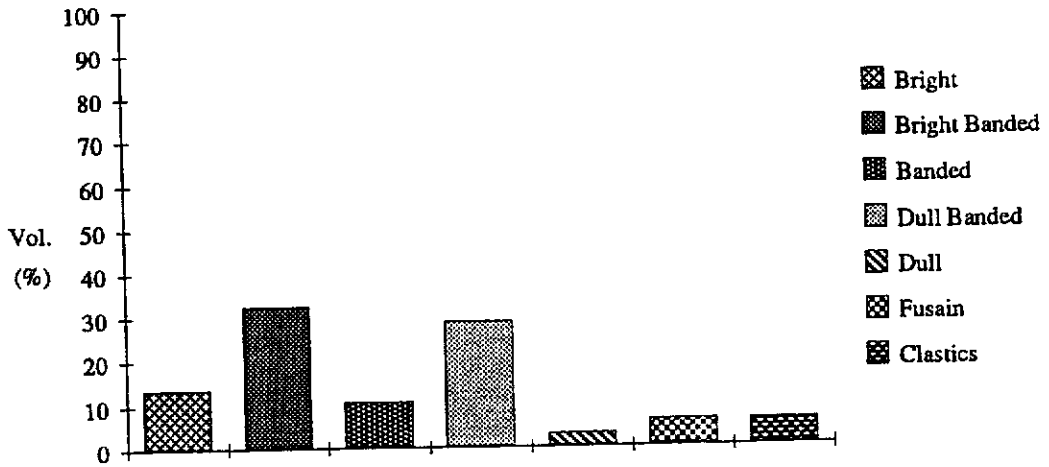

Figure 4.5. Lithotype and clastics distribution of sub-seam G3, drill hole CPCH 1.

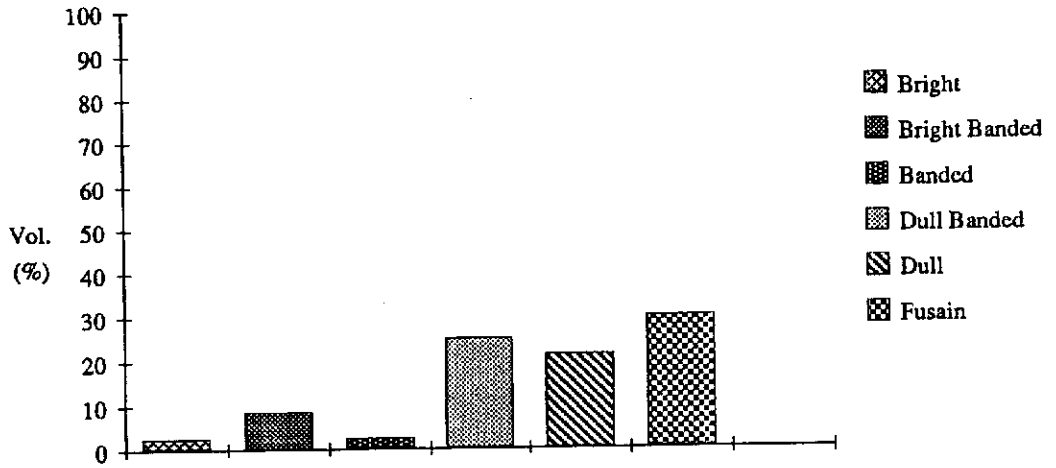

Figure 4.6. Lithotype distribution of sub-seam G 4, drill hole CPCH 1.

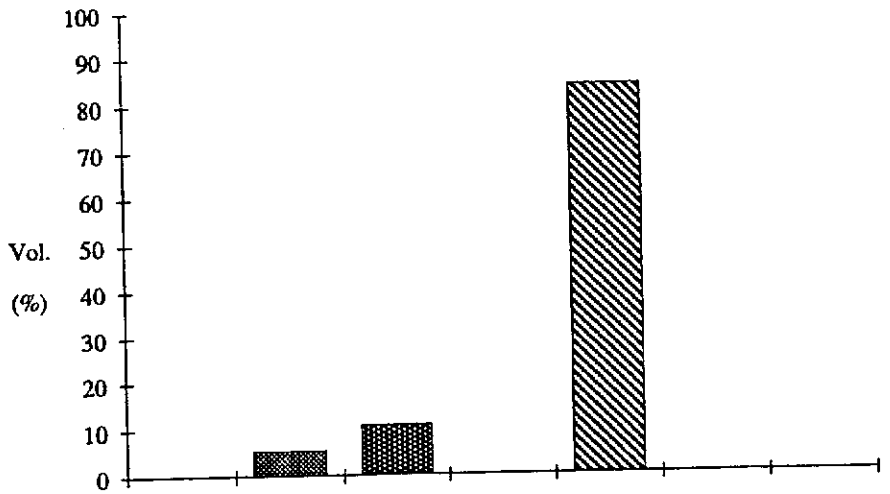

Figure 4.7. Lithotype distribution of sub-seam G 5, drill hole CPCH 1.

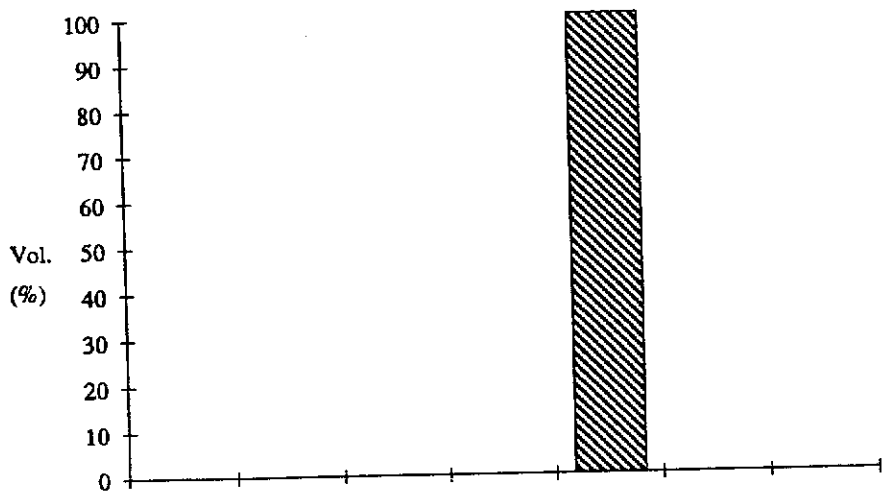

Figure 4.8. Lithotype distribution of sub-seam G 6, drill hole CPCH 1.

lithotypes are absent in this seam, (Figure 4.7). Sub-seam G6 with a thickness of 7 cm, is totally composed of friable dull lithotype, (Figure 4.8).

4.3. Maceral Groups

The characteristics of maceral groups identified in the Hill River coal and supported by photomicrographs taken in reflected light and fluorescence mode where appropriate, are described here. The maceral composition of coal is described under Mintaja and Gairdner Blocks where the drill holes are located.

4.3.1. Vitrinite Group

The vitrinite group occurs as disintegrated, degraded and fragmentary shreds and tissues, as well as microbands in the coal. The group consists of vitrinite A (telocollinite and telinite) and vitrinite B (desmocollinite, corpocollinite and minor vitrodetrinite). Figure 4.9 shows telinite and telocollinite macerals of vitrinite A sub-group, and desmocollinite and corpocollinite macerals of vitrinite B sub-group. In both Mintaja and Gairdner Block coal, vitrinite A is more dominant than vitrinite B (Table 4.5), and their ratio ranges from 0.71 to 1.57 (Tables 4.7 and 4.14).

Telocollinite is the dominant maceral in the coal and shows granular or spongy texture, and lower reflectance than other vitrinites. It usually shows a fairly uniform structure and reflectance, with medium to grey colour, sometimes with desiccation cracks. Transverse and oblique fractures and cleats are also prevalent. Desmocollinite always appears as groundmass (Figure 4.9 c). Corpocollinite usually occurs as discrete or in-situ excretion in sub-rounded to rounded shapes with various sizes

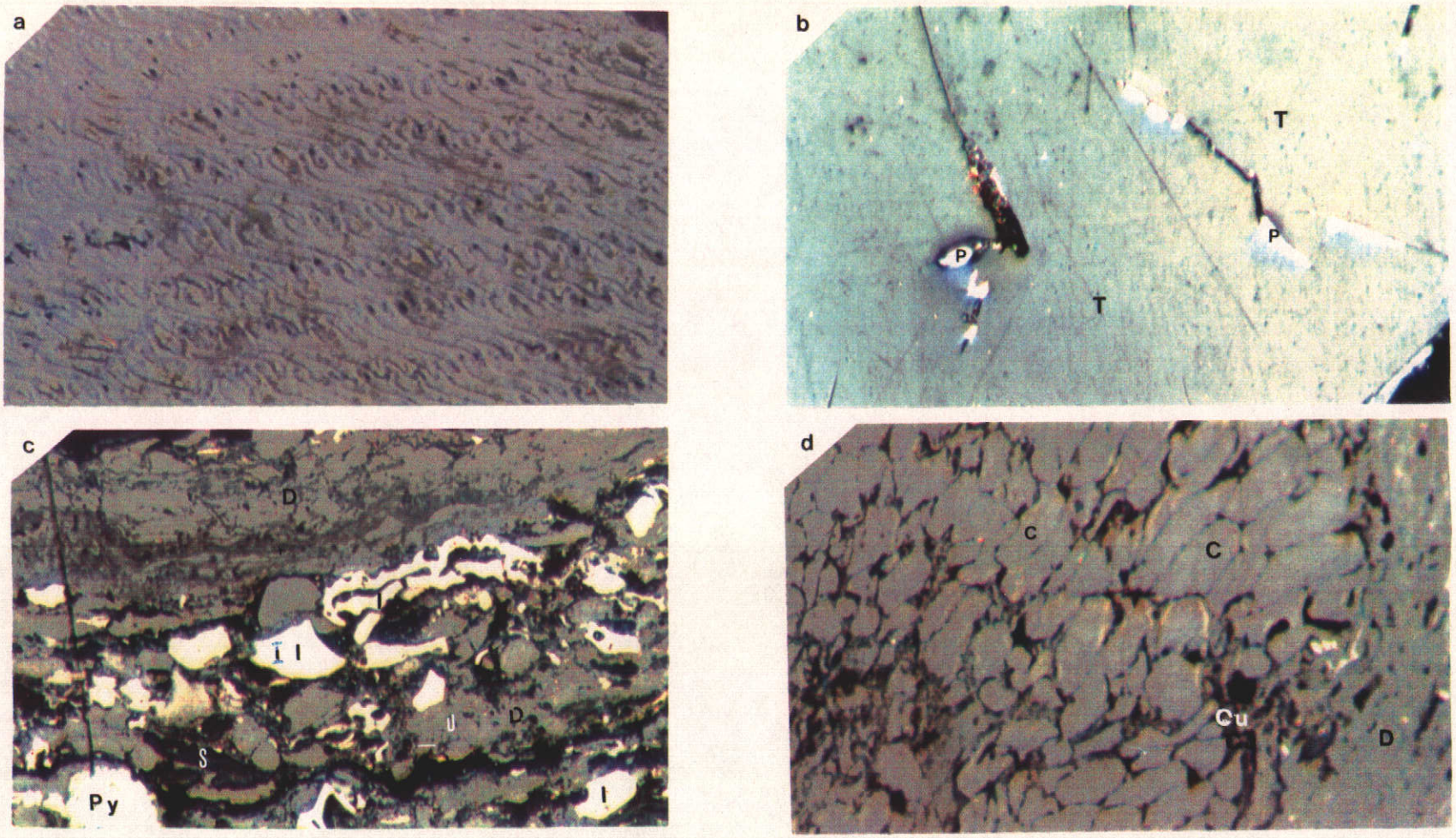

Figure 4.9. Photomicrographs of vitrinite A (a&b) and vitrinite (c&d). (Oil immersion), X 320, reflected light.
a. Telinite showing wood cells. (CPCH 37/G 5-6).
b. Telocollinite (T) and pyrite infillings (P). (CPCH 57/G 4).
c. Desmocollinite (D) forming groundmass, with sporinite (S) and inertodetrinite (I). (CPCH 39/G 6).
d. Corpocollinite (C), desmocollinite (D), cutinite (CU) and resinite (R). (CPCH 57/G 1).

(Figure 4.9 d). Telinite displaying a well-preserved tissue structure is rare (Figure 4.9 a) , which indicates that the coal has undergone a high degree of diagenesis.

In some samples, the presence of embedded inertodetrinite in the vitrinite is also recognised (Figure 4.9 c), suggesting that the inertodetrinite has undergone a high degree of degradation. Tiny specks, granules and framboids of pyrite are often recognised in vitrinite, particularly in desmocollinite and telocollinite macerals (Figures 4.9 b and c). The relatively high vitrinite content in most of the sub-seams of Mintaja and Gairdner Blocks, indicates that a reasonable degree of preservation of decayed plant material occurred, and vitrinite could be used as a measure of petrographic indices to interpret a peat depositional environment.

4.3.2. Inertinite Group

Semifusinite, fusinite and inertodetrinite are the most common macerals in Hill River coals, with minor macrinite and rare sclerotinite and micrinite. Semifusinite dominates over other inertinite macerals (Table 4.5) and occurs as layers, large lenses, bands or as isolated fragments, and it is generally associated with vitrinite and fusinite (Figure 4.10 a). Inertodetrinite maceral represents the second highest proportion of the inertinite group and it is present in all samples, in association with other macerals, particularly desmocollinite (Figure 4.10 c). Fusinite is common in the Hill River coal (Figures 4.10 a and b), and recognised as bands or threads. Fusinised resins (corpocollinites ?) are often recognised (Figure 4.10 d). Fusinite with "bogen" structure is also present in some samples (Figure 4.11 a). Macrinite occurs sporadically, as tiny pieces to dimensions of 25 microns to 300 microns (Figure 4.11 b). Sclerotinite of fungal origin with characteristic rounded shape is present in the coal (Figure 4.11 c). Micrinite occurs as traces associated with other macerals, especially with vitrinite in the coal (Figure 4.11 d).

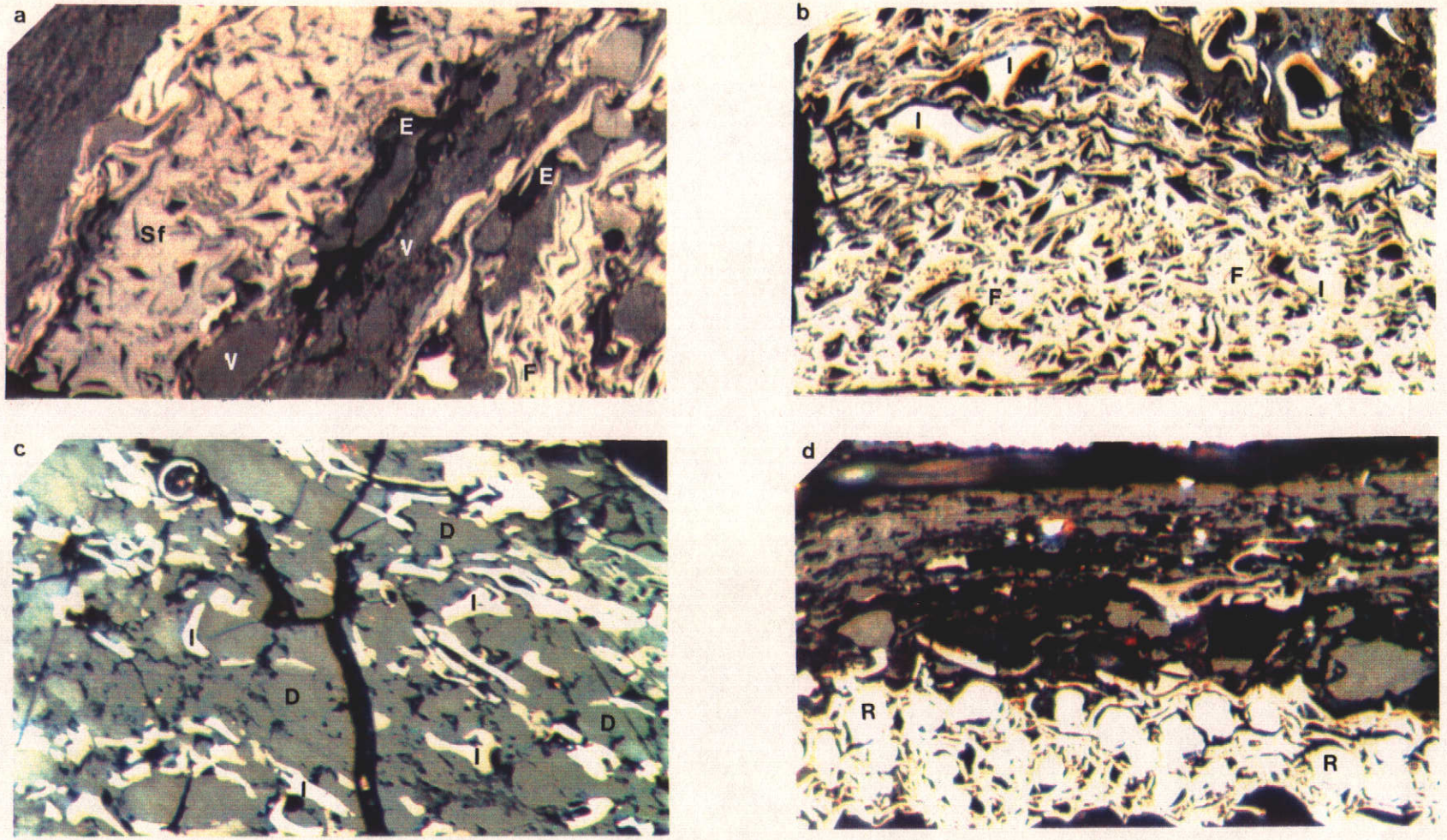

Figure 4.10. Photomicrographs of semifusinite, fusinite, and inertodetrinite. (Oil immersion), X 320, reflected light.
a. Semifusinite (Sf) associated with vitrinite (V), exinite (E) and fusinite (F). (CPCH 57/G 1).
b. Compressed fusinite (F) with inertodetrinite (I). (CPCH 1/G 1).
c. Inertodetrinite (I) embedded in desmocollinite (D). (CPCH 1/G 6).
d. Sub-rounded fusinite/oxydised resins (R) infilling cell cavities of fusinite. (CPCH 1/G 6).

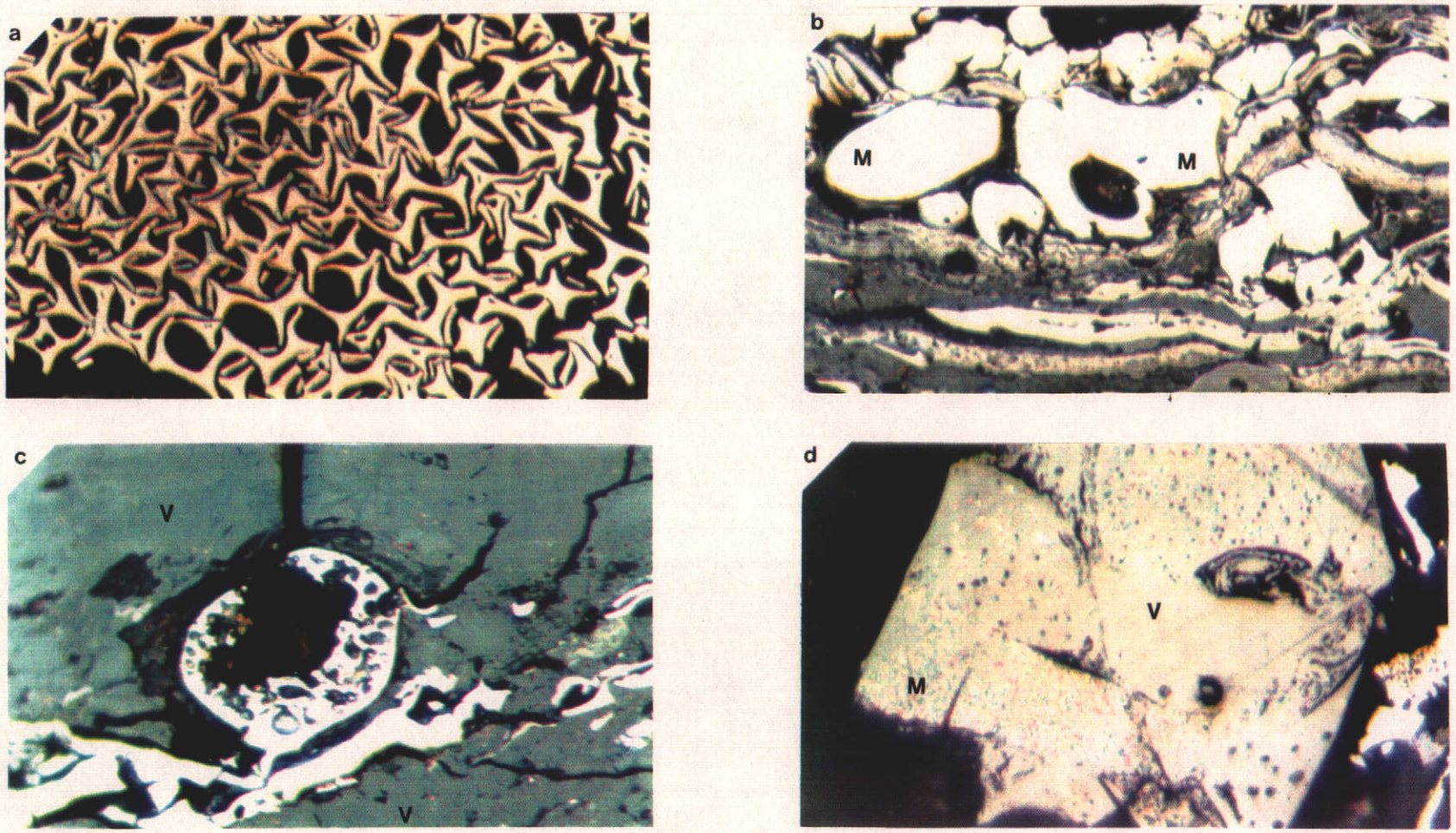

Figure 4.11. Photomicrographs of inertinite macerals. (Oil immersion), reflected light.
a. Fusinite showing "bogen" structure. Some cell cavities are infilled with clay minerals (CL). (CPCH 39/G 4), X 320.
b. Macrinite (M) occurring sporadically. (CPCH 37/G 3), X 320.
c. Sclerotinite showing fungal remains, embedded in vitrinite (V). (CPCH 39/G 4), X 320.
d. Micrinite (M) associated with vitrinite (V). (CPCH 1/G 1), X 500.

4.3.3. Exinite Group

In order of decreasing proportions, the exinite macerals of the Mintaja and Gairdner coals are sporinite, alginite, cutinite, liptodetrinite and resinite. The sporinite, cutinite and alginite predominate , with minor amounts of resinite and liptodetrinite. Sporinite appears as streaky spore exines, flattened along the bedding, and it is distributed throughout the samples in occasional densely packed patches or bands. It is represented in clarite, trimacerite and durite microlithotypes. Thin walled-sporinite (tenuisporinite) (Figure 4.12 a and b) is the dominant component within the exinite in the Hill River coal. However, sporangia and thick-walled sporinite (crassisporinite) are also present (Figures 4.12 c & d, and 4.13 a & b). Sporinite shows fluorescing colours from yellow, orangish yellow to yellowish orange . This colour variation is probably due to the rank of the coal. Cutinite occurs as both thin and thick bodies (Figures 4.13 c & d, and 4.14 a & b). It ranges from well-preserved to highly degraded structures , which is distributed sparsely or in densely packed units. This maceral fluoresces in orange, brownish orange and yellowish orange with varying intensities. Cutinite has been observed to be associated with and enclose vitrinite B (corpocollinite), and it flanks leaf structure (Figure 4.14 c and d). It is likely that it is the remnants of leaf tissues. Cutinite often exhibits its typical serrated edge of cuticles (Figure 4.13 c&d). The highly degraded cutinites are often associated with liptodetrinite. Alginite occurs sporadically in the coal. It is commonly associated with sporinite, liptodetrinite fractions and vitrinite. Under normal reflected light, the alginite is hardly distinguished from lumps or block granular clay minerals (Figure 4.14 c). Under ultra-violet excitation, alginite fluoresces with strong intensity, showing bright yellow to orangish yellow colours (Figure 4.14 d), which is stronger than yellow resinites. Alginite colonies have also been identified in the coal. Liptodetrinite, is chiefly composed of detrital and degraded sporinite, cutinite, alginite and undifferentiated substances, which are embedded in desmocollinite groundmass. Liptodetrinite of Hill River coal is rich in cutinite, alginite, and sporinite fragments.

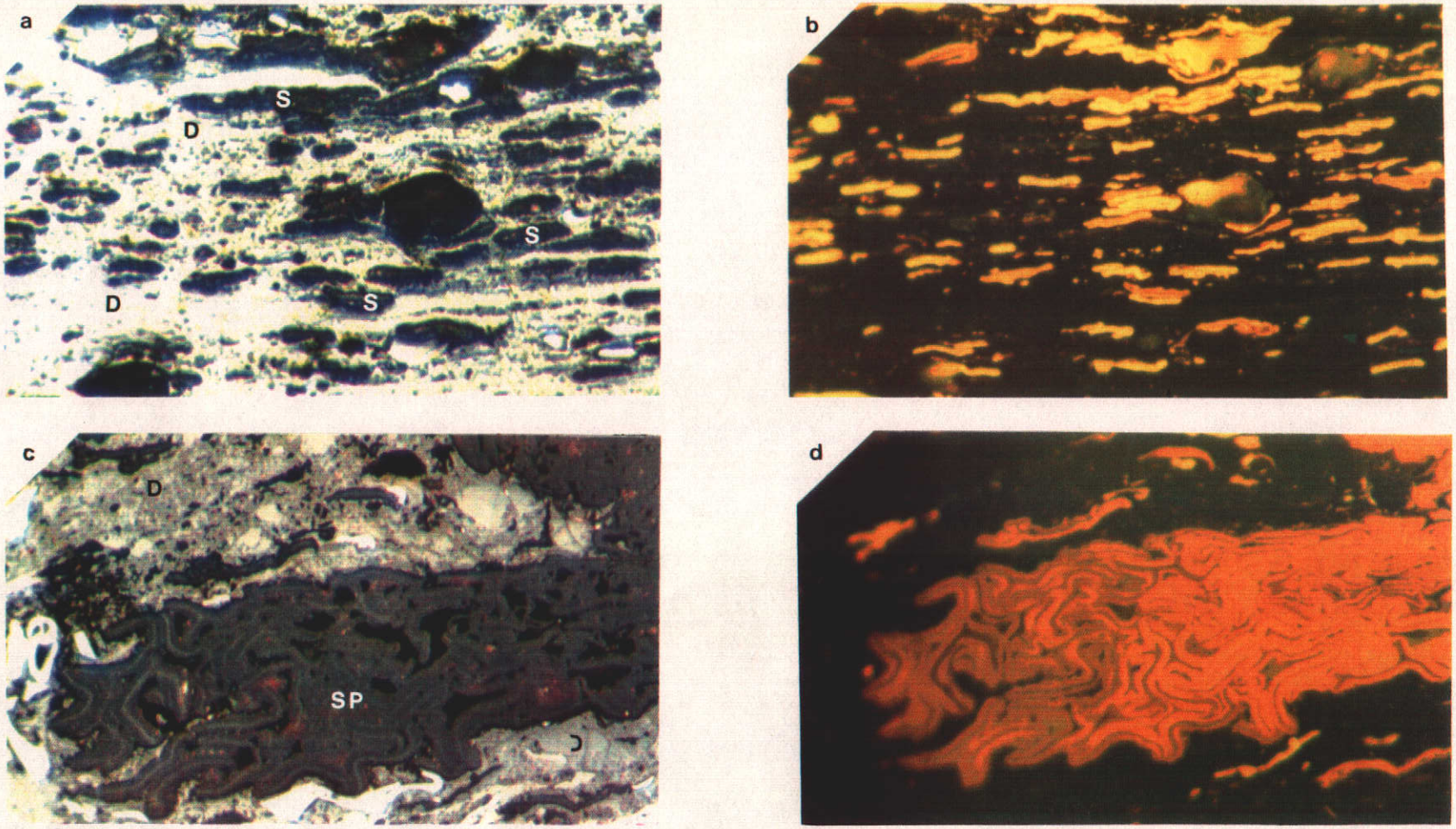

Figure 4.12. Photomicrographs of sporinite macerals. (Oil immersion), X 320.
a. "Layering" of thin walled- sporinite (S)/tenuisporinite, embedded in desmocollinite (D). (CPCH 1/G 6), reflected light.
b. The same figure as (a), under fluorescence mode.
c. Sporangia (SP) embedded in desmocollinite (D). (CPCH 1/G 1), reflected light.
d. The same as (c), under fluorescence mode.

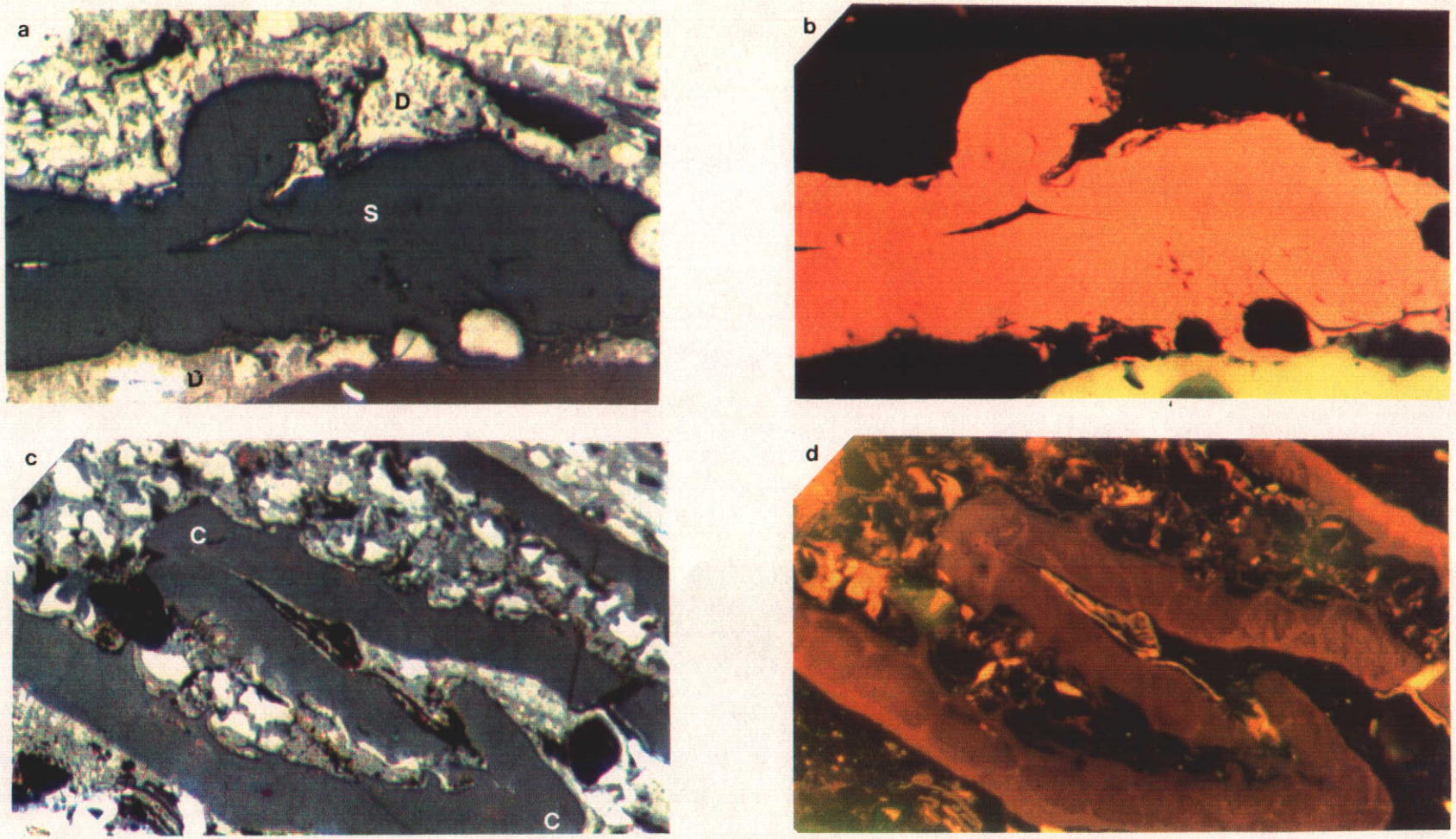

Figure 4.13. Photomicrographs of exinite macerals. (Oil immersion), X 320.
a. Thick-walled (macro-) sporinite (S) associated with desmocollinite (D). (CPCH 39/G 4), reflected light.
b. The same as (a), under fluorescence mode.
c. Well-preserved thick cutinite (C) showing serrated edge. (CPCH 1/G 1), reflected light.
d. The same as (c), under fluorescence mode.

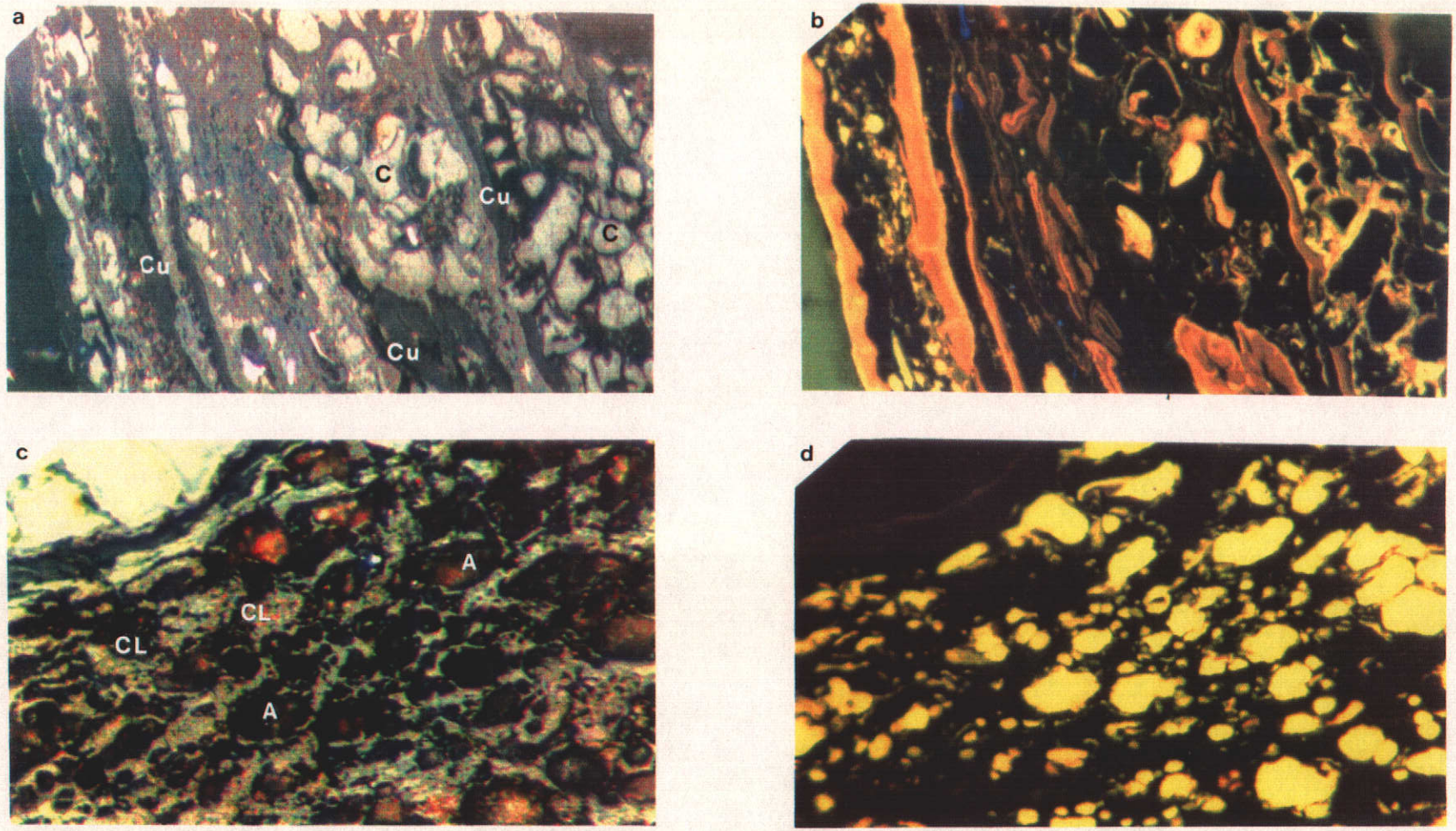

Figure 4.14. Photomicrographs of exinite macerals. (Oil immersion), X 320.
a. Thin cutinite (Cu) encloses corpocollinite (C), and resinite filling cell cavities. (CPCH 47/G 1), reflected light.
b. The same as (a), under fluorescence mode.
c. Scattered sub-rounded alginite (A) which is hardly distinguished from clay minerals (CL). (CPCH 37/G 4), reflected light.
d. The same as (c), under fluorescence mode.

Intensity and fluorescence colours of liptodetrinite vary from dull yellowish to orangish brown (Figure 4.15 a and b), which probably depends on the constituents of macerals fragments. Resinite is present as discrete oval, elliptical, globular bodies, filling cell lumens or embedded as thin layers within vitrinite (Figure 4.15 c and d). It displays varying fluorescence intensity and colour among the exinite macerals. The colour varies from bright yellow to light brown. The resinite within this coal has yellow, yellowish orange and brownish yellow colours .

4.4. Microlithotypes

The macerals in Hill River coal are mostly present in associations, in which one of the maceral groups tends to be dominant. On the basis of whether they consist of one or more maceral groups, microlithotype examination of Mintaja and Gairdner Block coal revealed four microlithotypes:

- Monomaceral
- Bimaceral
- Trimaceral
- Carbominerite

4.4.1. Monomaceral

This microlithotype is composed of vitrite, liptite, and inertite. Vitrite in Mintaja and Gairdner Blocks coal occurs as a predominant constituent often present as microbands of vitrinite (Figure 4.16 a). Liptite occurs rarely, and it is composed mainly of algite and sporite with minor cutite (Figures 4.16 b, c and d). Inertite, predominantly consists of semifusite and fusite with minor macroite (Figure 4.17 a, b and c).

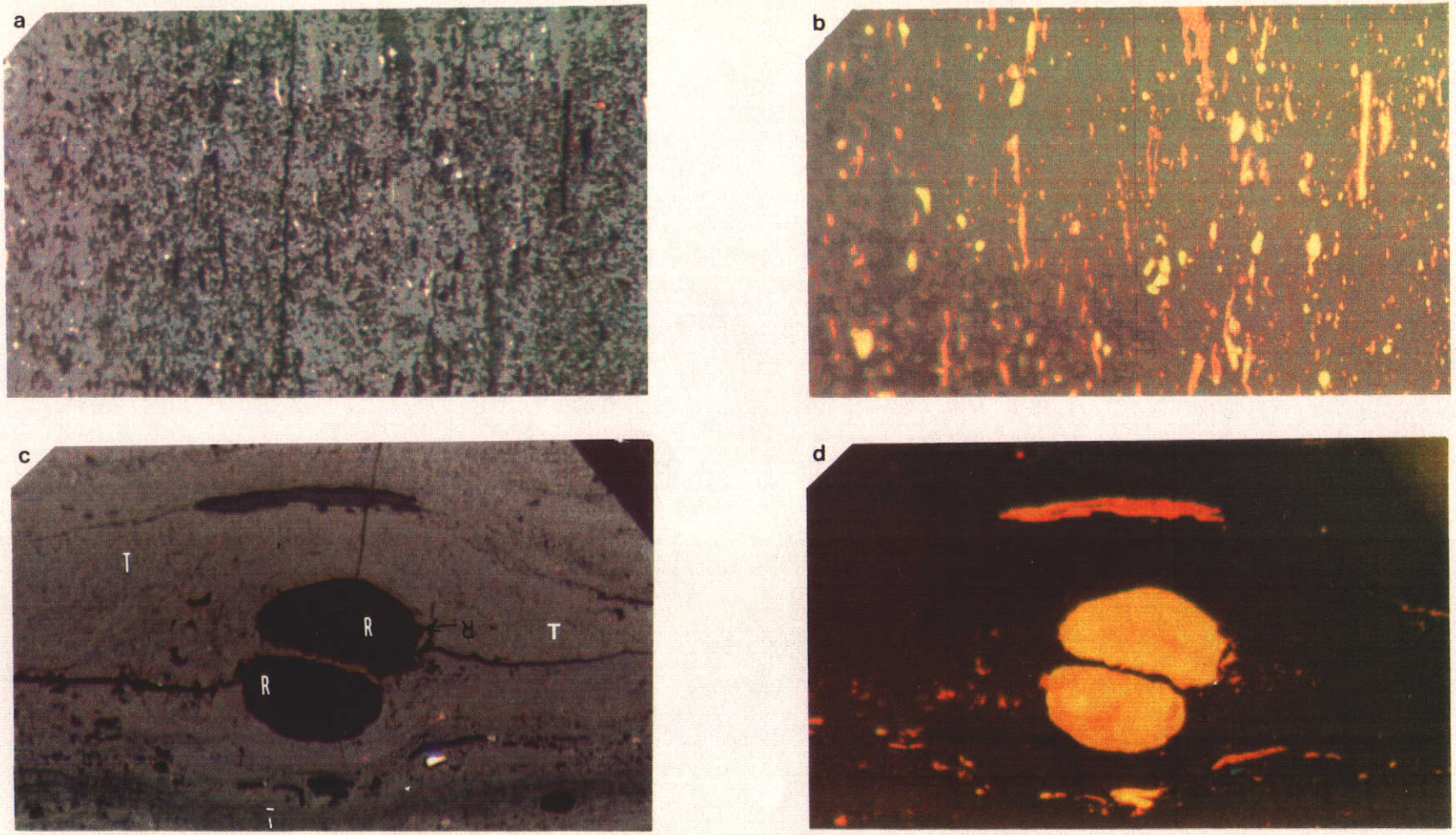

Figure 4.15. Photomicrographs of liptodetrinite and resinite. (Oil immersion), X 320.
a. Liptodetrinite embedded in desmocollinite. (CPCH 1/G 1), reflected light.
b. The same as (a), under fluorescence mode.
c. Elliptical resinites (R) embedded in telocollinite (T). (CPCH 1/G 1), reflected light.
d. The same as (c), under fluorescence mode.

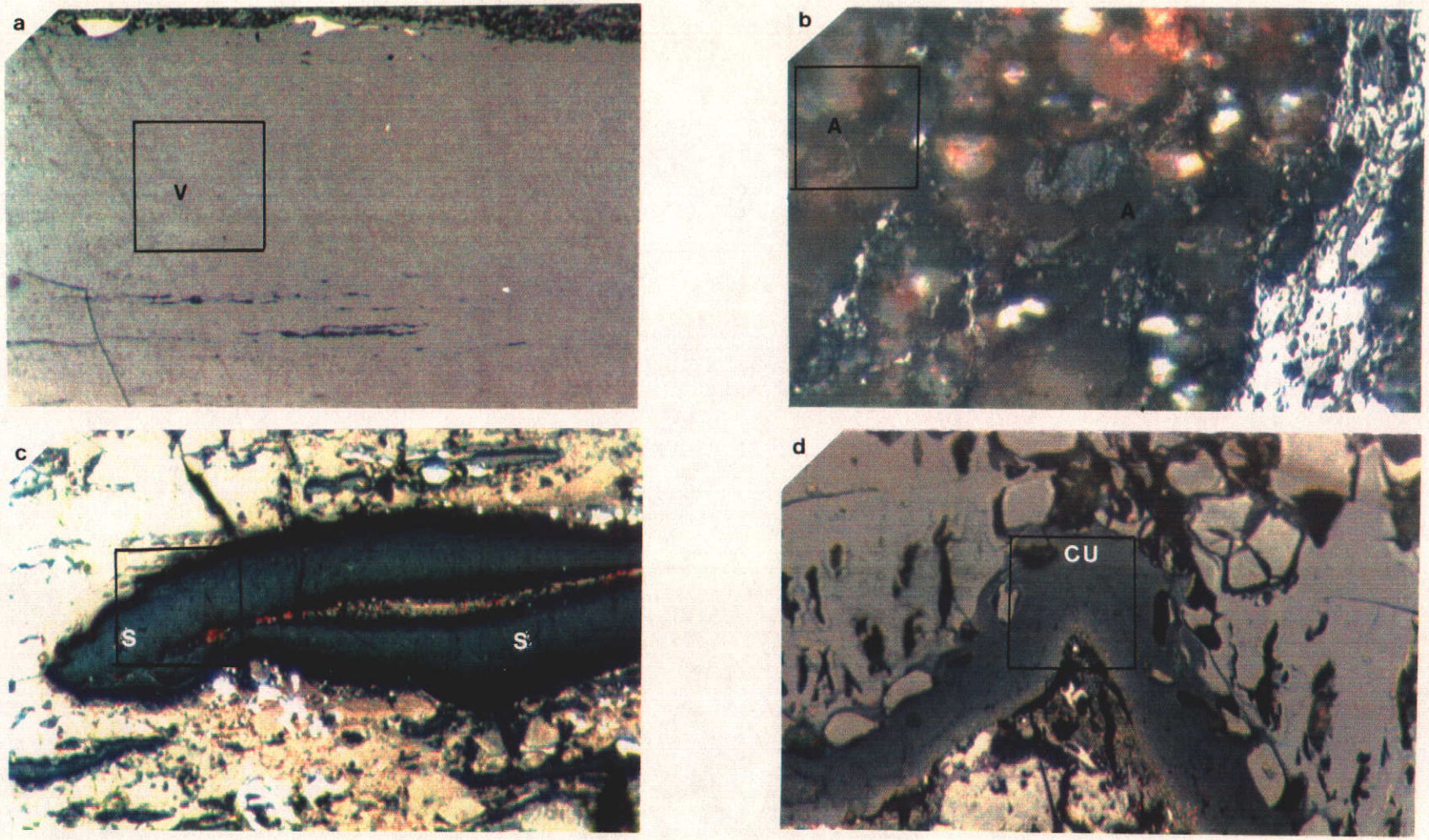

Figure 4.16. Photomicrographs of monomaceralic microlithotypes of Hill River coal. (Oil immersion), X 320.
a. Vitrite consisting of microbands of vitrinite (V). (CPCH 1/G 2).
b. Liptite composed of alginite (algite) (A). (CPCH 47/G 4).
c. Sporite (S) constitutes liptite. (CPCH 1/G 1).
d. Cutite (CU). (CPCH 1/G 6).

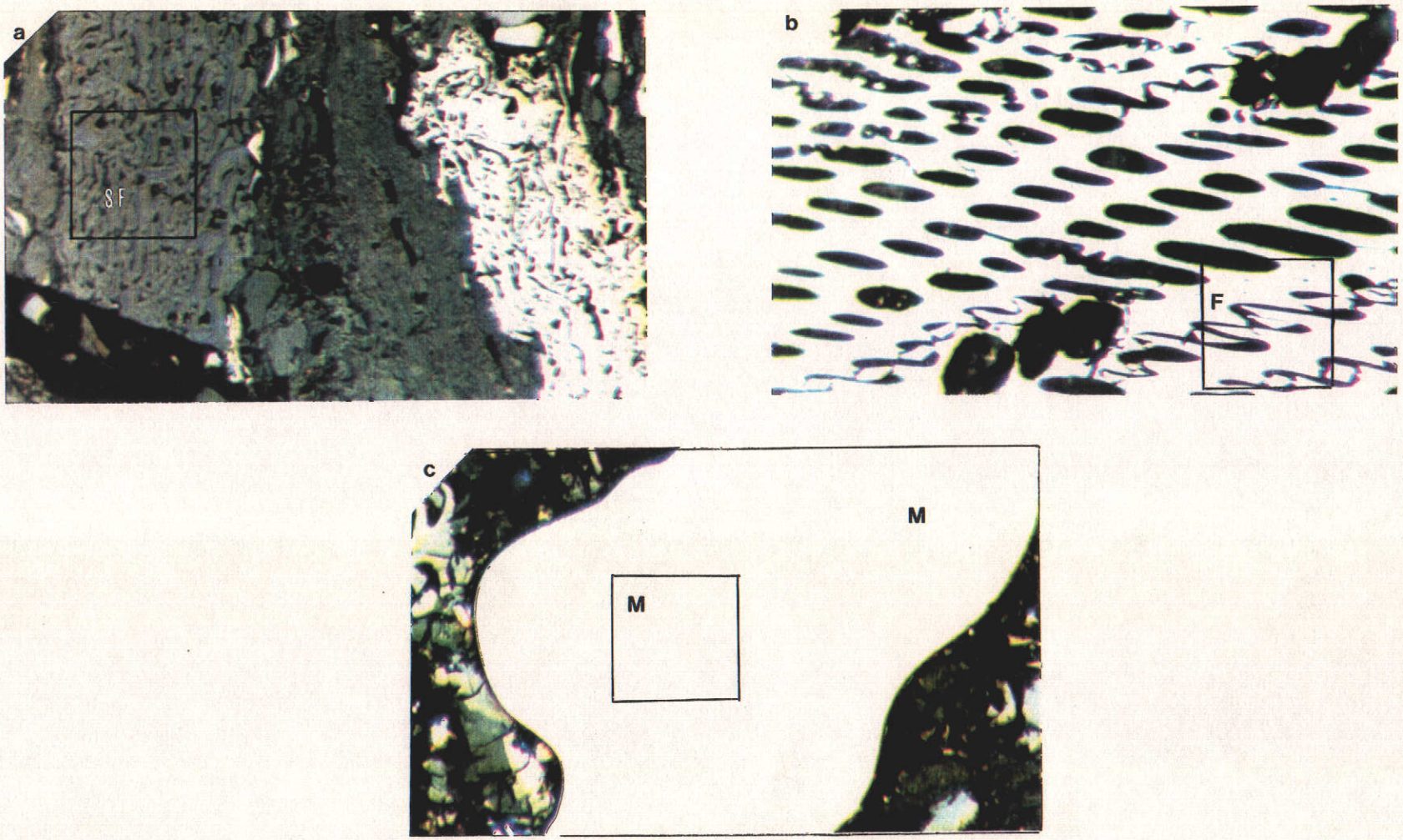

Figure 4.17. Photomicrographs of monomaceralic microlithotypes. (Oil immersion), X 320.
a. Semifusinite constituting semifusite (SF). (CPCH 39/G 6).
b. Fusite composed of fusinite (F). (CPCH 39/G 5).
c. Macroite consisting of macrinite (M). (CPCH 1/G 2).

4.4.2. Bimaceral

Within this type, clarite is the most common constituent, followed by vitrinite and durite. Clarite consists of vitrinite plus exinite. The vitrinite-rich clarite is identified as clarite-V (Figure 4.18 a) and exinite-rich clarite as clarite-E (Figure 4.18 b). The clarite-E is sub-divided into sporoclarite and cuticloclarite. The sporoclarite is present as an association of desmocollinite with dominant embedded sporinite (Figure 4.18 c), while cuticloclarite or cutinite-rich clarite-E is an association of desmocollinite as a groundmass with embedded cutinite maceral (Figure 4.18 d). Vitrinertite is composed of vitrinite and inertinite group of macerals, and is sub-divided into vitrinite-rich vitrinertite identified as vitrinertite-V (Figure 4.19 a) and inertinite-rich vitrinertite as vitrinertite-I (Figure 4.19 b). Durite is a combination of the inertinite plus exinite group of macerals, and it is sub-divided into inertinite-rich durite or durite-I (Figure 4.19 c) and exinite-rich durite or durite-E (Figure 4.19 d). In the Mintaja and Gairdner Block coal, durite-I is more common than durite-E.

4.4.3. Trimaceral

This microlithotype is an association of vitrinite, exinite and inertinite groups, and sub-divided into duroclarite, clarodurite and vitrinertoliptite. Duroclarite dominates in Mintaja and Gairdner Block coal. The duroclarite is characterised by an association of dominant vitrinite group with a minor amount of exinite and inertinite groups (Figure 4.20 a). Commonly, it is observed as vitrinite and sporinite with alginite or cutinite, associated with inertodetrinite and macrinite. Clarodurite is an association of predominant inertinite with vitrinite and exinite (Figure 4.20 b). The concentration of clarodurite is much less than duroclarite. It occurs usually as a combination of thin to thick band of semifusinite or fusinite with vitrinite B and exinite macerals. Generally, mineral matter is found to be associated in the clarodurite (Figure 4.20 c).

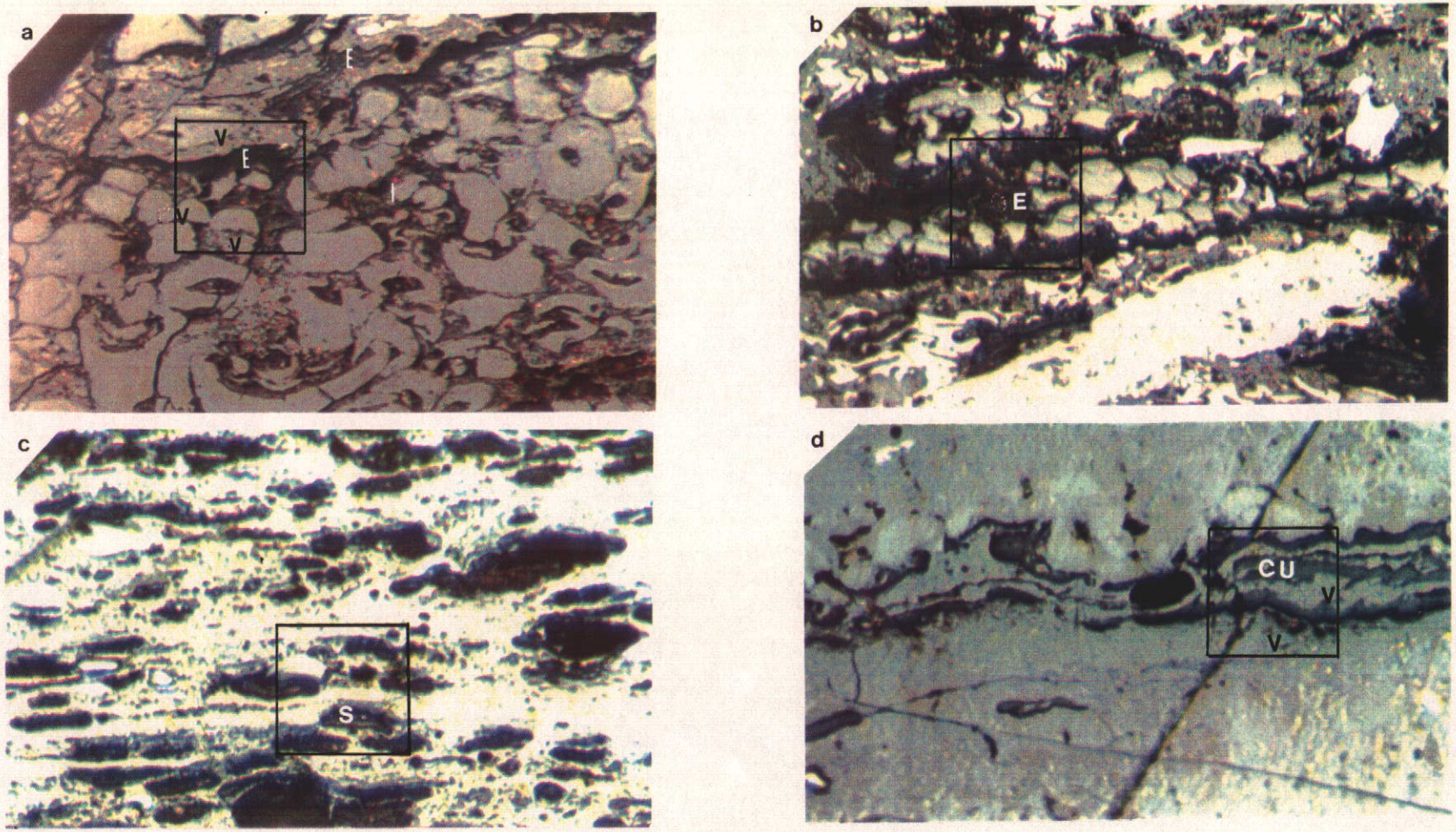

Figure 4.18. Photomicrographs of bimaceralic microlithotypes. (Oil immersion), X 320.
a. Vitrinite-rich clarite (clarite-V). Vitrinite (V), exinite (E). (CPCH 47/G 3).
b. Exinite-rich clarite (clarite-E). Exinite (E), vitrinite (V). (CPCH 57/ G 2).
c. Sporoclarite showing dominant sporinite (S); V = vitrinite.(CPCH 37/ G 4).
d. Cuticloclarite dominated by cutinite (CU); V = vitrinite. (CPCH 57/ G 5).

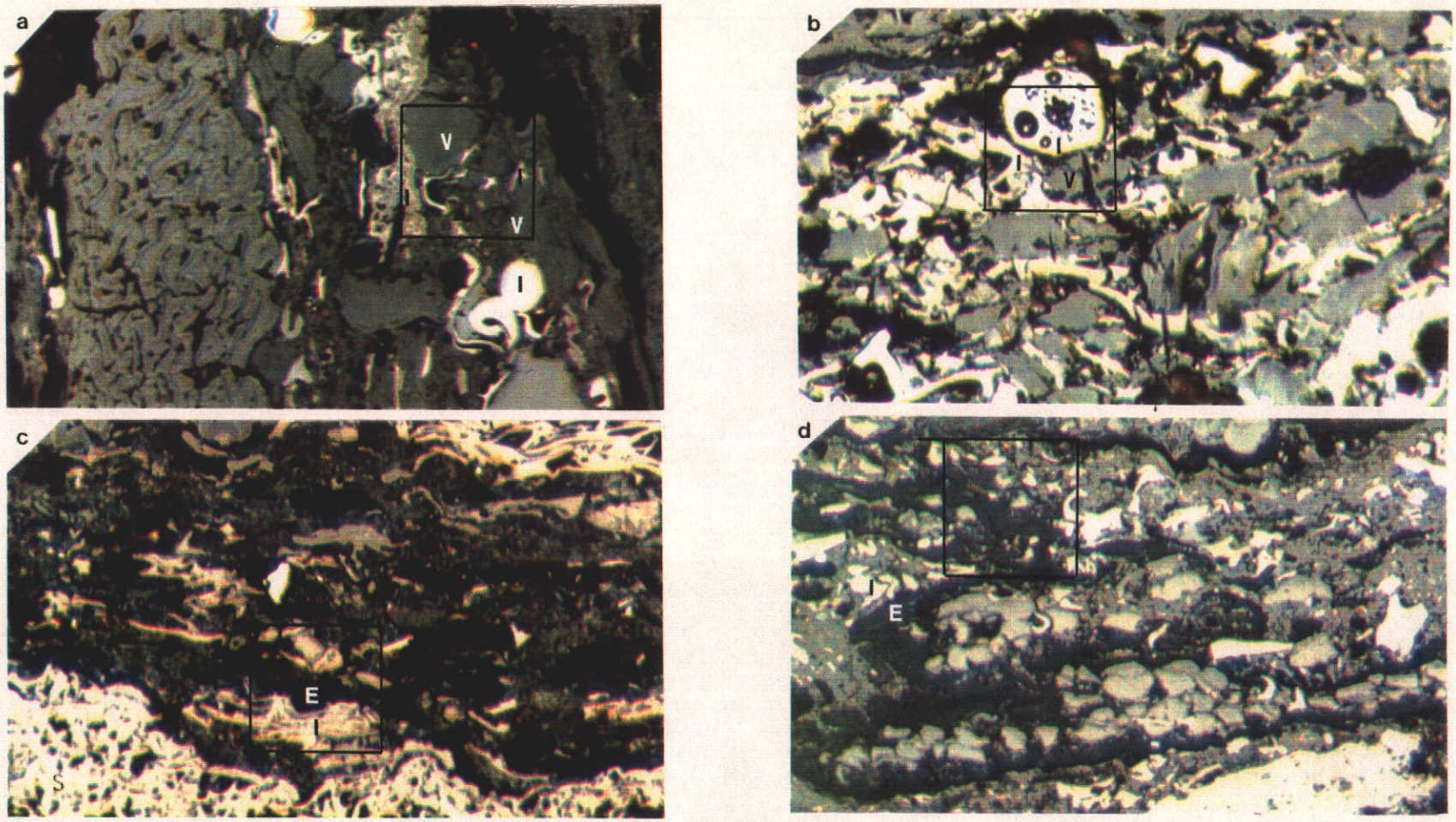

Figure 4.19. Photomicrographs of bimaceralic microlithotypes. (Oil immersion),X 320.
a. Vitrinertite-V showing vitrinite-rich vitrinertinite; V = vitrinite, I = inertinite. (CPCH 37/ G 3).
b. Vitrinertite-I characterised by abundance of inertinite (I); V = vitrinite. (CPCH 37/ G 5).
c. Durite-I composed of dominant inertinite (I) and exinite (E). (CPCH 39/G 3).
d. Durite-E composed of dominant exinite (E) and inertinite (I). (CPCH 39/G 6).

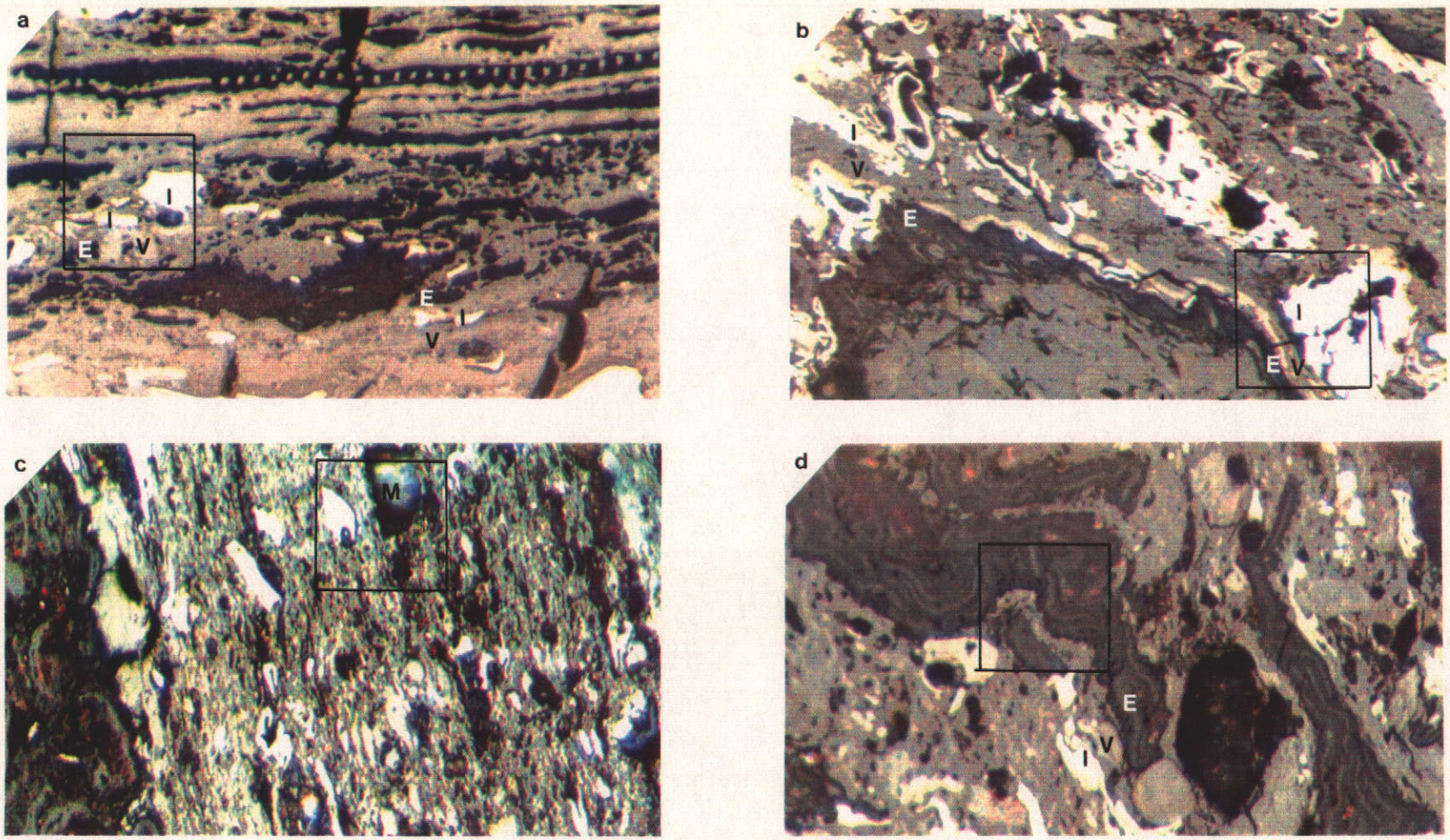

Figure 4.20. Photomicrographs of trimaceralic microlithotypes. (Oil immersion), X 320.
a. Duroclarite dominated by vitrinite (V), with a lesser extent of exinite (E) and inertinite (I). (CPCH 1/G 1).
b. Clarodurite showing predominant inertinite (I), with vitrinite (V) and exinite (E). (CPCH 57/G 1).
c. Mineral matter (M) associated with clarodurite. (CPCH 1/G 2).
d. Vitrinertoliptite constituted by dominance of exinite (E) with minor vitrinite (V) and inertinite (I). (CPCH 57/G 1).

Vitrinertoliptite is observed in a similar amount to clarodurite. This microlithotype is composed of dominated exinite over minor amounts of vitrinite and inertinite maceral groups (Figure 4.20 d). Exinite is present in the forms of mega-sporinite, sporangia, thick cutinite and alginite.

4.4.4. Carbominerite

The carbominerite group of the Hill River coal is sub-divided on the basis of the type and content of mineral matter which is associated with macerals. The sub-division of the carbominerite is presented in Table 3.4. Association of macerals with 20 % to 60% clay minerals is categorised as carbargillite (Figure 4.21 a). The carbargillite is present as the dominant carbominerite of the Hill River coal. A mixture of 5 % to 20 % pyrite and maceral which exists as the second major carbominerite of the Hill River coal, is classified as carbopyrite (Figure 4.21 b). The carbankerite with 5.0 % to 20.0 % carbonate association is present in the coal (Figure 4.21 c). Figure 4.21 d represents carbopolyminerite showing an association of macerals and 20.0 % to 60.0 % mixture of clay minerals and pyrite.

4.5. Mintaja Block and Surrounds (CPCH 1, 37, 39 and 47)

The petrographic data on maceral and microlithotype analyses of lithotypes of coal from the Mintaja Block drill holes is presented first for the drill hole CPCH 1, followed by the analyses of CPCH 1, 37, 39 and 47. As pointed out earlier, maceral and microlithotype analyses were completed on the lithotypes of the coal in the drill hole CPCH 1, followed by the analyses on other drill holes in the block, where only the crushed samples of coal were available.

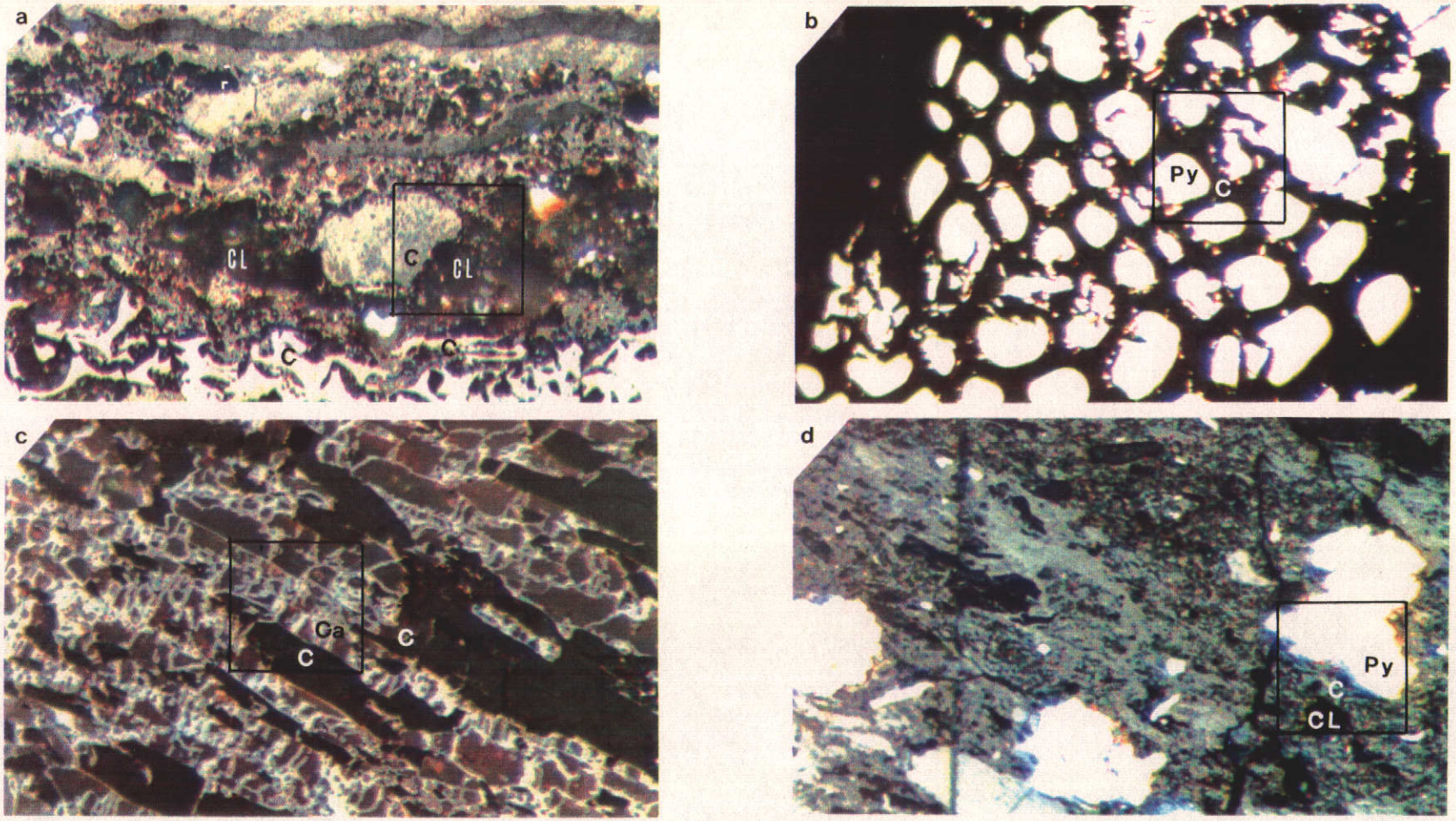

Figure 4.21. Photomicrographs of carbominerites. (Oil immersion), X320.
a. Carbargillite shown as an association of coal maceral (C) with clay minerals (CL). (CPCH 1/G 6).
b. Coal maceral (C) and pyrite (Py) constitute carbopyrite. (CPCH 47/G 1).
c. Carbankerite present as a mixture of coal maceral (C) and carbonate (Ca). (CPCH 57/G1).
d. Carbopolyminerite composed of coal maceral (C), clay mineral (Cl) and pyrite (Py). (CPCH 1/G5).

4.5.1. Maceral, Mineral Matter, and Microlithotype Analyses of Lithotypes, Drill Hole CPCH 1

Maceral and microlithotype analyses of lithotypes present in the coal of drill hole CPCH 1, were carried out to establish the distribution of macerals, mineral matter, and microlithotypes in the individual lithotypes . The proportions of macerals and mineral matter in the individual lithotypes of the sub-seams is presented in Table 4.2. The microlithotype distribution of the individual lithotypes is given in Table 4.3.

Maceral analyses of the individual lithotypes from sub-seams G1 to G5 are also displayed in Figures 4.22 and 4.23. As expected there is a marked increase in vitrinite content from dull to bright types, and the content of exinite shows a gradual decrease from duller to brighter types, particularly sporinite and alginite constituents (Table 4.2). Inertinite, in general decreases from dull to bright types, while in sub-seams G 1, G 2 and G 3 inertodetrinite and inertinite constituents show an increasing trend. The increase of inertodetrinite is due to either the increased in-situ disintegration of structured inertinite under drying conditions or increased transport under wet conditions. Mineral matter decreases from dull to bright lithotypes, and it is dominated by clay, and pyrite. On the basis of maceral analyses, "dullness" in coal is due to the relatively high content of structured inertinites, non-structured vitrinites (desmocollinite, corpocollinite), inertodetrinite, sporinite, alginite, and mineral matter; and "brightness" is attributable to vitrinite, especially telocollinite and telinite.

Figure 4.24 depicts a ternary plot of maceral compositions for each individual lithotype on a mineral matter free basis. The general trend of increasing vitrinite but decreasing inertinite contents along the dull to bright coals is present. There is a remarkable overlap between bright and bright banded coal, and also between bright banded and banded types. Variation in microlithotype associations occur from bright

Table 4. 2 . Maceral and mineral contents of lithotypes from drill hole CPCH 1.

Maceral	G 1					G 2					G 3					G4					G 5			G 6
	B	BB	BD	DB	D	B	BB	BD	DB	D	B	BB	BD	DB	D	B	BB	BD	DB	D	BB	BD	D	D
Telinite	2.2	1.8	3.0	1.0	0.2	5.0	2.4	3.4	0.6	5.0	1.8	2.6	2.2	4.2	3.2	1.4	0.8	2.8	0.0	0.0	0.0	0.2	1.2	0.3
Telocollinite	31.8	49.8	15.6	17.0	6.6	62.2	51.8	36.2	6.2	13.8	43.6	53.2	40.6	9.6	6.0	52.0	44.4	27.8	19.6	0.8	58.4	40.2	14.4	22.5
Vitrinite A	34.0	51.4	18.6	18.0	6.8	67.2	54.2	39.6	6.8	18.8	45.4	55.8	42.8	13.8	9.2	53.4	45.2	30.0	19.6	0.8	58.4	40.4	15.6	22.8
Corpocollinite	5.0	4.4	8.2	3.0	1.4	4.2	0.4	9.4	0.8	1.8	0.0	8.0	0.2	6.4	7.2	0.0	1.6	0.2	0.0	0.6	6.0	6.6	0.6	2.2
Desmocollinite	43.6	25.0	32.4	23.8	15.4	16.6	9.6	23.0	34.2	14.4	34.8	16.6	28.8	31.2	32.2	24.6	30.4	41.0	46.0	11.0	10.8	24.4	15.0	10.4
Vitrodetrinite	0.0	0.0	0.4	2.8	0.6	0.8	0.0	0.4	0.0	0.0	0.0	0.0	0.0	0.0	1.4	0.0	0.0	0.0	0.0	0.0	0.0	0.0	0.2	0.0
Vitrinite B	48.6	29.4	40.6	29.6	17.6	11.6	10.0	32.8	35.0	16.2	34.8	17.4	29.0	37.6	41.2	24.6	32.0	41.2	46.0	11.6	16.8	31.0	15.8	12.6
VITRINITE	82.6	80.8	59.2	47.6	24.2	88.8	64.2	72.4	41.8	35.0	80.2	73.2	71.8	51.4	50.4	78.0	77.2	71.8	65.6	12.4	75.2	71.4	31.4	35.4
Sporinite	9.2	4.2	10.8	12.4	19.6	3.8	4.4	6.6	11.8	11.0	12.8	3.8	7.0	11.6	7.6	8.6	8.2	6.2	22.2	12.6	7.0	6.4	9.2	6.2
Alginite	1.4	2.0	3.2	0.8	3.2	0.4	1.2	0.8	1.8	2.6	0.0	1.2	0.2	1.8	8.0	1.4	2.2	0.8	1.4	4.4	2.0	3.0	6.6	6.4
Liptodetrinite	0.2	0.6	0.8	1.0	0.2	0.4	1.4	1.0	1.2	1.0	0.0	0.2	0.4	0.2	0.0	0.4	0.0	1.4	0.0	1.8	0.2	0.4	0.6	1.0
Other exinites	1.6	0.6	8.0	0.0	0.8	0.0	0.4	4.8	0.6	0.2	0.8	1.2	3.6	3.2	2.0	0.8	1.8	4.2	1.6	0.6	0.4	0.6	0.6	0.4
EXINITE	12.4	7.4	22.8	14.2	23.8	4.4	7.4	13.2	15.4	14.8	13.6	6.4	10.2	16.8	17.6	11.2	12.2	12.6	25.2	19.4	9.6	10.4	17.0	14.0
Semifusinite	0.0	1.2	0.2	5.4	16.8	1.8	3.4	3.8	5.6	10.4	0.2	2.2	0.0	7.4	2.2	0.2	0.2	1.4	0.0	5.8	0.2	0.6	8.4	8.0
Fusinite	0.0	0.0	1.2	10.0	12.6	1.2	8.8	1.6	7.2	14.0	0.0	1.0	0.2	2.2	1.2	0.0	0.0	1.8	0.0	1.2	0.2	0.2	7.0	6.0
Inertodetrinite	2.4	6.2	10.2	8.4	14.8	3.0	10.8	3.4	22.6	15.8	1.6	8.8	7.8	11.2	16.0	2.2	2.6	2.2	0.8	19.2	4.0	4.2	10.0	10.8
Other inertinites	0.0	0.2	0.0	0.6	0.2	0.0	0.0	0.2	1.0	0.8	0.0	0.4	0.8	0.2	0.2	0.0	0.0	0.0	0.0	0.0	0.8	2.8	1.8	0.6
INERTINITE	2.4	7.6	11.6	24.4	44.4	6.0	23.0	9.0	36.4	41.0	1.8	12.4	8.8	21.0	19.6	2.4	2.8	5.4	0.8	26.2	5.2	7.8	27.2	25.4
Pyrite	0.6	0.0	1.0	1.4	1.0	0.0	1.6	0.2	0.2	0.0	1.6	0.2	0.6	0.2	1.0	3.4	0.0	4.2	2.6	0.4	3.0	3.2	4.8	6.2
Clay	1.8	4.0	5.4	12.4	6.6	0.8	2.6	5.2	6.2	9.2	2.8	7.8	8.6	10.6	11.2	6.6	7.8	2.2	5.8	40.4	7.0	7.2	18.0	18.8
Other M.M.	0.2	0.2	0.0	0.4	0.0	0.0	1.2	0.0	0.0	0.0	0.0	0.0	0.0	0.0	0.2	0.0	0.0	3.8	0.0	0.2	0.0	0.0	1.6	0.2
MINERAL MATTER	2.6	4.2	6.4	13.8	7.6	0.8	5.4	5.4	6.4	9.2	4.4	8.0	9.2	10.8	12.4	10.0	7.8	10.2	8.4	41.0	10.0	10.4	24.4	25.2

B = Bright , BB = Bright Banded , BD = Banded , DB = Dull Banded , D = Dull.

Table 4.3 . Microlithotype analyses of individual lithotype of drill hole CPCH 1.

Sub-Seam	Lithotype	Vitrite	Liptite	Inertite	Clarite	Durite	Vitrinertite	Duroclarite	Vitrinertoliptite	Clarodurite	Carbominerite
G 1	B	57.00	0.00	0.00	18.00	0.00	1.20	20.00	0.00	0.00	3.00
	BB	53.00	0.20	4.40	10.80	0.00	6.60	17.60	0.20	0.00	8.20
	BD	26.60	0.80	3.80	27.40	0.20	9.60	28.60	0.20	0.20	2.00
	DB	22.80	0.00	7.40	11.60	0.00	14.00	20.40	0.40	1.60	17.60
	D	5.60	0.20	49.40	12.20	2.40	6.60	13.20	1.20	1.80	5.40
G 2	B	70.60	0.20	1.60	1.00	0.00	2.00	20.60	0.20	0.20	1.00
	BB	60.40	0.00	2.60	4.60	1.40	4.00	21.20	0.20	0.20	3.00
	BD	46.60	0.20	0.60	9.80	0.00	2.20	35.40	0.00	0.00	5.60
	DB	20.20	3.00	30.00	9.20	2.60	3.80	11.80	1.10	0.40	9.00
	D	8.40	0.80	15.00	5.40	2.00	8.80	10.60	7.20	0.40	4.20
G 3	B	53.40	0.60	1.00	13.60	0.00	0.20	26.00	4.00	0.00	0.80
	BB	53.20	0.20	2.80	2.40	0.20	7.00	21.00	0.00	1.80	7.00
	BD	44.20	0.80	4.00	6.40	0.00	4.20	25.00	0.60	5.00	8.60
	DB	22.60	5.20	13.60	10.40	0.00	2.60	22.00	4.00	0.00	6.00
	D	15.00	0.40	25.60	4.60	0.20	7.40	20.00	5.00	6.20	8.80
G 4	B	63.20	0.20	0.20	9.60	0.20	0.00	20.00	0.00	0.00	6.60
	BB	57.60	0.60	0.40	12.60	0.00	0.80	22.00	3.00	0.00	3.00
	BD	38.00	4.20	0.60	15.80	0.00	0.60	25.00	0.00	0.00	5.00
	DB	33.80	2.20	1.40	10.00	1.80	5.60	8.00	6.20	0.20	7.00
	D	9.40	2.80	13.00	2.80	4.80	7.20	18.00	0.00	8.20	34.00
G 5	BB	59.60	0.20	2.20	1.20	1.00	4.00	22.00	0.00	0.00	9.80
	BD	47.40	0.00	2.40	3.20	0.00	1.60	26.00	0.00	0.00	19.40
	D	17.00	0.80	8.40	10.00	0.00	10.40	23.40	1.20	2.20	26.60
G 6	D	24.20	0.00	14.00	3.00	0.60	5.80	12.20	0.60	1.40	38.20

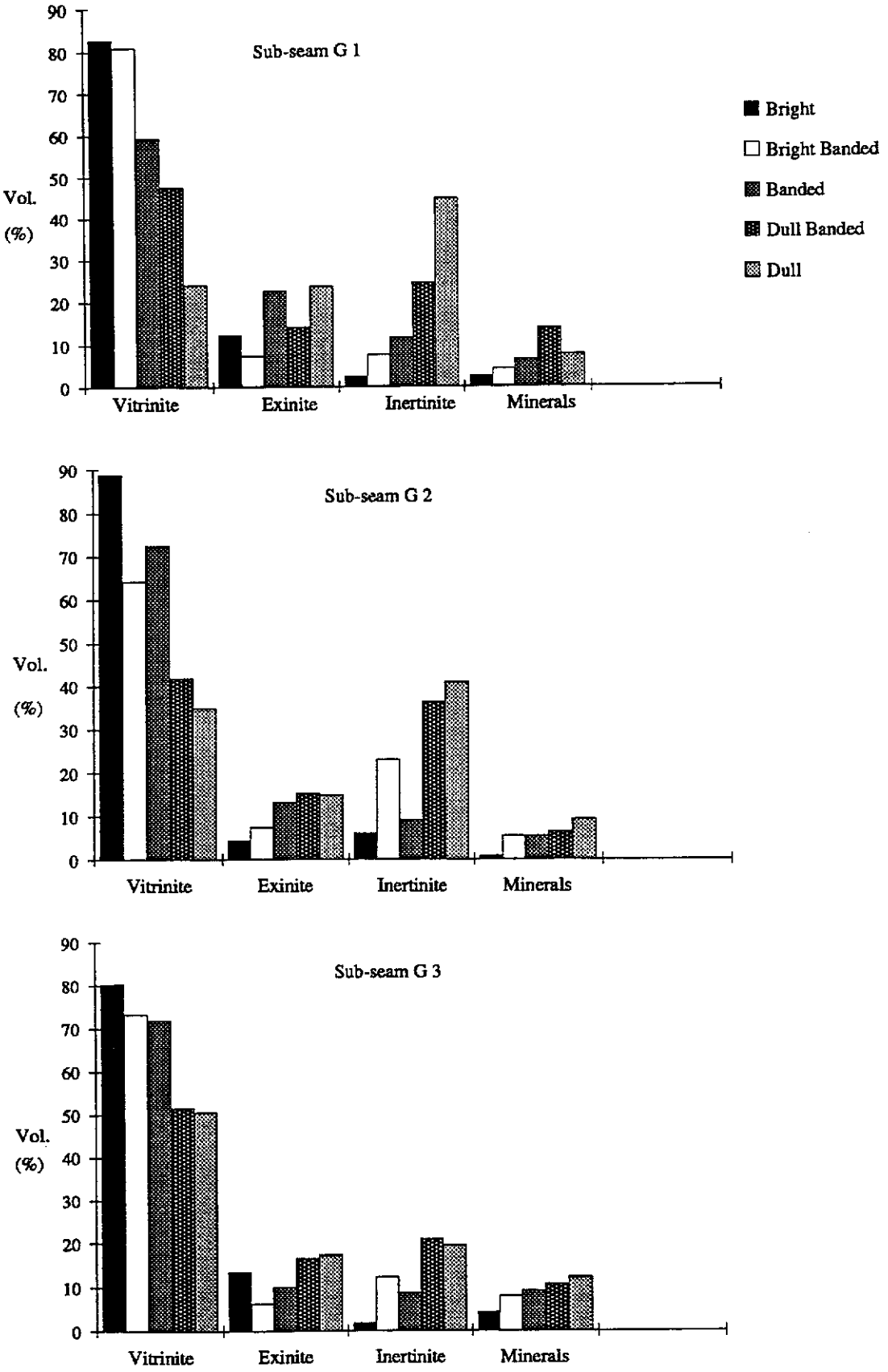

Figure 4.22. Maceral and mineral matter distributions of lithotypes of sub-seams G1, G2 and G3, drill hole CPCH 1.

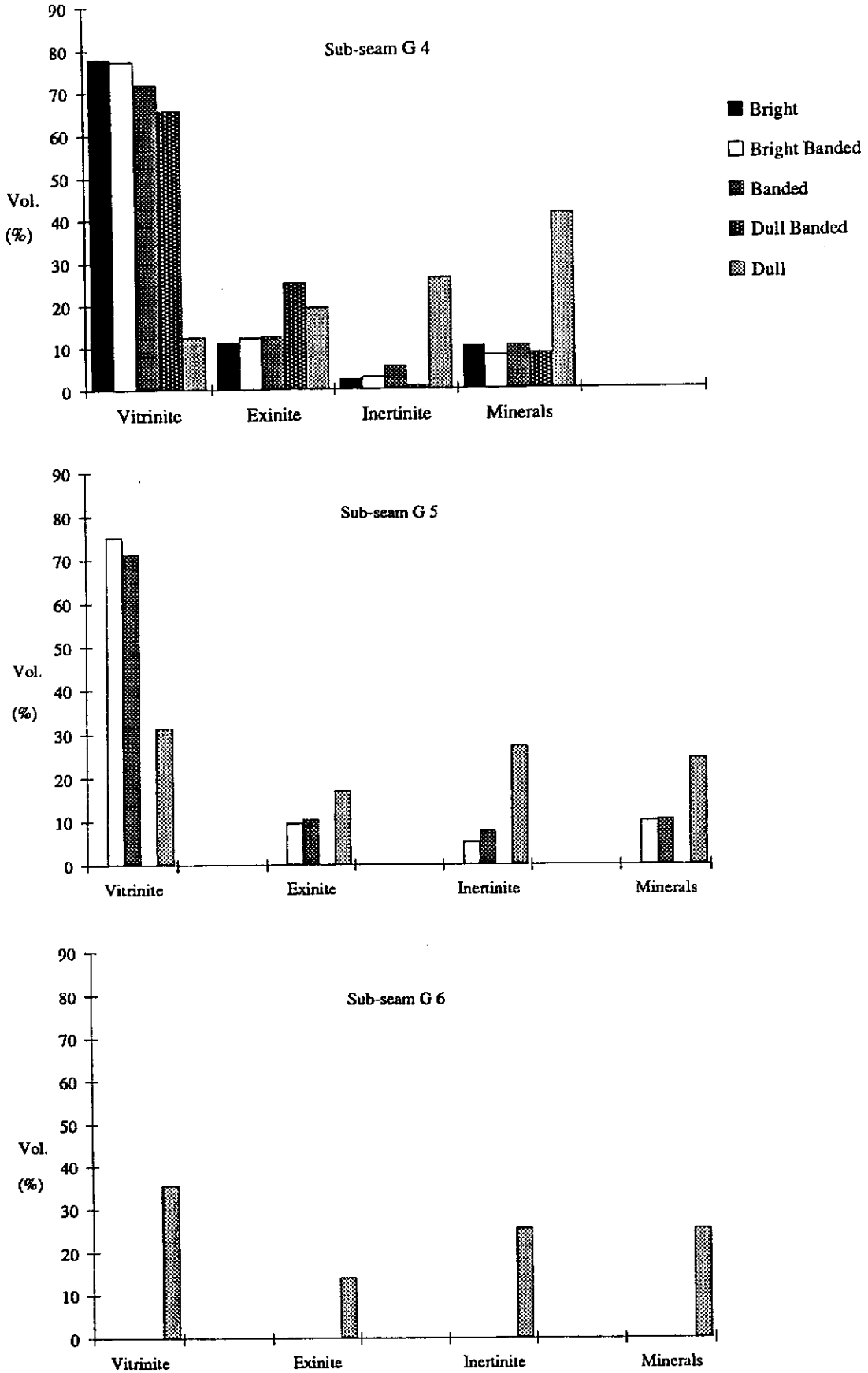

Figure 4.23. Maceral and mineral matter distributions of lithotypes of sub-seams G 4, G 5 and G 6, drill hole CPCH 1.

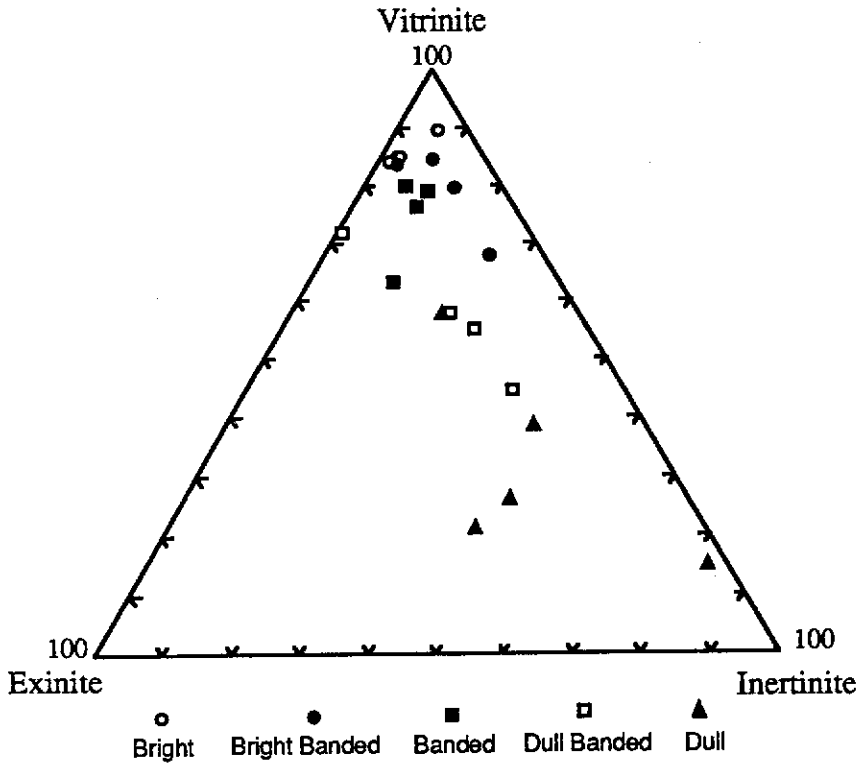

Figure 4.24. Maceral composition of lithotypes (mineral matter free), drill hole CPCH 1.

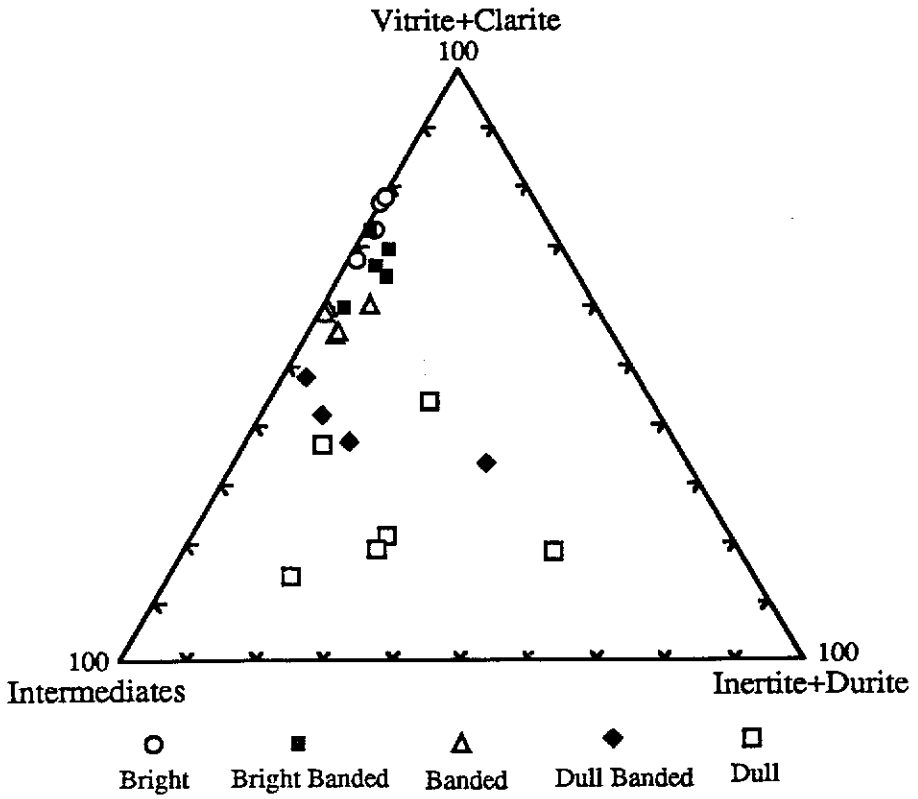

Figure 4.25. Microlithotype composition of coal lithotypes, drill hole CPCH 1.

to dull coal (Table 4.4). Vitrite plus clarite content decreases from bright to dull types, while intermediates and inertite plus durite show a reverse trend. Bright and bright banded lithotypes are characterised by high amounts of vitrite plus clarite, while dull banded and dull coals are dominated by either intermediates or inertite plus durite. Within the banded type, there is a close similarity in content between vitrite plus clarite and intermediates. Inertite plus durite exists as a minor component. Figure 4.25 illustrates a ternary diagram showing microlithotype associations for individual lithotypes. A remarkable overlap occurs between bright and bright banded type, as well as between bright banded and banded types. Hence, there is a similarity between maceral composition and microlithotype association. The brighter lithotype which is dominated by vitrinite content is also dominated by vitrite plus clarite association.

4.5.2. Maceral and Mineral Matter Analyses of CPCH 1, 37, 39 and 47

The data on maceral and mineral matter analyses of all sub-seams from four cores are presented in Table 4.5. The relative content of individual macerals vary considerably within the sub-seams, and are categorised as low, medium and high values. The terms "low", "medium" and "high" for maceral and mineral matter analyses are defined by Hunt and Hobday (1984) and Mishra (1989), and these are :

. Low - Vitrinite and Inertinite < 40.0%
Exinite and Mineral matter < 5.0 %

. Medium - Vitrinite and Inertinite 40.0 - 60.0 %
Exinite and Mineral matter 5.0 - 10.0 %

. High - Vitrinite and Inertinite > 60.0 %
Exinite and Mineral matter > 10.0 %

The Mintaja Block coal has consistently medium to high proportions of vitrinite (44.80 - 73.00 %), a low range of inertinite constituent (10.40 - 24.80 %) and

Table 4. 4 . Microlithotype associations of lithotypes, drill hole CPCH 1.

Sub-Seam	Lithotype	Vitrite+Clarite	Intermediates	Inertite+Durite
G 1	B	75.00	22.00	0.00
	BB	63.80	23.40	4.40
	BD	54.00	39.20	4.00
	DB	34.40	40.60	7.40
	D	17.80	24.80	51.80
G 2	B	71.60	25.60	1.60
	BB	65.00	28.00	4.00
	BD	56.40	37.20	0.60
	DB	29.40	26.00	32.60
	D	13.80	64.20	17.00
G 3	B	67.00	30.60	1.00
	BB	55.60	34.20	3.00
	BD	50.60	36.00	4.00
	DB	33.00	42.20	13.60
	D	19.60	45.40	25.80
G 4	B	72.80	20.00	0.40
	BB	70.20	25.80	0.40
	BD	53.80	36.40	0.60
	DB	43.80	43.80	3.20
	D	12.20	33.20	17.80
G 5	BB	60.80	26.20	3.20
	BD	50.60	27.60	2.40
	D	27.00	38.00	8.40
G 6	D	27.20	20.00	14.60

Table 4. 5 . Maceral and mineral matter analyses of Hill River Coal, Mintaja Block.

Maceral	CPCH 1						CPCH 37					CPCH 39						CPCH 47				
	G 1	G 2	G 3	G 4	G 5	G 6	G 1	G 2	G 3	G 4	G5/6	G 1	G 2	G 3	G 4	G 5	G 6	G 1	G 2	G 3	G 4	G 5
Telinite	0.60	1.00	0.40	0.20	0.20	0.40	0.00	1.00	1.60	0.80	1.00	0.60	1.20	2.20	0.80	1.80	0.20	0.60	1.00	0.40	2.60	2.40
Telocollinite	29.20	35.50	33.00	25.60	29.20	19.60	34.00	37.80	36.20	38.40	30.00	23.80	34.00	37.60	42.20	33.00	28.00	33.40	36.00	39.80	36.80	23.80
Vitrinite A	29.80	36.50	33.30	25.80	29.40	20.00	34.00	38.80	37.80	39.20	31.00	24.40	35.20	39.80	43.00	34.80	28.20	34.00	37.00	40.20	39.40	26.20
Desmocollinite	22.30	20.30	24.00	23.80	22.40	18.60	24.60	23.20	19.40	23.80	23.00	31.20	30.20	26.40	28.80	24.60	23.00	24.60	28.80	21.00	24.00	26.00
Corpocollinite	8.60	5.00	5.40	2.60	3.60	6.20	3.40	2.10	6.00	1.20	1.00	3.00	0.40	1.00	1.20	1.00	0.60	2.00	1.40	3.20	4.00	1.60
Vitrodetrinite	0.30	0.10	0.20	0.00	0.00	0.00	0.20	0.10	0.00	0.00	0.00	0.20	0.00	0.00	0.00	0.00	0.00	0.20	0.00	0.60	0.20	0.00
Vitrinite B	31.20	25.40	29.60	26.40	26.00	24.80	28.20	25.40	25.40	25.00	24.00	34.40	30.60	27.40	30.00	25.60	23.60	26.80	30.20	24.80	28.20	27.60
VITRINITE	61.00	61.90	63.00	52.20	55.40	44.80	62.20	64.20	63.20	64.20	55.00	58.80	65.80	67.20	73.00	60.40	51.80	60.80	67.60	65.00	67.60	53.80
Sporinite	5.30	5.60	8.30	8.60	7.00	5.60	5.80	4.60	5.50	4.60	2.80	6.10	6.40	8.40	8.80	5.80	4.20	5.70	4.80	5.00	5.80	5.20
Cutinite	2.00	0.90	1.10	1.40	2.20	1.00	1.00	0.40	2.10	1.00	1.20	1.50	0.60	0.60	1.40	0.80	1.80	0.60	0.40	1.80	1.40	1.00
Resinite	1.00	0.60	0.70	1.00	0.60	0.20	1.00	0.40	0.60	0.20	0.20	0.40	0.00	0.40	0.20	0.60	0.20	0.60	0.60	0.60	0.00	0.20
Alginite	4.10	4.60	3.40	8.00	5.60	8.20	1.40	1.40	0.60	0.60	2.00	1.00	0.20	0.60	0.20	1.40	1.20	1.50	0.40	0.40	0.60	1.80
Liptodetrinite	0.40	0.10	0.30	1.80	0.60	0.80	0.20	0.00	1.20	0.40	0.40	1.00	0.00	0.20	0.80	0.60	0.20	0.00	0.00	0.00	0.60	0.40
EXINITE	12.80	11.80	13.80	20.80	16.00	15.80	9.40	6.80	10.00	6.80	6.60	10.00	7.20	10.20	11.40	8.20	7.60	8.40	6.20	7.80	8.40	8.60
Semifusinite	10.80	8.90	6.30	8.20	5.40	5.00	9.20	7.60	6.60	6.40	7.60	9.00	10.40	6.40	4.40	5.80	11.60	11.00	8.60	9.80	6.80	7.40
Fusinite	2.50	2.30	1.90	1.20	1.60	1.00	2.00	2.40	4.40	1.60	1.40	3.40	2.40	2.20	0.80	1.80	4.20	3.80	3.00	3.00	3.40	3.00
Sclerotinite	0.10	0.10	0.20	0.00	0.20	0.40	0.40	0.40	0.00	0.20	0.40	0.40	0.00	0.00	0.00	0.40	0.20	0.00	0.00	0.00	0.20	0.00
Macrinite	3.10	3.80	2.10	3.00	1.40	4.00	2.20	1.20	1.40	1.20	1.40	1.80	1.60	1.00	1.00	1.00	1.00	0.80	1.60	1.60	1.00	0.60
Micrinite	0.20	0.50	0.60	0.20	0.40	0.00	0.20	0.60	1.40	0.00	0.40	0.20	0.20	0.00	0.00	0.20	0.00	0.20	0.00	0.60	0.60	0.40
Inertodetrinite	5.00	6.20	4.60	6.00	6.40	5.00	7.00	11.00	7.60	4.80	6.40	10.00	7.00	8.00	4.20	5.00	6.20	8.60	7.60	6.00	5.40	7.00
INERTINITE	21.70	21.80	15.70	18.60	15.40	15.40	21.00	23.20	21.40	14.20	17.60	24.80	21.60	17.60	10.40	14.20	23.20	24.40	20.80	21.00	17.40	18.40
Clay	3.10	2.20	5.80	3.60	9.00	17.60	4.80	2.40	2.20	8.40	14.20	4.00	2.00	2.20	1.00	15.20	10.40	2.60	1.80	3.60	2.00	12.80
Pyrite	1.20	2.30	1.50	4.60	4.00	6.00	1.80	1.80	2.20	5.20	3.80	1.00	1.60	1.80	3.20	1.20	5.20	2.40	2.40	1.80	3.40	5.80
Carbonate	0.00	Trace	0.00	0.00	0.00	0.40	0.20	1.40	1.00	0.80	2.80	1.40	1.60	1.00	1.00	0.80	1.80	1.40	1.20	0.80	1.20	0.60
Quartz	0.20	Trace	0.20	0.20	0.20	0.00	0.60	0.20	0.00	0.40	0.00	0.00	0.20	0.00	0.00	0.00	0.00	0.00	0.00	0.00	0.00	0.00
MINERAL MATTER	4.50	4.50	7.50	8.40	13.20	24.00	7.40	5.80	5.40	14.80	20.80	6.40	5.40	5.00	5.20	17.20	17.40	6.40	5.40	6.20	6.60	19.20
THICKNESS (m)	1.21	4.42	1.33	1.13	0.37	0.07	1.22	4.71	1.28	1.15	0.85	1.48	4.20	1.33	0.95	0.20	0.87	1.39	6.51	1.87	1.14	0.43

medium to high exinite content (6.20 - 20.80 %). Table 4.6 presents maceral distribution on a mineral matter free basis, which is also illustrated in Figure 4.26 and Figure 4.27 in terms of vitrinite, exinite and inertinite macerals. This later figure depicts vitrinite domination over other macerals followed by inertinite. Low to medium "semifusinite ratio" and high "vitrinite content" characterise Mintaja coal (Figure 4.28). However, an exception is present in G4 of CPCH 39, which shows very low "semifusinite ratio", and G6 of CPCH 1 displaying a medium value. Generally, low "semifusinite ratio" dominates Mintaja coal.

The most important maceral group in the coal is the vitrinite, and its content ranges between 44.80 % to 73.00 % or 57.00 % to 77.00 % (mmf). The macerals of this group in order of abundance, are telocollinite, desmocollinite, and corpocollinite. Telocollinite content ranges between 33.80 - 52.60 %, and desmocollinite content is from 9.40 % to 21.20 %. However, there is a low corpocollinite content and this varies from 0.40 % in sub-seam G2 of CPCH 39 to 8.60 % in sub-seam G1 of CPCH 1 (Table 4.5). Telinite occurs in low amounts, and constitutes 0.10 % - 2.60 %, while the vitrodetrinite content is between 0.10 % to 0.60 %. The ratio of vitrinite A to vitrinite B has a value between 0.71 and 1.57 (Table 4.7), and it indicates that the amount of structured vitrinite is higher than non-structured vitrinite. In high vitrinite-subseams, semifusinite and sporinite are always the most abundant inertinite and exinite macerals.

A common characteristic of Mintaja coal is its relatively high exinite content, which varies from 6.20 % to 20.80 %, and the macerals in order of abundance are sporinite, alginite and cutinite . Liptodetrinite and resinite occur in relatively low amounts. Exinite content shows distinct variation in the relative proportion of the individual maceral. Sporinite has a range between 2.80 % to 8.80 % quantitatively, and it is also the dominant maceral of this group; followed by alginite (0.20 % to 8.20 %) and cutinite (0.40 % - 2.20 %). Resinite and liptodetrinite contents range between

Table 4. 6 . Maceral analysis (mineral matter free) of Hill River coal from Mintaja Block.

Drill hole	Sub-Seam	Vitrinite	Exinite	Inertinite
CPCH 1	G 1	63.9	13.4	22.7
	G 2	64.8	12.1	23.1
	G 3	68.1	14.9	17.0
	G 4	57.0	22.7	20.3
	G 5	63.8	18.4	17.8
	G 6	58.9	20.8	20.3
CPCH 37	G 1	67.2	10.1	22.7
	G 2	68.2	7.2	24.6
	G 3	66.8	10.6	22.6
	G 4	75.3	8.0	16.7
	G 5	69.4	8.3	22.3
CPCH 39	G 1	62.7	10.7	26.6
	G 2	69.5	7.6	22.9
	G 3	70.7	10.7	18.6
	G 4	77.0	12.0	11.0
	G 5	72.9	9.9	17.2
	G 6	62.7	9.2	28.1
CPCH 47	G 1	64.9	9.0	26.1
	G 2	71.4	6.5	22.1
	G 3	69.3	8.3	22.4
	G 4	72.4	9.0	18.6
	G 5	66.6	10.6	22.8

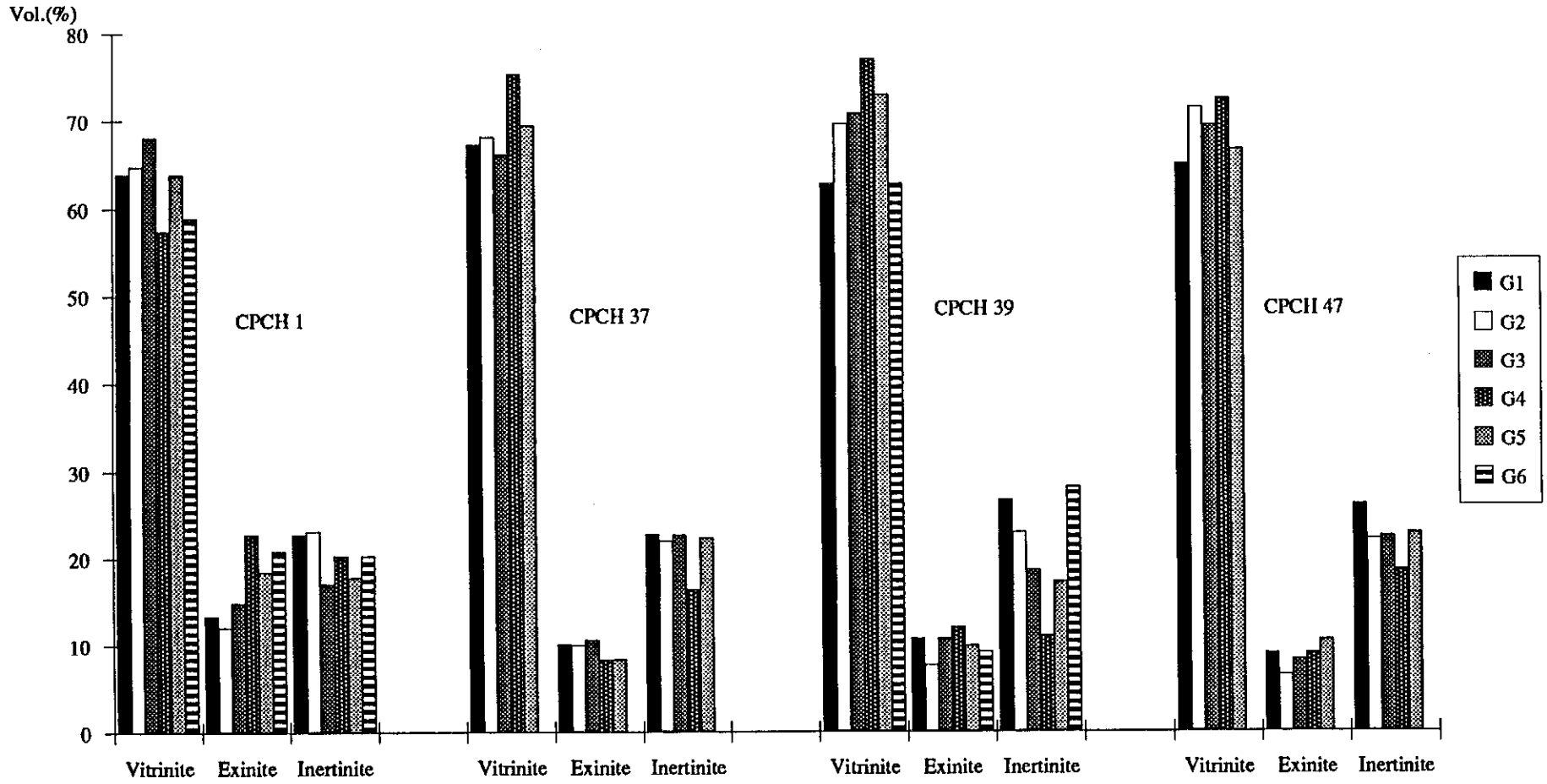

Figure 4.26. Maceral distributions (mineral matter free) of Hill River coal from Mintaja Block.

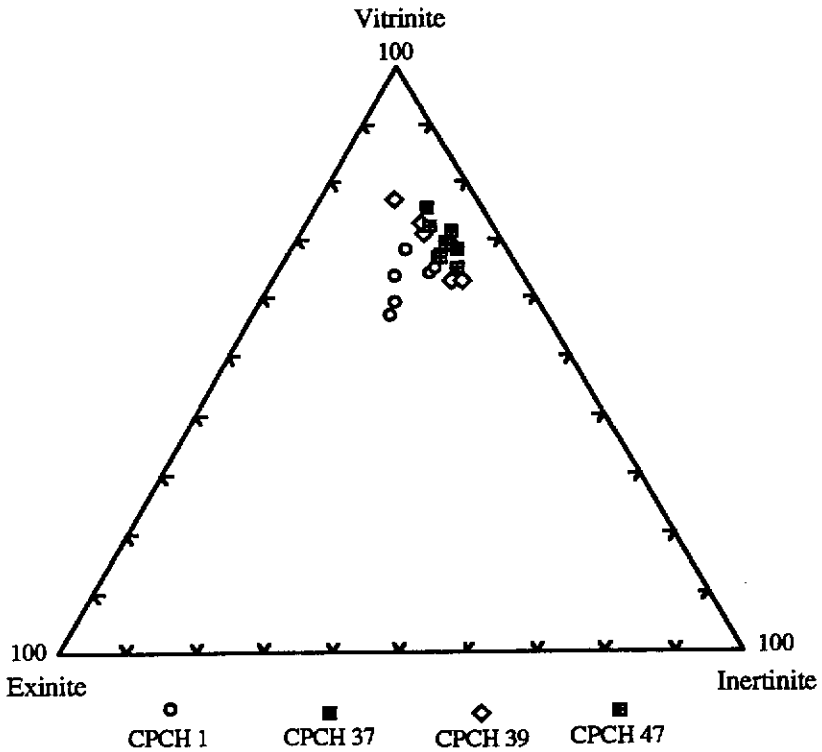

Figure 4.27. Maceral composition (mineral matter free) of Hill River coal, Mintaja Block.

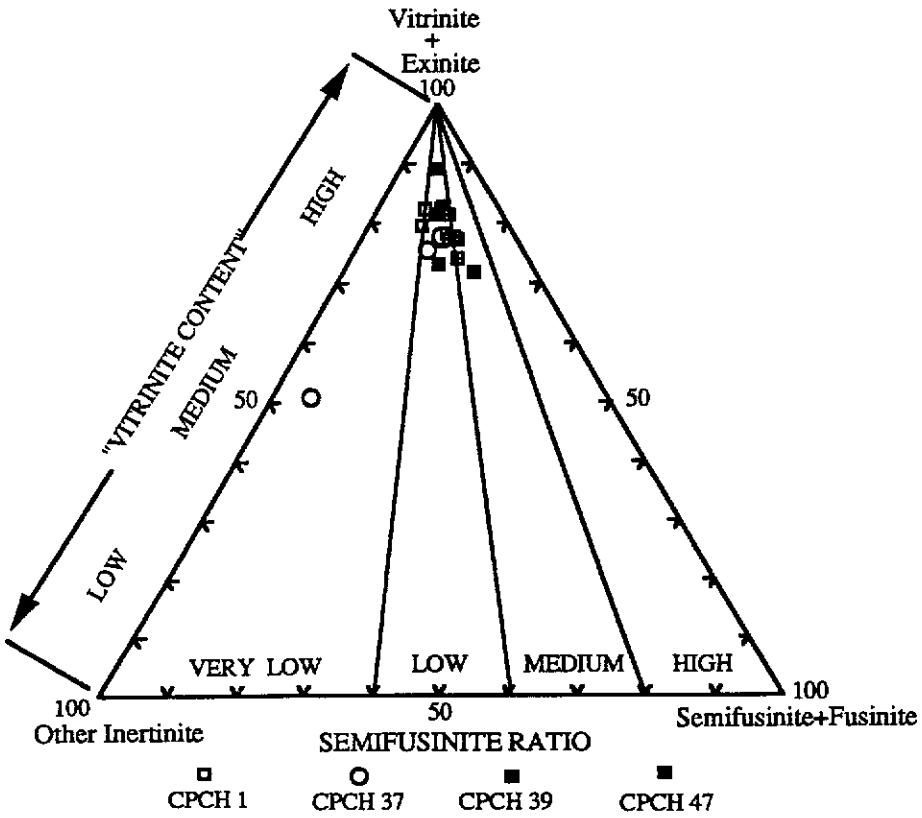

Figure 4.28. Maceral composition diagram of Hill River coal from Mintaja Block showing "vitrinite content" and "semifusinite ratio".

Table 4. 7. Petrographic indices of Hill River coal from Mintaja Block.

Borehole	Sub-Seam	A/B	T/F	SF/F	W/D	GI	TPI
CPCH 1	G 1	0.95	2.24	4.32	3.22	3.50	1.11
	G 2	1.44	3.26	3.87	3.27	3.77	1.35
	G 3	1.13	4.06	3.31	2.77	5.10	1.15
	G 4	0.98	2.74	6.83	2.00	3.58	0.99
	G 5	1.13	4.20	3.37	2.46	4.24	1.08
	G 6	0.81	3.33	5.00	1.78	4.44	0.77
CPCH 37	G 1	1.21	3.70	4.60	2.88	3.54	1.22
	G 2	1.53	3.88	3.17	2.90	3.10	1.30
	G 3	1.49	3.43	1.50	3.37	3.47	1.42
	G 4	1.57	4.90	4.00	4.45	5.11	1.52
	G 5	1.29	3.44	5.43	3.77	3.70	1.26
CPCH 39	G 1	0.71	1.97	2.65	2.07	2.70	0.80
	G 2	1.15	2.75	4.33	3.20	3.40	1.22
	G 3	1.45	4.63	2.91	2.78	4.10	1.22
	G 4	1.43	8.27	5.50	3.44	7.80	1.37
	G 5	1.36	4.58	3.22	3.59	4.80	1.34
	G 6	1.19	1.78	2.76	3.86	2.40	1.43
CPCH 47	G 1	1.30	2.30	2.89	3.23	2.63	1.36
	G 2	1.22	3.19	2.87	3.47	3.60	1.23
	G 3	1.60	3.14	3.27	4.21	3.50	1.67
	G 4	1.40	3.86	2.00	4.07	4.40	1.44
	G 5	0.95	2.52	2.47	2.86	3.13	1.04

A/B = Telinite+Telocollinite/Remaining Vitrinite
SF/F = Semifusinite/Fusinite
T/F = Telinite+Telocollinite/Semifusinite+Fusinite
W/D = Telinite+Telocollinite+Semifusinite+Fusinite/Inertodetrinite+Macrinite+Sporinite
TPI = Telinite+Telocollinite+Semifusinite+Fusinite/Desmocollinite+Corpocollinite+Macrinite+ Inertodetrinite
GI = Vitrinite+Macrinite/Semifusinite+Fusinite+Inertodetrinite

0.20 % to 1.00 % and 0.10 % - 1.80 % , respectively (Table 4.5). Assessment of the alginite content was carried out under both normal reflected light and ultra-violet excitation. The ternary diagram shown in Figure 4.29, illustrates the composition of exinite macerals of coal from individual sub-seams based on the three types of exinite macerals. These are, sporinite, cutinite and other exinite (alginite, resinite and liptodetrinite). This diagram shows that exinite maceral is dominated by sporinite, while other exinite is the second abundance.

The inertinite content in the Mintaja Block coal has an intermediate value between 10.40 % and 24.80 % (Table 4.5) or 11.00 % and 28.10 % on a mineral matter free basis (Table 4.6). The highest inertinite content (inertodetrinite and semifusinite) is recorded in sub-seam G1 of CPCH 39. The fusinite is relatively low, with amounts of 0.40 % to 4.40 %, and with the semifusinite content between 5.00 % - 11.60 %. This is always higher than fusinite content. The fusinite and semifusinite probably appear to be formed mainly from the degradation and oxidation process of humic substances. The macrinite shows a range of 0.60 % to 4.00 %, while sclerotinite and micrinite are very low constituents in the coal, having contents of 0.10 % - 0.40 % and 0.20 % - 1.40 %, respectively. Figure 4.30 depicts a ternary diagram of inertinite composition of individual sub-seams of the Mintaja Block, in terms of three apices representing semifusinite, fusinite and other inertinite (inertodetrinite, macrinite, micrinite, and sclerotinite). The semifusinite and other inertinite macerals are dominant in the coal, in comparison to fusinite. The semifusinite ratio of coal in Mintaja Block, is illustrated in Figure 4.28, which is in the range of very low to medium, with the majority in the low category. The low to medium ratio is evidence of lower oxidation of the coal in the Mintaja block. From the maceral analyses, petrographic indices such as the ratio of vitrinite A over vitrinite B (A/B), the Gelification Index (GI), the Tissue Preservation Index (TPI), Wood Ratio (W/D), and the ratio of structured vitrinite to structured inertinite (T/F) are calculated , and shown in Table 4.7. The value of TPI of Mintaja Block coal occupies a compositional

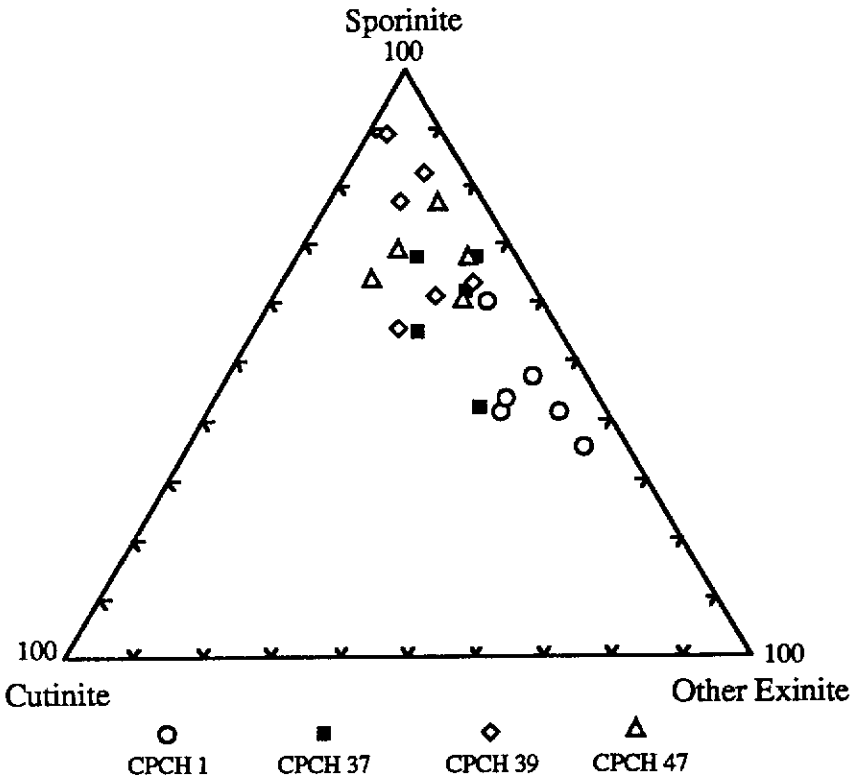

Figure 4.29. Composition of exinite group, Hill River coal, Mintaja Block.

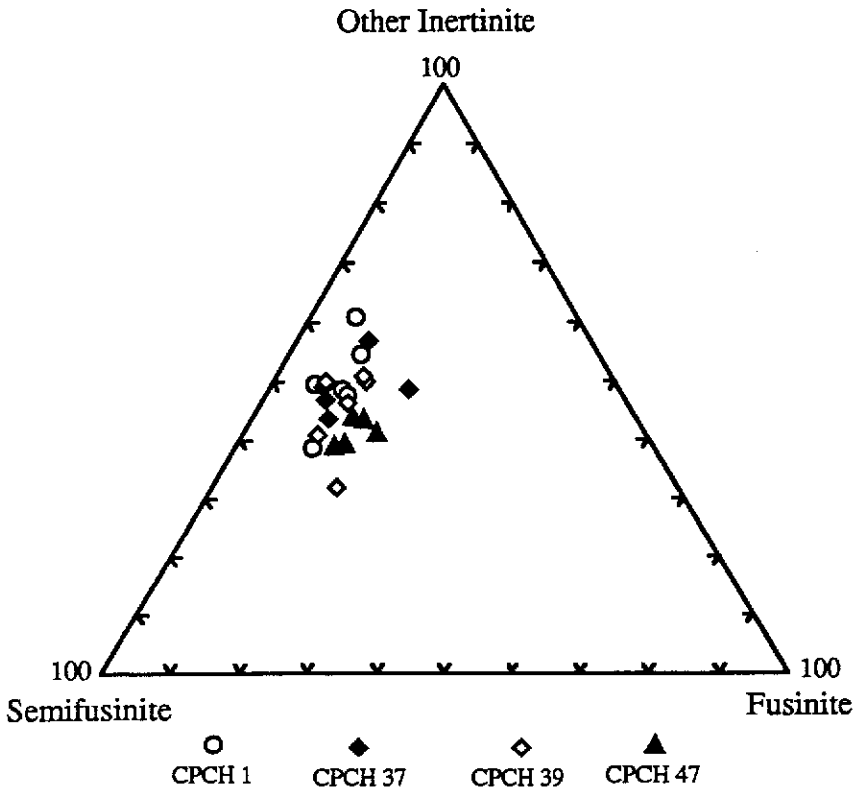

Figure 4.30. Composition of inertinite group, Hill River coal, Mintaja Block.

zone around 0.77 - 1.67 which indicates that well preserved plant tissues are present in the coal, which is also supported by the high value of the wood ratio ranging from 2.00 to 4.45. The GI, showing values between 2.40 to 7.80 supported by a high T/F value which ranges between 1.78 to 8.27, indicates that Mintaja Block coal has a low degree of oxidation .

The maceral variations (mineral matter-free basis) of the sub-seams are depicted in Figures 4.31 to 4.34. These figures illustrate four core profiles, and exhibit that the vitrinite and inertinite contents show remarkable variation. The increase in vitrinite content is marked by the decrease in the inertinite content. Thus the vitrinite content varies inversely to the inertinite content. In sub-seams G3 - G6 of CPCH 1, G2 - G5 of CPCH 37, G1 - G2 of CPCH 39 and G1 - G3 of CPCH 47, the vitrinite contents vary inversely against the exinite contents. The variations of "vitrinite content" and the "semifusinite ratio" of all sub-seams of the four cores, are also illustrated in Figures 4.31 to 4.34. In general, all sub-seams are occupied by coals of low to medium "semifusinite ratio". Within CPCH 1, the lowest semifusinite ratio is present in G6, while the highest one is in G1. In CPCH 37, the highest value occurs within G4, whereas the lowest is within G2. The lowest ratio in CPCH 39 occurs within G3 and the highest is in G6. Moreover, in CPCH 47, the lowest ratio is in G5 and the highest one within G3. The decrease in "vitrinite content" compensated by an increase in "semifusinite ratio", characterises CPCH 39 and 47, whereas, in CPCH 1 and 39, the increase in "vitrinite content" is followed by an increase in the "semifusinite ratio". The "semifusinite ratio" of the four boreholes, predominantly is of low degree. However, it ranges from low to medium. This low to medium "semifusinite ratio" with a high "vitrinite content" characteristic is in agreement with the value of "semifusinite ratio" and "vitrinite content" plotted on a ternary diagram (Figure 4.28).

The vertical and lateral variations of maceral groups and mineral matter contents of

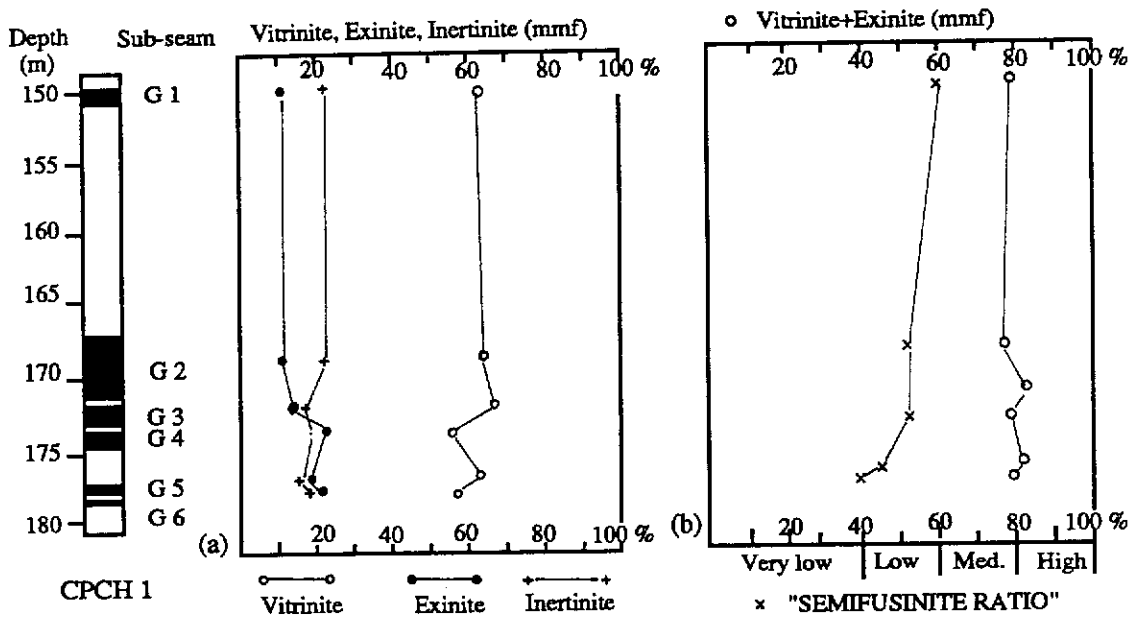

Figure 4.31. (a) Variation in vitrinite, exinite and inertinite, and (b) variation of "vitrinite content" and the "semifusinite ratio" of sub-seams G1 - G6 of Hill River coal, drill hole CPCH 1 from Mintaja Block.

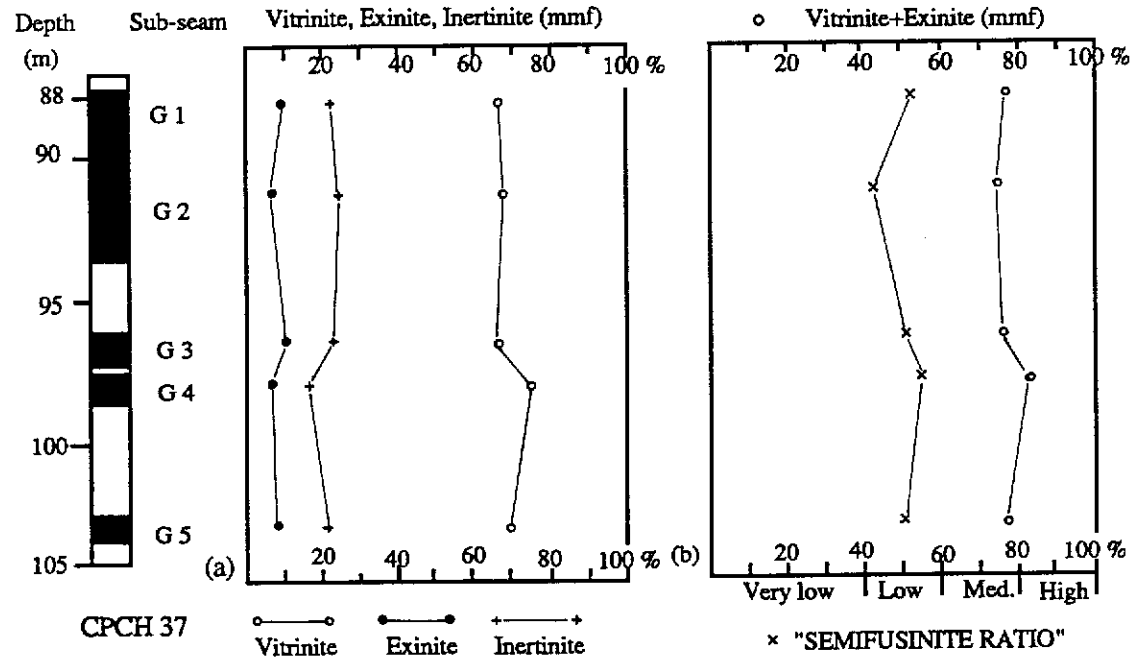

Figure 4.32. (a) Variation in vitrinite, exinite and inertinite, and (b) variation of "vitrinite content" and the "semifusinite ratio" of sub-seams G1 - G5 of Hill River coal, drill hole CPCH 37 from Mintaja Block.

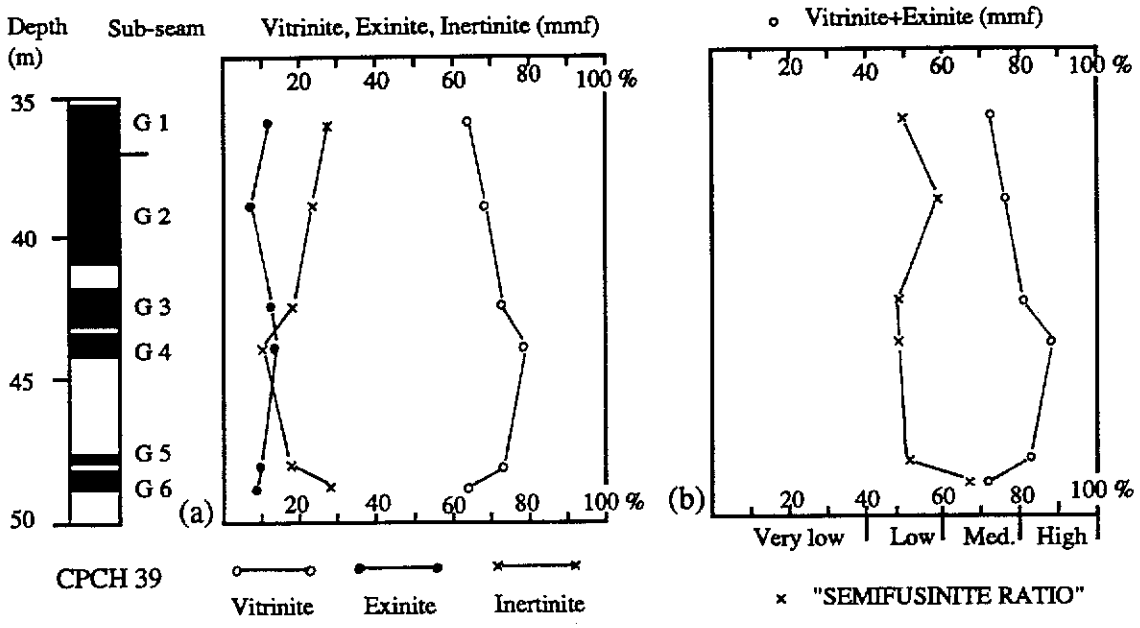

Figure 4.33. (a) Variation in vitrinite, exinite and inertinite, and (b) variation of "vitrinite content" and the "semifusinite ratio" of sub-seams G1 - G6 of Hill River coal, drill hole CPCH 39 from Mintaja Block.

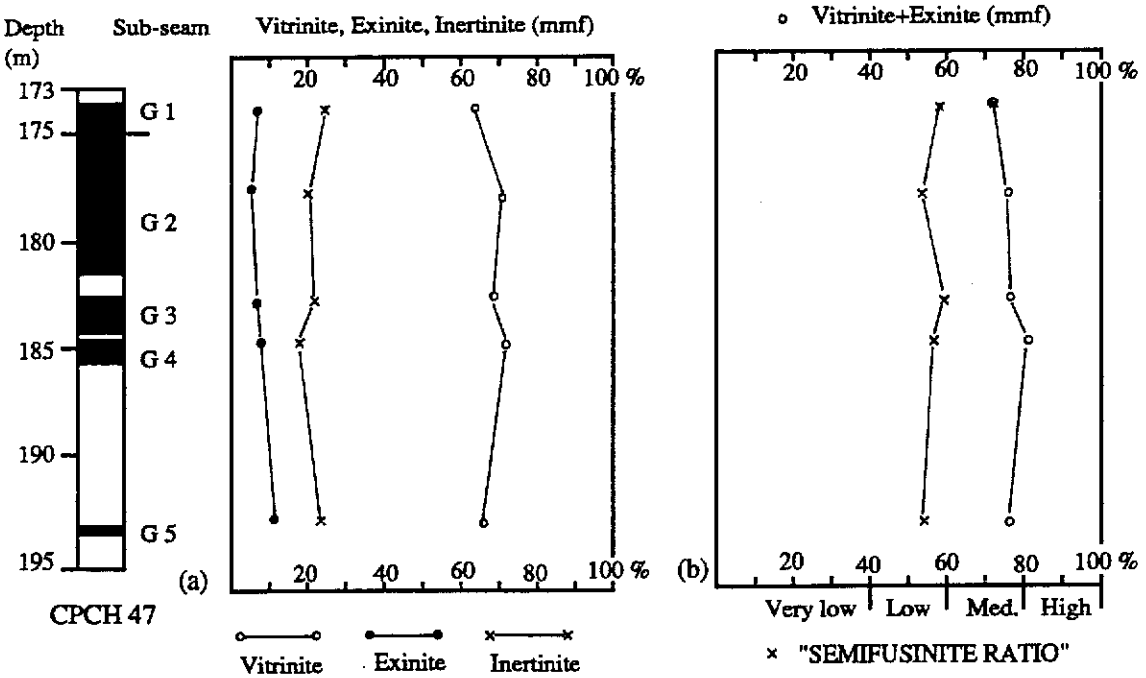

Figure 4.34. (a) Variation in vitrinite, exinite and inertinite , and (b) variation of "vitrinite content" and the "semifusinite ratio" of sub-seams G1 - G5 of Hill River coal, drill hole CPCH 47 from Mintaja Block.

the Mintaja Block coal are illustrated in Figures 4.35. Vertically, vitrinite content in all cores decreases in abundance downward, except within G1 to G2. The exinite content does not show remarkable variation from one sub-seam to another. The inertinite content is varied in the sub-seams, however the mineral matter content increases from G1 to G6. The variation is attributed to the variation in depositional environment of the individual sub-seam.

The lateral variation of macerals in the Mintaja Block coal can be observed within sub-seam G1 to G6 in drill holes CPCH 1 and 39, and G1 to G5 in drill holes CPCH 37, in SE to NW directions. In general, the abundance of each maceral group and mineral matter in each sub-seam varies to a limited extent. However, there is a maceral content deviation occurring in sub-seams G2 of CPCH 47, sub-seam G4, G5 and G6 of CPCH 1. In sub-seam G1, the lateral variation of maceral content does not show a marked trend. It displays a similar pattern from SE to NW areas, which indicates that coal-precursor deposition in all drill holes had a similar condition, consistent with a relatively constant water table. Within sub-seam G2 of drill holes CPCH 1, 39 and 37, a similar pattern occurs. However, in CPCH 47, the exinite content is higher, which is compensated for by a lower content of vitrinite, compared to other drill holes. It reflects the idea that a lowered water table has occurred, which leads to the higher degree of oxidation within the peat. Furthermore, there was either a floral change or an increased contribution of plants forming undergrowth around drill hole CPCH 47 which produced more spores. The sub-seam G3 is characterised by a similar condition throughout the drill holes. The fluctuation in the exinite content from SE to NW areas, characterises sub-seam G4. A low content of vitrinite macerals in drill hole CPCH 1 is probably due to a decrease in woody plants in the SE area of Mintaja Block. Within sub-seam G5, the similarity in vitrinite and exinite contents in all drill holes may indicate that the water table and oxidation or decomposition process from SE to NW areas were relatively constant. However, in drill hole CPCH 1 exinite content is much higher than in the other three drill holes. Probably it reflects a change in plant community around this location. The sub-seam

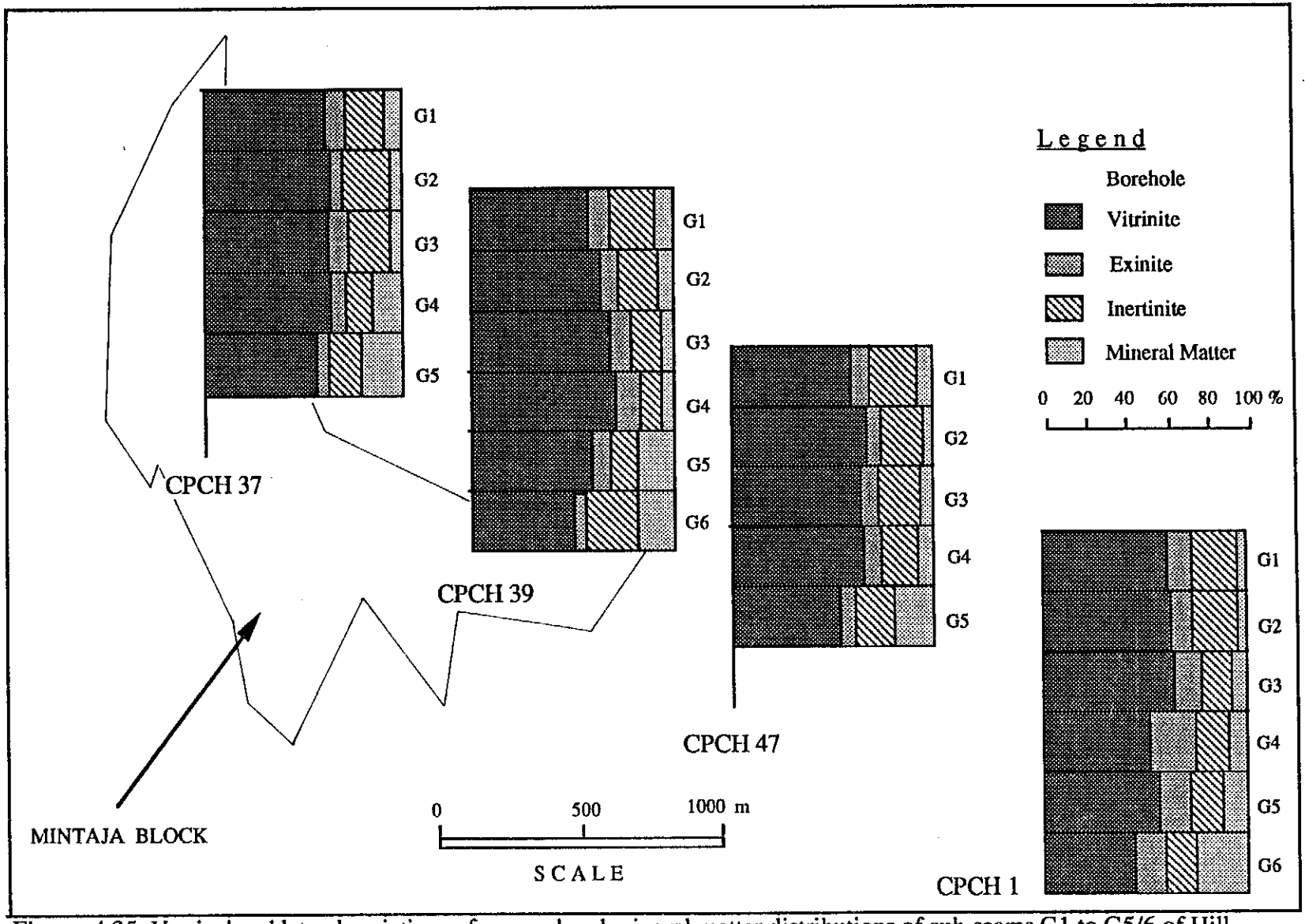

Figure 4.35. Vertical and lateral variations of maceral and mineral matter distributions of sub-seams G1 to G5/6 of Hill River coal in Mintaja Block.

G6 is only recognised in drill holes CPCH 1 and 39. These two drill holes show a difference in the content of individual maceral groups. The vitrinite and inertinite content of CPCH 1 is lower than that of CPCH 39, while exinite value is higher. This condition may be due to a difference in the type of depositional environment. It suggests that CPCH 1 is dominated by a continuously shallow/sub aerial flooding which also leads to the deposition of a high content of mineral matter.

4.5.3. Maceral and Mineral Matter Distribution in Coal Size Fractions (CPCH 1)

Table 4.8 shows maceral analyses of coal size fractions and distribution of mineral matter in sub-seams G1 to G5/6 from borehole CPCH 1, which is also depicted in Figures 4.36 and 4.37 . In all size fractions of the sub-seams, the increase in vitrinite content is marked by the corresponding decrease in inertinite content. Overall, the exinite content decreases with the decrease in size fractions from > 4 mm to < 1/4 mm. The mineral matter content is greater in finer size fractions in comparison to the coarse ones.

4.5.4. Microlithotype Analysis of CPCH 1, 37, 39 and 47

Microlithotype analysis is used to identify specific environment of peat deposition, Teichmuller and Thompson (1958), Hacquebard and Donaldson (1969), and Teichmuller (1982). The coal type may not be related to the sedimentary environment, but to the extent of wetness of the environment , Stavrakis and Smyth (1991).

The typical microlithotypes observed in the coal comprise vitrite, vitrinite-rich clarite (clarite-V),inertite, duroclarite, trimacerites, vitrinite-rich vitrinertite (vitrinertite-V),

Table 4. 8. Maceral and mineral matter analyses of size fractions of drill hole CPCH 1

Sub-Seam	Size Fraction (mm)	Vitrinite	Exinite	Inertinite	Mineral Matter
G 1	> 4	51.40	18.20	21.80	8.60
	4 X 2	47.80	18.60	22.80	10.80
	2 X 1	54.40	13.60	21.60	10.40
	1 X 1/2	52.00	10.20	26.80	11.00
	1/2 X 1/4	53.40	10.60	25.80	10.20
	< 1/4	54.00	7.40	34.00	4.60
G 2	> 4	58.60	15.00	18.40	8.00
	4 X 2	61.40	12.40	18.40	7.80
	2 X 1	62.40	9.80	23.60	4.20
	1 x 1/2	58.20	10.20	25.20	6.40
	1/2 x 1/4	58.20	6.80	30.00	5.00
	< 1/4	56.20	8.20	29.00	6.60
G 3	> 4	61.20	14.40	18.00	6.40
	4 X 2	64.40	11.40	15.20	9.00
	2 X 1	60.00	11.80	22.80	5.40
	1 X 1/2	62.80	7.20	20.60	9.40
	1/2 X 1/4	63.40	10.40	20.40	5.80
	< 1/4	58.60	8.40	26.00	7.00
G 4	> 4	49.60	17.00	16.20	17.20
	4 X 2	56.00	12.20	15.20	16.60
	2 X 1	49.80	13.20	20.60	16.40
	1 x 1/2	54.00	11.20	19.20	15.60
	1/2 X 1/4	55.60	15.40	17.60	11.40
	<1/4	53.40	9.80	20.80	16.00
G 5/6	> 4	44.00	20.00	15.80	20.20
	4 X 2	53.20	16.60	17.20	13.00
	2 X 1	52.60	14.20	19.40	13.80
	1 X 1/2	51.60	11.40	15.60	21.40
	1/2 x 1/4	53.60	13.00	14.00	19.40
	< 1/4	54.40	14.20	17.20	14.20

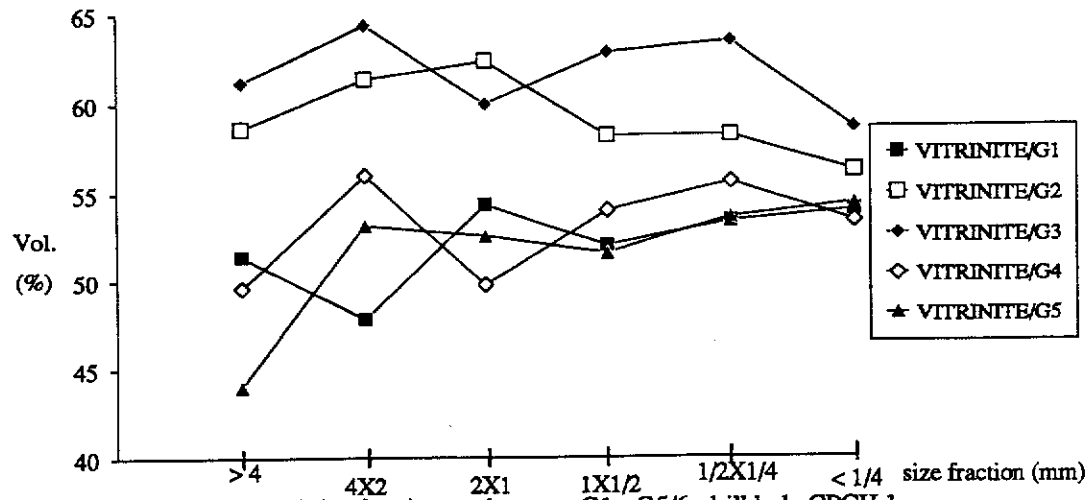

a. Vitrinite content of size fractions, sub-seams G1 - G5/6, drill hole CPCH 1.

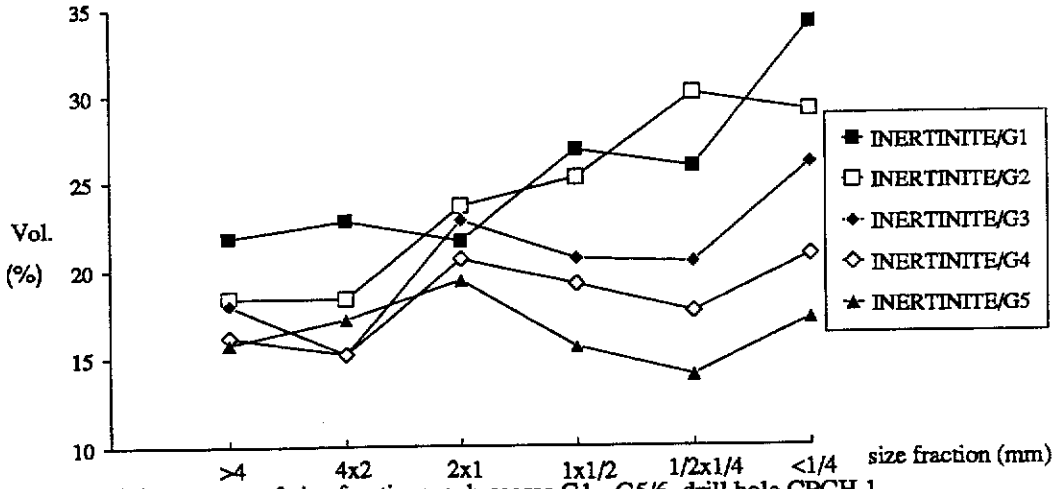

b. Inertinite content of size fractions, sub-seams G1 - G5/6, drill hole CPCH 1.

Figure 4.36. Vitrinite and inertinite content variations of size fractions, sub-seams G1 - G5/6, drill hole CPCH 1.

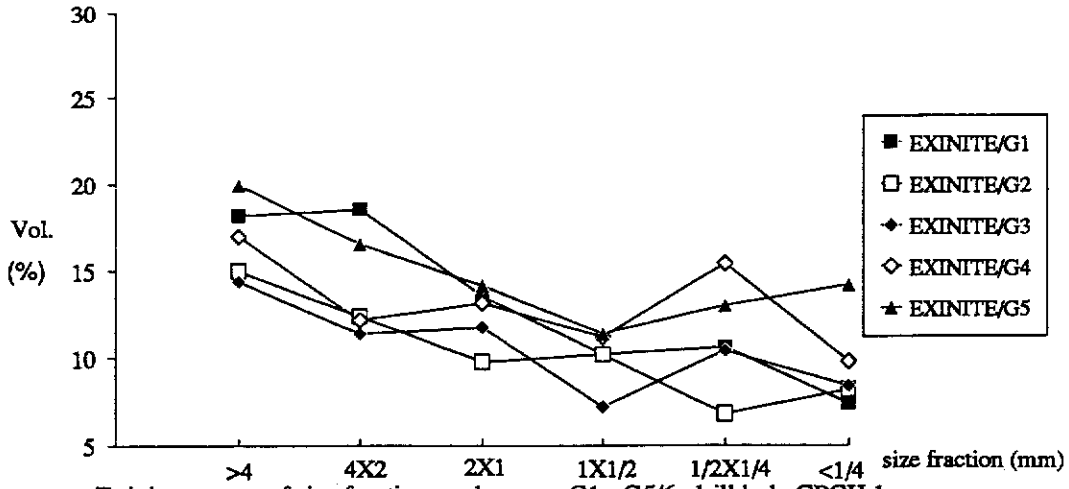

a. Exinite content of size fractions, sub-seams G1 - G5/6, drill hole CPCH 1.

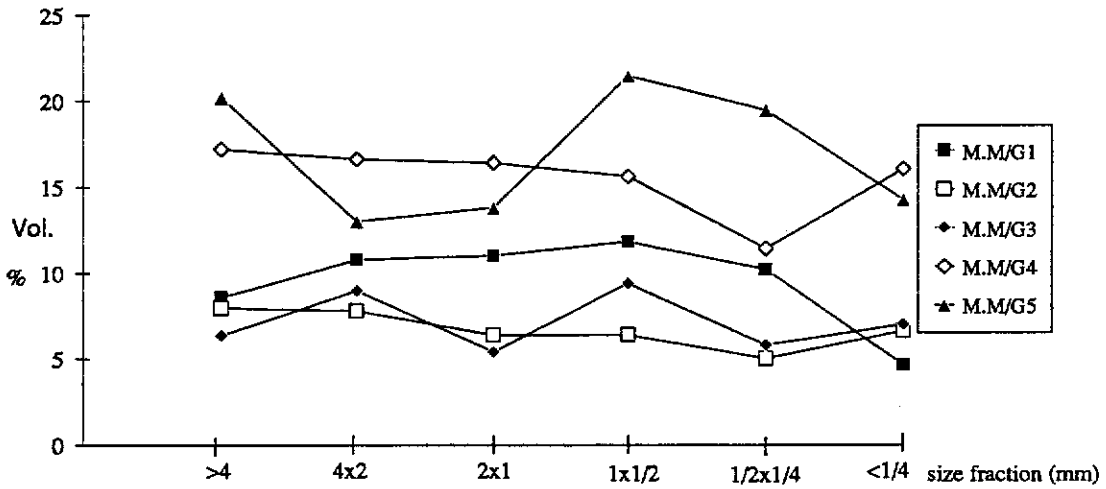

b. Mineral matter content of size fraction, sub-seams G1-G5/6, drill hole CPCH 1.

Figure 4.37. Exinite and mineral matter content variations of size fractions, sub-seams G1 - G5/6, drill hole CPCH 1.

and clarodurite. The liptite occurs in low amount in the coal. The carbominerite is dominated by carbargilite and carbopyrite. In terms of concentration, the coal of the Mintaja Block consists of mostly vitrite+clarite .

Vitrite, duroclarite and clarite are the major microlithotypes occurring in the Mintaja Block coal (Table 4.9), and their contents range between 25.20 % and 45.50 %, 13.20 % to 37.80 %, and 2.80 % to 13.80 %, respectively. These are followed by inertite ranging between 3.80 % and 12.80 %, and vitrinertite with a range of 3.40 % to 11.40 %. The subordinate microlithotypes are liptite, durite, vitrinertoliptite and clarodurite which occur within the range of 0.10 % to 3.0 %. The carbominerites predominantly comprise carbargilite and carbopyrite. Range of carbargilite content is between 4.30 % and 21.20 %, while carbopyrite shows a value of around 0.40 % to 8.60 %. Carbankerite and carbosilicate display a nearly similar amount, which range from 0.10 % to 0.60 %.

The microlithotype composition of Mintaja Block coal is listed in Table 4.10 and also plotted in a ternary diagram. The apices consist of three components, which are vitrite+clarite, intermediates and inertite+durite (Figure 4.38). Most of the sub-seams are dominated by the microlithotypes vitrite+clarite with amounts of more than 50 %. In general, sub-seams containing high trimacerite content, also have high a inertinite content.

In Figure 4.39 microlithotype and carbominerite compositions are illustrated for the individual boreholes. Generally, the abundance of vitrite+clarite varies downward through the borehole, and in CPCH 47, it shows a slight decrease downward from G1 to G5, and from G2 to G4 of CPCH 1, and G2 to G 5 of CPCH 37. The vertical distribution of intermediates also shows a similar variation. It has an almost similar amount with small variations throughout the sub-seams and shows a reverse trend which is concomitant with the vitrite+clarite composition. However, the lowest sub-

Table 4. 9 . Microlithotype analyses of Hill River coal from Mintaja Block.

Drill hole	Sub-Seam	Vitrite	Liptite	Inertite	Clarite	Durite	Vitrinertite	Duroclarite	Vitrinerto-liptite	Clarodurite	Carbopyrite	Carbargillite	Carbo-minerite
CPCH 1	G 1	35.60	0.50	6.20	12.90	0.30	8.90	24.20	0.10	0.00	0.90	9.20	10.40
	G 2	45.50	0.10	9.40	3.80	0.20	8.40	25.70	0.40	1.00	0.90	4.30	5.50
	G 3	39.60	0.00	4.90	3.30	0.20	8.40	33.60	1.10	3.00	1.40	4.30	5.90
	G 4	25.20	0.20	4.20	13.80	1.20	3.40	37.80	2.60	1.80	3.00	6.80	9.80
	G 5	39.00	0.00	5.20	8.40	0.00	10.60	22.40	0.40	0.60	6.60	6.80	13.40
	G 6	36.40	0.00	10.00	2.80	0.40	5.20	13.40	0.40	1.60	8.60	21.20	29.80
CPCH 37	G 1	36.80	0.00	9.00	8.80	0.80	8.40	23.00	2.20	2.00	2.60	6.00	9.00
	G 2	42.20	0.60	12.20	5.40	0.00	6.20	22.60	0.40	1.40	1.20	7.40	9.00
	G 3	44.00	0.40	8.80	7.80	0.40	6.20	23.60	1.00	1.40	1.20	5.00	6.40
	G 4	34.40	0.40	3.80	13.20	0.20	5.40	26.20	0.20	1.20	3.80	11.00	16.20
	G 5	38.40	0.20	9.40	2.60	0.40	10.00	16.40	0.00	0.40	5.20	17.00	22.20
CPCH 39	G 1	31.40	0.20	12.80	6.80	2.00	8.60	24.60	1.40	2.20	0.40	9.60	10.00
	G 2	42.00	0.20	7.60	9.00	0.40	8.60	20.80	0.40	1.40	1.40	7.60	9.60
	G 3	35.60	1.00	11.00	3.80	1.40	6.80	29.20	2.00	0.40	2.40	6.00	8.80
	G 4	42.80	0.20	5.60	11.60	0.80	7.80	20.40	0.40	0.80	3.20	6.40	9.80
	G 5	34.20	0.40	4.60	5.40	0.20	6.40	24.80	1.20	0.40	1.60	20.60	22.40
	G 6	35.60	0.00	12.60	5.40	0.20	6.80	15.60	0.40	1.20	3.00	19.20	22.20
CPCH 47	G 1	45.20	0.40	12.00	3.20	0.20	11.40	13.20	0.80	1.00	2.80	9.40	12.60
	G 2	44.00	0.40	12.60	4.00	0.00	8.20	18.00	1.20	2.40	2.40	6.40	9.20
	G 3	43.20	0.00	12.80	5.20	0.20	10.40	17.00	0.60	1.20	3.00	6.40	9.40
	G 4	42.20	0.60	6.80	9.40	0.00	6.40	18.00	2.40	1.80	6.40	5.80	12.60
	G 5	35.40	0.00	8.80	5.80	0.00	7.00	15.60	1.00	1.60	6.60	18.20	24.80

Table 4.10 . Microlithotype compositions of Hill River coal from Mintaja Block.

Drill hole	Sub-Seam	Vitrite+Clarite	Intermediates	Inertite+Durite
CPCH 1	G 1	54.40	38.30	7.30
	G 2	52.20	37.60	10.20
	G 3	45.60	49.00	5.40
	G 4	43.30	50.70	6.00
	G 5	54.70	39.30	6.00
	G 6	55.80	29.30	14.90
CPCH 37	G 1	50.10	39.10	10.80
	G 2	52.60	33.80	13.60
	G 3	55.60	34.50	9.90
	G 4	57.10	38.10	4.80
	G 5	52.80	34.50	12.70
CPCH 39	G 1	42.50	41.00	16.50
	G 2	56.50	34.60	8.90
	G 3	44.10	42.10	13.80
	G 4	60.40	32.40	7.20
	G 5	50.30	43.50	6.20
	G 6	52.70	30.80	16.50
CPCH 47	G 1	55.60	30.30	14.10
	G 2	53.10	33.00	13.90
	G 3	53.40	32.20	14.40
	G 4	59.40	32.70	7.90
	G 5	54.80	33.50	11.70

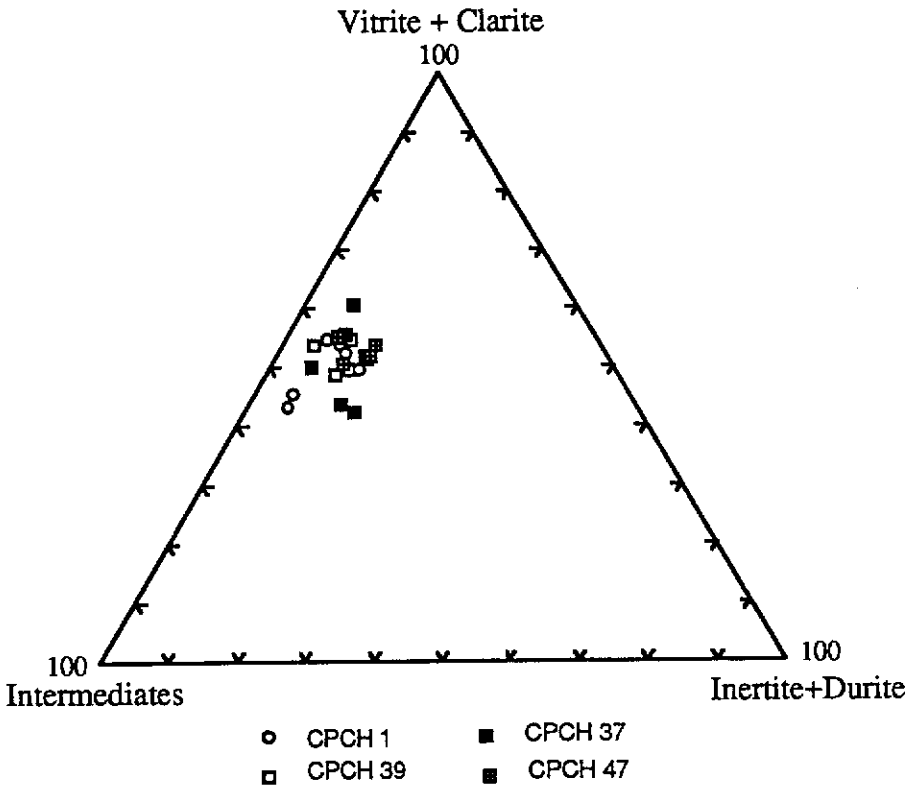

Figure 4.38. Microlithotype composition of Hill River coal from Mintaja Block.

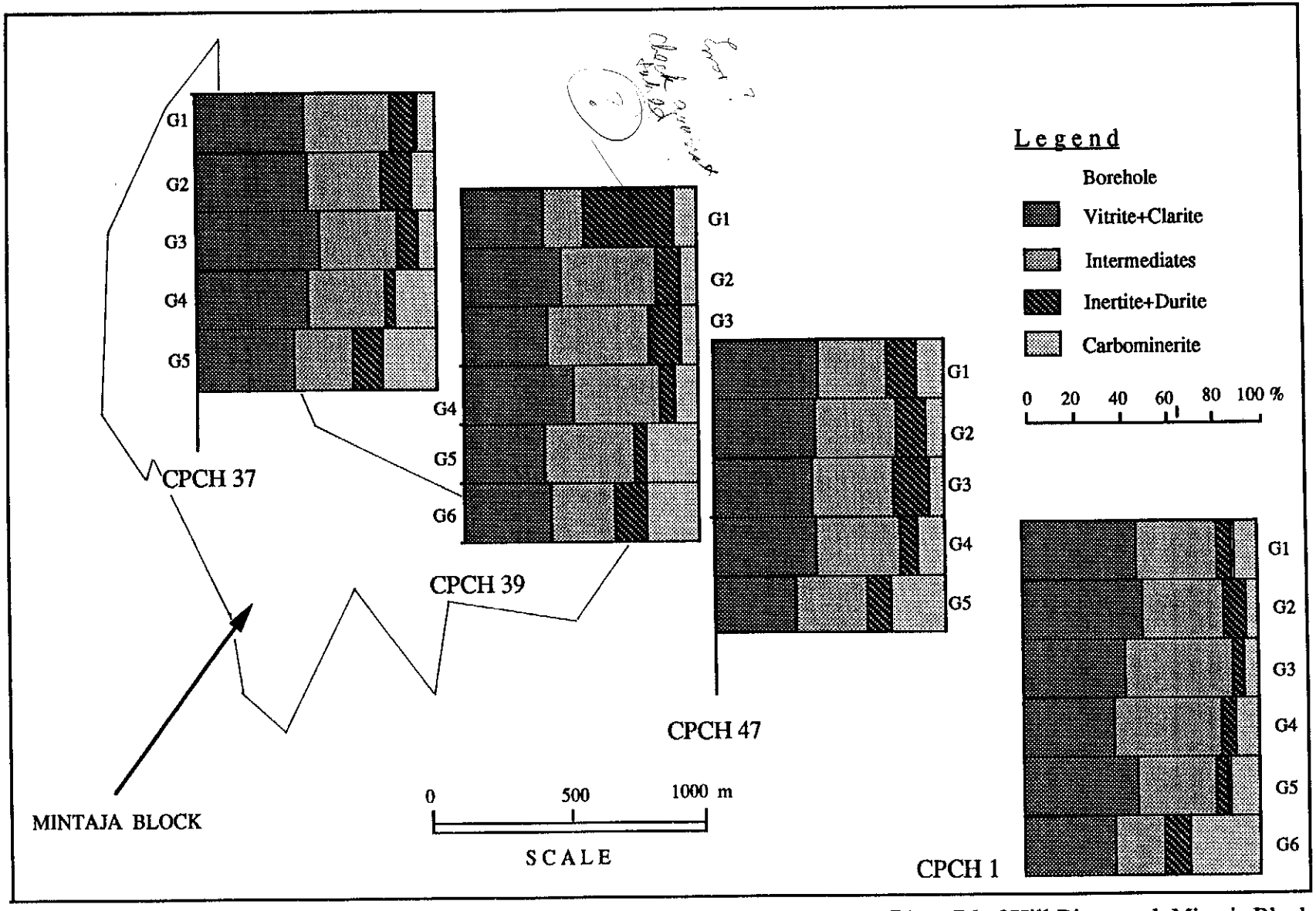

Figure 4.39. Vertical and lateral variations of microlithotype associations of sub-seams G1 to G6 of Hill River coal, Mintaja Block.

seam of CPCH 1, 37 and 39 shows the least "intermediates" values. In all boreholes, carbominerite has a remarkable trend, which decreases in content upward through the borehole. Inertite+durite composition exhibits variegated values throughout the boreholes.

Based on the study of Teichmuller (1982), coal of the Mintaja Block, which is rich in vitrite plus exinite-poor clarite, developed in a forest swamp, and represents detritus of stems, branches, barks, spores and cuticles. The semifusinite- and sporinite-rich durites observed in G1 of CPCH 1, and in G2 and G3 of CPCH 39, are interpreted to accumulate sub-aquatically in well-oxygenated water, Smith (1968).

4.5.5. Rank Variation and Classification

In the present study, mean maximum reflectance of vitrinite is used to measure coal rank. Vitrinite reflectance measurements of Mintaja Block coal were taken on 22 samples from four drill cores. The results of measurements are given in Table 4.11. Mean maximum reflectance value of the Mintaja coal varies between 0.47 % and 0.52 %, and range of maximum reflectance value is present from 0.42 % to 0.58 % (Table 4.11) . The mean reflectance values of Mintaja coal are plotted against the Australian, North American (ASTM), German, and USSR classifications (Figure 4.40). The reflectance values of Mintaja coal indicate a coalification stage at sub-bituminous level according to the Australian rank value, which approximately corresponds to the sub-bituminous A and B rank of ASTM classification, Bright Brown Coal of Germany Din and into B3 - D rank of USSR. Pareek (1987), pointed out that coal having maximum reflectance value between 0.40 % and 0.60 % is assigned as a metalignitous type. Thus, the Mintaja Block coal showing maximum vitrinite reflectance from 0.42 % to 0.58 % is categorised as metalignitous rank.

Table 4.11 . Maximum vitrinite reflectance of Hill River coal from Mintaja Block.

Drill hole	Sub-Seam	Range of Ro max (%)	Ro max (%)
CPCH 1	G 1	0.42 - 0.55	0.47
	G 2	0.44 - 0.54	0.49
	G 3	0.43 - 0.56	0.50
	G 4	0.44 - 0.56	0.50
	G 5	0.45 - 0.54	0.49
	G 6	0.45 - 0.55	0.50
CPCH 37	G 1	0.44 - 0.55	0.49
	G 2	0.43 - 0.54	0.50
	G 3	0.46 - 0.57	0.49
	G 4	0.44 - 0.54	0.49
	G 5	0.45 - 0.53	0.52
CPCH 39	G 1	0.46 - 0.58	0.51
	G 2	0.46 - 0.53	0.50
	G 3	0.45 - 0.57	0.51
	G 4	0.43 - 0.55	0.52
	G 5	0.48 - 0.55	0.52
	G 6	0.42 - 0.57	0.51
CPCH 47	G 1	0.44 - 0.49	0.47
	G 2	0.42 - 0.52	0.48
	G 3	0.46 - 0.54	0.49
	G 4	0.45 - 0.53	0.49
	G 5	0.44 - 0.56	0.51

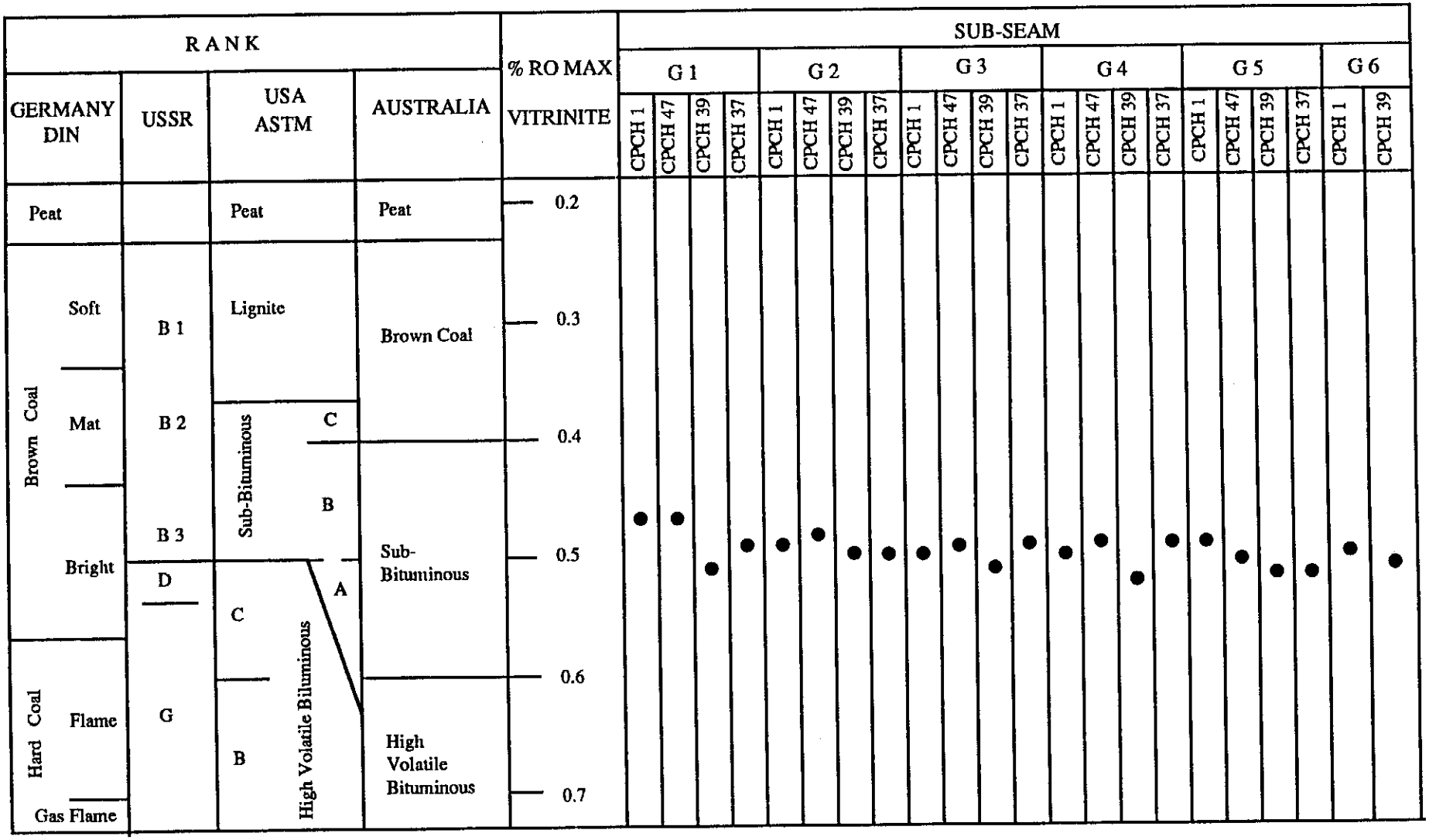

Figure 4.40. Rank and classification of Hill River coal from Mintaja Block.

The relationship of maximum vitrinite reflectance with depth of the Mintaja coal is illustrated in Figure 4.41. It shows that a positive relationship exists between reflectance and depth in Mintaja coal. Generally, the rank of coal exhibits slight increase with depth in all boreholes. The slight increasing trend in rank from G1 to G5/6 in CPCH 1 and 47, is possibly related to the burial depth and geothermal gradient in this area. However, CPCH 37 and 39 show fluctuating reflectance values from G1 to G5/6. The gradual change in reflectance of vitrinite indicates that the sub-seams are tectonically undisturbed, as well as almost free from the intrusive influence of igneous rocks.

According to Bennet and Taylor (1970) and Sappal (1986), Mintaja coal can also be classified on the basis of vitrinite content and maximum reflectance of vitrinite. This classification is shown in Figure 4.42. The vitrinite content of individual samples is plotted against its maximum reflectance of vitrinite. Points fall in the rectangular "boxes" indicate the class/type of coal.

The coal samples from Mintaja Block range from 045 to 046 and from 054 to 057. For example, the 045, means that the reflectance of vitrinite is situated between 0.40 % and 0.50 % and the vitrinite content between 50.0 % to 59.0 %. This value is within the range of sub-bituminous rank according to the Australian Classification or sub-bituminous B rank of North American Standard (ASTM).

On the basis of Sen's classification of coal (Table 3.8), vitrinite content of coal from CPCH 1 and CPCH 39, with values between 57.00% to 77.00 % belongs to "Ortho-vitrinous A" and "Meta-vitrinous B", in group member "5" and "6". The CPCH 37 and CPCH 47 display vitrinite values from 64.90 % to 75.30 % and this range of vitrinite content occupies "Meta-vitrinous B" of group member "6". The exinite content of CPCH 1 and CPCH 39 which ranges between 7.60% to 22.70% is classified into "Ortho-exinous A" to "Per-exinous A" and grouped to member "3 to

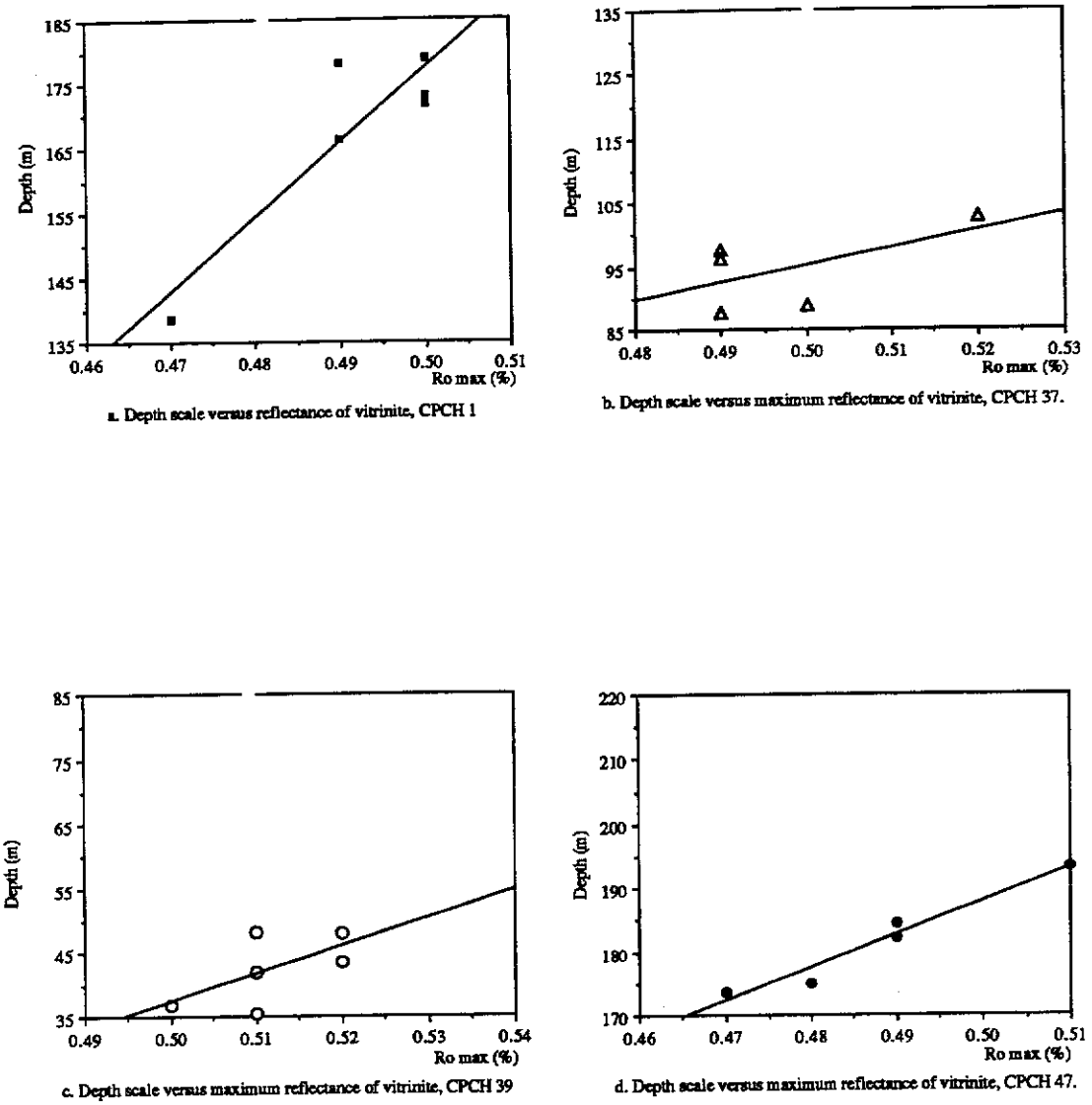

Figure 4.41. Relationship between depth and maximum vitrinite reflectance of Hill River coal from Mintaja Block.

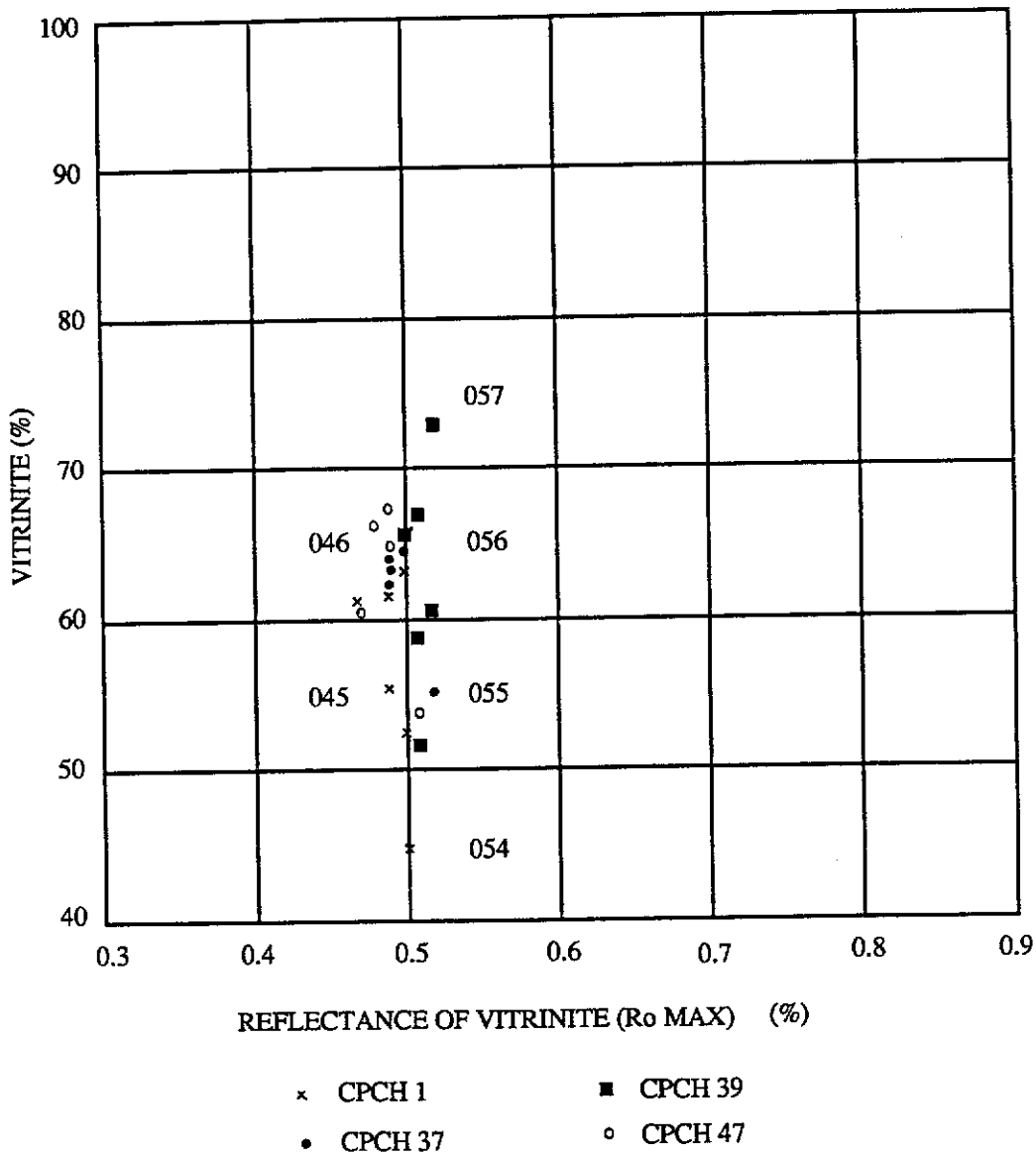

Figure 4.42. Classification and variation of Hill River coal from Mintaja Block.

5". The exinite content of CPCH 37 and CPCH 47 is classified into "Ortho-exinous A" of group member "3", because their exinite content is of 7.20 % to 10.60 %. Reflectance number of CPCH 1, 37, 39 and CPCH 47 fall into "1", "1 to 2", "1 to 2" and "1", respectively. Therefore, the typical code classification for CPCH 1 are "531" to "651"; CPCH 37 are "631" to "632"; CPCH 39 varies from "531" to "652", while CPCH 47 is "631". Generally, these types of coal are mainly "non-caking".

According to Mishra *et al.* (1990), coal having a vitrinite reflectance of 0.38 % - 0.80 %, supported by a high exinite content (10.00 % -23.00%), is more suitable for liquefaction purposes. Chandra *et al.* (1981) indicated that coal showing a vitrinite content between 44.00 % -68.00 % (mmf), an exinite content of 3.00 % to 15.00 %, an inertinite content from 20.00 % to 44.00 %, and a maximum vitrinite reflectance between 0.48 % - 0.88 %, is suitable for fertiliser material. Most of the coals from Mintaja Block have these characteristics.

4.5.6. Petrographic Characters

On the basis of petrographic examinations, the Mintaja Block coal has the following characters:

- The dominant lithotypes of the coal are banded, dull banded, and dull; while bright, bright banded and fusainous types are present as minor constituents. A progressive increase in vitrinite and a decrease in inertinite contents are present from the duller to the brighter lithotypes.

- The predominance of vitrinite is present in all sub-seams in the four drill cores. Its content is moderate to high. Thus the Mintaja Block coal can be

regarded as a vitrinite-rich coal. The lack of telinite indicates a slow burial and high pH of swamp water, Rimmer and Davis (1988). The vitrinite A content is higher than vitrinite B in the coal.

- The inertinite contents show low values, which reflect that a low degree of oxidation occurred in Mintaja Block coal. Inertinite is mostly present to form micro- to macrobands. These bands are composed mainly of semifusinite, inertodetrinite and fusinite with sporadic concentration of macrinite. The inertinite macerals are the result of an in-situ oxidation process, while inertodetrinite may also have been subjected to transportation from other areas of the basin.

- The exinite content is medium to high. Sporangia and megasporinite are easily recognised. The association of cutinite with varieties of vitrinite B especially with corpocollinite, suggest a leaf source for the peat. The finely laminated nature of vitrinite B is suggestive of compressed leaves. The abundance of resinite-rich leaf remains observed in Mintaja Block coal, may indicate shrubby vegetation rather than forest ones.

- The vitrite plus clarite content, in general, is more than 50 %, which shows an occurrence of forest in the Mintaja Block. The content of vitrite +clarite > 50% is due to the increased level of standing water and water table, with concomitant change in floral type and preservation of organic accumulation from oxidation processes.

- On the basis of reflectance measurement, the coal is designated as sub-bituminous stage A-B, or metalignitous type.

4.6. Gairdner Block

The petrographic analyses of the crushed coal samples obtained from the drill holes CPCH 57 and 60 are described here.

4.6.1. Maceral and Mineral Matter Analyses of CPCH 57 and CPCH 60

Maceral and mineral matter analyses of Gairdner Block coal were performed on sub-seams G1 to G 5 of the drill cores CPCH 57 and 60. The maceral and mineral matter distributions in the sub-seams are given in Table 4.12. The vitrinite is present as the dominant maceral groups, ranging moderately to highly from 41.60 % to 67.60 %. The exinite content shows a range between 7.80 % and 13.80 %. The inertinite content is present in low amounts, which varies from 14.20 % to 24.80 %. The maceral analysis on a mineral matter free basis is given in Table 4.13, and maceral composition of individual cores is depicted as histograms in Figure 4.43, and also in Figure 4.44 as a ternary diagram. This ternary diagram is depicted in terms of three apices constituting of vitrinite, exinite and inertinite maceral contents, and it shows the richness of vitrinite in the coal. Several petrographic indices like the ones for the Mintaja Block coal are used to interpret coal precursors condition and facies which are calculated from maceral analyses, and shown in Table 4.14. The ratio of vitrinite A to vitrinite B is very low to low, and ranges between 0.88 and 1.43. TPI value is low, and varies from 0.79 to 1.55, and GI is also low ranging between 2.73 and 4.77. The wood ratio (W/D) has a range of 3.03 - 5.43, while the degree of gelification of woody tissue (T/F) is 1.60 to 4.51. The coal is characterised by the high "vitrinite content" with low to medium "semifusinite ratio" (Figure 4.45).

The vitrinite group is a major constituent of the Gairdner Block coal, and dominant in all the sub-seams (Figure 4.43). Its range is between 41.60 % and 69.40 %. The

Table 4.12 . Maceral and mineral matter analyses of Hill River coal, Gairdner Block

Maceral	CPCH 57					CPCH 60				
	G 1	G 2	G 3	G 4	G 5	G 1	G 2	G 3	G 4	G 5
Telinite	0.40	0.40	0.40	0.00	0.00	0.00	0.00	0.20	0.20	0.00
Telocollinite	31.40	35.80	30.40	32.20	16.60	32.20	32.20	31.60	33.80	15.40
Vitrinite A	31.80	36.20	30.80	32.20	16.60	32.20	32.40	31.80	34.00	15.40
Desmocollinite	27.60	23.00	24.40	30.80	29.60	30.60	34.40	27.60	30.60	23.80
Corpocollinite	3.80	2.20	2.00	2.60	1.00	2.20	2.40	7.20	3.00	2.40
Vitrodetrinite	0.20	0.20	0.20	0.00	0.00	0.20	0.20	0.40	0.00	0.00
Vitrinite B	31.60	25.40	26.60	33.40	30.60	33.00	37.00	35.20	33.60	26.20
VITRINITE	63.40	61.60	57.40	65.60	47.20	65.20	69.40	67.00	67.60	41.60
Sporinite	5.60	5.00	7.40	6.70	4.60	3.80	4.00	4.60	4.60	1.80
Cutinite	2.10	1.90	2.10	2.70	1.80	2.00	2.00	4.60	3.00	2.00
Resinite	0.40	0.60	0.60	0.40	0.40	0.00	0.00	0.60	0.60	0.00
Alginite	1.70	2.30	1.50	1.20	3.20	1.40	1.80	0.60	0.60	1.40
Liptodetrinite	0.60	0.00	0.00	0.20	3.80	0.80	0.00	0.20	0.00	3.40
EXINITE	10.40	9.80	11.60	11.20	13.80	8.00	7.80	10.60	8.80	8.60
Semifusinite	9.80	12.80	7.20	6.80	8.00	7.60	7.40	7.80	5.60	6.60
Fusinite	2.80	2.80	5.00	3.60	4.60	3.60	2.00	3.60	4.60	3.00
Sclerotinite	0.00	0.20	0.00	0.00	0.40	0.00	0.40	0.00	0.20	0.60
Macrinite	0.80	1.20	1.60	1.20	1.40	0.80	0.80	1.20	0.40	0.20
Micrinite	0.40	0.80	0.60	0.20	0.00	0.20	0.20	0.20	0.20	0.00
Inertodetrinite	8.20	7.00	5.20	4.60	5.00	7.20	9.20	4.00	5.40	3.80
INERTINITE	22.00	24.80	23.60	15.40	19.40	19.40	20.00	16.80	16.40	14.20
Clay	2.00	1.00	3.20	5.20	12.60	3.00	1.00	1.80	1.00	27.00
Pyrite	1.20	1.60	2.80	1.40	4.80	2.20	1.20	2.40	5.60	7.20
Carbonate	1.00	1.20	1.40	1.20	2.00	2.20	0.60	1.40	1.20	3.60
Quartz	0.00	0.00	0.00	0.00	0.20	0.00	Trace	Trace	0.00	Trace
MINERAL MATTER	4.20	3.80	7.40	7.80	19.60	7.40	2.80	5.60	7.20	35.60
THICKNESS (m)	1.48	3.68	1.16	1.06	0.68	1.40	4.53	1.42	1.17	0.24

Table 4.13. Maceral analysis (mineral matter free) of Hill River coal from Gairdner Block.

Drill hole	Sub-Seam	Vitrinite	Exinite	Inertinite
CPCH 57	G 1	66.2	10.8	23.0
	G 2	64.0	10.2	25.8
	G 3	62.0	12.5	25.5
	G 4	71.1	12.1	16.8
	G 5	58.7	17.2	24.1
CPCH 60	G 1	70.4	8.6	21.0
	G 2	71.4	8.0	20.6
	G 3	71.0	11.2	17.8
	G 4	72.8	9.5	17.7
	G 5	64.6	13.3	22.1

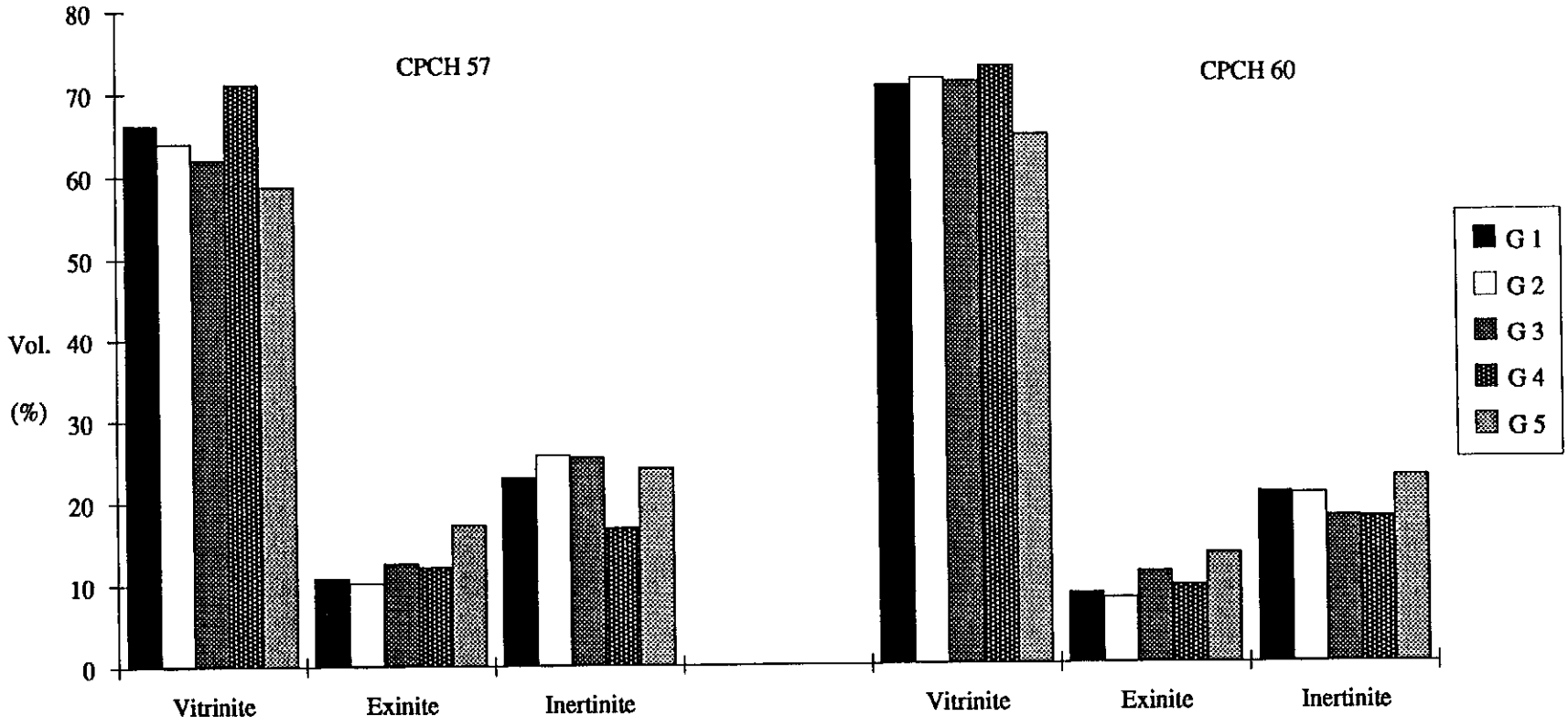

Figure 4.43. Maceral distributions (mineral matter free) of drill holes CPCH 57 and CPCH 60, Gairdner Block.

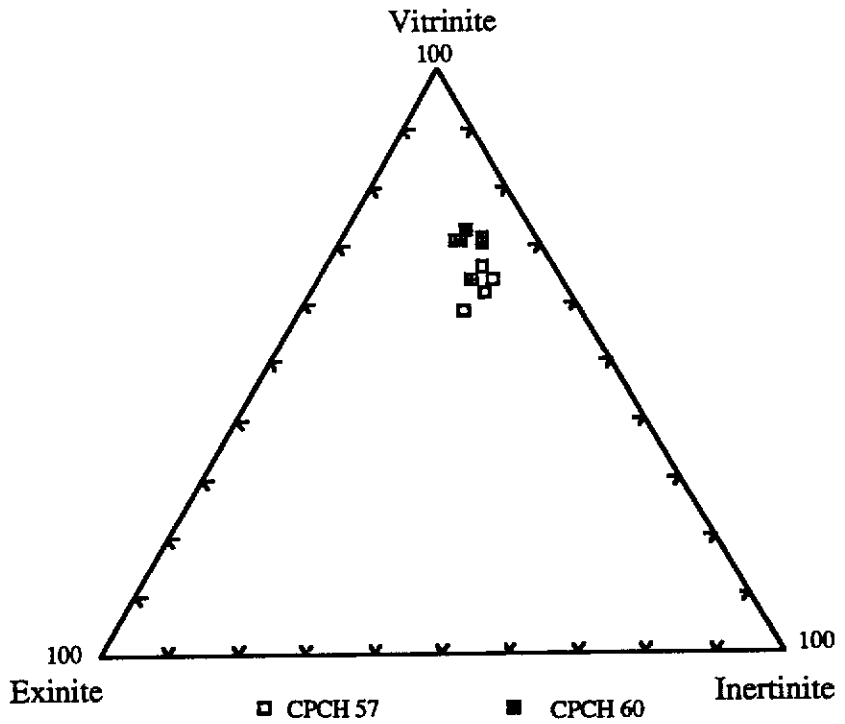

Figure 4.44. Maceral composition (mineral matter free) of Hill River coal, Gairdner Block.

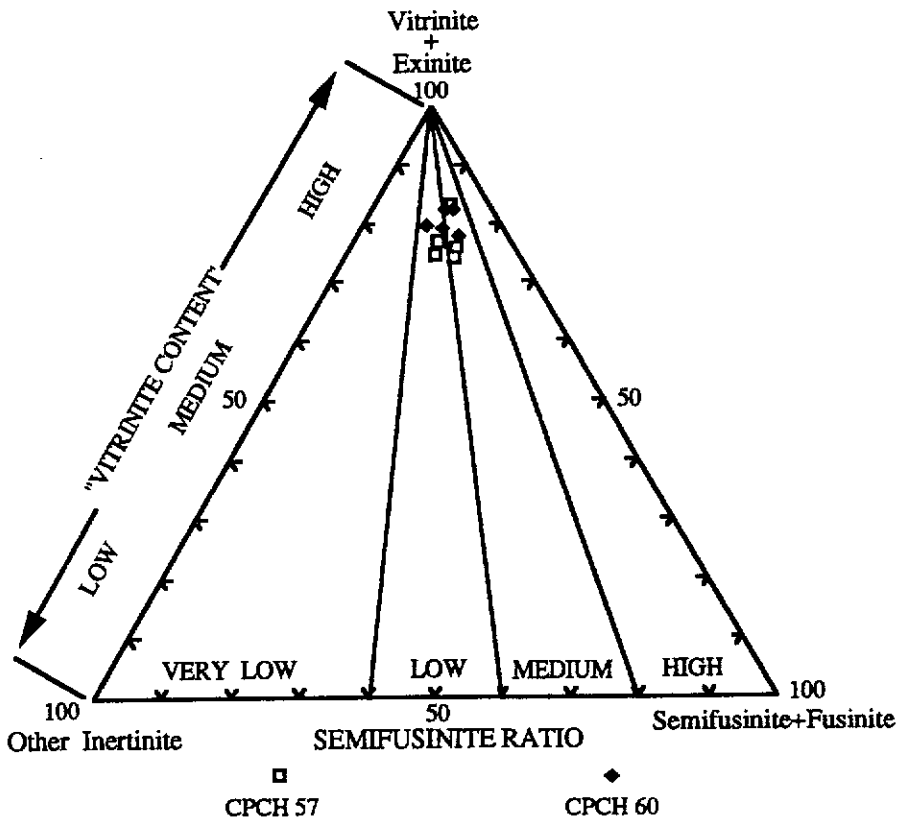

Figure 4.45. Maceral composition diagram of Hill River coal from Gairdner Block showing "vitrinite content" and "semifusinite ratio".

Table 4.14 . Petrographic indices of Hill River coal from Gairdner Block.

Drill hole	Sub-Seam	A/B	T/F	SF/F	W/D	GI	TPI
CPCH 57	G 1	1.01	3.32	3.50	3.73	3.08	1.10
	G 2	1.43	2.96	4.57	4.68	2.78	1.55
	G 3	1.16	2.52	1.44	3.03	2.73	1.30
	G 4	0.96	4.06	1.89	4.21	4.77	1.07
	G 5	0.87	2.11	1.74	3.56	2.76	0.79
CPCH 60	G 1	0.98	2.87	2.11	3.68	3.59	1.06
	G 2	0.88	4.51	3.70	3.70	3.77	0.89
	G 3	0.90	3,67	2.17	5.43	4.40	1.08
	G 4	1.01	3.33	1.22	4.25	4.36	1.12
	G 5	0.91	1.60	2.20	4.31	3.10	0.83

A/B = Telinite+Telocollinite/Remaining Vitrinite

SF/F = Semifusinite/Fusinite

T/F = Telinite+Telocollinite/Semifusinite+Fusinite

W/D = Telinite+Telocollinite+Semifusinite+Fusinite/Inertodetrinite+Macrinite+Sporinite

TPI = Telinite+Telocollinite+Semifusinite+Fusinite/Desmocollinite+Corpocollinite+Macrinite+Inertodetrinite

GI = Vitrinite+Macrinite/Semifusinite+Fusinite+Inertodetrinite

telocollinite has the highest content, and ranges from 15.40 % to 45.80 %. Figure 4.44 also illustrates the domination of vitrinite over other maceral groups in the Gairdner Block coal. The ratio of vitrinite A to vitrinite B varying between 0.88 and 3.00 (Table 4.14), reflects that structured vitrinite or woody tissue is low to moderate in the coal.

The exinite content of Gairdner Block coal does not display a remarkable variation. It ranges between 7.80 % and 13.80 % with sporinite, cutinite and alginite having high contents compared to the remaining exinite macerals. Sporinite dominates the exinite group and varies between 1.80 % to 7.40 %. The exinite composition of individual sub-seams and the whole sample of the Gairdner Block coal dominated by sporinite with minor other exinite, is given in Figure 4.46.

The predominance of semifusinite and inertodetrinite is evident in the coal, with a range of 5.60 % - 12.80 % and 3.80 % - 9.20 %, respectively. The fusinite which is relatively low in content, occurs in amounts between 2.00 % and 5.00 % (Table 4.12). The ratio of semifusinite to fusinite (SF/F) is between 1.22 and 4.57 (Table 4.14). The sclerotinite, macrinite and micrinite occur in very low amounts, and sclerotinite ranges from 0.20 % to 0.60 %, while macrinite and micrinite range from 0.20 % to 1.60 % and 0.20 % to 0.80 %, respectively. Figure 4.47 depicts a ternary diagram of inertinite maceral composition of individual sub-seams and the whole Gairdner Block coal, and it shows the predominance of semifusinite and other inertinite over the fusinite.

In conclusion, preservation of woody material increases from G5 to G1 (bottom part to upper part of the sequence), as shown by the increase in the content of vitrinite A (structured vitrinite), and semifusinite and fusinite (structured inertinite). A relatively medium to high TPI value suggests that more well preserved plant tissues are present in almost all sub-seams, except in G5 of CPCH 60 displaying low TPI

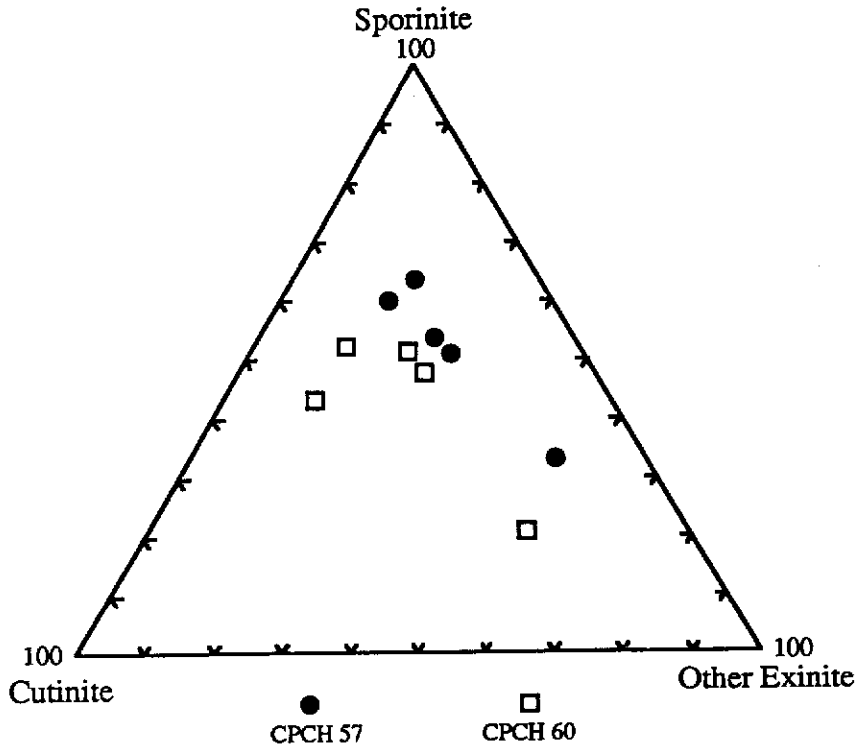

Figure 4.46. Composition of exinite group, Hill River coal, Gairdner Block.

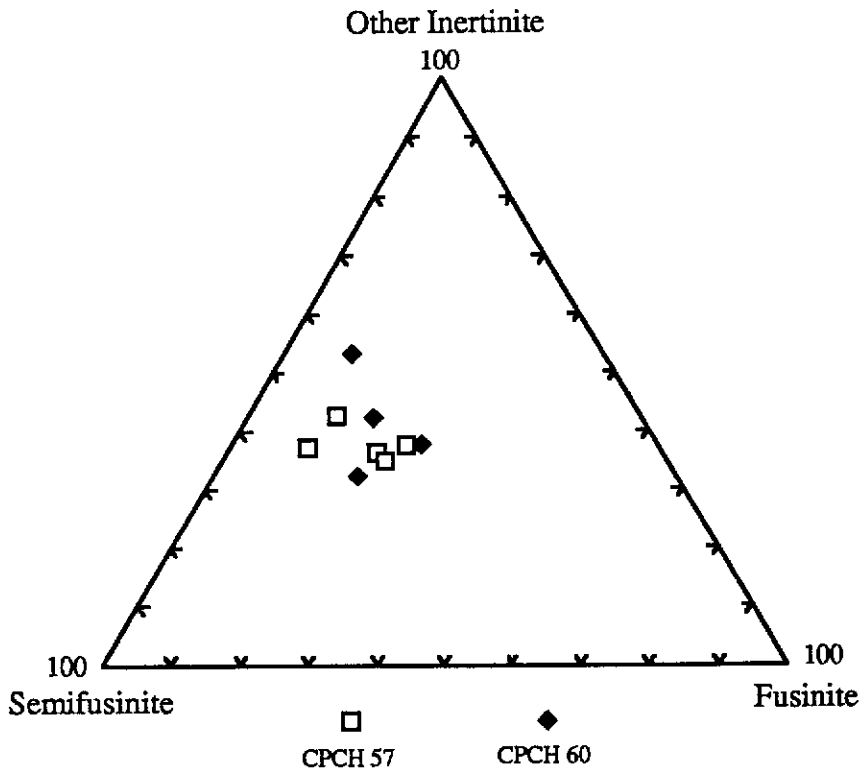

Figure 4.47. Composition of inertinite group, Hill River coal, Gairdner Block.

(0.90). Additionally, the high wood ratio (W/D) value is evidence of high preservation of woody tissues. A low degree of oxidation which is indicated by the high GI value and supported by high T/F value, affected the Gairdner Block coal.

The vertical maceral variations (mineral matter free basis) of all sub-seams are illustrated in Figures 4.48 and 4.49, and in these figures, a relationship of vitrinite, exinite and inertinite is shown. The vitrinite content varies inversely to the inertinite content, from sub-seams G1 to G5. Moreover, within G1 to G3 of both boreholes, exinite content distributes inversely against the inertinite content. The semifusinite ratio for all the sub-seams is also shown in Figures 4.48 and 4.49. Most of the sub-seams analysed have "vitrinite content" between 75 % and 85 %, and are categorised as medium to high values (Figure 4.48 b and 4.49 b). However, the medium value ranging between 75 % to 80 %, is predominant. In CPCH 57, it shows a variation, while in CPCH 60, the "vitrinite content" from G1 to G5 has a similar value. The "semifusinite ratio" ranges from low to medium. In CPCH 57, the lowest degree of "semifusinite ratio" occurs within G3, whereas the highest is in G4. In CPCH 60, G2 is occupied by the lowest ratio, and G5 by the highest one. In general, there is no remarkable relationship of "vitrinite content" and "semifusinite ratio". However, in G1-G3 within CPCH 57 and G4 to G5 of CPCH 60, the decrease in "vitrinite content" is compensated for by an increase in the "semifusinite ratio". In addition, from G3 to G5 of CPCH 57, the value of "vitrinite content" coincides with the value of "semifusinite ratio". The results obtained from Figures 4.48 and 4.49 are comparable to those shown in Figure 4.45. Both have low to medium "semifusinite ratio" and medium to high "vitrinite content", similar to the Mintaja Block coal. This indicates that the degree of oxidation in the peat was low, which resulted in a high vitrinite content in the coal.

The vertical and lateral variations in maceral and mineral matter contents in all the sub-seams of the drill holes CPCH 57 and 60 are shown in Figure 4.50. The vitrinite

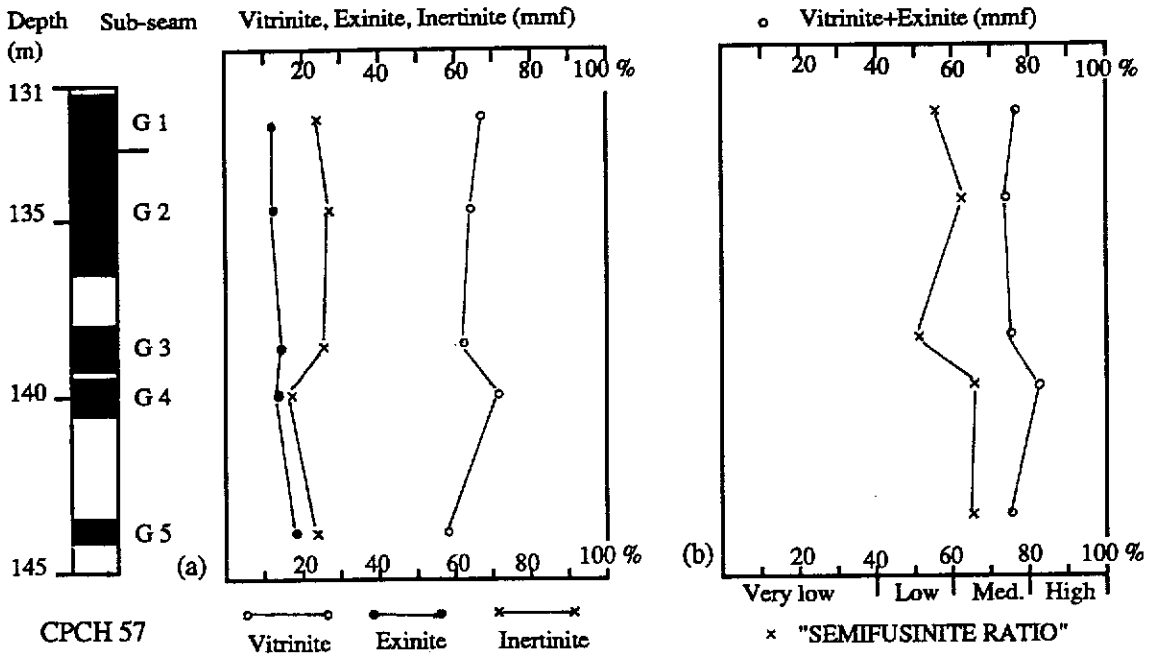

Figure 4.48. (a) Variation in vitrinite, exinite and inertinite, and (b) variation of "vitrinite content" and the "semifusinite ratio" of sub-seams G1 -G5 of Hill River coal, drill hole CPCH 57 from Gairdner Block.

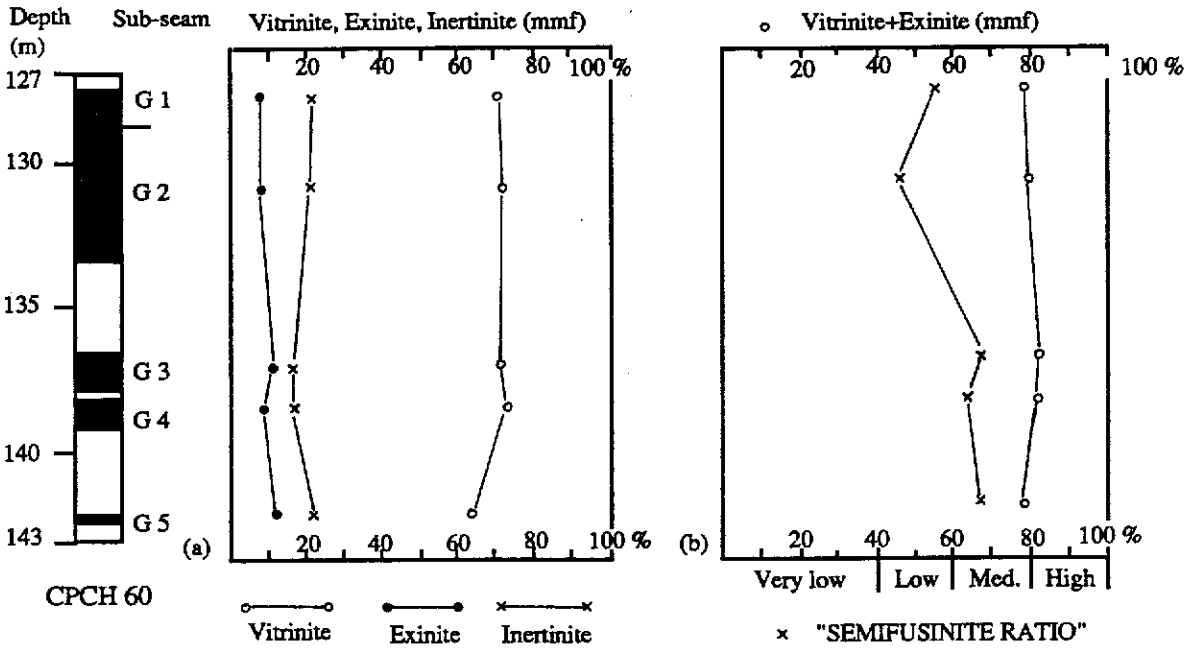

Figure 4.49. (a) Variation in vitrinite, exinite and inertinite, and (b) variation of "vitrinite content" and the "semifusinite ratio" of sub-seams G1 - G5 of Hill River coal, drill hole CPCH 60 from Gairdner Block.

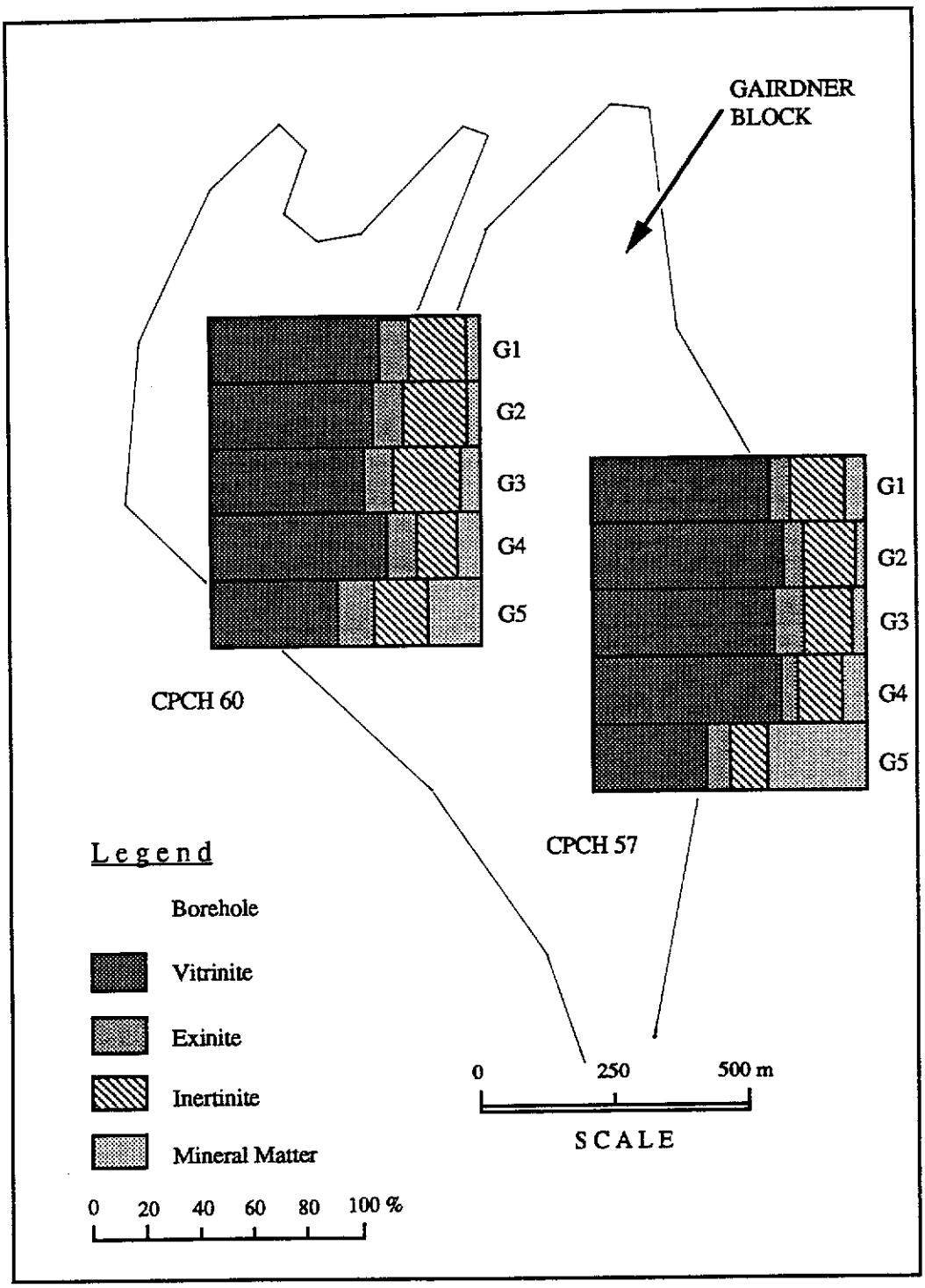

Figure 4.50. Vertical and lateral variations of maceral and mineral matter distributions of sub-seams G1 to G5 of Hill River coal in Gairdner Block.

content, in general, decreases downward in the sub-seams, except G 3 to G 4 of CPCH 57 and G 1 to G 2 of CPCH 60. However, inertinite and mineral matter contents show a reverse trend. This evidence indicates that an increasing oxidation down the sequence has taken place. An increase in mineral matter content is due to the increased flooding which produced fine mineral matter in the coal. The amount of exinite in sub-seams of CPCH 60 is relatively uniform and does not exhibit a remarkable trend. It shows values between 7.80 % o 10.60 %. However, in CPCH 57, its amount increases down the sequence. The vertical variations in proportions of vitrinites and inertinites reflect decomposition or the degree of oxidation in the peat, which is due to frequent fluctuations in water level, periodic flooding, desiccation and burning of the peat.

The lateral variation of maceral distribution in the Gairdner Block coal shown in Figure 4.50 indicates that vitrinite distribution increases towards a northwest direction, except in sub-seam G1 and G5. The exinite content has a similar pattern throughout the sub-seams, and it decreases along SE - NW direction. A decrease in inertinite content from the southeast to the northwest can be recognised within sub-seams G2 to G5. However, in sub-seam G1 a similar content occurs. The decrease in inertinite content, is compensated by an increase in vitrinite content, except in G5. In sub-seams G 1 and G5 an increase in mineral matter content from a southeast to a northwest direction, is present. These maceral and mineral matter variations are due to vegetational characteristics, differences in the rate of accumulation and decomposition or oxidation of plant communities, and variations in the ground water table in the basin.

4.6.2. Microlithotype Analyses

Microlithotype analyses were undertaken on the Gairdner Block coal, in terms of

vitrite, clarite, inertite, trimacerite, duroclarites, clarodurite and vitrinertite. Liptite is also observed in the coal, although it is present in low amounts. Carbominerite which predominantly consists of carbargilite and carbopyrite, is also recorded in the coal (Table 4.15).

The microlithotype analyses of Gairdner Block coal listed in Table 4.15, shows that vitrite is a predominant constituent, which ranges between 29.0 % and 45.0 %. It is followed by duroclarite and inertite displaying contents of 13.20 % to 20.20 % and 8.00 % to 13.80 %, respectively. The clarite and vitrinertite contents range between 2.40 % to 10.20 % and 5.20 % to 13.20 %, respectively. With the durite, vitrinertoliptite, liptite, and clarodurite , each of them have very low content, with the range between 0.20 % and 2.60 %. The carbominerites dominated by carbargilite and carbopyrite have low to high values, which range from 6.20 % to 33.60 %. The content of carbargilite is between 4.60 % and 27.80 %, while carbopyrite shows amounts of 0.60 % to 5.20 %. The data on microlithotype composition of the Gairdner Block coal is also given on a group basis in Table 4.16 and illustrated in Figure 4.51. Predominantly, the coal is constituted by an association of vitrite plus clarite, followed by intermediates and then inertite plus durite.

Based on the study of Teichmuller (1982) regarding the relationship between microlithotype association and its environmental deposition, the coal of Gairdner Block was formed from vegetation which grew in forest swamp.

Figure 4.52 depicts the microlithotype and carbominerite variations in boreholes CPCH 57 and 60. In general, the vitrite+clarite content increases downward from G1 to G4, and then it decreases from G4 to G5. Intermediates association within CPCH 57 has a reverse trend compared to vitrite+clarite content, while in CPCH 60 intermediate content shows a relatively constant value throughout borehole. The inertite+durite content does not show any special trend and its amount varies. The

Table 4. 15 . Microlithotype analyses of Hill River coal from Gairdner Block.

Drill hole	Sub-Seam	Vitrite	Liptite	Inertite	Clarite	Durite	Vitrinertite	Duroclarite	Vitrinerto-liptite	Claro-durite	Carbo-pyrite	Carbargillite	Carbo-minerite
CPCH 57	G 1	35.8	0.0	13.8	2.4	0.6	12.8	18.4	0.4	2.0	0.6	12.0	14.0
	G 2	44.2	0.2	9.0	4.0	0.0	13.2	20.2	0.4	2.6	1.4	4.6	6.2
	G 3	44.2	0.2	16.2	5.4	0.4	6.6	16.4	0.8	0.0	1.2	7.6	9.8
	G 4	45.0	0.0	8.0	9.6	0.0	5.8	14.6	0.6	0.4	4.6	10.8	15.8
	G 5	29.2	0.4	10.0	5.4	0.2	5.2	13.8	0.6	1.2	5.2	27.8	33.6
CPCH 60	G 1	42.6	0.2	12.8	3.4	0.6	6.0	14.8	1.2	1.2	3.4	13.4	16.8
	G 2	44.2	0.4	11.8	3.6	0.2	9.2	13.2	0.8	1.2	4.0	11.4	15.4
	G 3	40.2	0.0	13.2	5.4	0.2	7.8	15.8	0.8	1.4	3.8	11.2	15.0
	G 4	38.0	0.6	9.2	10.2	0.2	8.6	16.8	0.4	2.2	4.2	9.4	13.6
	G 5	29.0	0.2	12.2	6.8	0.4	6.4	14.2	0.0	0.2	4.0	26.6	30.6

Table 4.16 . Microlithotype compositions of Hill River coal from Gairdner Block.

Drill hole	Sub-Seam	Vitrite+Clarite	Intermediates	Inertite+Durite
CPCH 57	G 1	44.4	38.6	17.0
	G 2	51.5	38.9	9.6
	G 3	55.1	26.4	18.5
	G 4	64.8	25.4	9.8
	G 5	52.4	31.5	16.1
CPCH 60	G 1	55.4	27.9	16.7
	G 2	56.8	29.0	14.2
	G 3	53.6	30.3	16.1
	G 4	56.2	32.6	11.2
	G 5	51.7	30.1	18.2

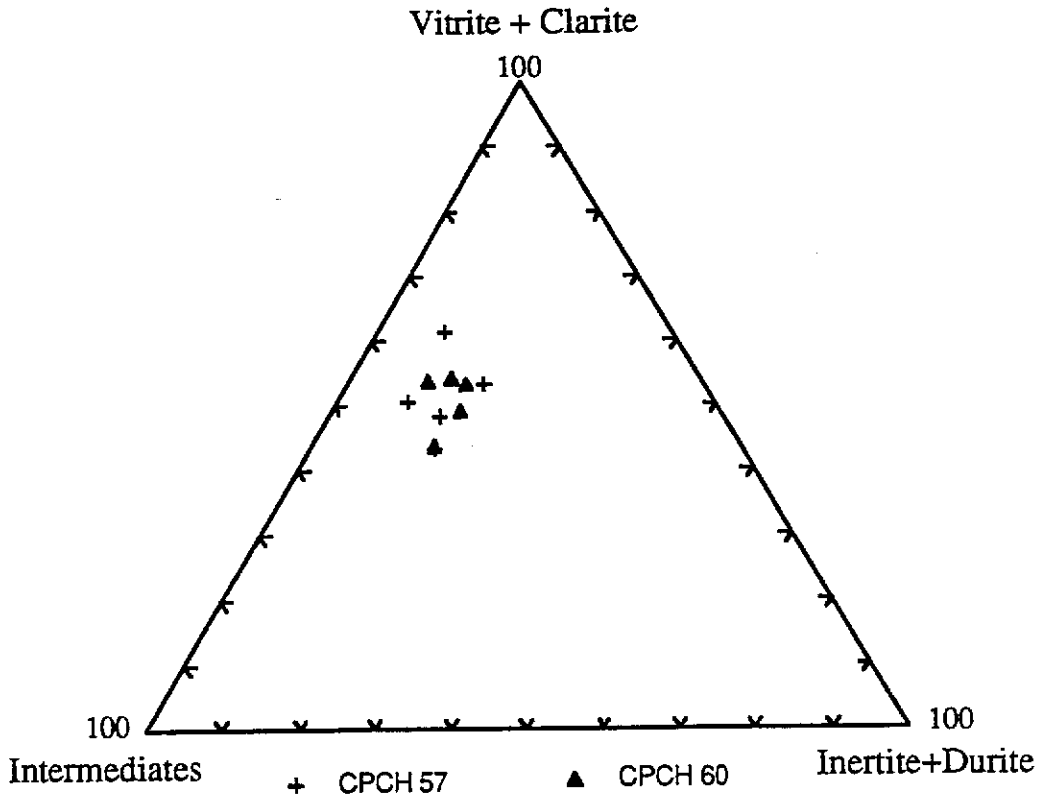

Figure 4.51. Microlithotype composition of Hill River coal from Gairdner Block.

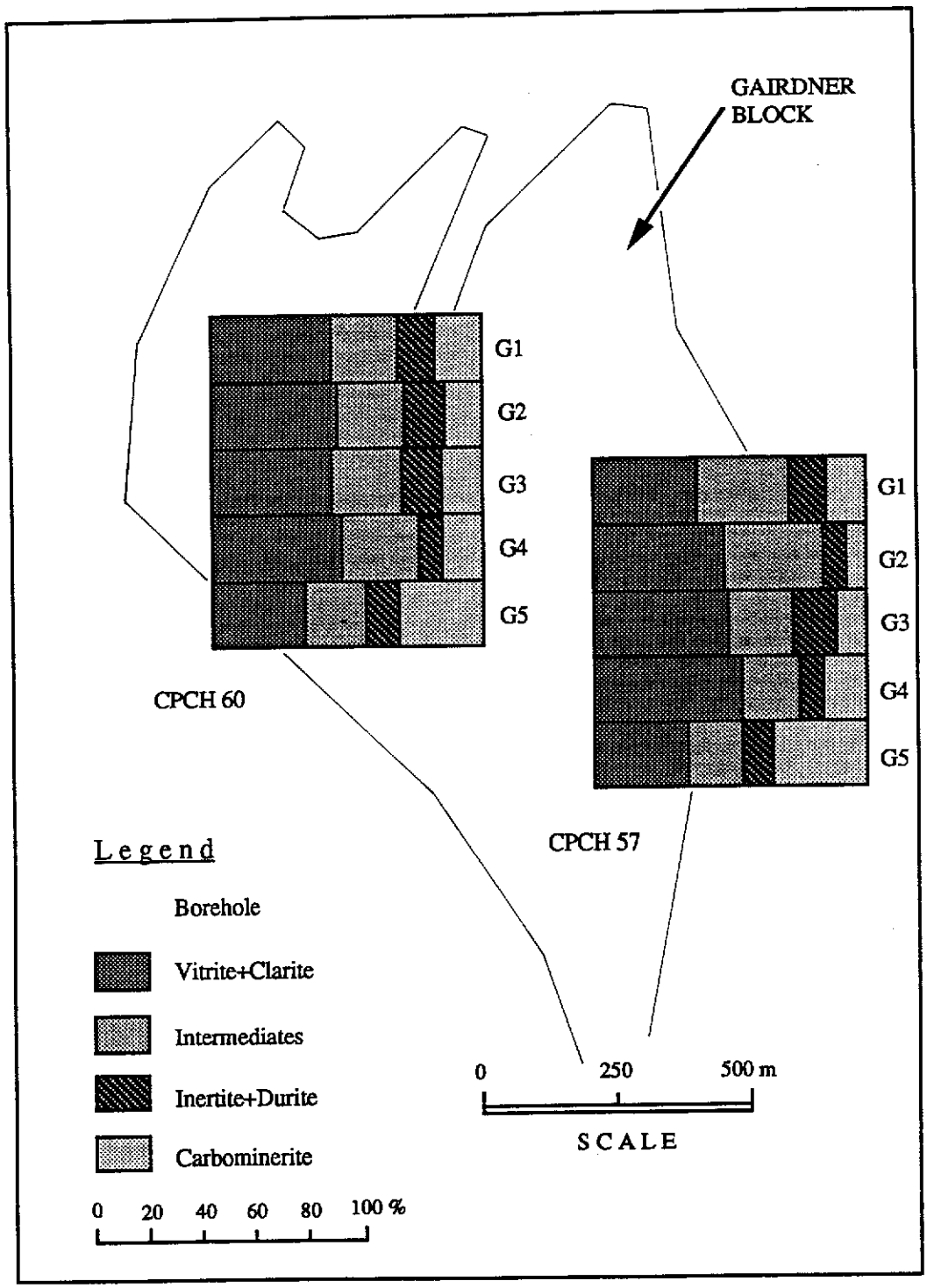

Figure 4.52. Vertical and lateral variations of microlithotype associations of sub-seams G1 to G5 of Hill River coal, Gairdner Block.

liptite because of its low amount is combined with carbominerite, and it shows a decrease upward through the boreholes.

The proportions of microlithotypes can be used as indicative of peat depositional environment , Teichmuller (1982). Stavrakis and Smyth (1991) stated that coal predominantly constituted by association of vitrite+clarite was deposited in the coastal marsh or lower delta-plain. Therefore, the depositional environment of the Gairdner Block coal precursor can be presumed as a forest swamp of coastal area/delta plain.

4.6.3. Rank Variation and Classification

The rank of the Gairdner Block coal is measured on the basis of mean maximum reflectance of vitrinite. The measurement of vitrinite reflectance on the coal was undertaken on 10 samples of sub-seams G1 to G5, from boreholes CPCH 57 and 60. Table 4.17 gives the result of reflectance measurements. The range of vitrinite reflectance of the coal is between 0.46 % to 0.61 %, while mean maximum reflectance varies from 0.51 to 0.54 % (Table 4.17). Figure 4.53 depicts reflectance and rank variation of Gairdner coal. The measurements obtained from coal of CPCH 57 and CPCH 60 are plotted against the Australian and North American Standards (ASTM), and also against German and USSR classifications. These values indicate a narrow range of rank within the sub-bituminous stage according to Australian rank, which corresponds to sub-bituminous A of USA standard (ASTM), Bright Brown Coal of Germany (Din) or Stage-D in USSR classification. On the basis of Pareek's classification (1987), the coal is classified as metalignitous rank, because its maximum vitrinite reflectance varies between 0.40 % to 0.60 %.

The vitrinite reflectance data in CPCH 57 show a slightly regular increase with depth (Figure 4.54 a), whereas, vitrinite reflectance data obtained from CPCH 60 display

Table 4.17. Maximum vitrinite reflectance of Hill River coal from Gairdner Block.

Drill hole	Sub-Seam	Range of Ro max (%)	Ro max (%)
CPCH 57	G 1	0.46 - 0.54	0.51
	G 2	0.47 - 0.55	0.52
	G 3	0.48 - 0.56	0.53
	G 4	0.46 - 0.58	0.53
	G 5	0.46 - 0.56	0.51
CPCH 60	G 1	0.47 - 0.56	0.52
	G 2	0.49 - 0.60	0.54
	G 3	0.50 - 0.56	0.53
	G 4	0.47 - 0.61	0.54
	G 5	0.46 - 0.54	0.52

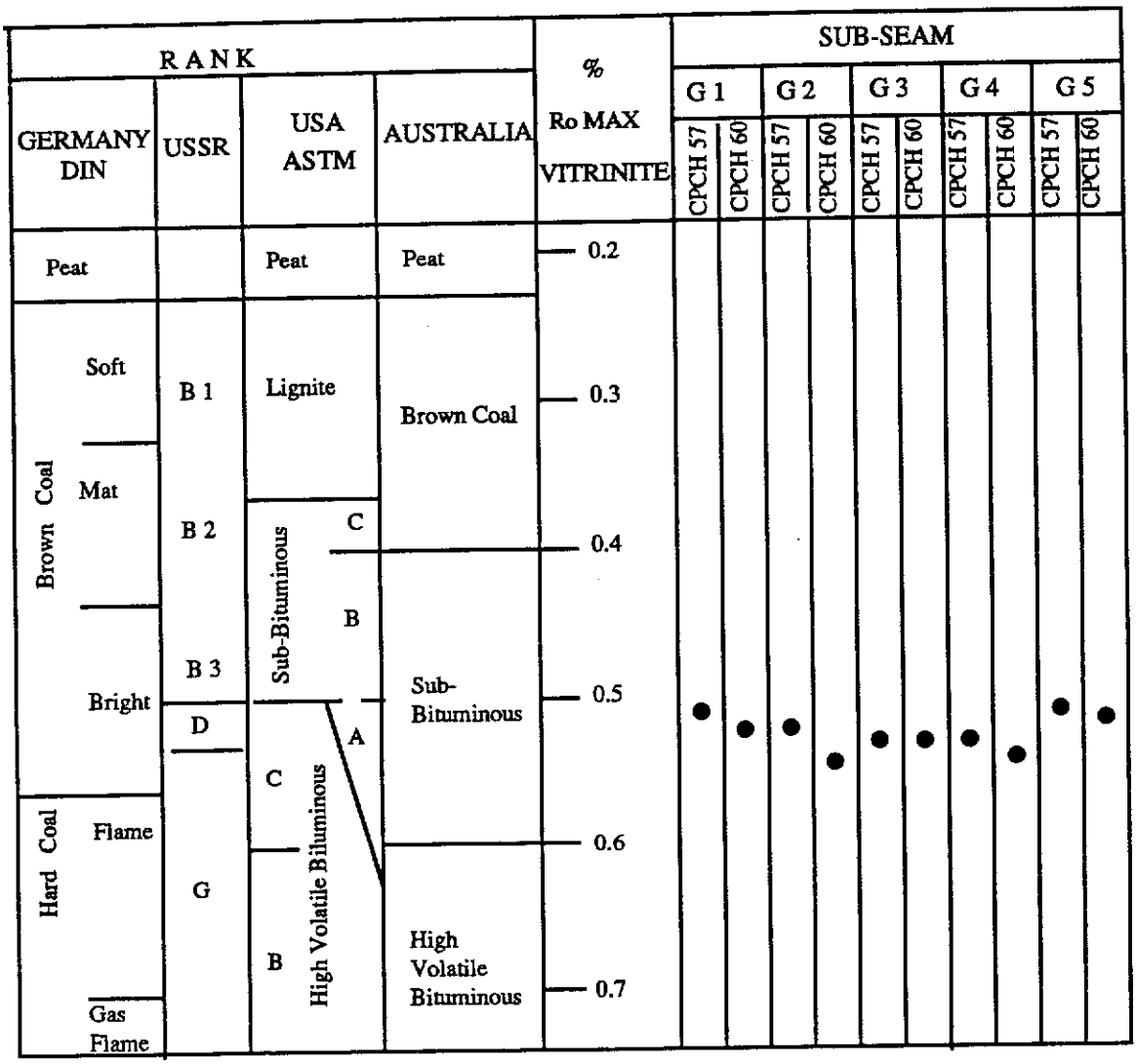

Figure 4.53. Rank and classification of Hill River coal from Gairdner Block.

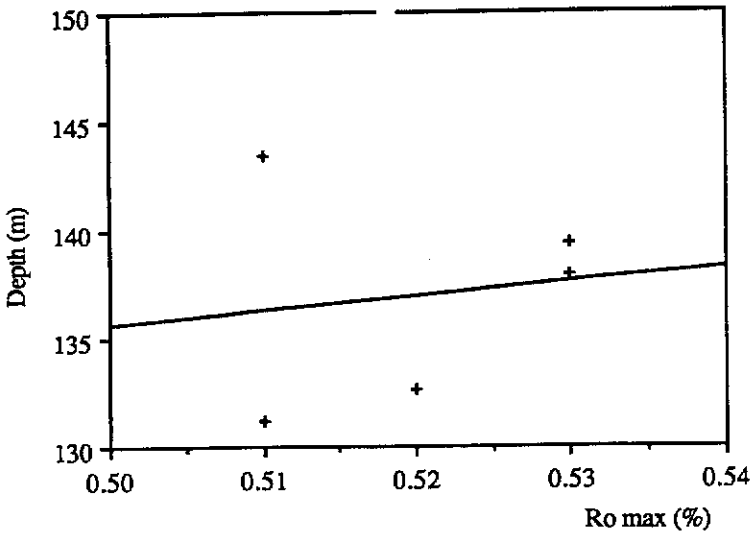

a.Depth scale versus maximum reflectance of vitrinite, CPCH 57.

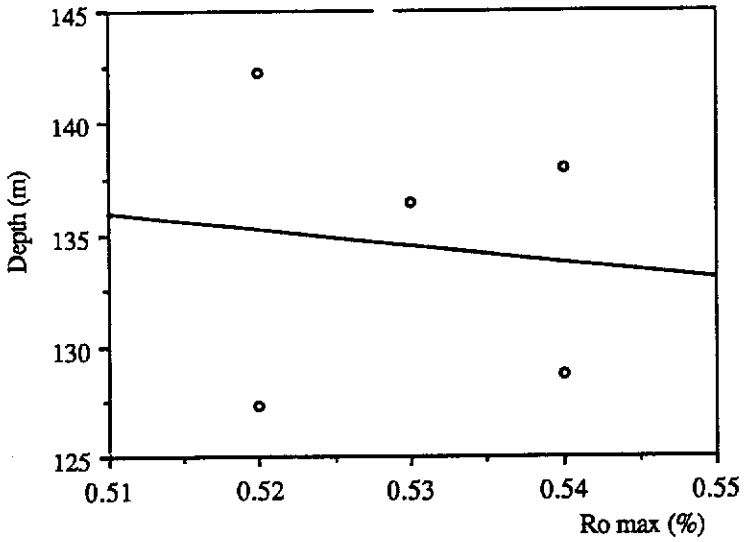

b. Depth scale versus maximum reflectance of vitrinite, CPCH 60.

Figure 4.54. Relationship between depth and maximum vitrinite reflectance of Hill River coal from Gairdner Block.

a fluctuating value downward through the borehole and does not show a remarkable relationship with depth (Figure 4.54 b). However, these two figures do not represent the whole seam of CPCH 57 and 60, because of a very limited number of samples.

The Gairdner Block coal can be classified on the basis of vitrinite content and maximum reflectance of vitrinite, in accordance with Bennet and Taylor (1970) and Sappal (1986). The maximum vitrinite reflectance of the vitrinite in the individual samples is plotted against the vitrinite content (Figure 4.55). The class/type of coal is indicated in the rectangular "boxes", and the classification/type of the Gairdner Block coal which ranges from 054 to 056 indicates that the vitrinite reflectance is between 0.50 % and 0.60 %. This range of value falls into the sub-bituminous rank of the Australian Classification or the sub-bituminous A of the USA Standard (ASTM), and the vitrinite content in the coal is between 40 % to 59 %.

In accordance with Sen's classification (Table 3.8), coal from CPCH 57 is classified into "Ortho-vitrinous A" to "Meta-vitrinous B" which belongs to group members "5" and "6", respectively. However, coal from CPCH 60 showing a vitrinite content between 64.6% to 72.8 % (mmf) is of "Meta-vitrinous B" of group member "6". The exinite content of CPCH 57 ranges between 10.2 and 17.20 %, and it is of "Ortho-exinous B" to "Per-exinous A" genera, which can be grouped into members "4" to "5", respectively. CPCH 60 which has an exinite content between 9.50 to 13.30 % falls into "Ortho-exinous A-B" of group member "3-4". Reflectance showing value between 0.51 and 0.54 %, is classified to reflectance number "2". Thus, on the basis of Sen's classification, the typical code of CPCH 57 is between "542" and "652", while CPCH 60 is of "632" to "642". These coals are mainly "non-caking".

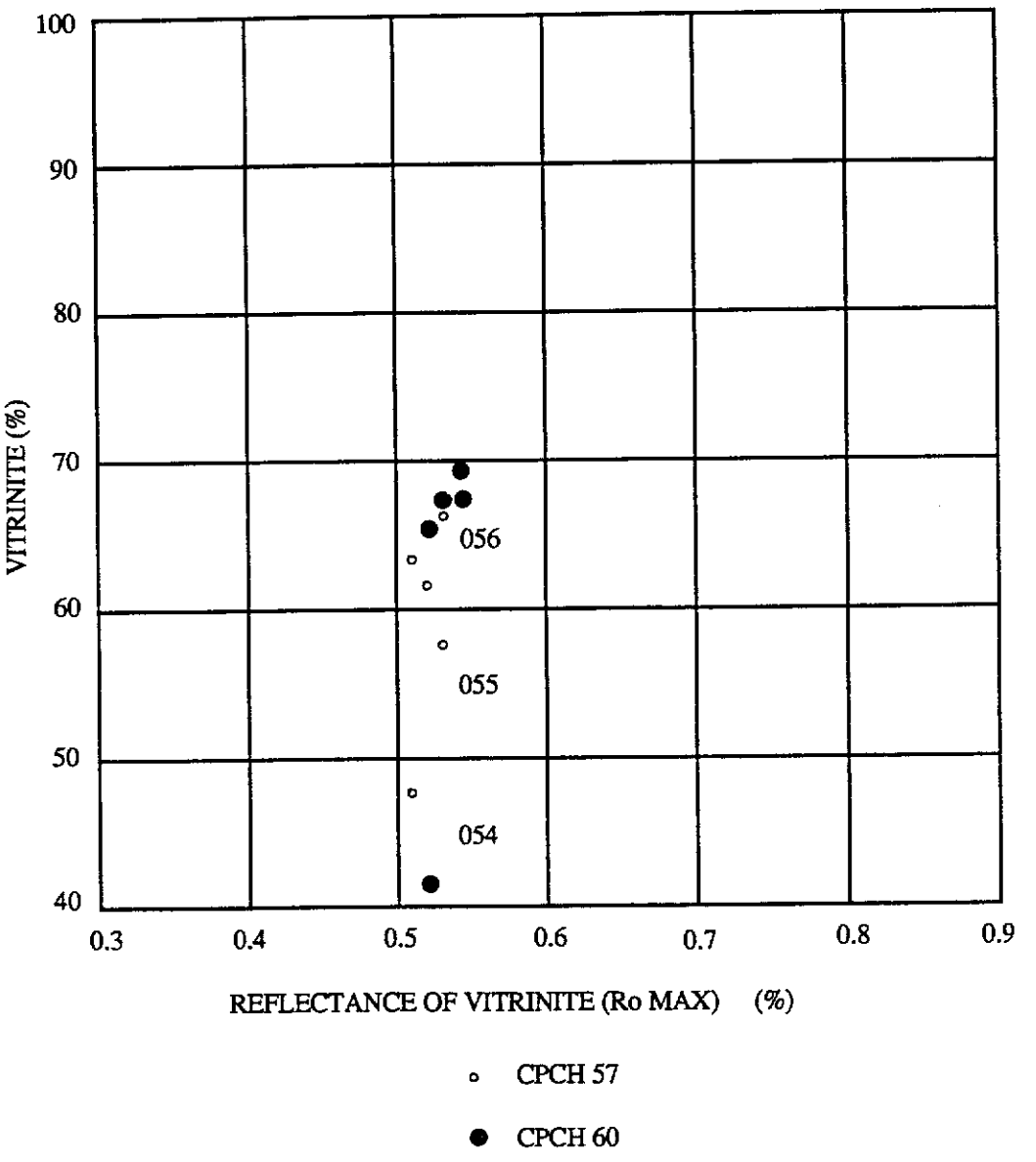

Figure 4.55. Classification and variation of Hill River coal from Gairdner Block.

4.6.4. Petrographic Characters

From the above petrographic data of the Gairdner Block coal, the coal has the following characters:

- Gairdner Block coal, predominantly has a moderate to high vitrinite content. The scarcity of well preserved cell-structure in the vitrinite, indicates that the coal has undergone high degree diagenesis.

- The inertinite content is low, which suggests a low degree of decomposition of peat.

- The exinite content is relatively high, and it is dominated by sporinite, cutinite and alginite. Association of cutinite with vitrinite B and resinite is recorded in the coal, which suggests a leafy vegetation precursor to the coal.

- The microlithotype analyses show that, vitrite plus clarite content of the Gairdner Block coal is more than 50.0 %. The higher content of vitrite plus clarite is perhaps due to the increase in the level of standing water and water table, in the environment of deposition.

- The coal is classified as sub-bituminous of Australian rank or sub-bituminous A stage of ASTM, or as metalignitous rank, on the basis of vitrinite reflectance.

No discussion of comparisons with constituents (if any) in adjacent thick

CHAPTER 5. MINERAL MATTER

5.1. Introduction

Most inorganic constituents occur in coal in the form of mineral matter, and they form the bulk of the ash after burning of coal. Two groups of inorganic constituents in coal can be distinguished based on their mode of origin, Francis (1961). The first group is of inherent ash, which is present in all coal forming plants, and the common compounds of their group consist of elements like Ca, Mg, Fe, Al, Na, K, Mn, Ti, S, Si, Cl and P. Some of the elements like Na, K, Mg and Cl are removed by water during the biochemical stage of coalification. The component of inherent inorganic constituents to the total mineral matter of coal is relatively small due to the fact that the proportion of inorganic matter contained in plant is usually less than 2 %. The second group of inorganic constituents include all mineral matter which was either washed into the coal swamp as detrital fragments or which was precipitated in the swamp from solutions, and this mineral matter is referred to as adventitious. Raymond, Cameron and Cohen (1990) considered that the type and amount of the inorganic matter in the coal is controlled by three factors. These are underlying bedrock or sediment, detrital source areas, and the ecology of the peat-forming botanical communities.

Application and complete understanding of the mineral matter studies in coals is of great significance to a variety of geological and industrial problems. Geological problems include aspects of coal formation such as genesis of macerals, coal depositional environment, and coal seam correlation. The nature of mineral matter in coal seam correlation is an additional characterising feature which may be of some aid in tracing a particular seam across an area or stratigraphic sequence. Seams or sub-seams that are close together in the sequence may have similar mineral matter as assemblage. Industrial problems include coal exploration, colliery dust, coal

washability, coal beneficiation and utilisation, with particular emphasis on the effect of the minerals present on ash fusion behaviour , Mackowsky (1968), and Cook and Kantsler (1982). The abrasiveness of the coal with respect to mining machinery or the toxicity of dusts released into the mine atmosphere may effect coal exploration. In coal utilisation, minerals may effect some aspects such as ash behaviour in combustion, or coke slag performance in the blast furnace. During the washing operations and in the behaviour of the resultant coke, the mineral matter content is of great importance. For example montmorillonite, because of its swelling properties and its tendency to form a fine suspension in water, leads to difficulties in most phases of the washing process, which include comminution, separation and dewatering operations. However, in some cases montmorillonite improves coke stability. Minerals and other inorganic matter in coal act as dilutants and reduce the proportion of hydrocarbon compound. The mineral matter content leads to a decrease in heat energy and other useful products.

In commercial uses, it can be termed as "coal" if its mineral matter content is more than 50.0 % weight, with carbonaceous matter > 70.0 % by volume. Coal having up to 50.0 % mineral matter content is categorised as an "impure" variety. Based on the mineral matter contents, Schlatter (1973) classified Western Europe coal into the following 8 grades for economic consideration :

. Grade 1 : 0 - 5 % mineral matter content
. Grade 2 : 5 - 10 % mineral matter content
. Grade 3 : 10 - 15 % mineral matter content
. Grade 4 : 15 - 20 % mineral matter content
. Grade 5 : 20 - 25 % mineral matter content
. Grade 6 : 25 - 30 % mineral matter content
. Grade 7 : 30 - 35 % mineral matter content
. Grade 8 : 35 - 40 % mineral matter content

Furthermore, grade 1 is categorised as the "purest coal", grade 1+2 (0-10 %) as "high-grade coal", and grades 1 to 4 (1-20 %) as "normal-grade coal".

Capes *et al.* (1979) reported that up to 80.0 % of pyrite content could be removed by pulverising the coal to -325 mesh (45 microns) in size and following this with oil agglomeration. Referring to environmental purpose, Birk (1990) considered that abundance of mineral matter content in the size of 0.2 to 2.0 microns leads to the contribution to conspirable mine dust which influences the amount of combustion fly ash.

5.2. Occurrence and Classification

According to the Standard Association of Australia (AS 2418 part-2, 1982), mineral matter is described as " the minerals and other inorganic material in, and associated with coal". On the basis of this definition, Ward (1986) classified the mineral matter into three types:

. Discrete crystalline mineral particles in coal or associated strata, eg. intraseam non-coal bands.

. Inorganic elements or compounds, incorporated in the organic molecules of coal.

. Dissolved inorganic compound in the coal's pore water or surface water.

Cook and Kantsler (1982) described mineral matter in coal as :

. Discrete minerals which consist of detrital matter, mainly clay with rare quartz occurring as thick layers, streaks, intercalations and also disseminated matter within coal. Thick layers are commonly referred to as "dirt bands" which were usually formed early in the diagenesis of coal, Botz *et al.* (1986).

. Syngenetic chemical precipitates, which originated from solution or colloidal

suspension during the peat stage, are present either as clay or quartz (chalcedony), siderite pyrite and apatite. These minerals are disseminated throughout the coal, but may be concentrated as nodules replacing vitrinite.

. Epigenetic minerals formed from solution after the peat stage and occur in cracks, such as cleats or bedding planes, which partially replace coal. The most important minerals in this group are sulphides (eg. pyrite), carbonates of iron, calcium and magnesium (eg. siderite, calcite and ankerite).

. Inherent minerals represent "inorganic matter" present in the original organic compound or adsorbed by the organic material in the peat stage.

Stach *et al.* (1982) sub-divided mineral matter in coal, based on its origin, into the following three groups :

. Inorganic matter occurring in the original plants which contribute to coal formation.

. Associations of inorganic-organic matter and minerals formed at the early stage of the coalification process. Commonly, these constituents were transported into the swamp by water or wind during the coal formation.

. Minerals that developed during the late stage of the coalification process, and these minerals infilled cracks, fissures or cavities in the form of solution or alteration of primarily deposited minerals.

On the basis of genetic and practical connotations, Falcon and Snyman (1986) divided the mineral matter into intrinsic, extrinsic, adventitious and inherent (Table 5.1). They also schemed the type of distribution for the common mineral matter in coal, as shown in Table 5.2.

According to Spears (1987), detrital minerals in coal occur in dispersed or concentrated forms, the later is less intimately associated with macerals. The overall composition of detrital minerals is a function of grain size and their environment of

Table 5.1 . Classification of mineral matter (after Falcon and Snyman, 1986).

Basis of Classification	Type/ Category		Characteristics
Genetic	Intrinsic		Inorganic matter. Present in their original living plant tissue. Ultimately trapped in the form of sub-microscopical mineral grains and organo-metallic complexes. Some as discrete, coarse grained minerals.
	Extrinsic	Primary or Syngenetic	From accumulation of the minerals at the time of peat accumulation by wind and water or precipitation in-situ.
		Secondary or Epigenetic	Deposited by percoling waters into fractures, cavities, and pores within the coal seams long after initial accumulation of the peat.
Practical conotations	Adventitious		At a particular size the minerals can be easily liberated by milling, and can be removed by beneficiation processes.
	Inherent		Minerals are not yet liberated.

Table 5.2 . Distribution of the more common minerals (after Falcon and Snyman, 1986).

Group of minerals	Syngenetic Interlaminated or associated with macerals	Epigenetic In cleats or fractures
Clay minerals	Kaolinite Illite Montmorillonite	
Carbonates	Calcite Siderite	Calcite Siderite
Sulphides	Pyrite	Pyrite
Quartz	Quartz grains	Quartz

deposition, which could be aqueous or aeolian. He also divided diagenetic minerals in coal into early and late diagenetic ones. The early diagenetic minerals are formed in pre-cleat form, and these are framboids and associated microcrystalline pyrite. The late diagenetic matter include cleat minerals consisting of non-framboidal granular to massive aggregates, and fibrous radiating microscopic pyrite.

On the basis of the timing of mineralisation related to coalification process, Diessel (1992) sub-divided mineral matter in the coal into syngenetic and epigenetic types. The syngenetic mineral is formed at the same time as peat accumulation, whereas the epigenetic type is the result of chemical precipitation after the coal has been completely compacted.

A quantitative method for pyrite in coal using optical image techniques was suggested by Harris *et al.* (1977), and Creelman, Greenwood and Paulson(1986) proposed an automated mineral recognition under Quantitative Evaluation of Materials (QEM) by Scanning Electron Microscope (SEM). Ward (1986, 1992) reviewed the distribution and character of mineral matter of eastern and southern Australian bituminous coals, and also the application of various analytical techniques, like selective chemical leaching and oxygen-plasma techniques for its determination. Birk (1990) examined quantitatively minerals in coal of Sydney Coalfield, Nova Scotia, by SEM mode, computerised image analysis, and energy dispersive X-ray spectrometry (EDS).

The occurrence, form, origin and characteristics of cleat minerals in coal from Australia, North America and Europe have been studied and reported on by Mackowsky (1968), Hatch, Gluskoter and Lindahl (1976), Love, Coleman and Curtis (1983), Spears and Caswell (1986), Spears (1987), Frankie and Hower (1987), Bodily *et al.* (1991) and Demchuk (1992).

5.3. Mineral Matter in Hill River Coal

Petrographic study of the Hill River coal includes determination of mineralogical characters, occurrences, and vertical and lateral distributions of adventitious mineral matter in all the sub-seams. The distribution of the mineral matter in the Mintaja Block coal is presented in section 5.4.1 and for the Gairdner Block coal in section 5.4.2. The most common recognisable mineral matter in the coal is of the adventitious group, consisting of syngenetic, diagenetic, and epigenetic minerals. The syngenetic and diagenetic sub-groups, are generally intergrown intimately with the coal, while the epigenetic one tends to be coarsely intergrown and associated with cleats or fractures, such as coating or infillings in the coal. The epigenetic minerals were probably formed either at later stage of the coal diagenetic event or at an early stage of epigenetic event. The inherent mineral matter is hardly recognised under the microscope and therefore the SEM method is used for its identification. These minerals include small sub-angular particles, consisting of compounds of Co, P, Si, Cl, Ti, F, Al, and V. The macroscopic identification of mineral matter is possible when it occurs as thick discrete bands and laminae or lenticles of clay or pyritic materials, rounded pellets, and dispersed crystals within coal. Such occurrences indicate that these minerals were formed contemporaneously with peat in the basin. A brief description and distribution of adventitious minerals in the coal from the Mintaja and Gairdner Blocks is as follows :

5.3.1. Clays

The clay minerals are recognised as pellets or bands present among macerals (Figure 5.1 a). These also occur as cell cavity infillings in telinite (Figure 5.1 b), fusinite (Figure 5.1 c), and as cleat infillings. The pellets or nodular forms and infillings of

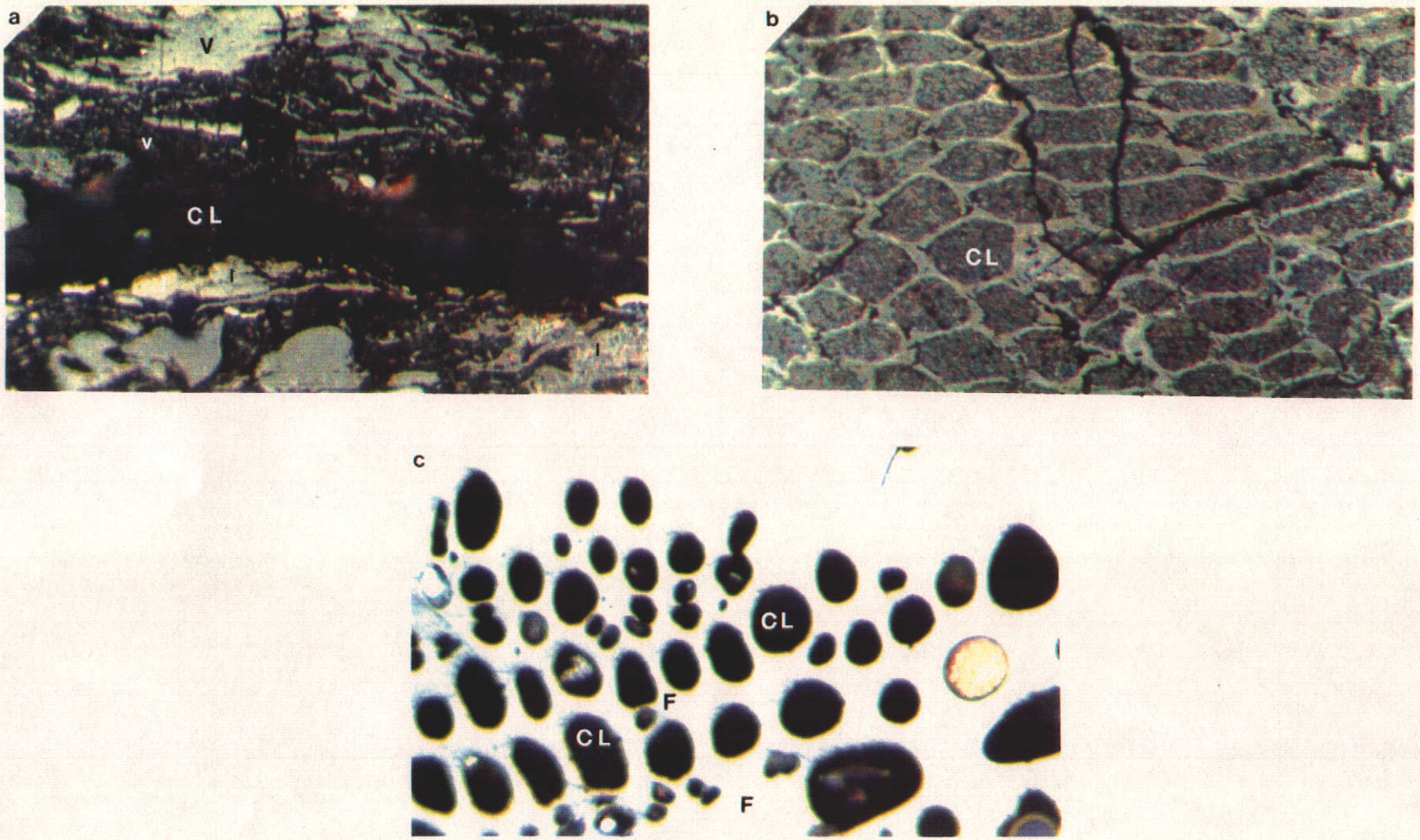

Figure 5.1. Photomicrographs of clay minerals in coal. (Oil immersion), X 320.
a. Band of fine-grained clays (CL) interstratified within vitrinite (V) and inertinite (I) groups. (CPCH 1/G 6).
b. Fine-grained clays (CL) infilling cell cavities of telinite. (CPCH 1/G 3).
c. Clays (CL) infilling fusinite (F) cell cavities. (CPCH 1/G 5).

cell cavities, are products of precipitation or remobilisation of the clay minerals at a later stage in the coal compaction, Ward (1989).

The SEM study undertaken on the selected samples of the Mintaja and Gairdner Blocks coal, indicates that clay minerals present in the coal, include illite (Figure 5.2 a), montmorillonite (Figure 5.2 b) and kaolinite (Figure 5.2 c). Under high magnification of the SEM mode, kaolinite forms "books" of crystals. Abundance of clay minerals in the coal in relation to pyrite and other minerals (carbonates and quartz) is shown in Figure 5.6 for the Mintaja Block coal and in Figure 5.7 for the Gairdner Block coal. The distribution of the clay minerals in the coal is discussed later in sections 5.4.1 and 5.4.2.

5.3.2. Pyrite

Pyrite is formed during the depositional and diagenetic phases of the precursor peat formation, Wiesse and Fyfe (1986). Pyrite is the most common iron-bearing mineral present in the Mintaja and Gairdner Block coal and can be sub-divided into syngenetic and epigenetic types. The syngenetic pyrite includes framboids, and cell fillings in macerals. The epigenetic type consists of isolated pyrite bodies, and cleat and fracture infillings in the coal.

Framboidal pyrite is present as clusters or individuals, up to 220 microns in size (Figure 5.3 a). The majority of framboids occur as inter layered constituents, but some are present as cleat and crack infillings. The massive pyrite showing framboidal relicts is recognised as a replacement of vitrinite and sporinite bodies (Figure 5.3 b). Figure 5.3 c shows massive pyrite infilling cell cavities of "sieve -structured" fusinite. The pyrite infilling vitrinite cell cavities is depicted in Figure 5.3 d. Massive pyrite occurs as infilling of cleat and fracture in telocollinite and is

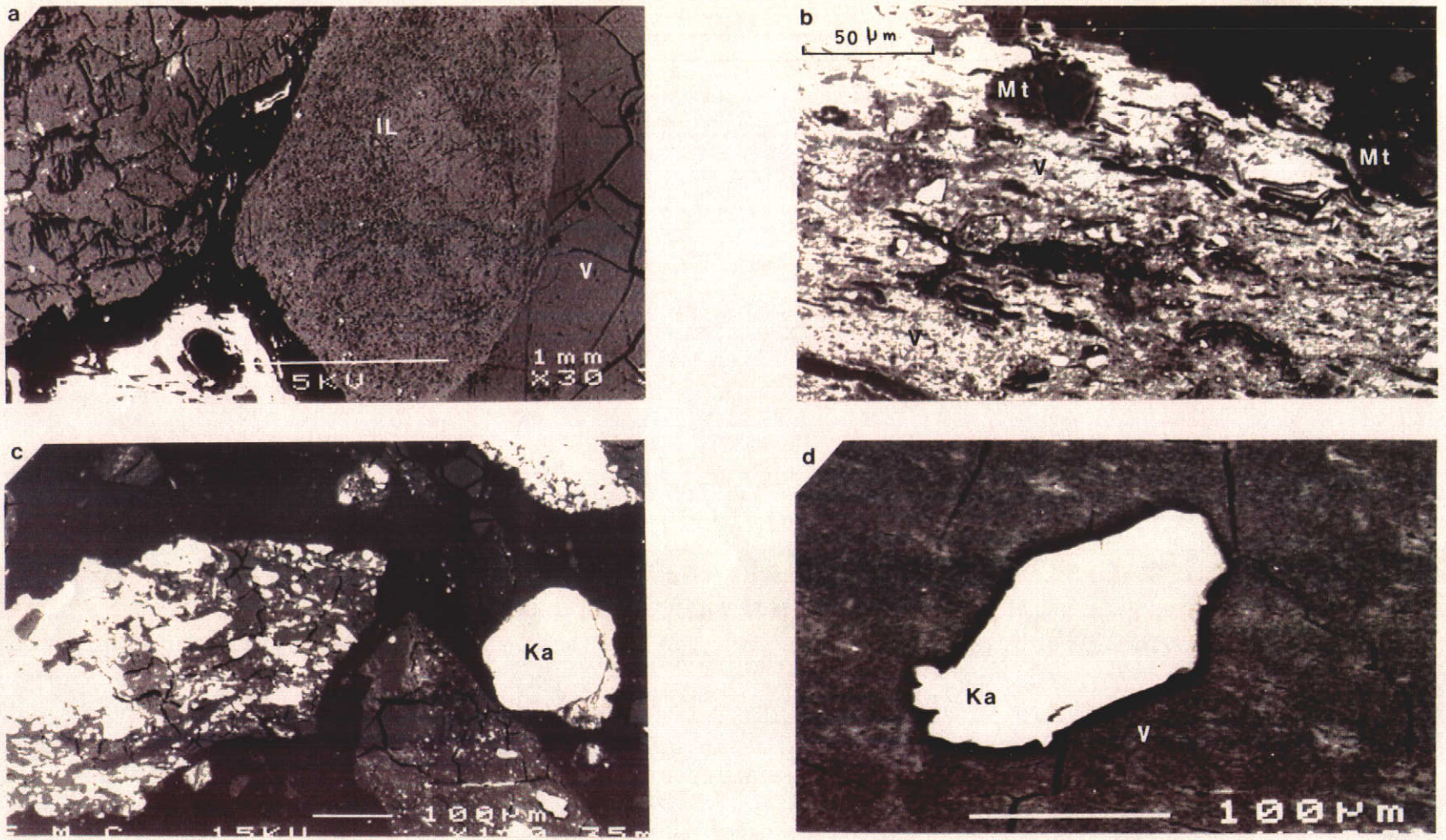

Figure 5.2. Photomicrographs of clay mineral varieties. (SEM mode).
a. Sub-rounded grain of illite (IL) embedded in vitrinite (V). (CPCH 57/G 5-6).
b. Scattered motmorilllonite (Mt) in vitrinite-B (V). (CPCH 57/G 5-6).
c. Kaolinite grains (Ka) embedded in vitrinite (V). (CPCH 57/G 5-6).
d. Single grain of kaolinite (Ka) embedded in vitrinite (V). (CPCH 37/G 4).

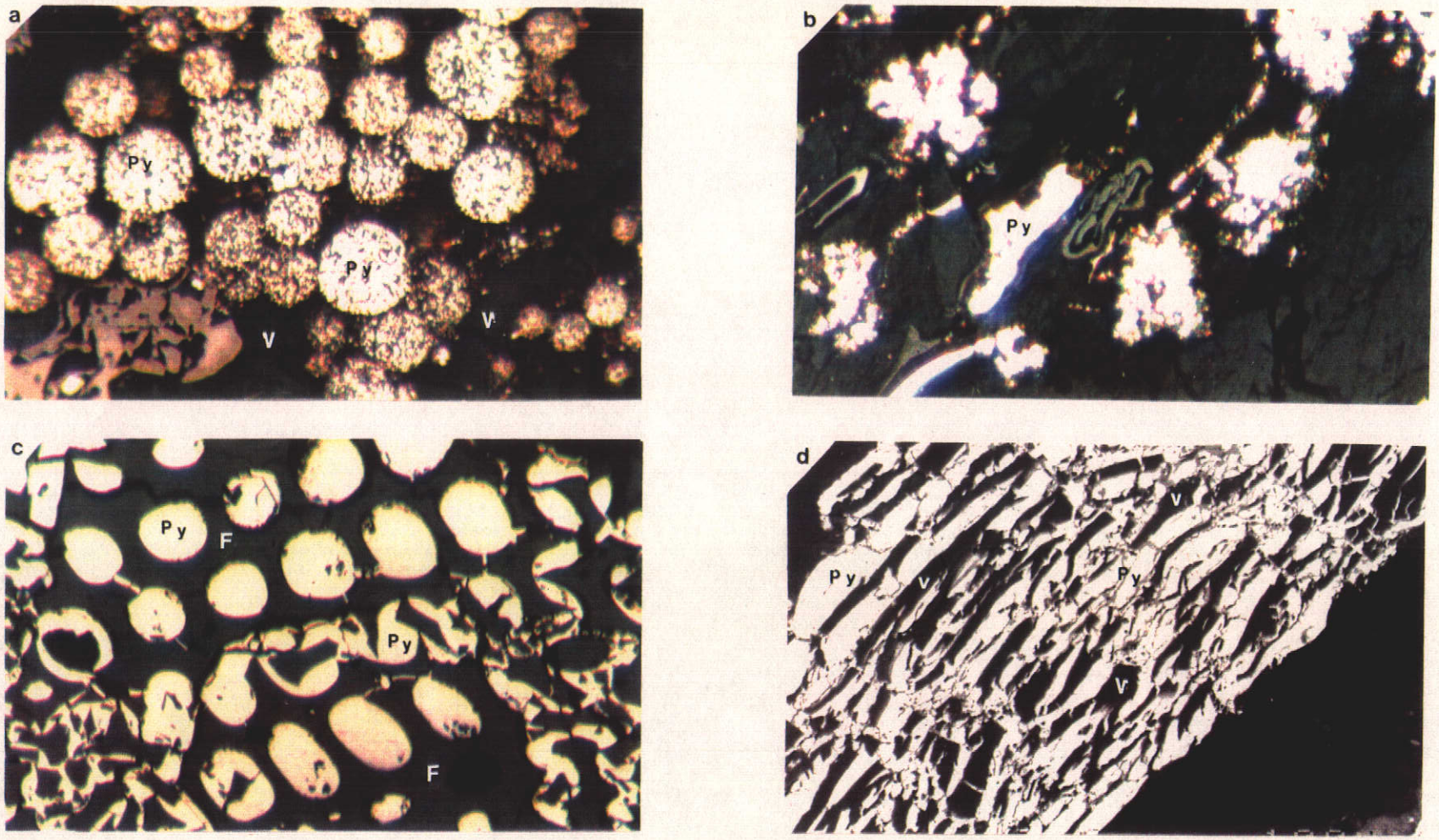

Figure 5.3. Photomicrographs of pyrite in coal. (a, b, and c under oil immersion objective, X 320; d under SEM mode).
a. A cluster of framboidal pyrite (Py) embedded in vitrinite (V). (CPCH 57/G 4).
b. Sporinite replaced with pyrite (Py). (CPCH 47/G 1).
c. Pyrite (Py) infilling cell cavities of "sieve-structured" fusinite (F). (CPCH 47/G 3).
d. Massive pyrite (Py) infilling cell cavities of vitrinite (V). (CPCH 57/G 5-6).

represented in Figure 5.4 a, and the isolated massive single body of pyrite of 300 microns is shown in Figure 5.4 b. According to Diessel (1992), the presence of cleat pyrite indicates a late mineralisation during tectonic deformation within a basin. The importance of clay in coal as a transporter of iron, was emphasised by Berner (1971) and Stanton (1972). A similar occurrence of pyrite infilling cell cavities in fusinite which are adjacent to cells filled with clay minerals is shown in Figure 5.4 c. In sub-seam G 6 of CPCH 1, tiny pieces of pyrite are embedded in clay minerals (Figure 5.4 d). Distribution of pyrite with reference to the Mintaja Block coal is discussed in section 5.4.1, and that of the Gairdner block coal in section 5.4.2. The presence of pyrite in coal contributes to sulphur content in coal. Hunt and Hobday (1984) classified Australian Permian coal on the basis of sulphur content as :

. Low : < 0.55 % (daf)

. Medium : 0.55 % to 1.00 % (daf)

. High : > 1.00 % (daf)

The total sulphur distribution of the sub-seams from the Mintaja and Gairdner Blocks is presented in Figure 5.7 and 5.10, and discussed briefly in the section 5.4.1.

5.3.3. Carbonates

The carbonate minerals including calcite and siderite, have been identified in the coal. The calcite occurs as cell wall infillings in fusinite and also as replacement in vitrinite (Figure 5.5.a and b). The calcite was formed as a result of precipitation by percolating water containing calcium carbonate which took place after compaction of coal. Hatch, Gluskoter and Lindahl (1976), Botz *et al.* (1986) and Spears (1987) considered that calcite in fracture fillings have been deposited during the later stage of diagenesis, at a temperature of up to more than 100 ° C. Spears (1987) also suggested that the calcium of calcite was derived from diagenetic modification of detrital minerals in and around the coal seam, whilst the carbonate was derived from

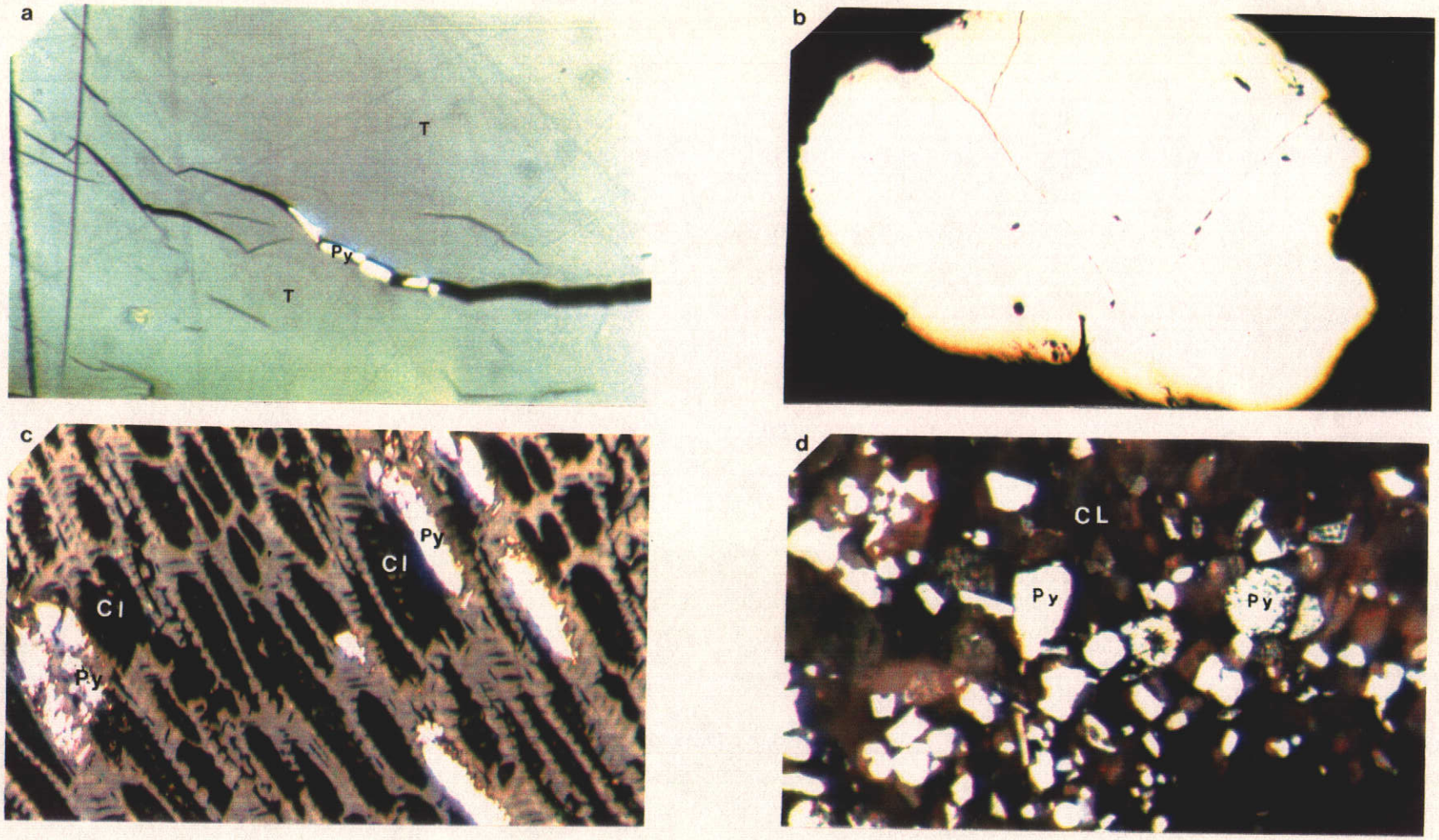

Figure 5.4. Photomicrographs of pyrite and clay minerals in coal. (Oil immersion), X 320.
a. Epigenetic pyrite (Py) infilling cleat of telocollinite (T). (CPCH 57/G 4).
b. Isolated massive sub-rounded pyrite. (CPCH 1/G 6).
c. Cell-cavity infilling pyrite (Py) adjacent to clay minerals (CL). (CPCH 1/G 5).
d. Scattered pyrite (Py) in association with clay minerals (CL). (CPCH 1/G 6).

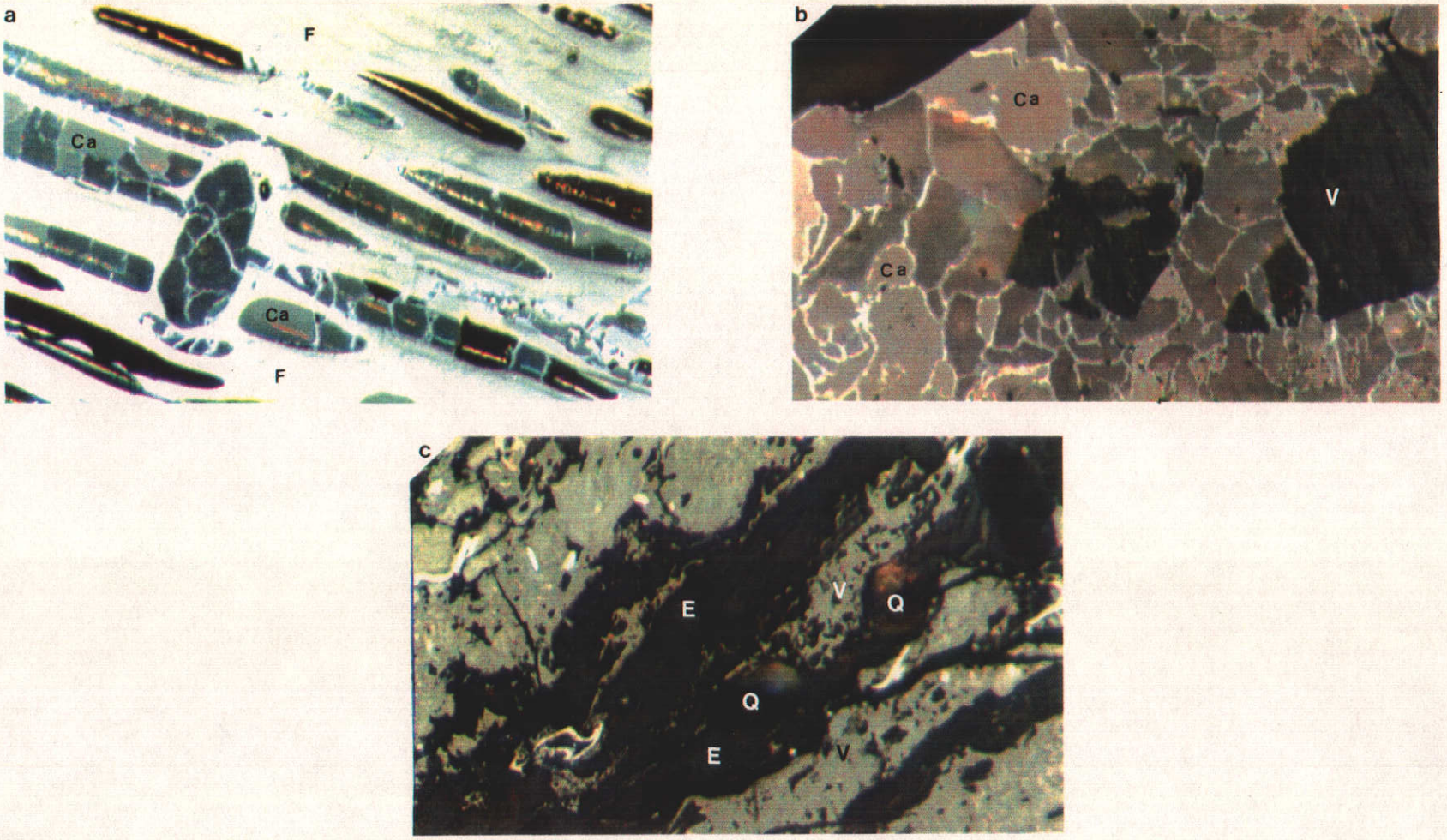

Figure 5.5. Photomicrographs of carbonate and quartz minerals.(Oil immersion objective), X 320.
a. Calcite (Ca) infilling cell-cavities of fusinite (F). (CPCH 57/G 4).
b. Calcite (Ca) replacing vitrinite maceral. (CPCH 57/ G 4).
c. Sub-rounded quartz grains (Q) embedded in exinite (E) and vitrinite (V) macerals. (CPCH 39/G 6).

decarboxylation and other reactions in the organic matter. However, the calcium is also a common compound of the organic matter itself in a number of low-rank coals, Nankeris and Furlong (1980). The possible origin of siderite may be due to interaction between iron in the peat's pore water and dissolved carbondioxide presented by fermentation of the organic matter, Gould and Smith (1979).

5.3.4. Quartz

The quartz is recognised in association with vitrinite and exinite in the form of sub-angular to sub-rounded grains (Figure 5.5 c). The quartz formed from solution with fine crystalline structure may be present in the coal, but it is difficult to identify under the microscope.

5.4. Mineral Matter Distribution

The study of mineral matter in the Hill River coal is valuable for the determination of how various minerals have both aggregated and associated with the macerals. The determinations of the mineral matter types, were successfully achieved by the combination of reflected light microscope, fluorescence mode and SEM method.

The mineral matter recognised in the coal consists mainly of clays, pyrite and minor amounts of carbonates and quartz. The clay minerals consist of montmorillonite, illite and kaolinite, and are present in low (< 5.0 %) to high (> 10.0 %) amounts. The pyrite content is low to moderate (5.0 - 10.0 %), and the carbonates and quartz contents are low .

5.4.1. Mineral Matter in the Mintaja Block Coal (CPCH 1, 37, 39 and 47)

The mineral matter analyses of the Mintaja Block coal were undertaken on sub-seams G1 to G6 from the drill cores CPCH 1, 37, 39 and 47. The mineral matter, vitrinite plus exinite, inertinite and the total sulphur for all the sub-seams are presented in Table 5.3 and illustrated in Figure 5.6. Additionally, association of mineral matter with macerals was also examined, which is given in Table 5.4. The vertical distribution of sulphur, pyrite, other minerals and macerals is presented in Figure 5.7 for all the sub-seams of the block.

The clay minerals are the most prominent in the coal, particularly in sub-seams G 5 of CPCH 1, 37, 39 and 47, and sub-seams G 6 of CPCH 1 and 39 (Table 5.3). The clay minerals range from 1.00 to 17.60 % in the sub-seams. The highest clay content occurs in sub-seam G 6 of CPCH 1, whereas, the lowest is recorded in sub-seam G 4 of CPCH 39. The clays are associated mostly with vitrinite B, followed by vitrinite A and inertinite, and minor association with exinite (Table 5.4).

The pyrite is the second dominant mineral in the coal (Table 5.3 and Figure 5.6). It has a low to medium value, which varies from 1.00 % to 6.00 % in the coal. The majority of pyrite is commonly associated with vitrinite B, and the lesser amounts recognised in association with vitrinite A , inertinite, and exinite (Table 5.4). The distribution of pyrite in the coal is of particular interest, because higher sulphur content requires desulphurisation in the power station to avoid pollution by sulphur dioxide. The total sulphur content of the Mintaja Block coal sub-seams is obtained from CRAE analyses (1989), and it ranges from 0.87 % to 3.55 %, which is categorised as medium to high value, Hunt and Hobday (1984). The total sulphur variation, macerals, mineral matter and pyrite distribution in the sub-seams is shown in Figure 5.7. This figure shows that pyrite distribution is concomitant with sulphur distribution and the increase in pyrite content is accompanied by an increase in

Table 5.3. Mineral matter, total sulphur and maceral analyses of Hill River coal, Mintaja Block.

Drill Hole	Sub-seam	Mineral Matter	Clays	Pyrite	Total Sulphur	Vitrinite+ Exinite	Inertinite
CPCH 1	G 1	4.5	3.1	1.2	0.92	73.8	21.7
	G 2	4.5	2.2	2.3	1.42	73.5	21.8
	G 3	7.5	5.8	1.5	1.17	76.8	15.7
	G 4	8.4	3.6	4.6	2.36	73.0	18.6
	G 5	13.2	9.0	4.0	N/A	71.4	15.4
	G 6	24.0	17.6	6.0	N/A	60.6	15.4
CPCH 37	G 1	7.4	4.8	1.8	1.18	71.6	21.0
	G 2	5.8	2.4	1.8	1.00	71.0	23.2
	G 3	5.4	2.2	2.2	1.09	73.2	21.4
	G 4	14.8	8.4	5.2	2.40	71.0	14.2
	G 5	20.8	14.2	3.8	1.82	61.6	17.6
CPCH 39	G 1	6.4	4.0	1.0	0.87	68.8	24.8
	G 2	5.4	2.0	1.6	1.19	73.0	21.6
	G 3	5.0	2.2	1.8	1.16	77.4	17.0
	G 4	5.2	1.0	3.2	2.35	84.4	10.4
	G 5	17.2	15.2	1.2	0.91	68.6	14.2
	G 6	17.4	10.4	5.2	1.97	59.4	23.2
CPCH 47	G 1	6.4	2.6	2.4	2.38	69.2	24.4
	G 2	5.4	1.8	2.4	1.57	73.8	20.8
	G 3	6.2	3.6	1.8	1.16	72.8	21.0
	G 4	6.6	2.0	3.4	1.95	76.0	17.4
	G 5	19.2	12.8	5.8	3.36	62.4	18.4

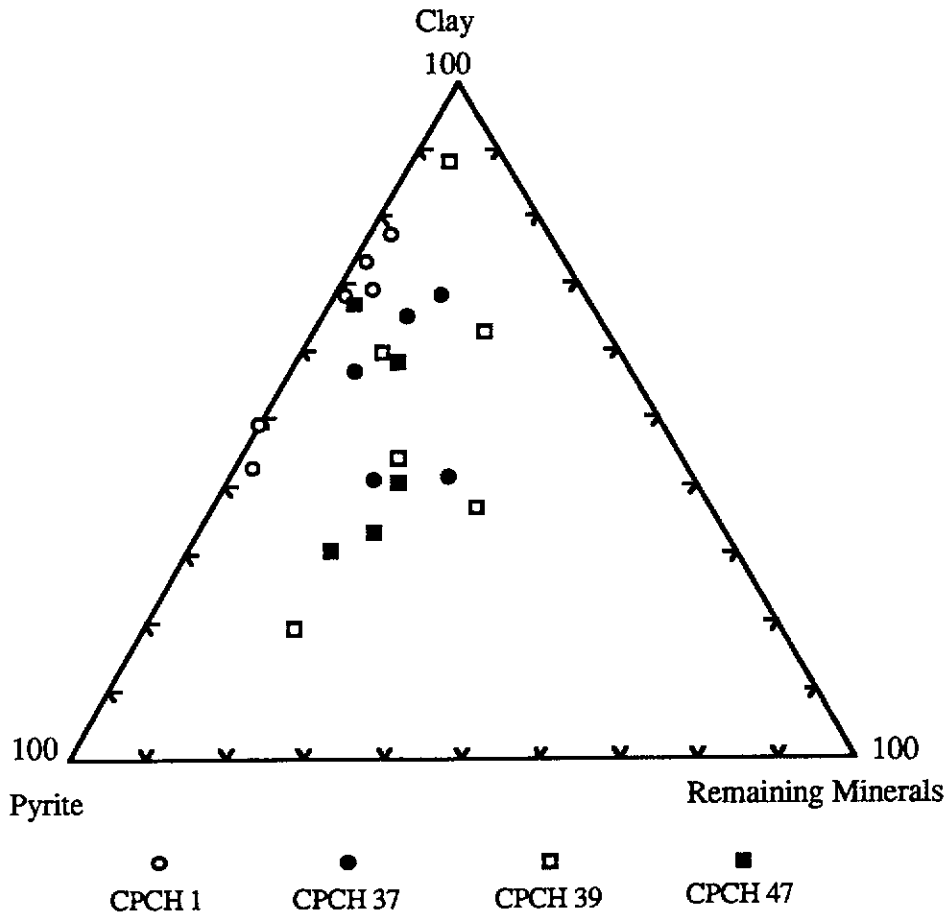

Figure 5.6. Composition of mineral matter, Hill River coal, Mintaja Block.

Table 5.4 . Distribution of mineral matter and maceral association, Hill River coal, Mintaja Block.

Mineral	Maceral	CPCH 1						CPCH 37					CPCH 39						CPCH 47				
		G 1	G 2	G 3	G 4	G 5	G 6	G 1	G 2	G 3	G 4	G 5	G 1	G 2	G 3	G 4	G 5	G 6	G 1	G 2	G 3	G 4	G 5
Clay	Vitrinite A			0.2		1.0	0.6	0.8		0.8	8.4		0.4				3.2	2.0			0.4		2.8
	Vitrinite B	2.8	2.0	4.0	3.0	7.2	15.0	4.0	2.4	1.4		14.0	2.8	2.0	2.0	1.0	12.0	6.6	2.0	1.8	2.8	2.0	9.6
	Exinite												0.4		0.2								
	Inertinite	0.3	0.2	0.6	0.6	0.8	2.0					0.2	0.4					1.8	0.6		0.4		0.4
Pyrite	Vitrinite A		0.2		0.4		0.4	1.2	0.2	0.6			0.2					0.4				0.6	1.0
	Vitrinite B	1.0	1.9	1.3	3.8	3.8	3.8	0.4	1.0	1.6	5.0	3.8	0.8	1.6	1.6	3.2	1.0	4.6	2.4	2.4	1.8	2.8	4.8
	Exinite										0.2												
	Inertinite	0.2	0.2	0.2	0.4		1.4	0.2	0.6						0.2		0.2	0.2					
Carbonates	Vitrinite A							0.2		0.4		0.2	0.8										
	Vitrinite B						0.3		1.4	0.6	0.8	2.2	0.6	1.6	1.0	1.0	0.8	1.6	1.4	1.2	0.6	1.2	0.6
	Exinite											0.2									0.2		
	Inertinite						0.1					0.2											
Quartz	Vitrinite A																						
	Vitrinite B	0.2		0.2	0.2	0.2		0.4	0.2		0.2			0.2									
	Exinite							0.2			0.2							0.2					
	Inertinite																						

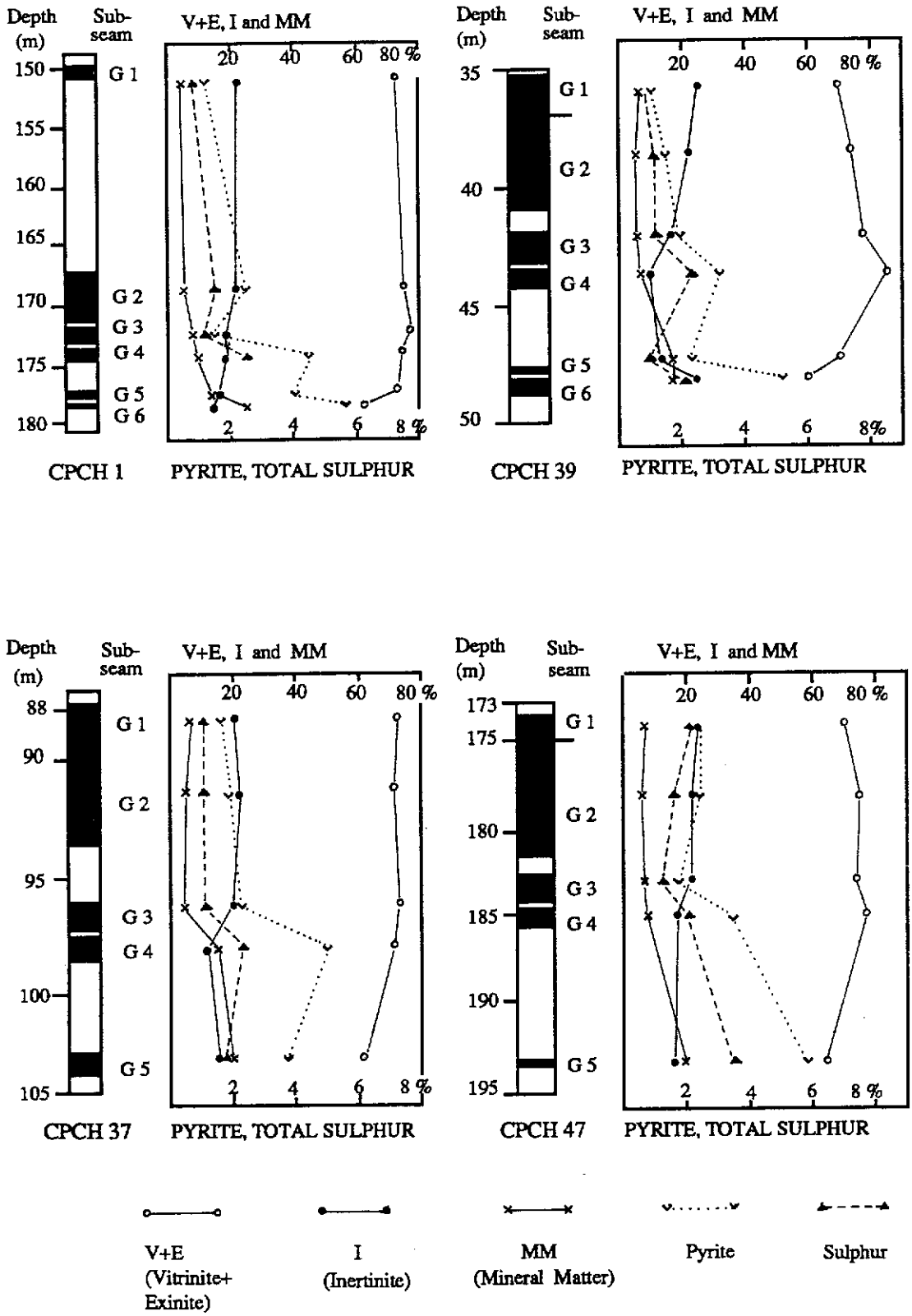

Figure 5.7. Vertical variation in vitrinite, exinite, inertinite, mineral matter, pyrite and sulphur contents of sub-seams G1 - G5/6 of Hill River coal, drill holes CPCH 1, 37, 39 and 47, Mintaja Block.

sulphur content. The random pattern of sulphur distribution in the coal is probably caused by different proportions of pyrite occurring in association with the macerals.

The carbonate minerals including calcite and siderite in the coal have a range between traces to 2.80 %, and mostly associated with vitrinite B_r in all the sub-seams of CPCH 37, 39 and 47 (Table 5.4). In the ternary diagram of mineral matter composition shown in the Figure 5.6, carbonates are combined with quartz as the remaining minerals, because of their minor content in the coal.

The quartz in the coal occurs microscopically in nearly all the sub-seams of CPCH 1 and CPCH 37. However, its content is very low varying from traces to 0.60 %. The majority of quartz is associated with vitrinite B, and to a lesser extent with exinite (Table 5.4). It is recognised as sub-angular to sub-rounded grains, probably of detrital origin introduced into the swamp by water or air-borne activities.

The vertical variation of mineral matter distribution in the Mintaja Block coal is depicted in Figures 4.36 and 5.7. In Figure 5.7, the total mineral matter content shows an increase from the sub-seam G2 to G 6, for the drill holes CPCH 1, 37 and 47. For the drill hole CPCH 39, the increase in the total mineral matter is recorded from the sub-seams G 3 to G 6. Lateral variation in the mineral matter content of the Mintaja Block coal in SE-NW direction is illustrated in Figure 4.36. The figure shows a remarkable trend in the sub-seam G 1, G 2 and G 5. The mineral matter content increases towards the NW direction, while in sub-seams G 3 and G 6, a decrease in mineral matter content occurs in the same direction. The relationship of the total mineral matter, pyrite, total sulphur, vitrinite plus exinite and inertinite distribution of the Mintaja Block coal is depicted in Figure 5.7. The total mineral matter content from sub-seams G 1 to G 4 in CPCH 37, G 2 to G 4 in CPCH 39, and G 2 to G 5 in CPCH 47 coincides with the content of pyrite and total sulphur. Moreover, in all the sub-seams of the four drill holes, pyrite content is concomitant

with the total sulphur content. Generally, from sub-seams G 1 to G 5/6, the total mineral matter, pyrite and total sulphur distribution shows an increase in value. However, a fluctuation of their distribution occurs in drill holes CPCH 1 and CPCH 39. In drill holes CPCH 37 and 47, the total mineral matter, pyrite and total sulphur content increases from sub-seams G 1 to G 4. This increasing value is still present from G 4 to G 5 of drill hole CPCH 47, whereas in CPCH 37 a decrease in content of those three matters occurs from sub-seams G 4 to G 5. In addition, the vitrinite plus exinite content varies inversely to the inertinite content in sub-seams G 1 to G 4 of all the drill holes.

Besides the above distribution of mineral matter, the distribution of mineral matter in coal size fraction of drill cores CPCH 1 has also been carried out, earlier described in Chapter 4 (section 4.4.2). The analyses of the coal from the CPCH 1 was possible due to the availability of the entire core, while from other holes only the crushed coal fractions were available. The total mineral matter inclusive of all minerals, clay minerals and pyrite distribution of coal size fractions from sub-seams G 1 to G 5/6 of drill core CPCH 1, is presented in Table 5.5 and depicted in Figure 5.8. There is a similarity of trend in the distribution between the total mineral matter and clay contents, from size fractions > 4 mm to 1/2X1/4 mm, in all the sub-seams, which reflects that the mineral matter of the size fractions is predominantly composed of clay minerals. The total mineral matter, clays and pyrite content of all size fractions shows an undulated variation in sub-seams G1, G2 and G3. The contents of total mineral matter and clays in sub-seam G4, show a decrease from size fraction > 4 mm to 1/2X1/4 mm, and an increase from 1/2X1/4 mm to < 1/4 mm. In sub-seam G5, the total mineral matter and clays show a decrease from size fraction > 4 mm to 4X2 mm, followed by an increase from size fraction 4X2 mm to 1X1/2 mm, and then a decreasing value from 1x1/2 mm to < 1/4 mm. The total mineral matter and clays distribution in all the sub-seams are less in coarser size fractions in comparison to the finer ones, except in sub-seams G1 and G2. The pyrite distribution in all the sub-

Table 5.5. Mineral matter analyses of size fractions of coal, drill hole CPCH 1

Sub-seam	Size Fraction (mm)	Total Mineral Matter	Clay	Pyrite
G 1	> 4	8.60	8.40	0.00
	4X2	10.80	9.80	1.00
	2X1	10.40	8.60	0.20
	1X1/2	11.00	9.80	0.20
	1/2X1/4	10.20	9.40	0.80
	< 1/4	4.60	2.80	1.00
G 2	> 4	8.00	6.40	1.00
	4X2	7.80	4.40	3.20
	2X1	4.20	2.40	1.40
	1X1/2	6.40	3.40	3.00
	1/2X1/4	5.00	3.60	1.40
	< 1/4	6.60	3.60	3.00
G 3	> 4	6.40	5.40	0.00
	4X2	9.00	7.00	1.40
	2X1	5.40	3.60	1.20
	1X1/2	9.40	7.80	1.20
	1/2X1/4	5.80	4.00	1.60
	< 1/4	7.00	2.80	2.80
G 4	> 4	17.20	10.40	4.40
	4X2	16.60	7.40	6.40
	2X1	16.40	6.60	8.00
	1X1/2	15.60	6.60	7.00
	1/2X1/4	11.40	3.80	5.20
	< 1/4	16.00	2.80	6.20
G 5/6	> 4	20.20	11.80	6.40
	4X2	13.00	5.00	6.80
	2x1	13.80	7.00	5.80
	1X1/2	21.40	11.60	7.40
	1/2x1/4	19.40	12.20	6.00
	< 1/4	14.20	6.80	4.20

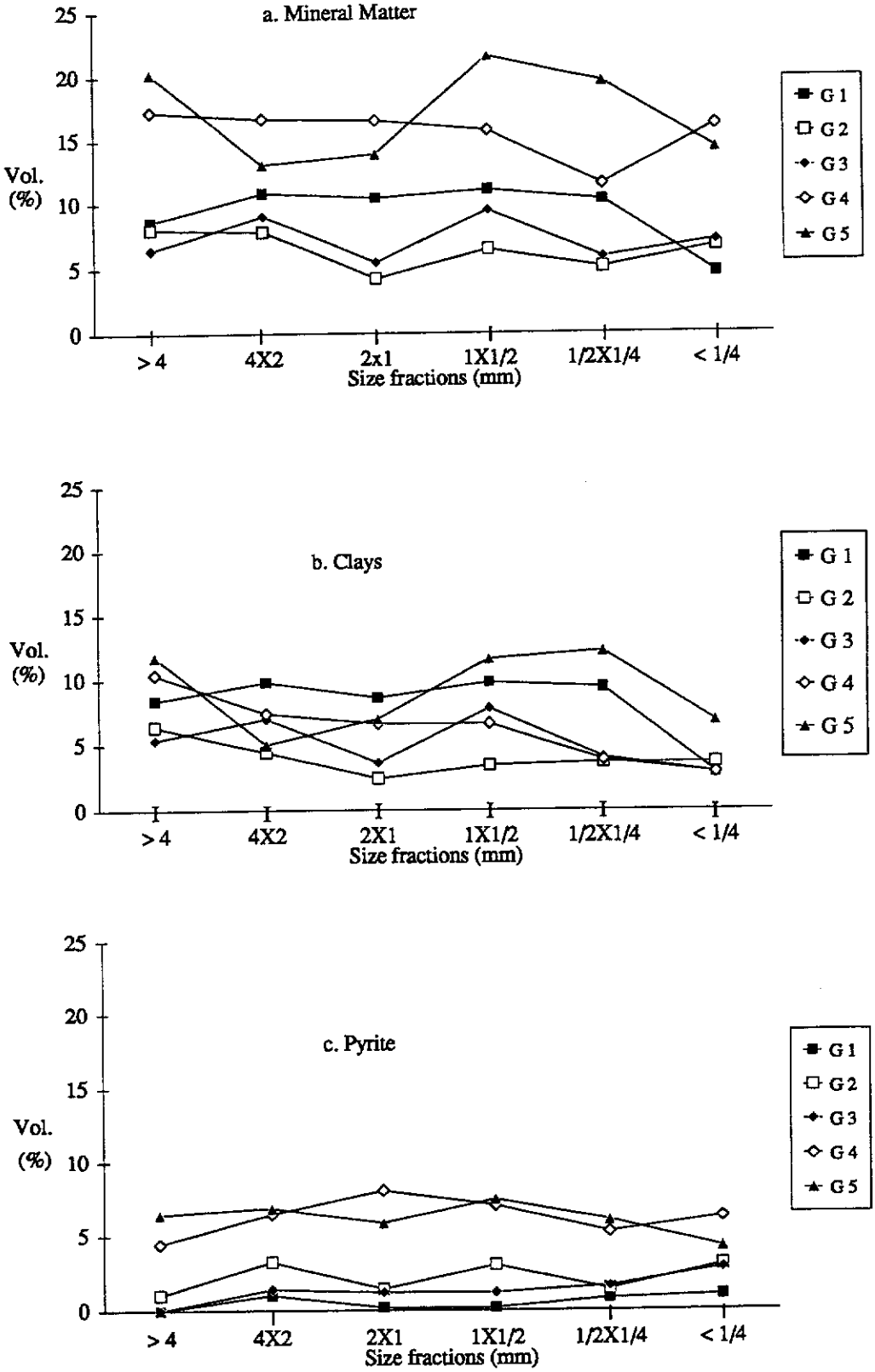

Figure 5.8. Mineral matter, clays, and pyrite content variation of size fractions, sub-seams G1 - G5/6, drill hole CPCH 1, Mintaja Block.

seams does not show great fluctuation, and it is represented in a slightly similar variation, particularly in sub-seams G1 and G3, and G2 and G5. The low content of the total mineral matter in the coal which ranges up to 5.40 %, is identified in size fraction < 1/4 mm of sub-seam G1, size fraction 1/2X1/4 mm of sub-seam G2, and size fraction 2X1 mm of sub-seam G3. The lower content of clays is recognised in size fraction 2X1 mm of sub-seam G2 (2.40 %) and size fraction < 1/4 mm of sub-seams G1 and G3 (2.80 %). The lowest pyrite content is present in size fraction 2X1 mm and 1X1/2 mm of sub-seam G1 and has a value of 0.20 %.

Based on the above mentioned description and the distribution of mineral matter, the Mintaja Block coal shows the following characteristics:

- Clay minerals represent the most widespread and abundant inorganic constituent in the coal.
- The mineral matter is predominantly associated with vitrinite B followed by the association with the inertinite.
- Distribution in size fractions shows that the mineral matter contents are more in finer size fractions in comparison to the coarser ones.
- Based on the mineral matter content, the coal is classified as a "normal-grade coal".

5.4.2. Mineral Matter in the Gairdner Block Coal (CPCH 57 and 60)

The mineral matter examination of the Gairdner Block coal from the drill cores CPCH 57 and 60, was also completed to determine its distribution, as well as its association with the macerals within the sub-seams G 1 to G 5. The analyses of mineral matter in the coal are shown in Table 5.6 and depicted in Figure 5.9 in terms of three apices consisting of clays, pyrite and the remaining minerals (carbonates and quartz). In addition, the Figure 5.10 shows the distribution of macerals, mineral matter, pyrite and the total sulphur in the sub-seams G 1 to G 5. The mineral matter

Table 5.6 . Mineral matter, total sulphur and maceral analyses of Hill River coal, Gairdner Block.

Drill hole	Sub-seam	Mineral Matter	Clays	Pyrite	Total Sulphur	Vitrinite+ Exinite	Inertinite
CPCH 57	G 1	4.20	2.00	1.20	0.85	73.80	22.00
	G 2	3.80	1.00	1.60	0.99	71.40	24.80
	G 3	7.40	3.20	2.80	1.63	69.00	23.60
	G 4	7.80	5.20	1.40	1.74	76.80	15.40
	G 5	19.60	12.60	4.80	2.10	61.00	19.40
CPCH 60	G 1	7.40	3.00	2.20	1.49	73.20	19.40
	G 2	2.80	1.00	1.20	1.00	77.20	20.00
	G 3	5.60	1.80	2.40	1.20	77.60	16.80
	G 4	7.20	1.00	5.60	1.92	76.40	16.40
	G 5	35.60	27.00	7.20	1.13	50.20	14.20

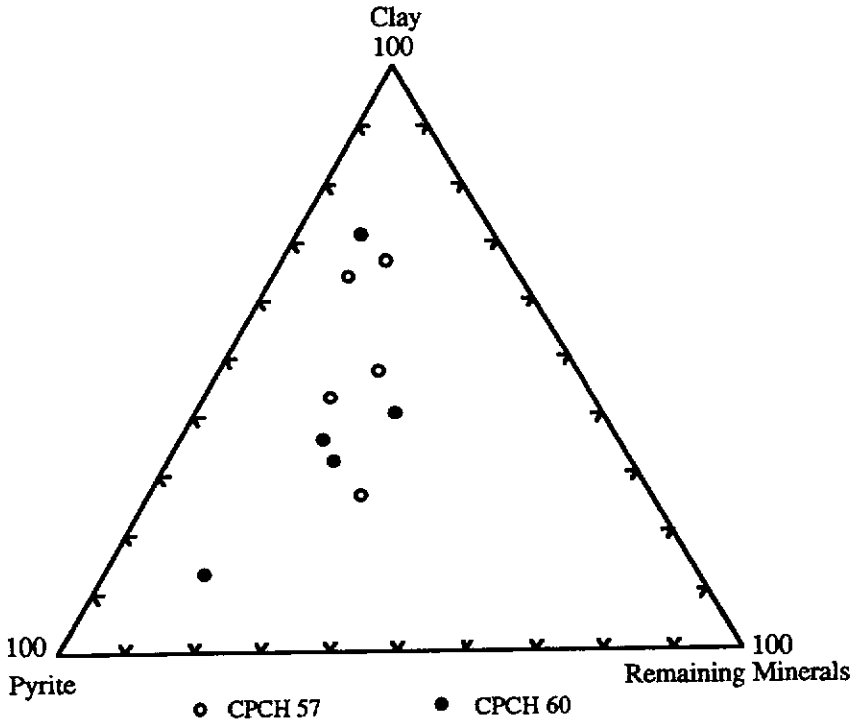

Figure 5.9. Composition of mineral matter, Hill River coal, Gairdner Block.

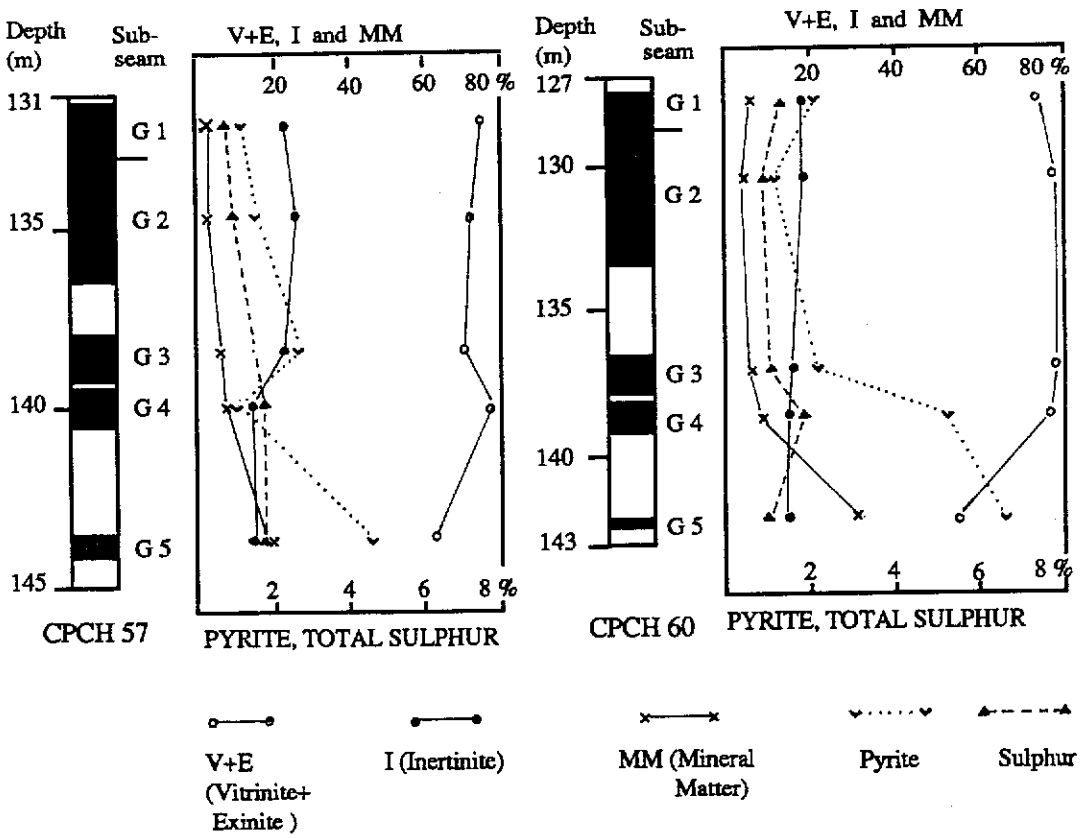

Figure 5.10. Vertical variation in vitrinite, exinite, inertinite, mineral matter, pyrite and sulphur contents of sub-seams G1 - G5 of Hill River coal, drill holes CPCH 57 and 60, Gairdner Block.

content ranges from 2.80 % to 35.60 % in all the sub-seams (Table 5.6). The lowest value of 2.80 % is recognised in sub-seam G 2 of CPCH 60, while the highest one of 35.60 % is present in sub-seam G 5 of CPCH 60. The mineral matter content is classified as low (< 5.0 %) to high (> 10.0 %). However, the dominant mineral matter content is medium, showing a value between 5.60 % and 7.80 %. In addition, the association of mineral matter with the macerals is also presented in Table 5.7.

The predominant mineral matter in the coal is clay as evidenced in Figure 5.9. The mineral content ranges from 1.00 % in G 2 (CPCH 57 and 60), to 27.00 % in G 5 of CPCH 60, which represents low to high amounts. The clay minerals are mostly associated with the vitrinite B, followed by the association with the inertinite. The minor association of clay minerals occurs in vitrinite A and exinite macerals (Table 5.7).

The pyrite content in the coal ranges between 1.20 % to 7.20 %, which represents low to medium values. The pyrite association with the vitrinite B is common in comparison to the association with the vitrinite A, inertinite and exinite (Table 5.7). The total sulphur content of the Gairdner Block coal obtained from CRAE (1989), ranges between 0.85 % to 2.10 % which compares favourably with the distribution of pyrite.

The carbonate minerals are calcite and siderite with contents ranging between 0.60 % to 3.60 %, which is relatively low in comparison to clay and pyrite. The majority of carbonates are associated with vitrinite B, while the association with exinite and inertinite occurs to a lesser extent (Table 5.7). The quartz recorded in the coal is very low in content, and its range is from traces to 0.20 %. The quartz is associated with vitrinite A, vitrinite B and exinite in the coal.

Table 5.7. Distribution of mineral matter and maceral association, Hill River coal, Gairdner Block.

Mineral	Maceral	CPCH 57					CPCH 60				
		G 1	G 2	G 3	G 4	G 5	G 1	G 2	G 3	G 4	G 5
Clay	Vitrinite A					3.8					1.8
	Vitrinite B	1.8	1.0	3.0	5.0	9.0	2.2	1.0	1.6	1.0	20.0
	Exinite						0.2				0.4
	Inertinite	0.2		0.2	0.2	0.2	0.6		0.2		4.8
Pyrite	Vitrinite A					0.4					0.6
	Vitrinite B	1.0	1.4	2.8	1.4	4.2	2.2	1.2	2.4	4.6	3.1
	Exinite		0.2			0.2					
	Inertinite	0.2								0.6	1.3
Carbonates	Vitrinite A										
	Vitrinite B	0.8	1.0	1.0	1.2	2.4	2.0		1.2	1.0	3.6
	Exinite						0.2	0.6	0.2	0.2	
	Inertinite		0.2	0.4							
Quartz	Vitrinite A					0.4					
	Vitrinite B										
	Exinite	0.2									
	Inertinite										

The vertical variation of mineral matter content in all the sub-seams from the drill cores CPCH 57 and 60 is depicted in Figure 4.54. An increase in mineral matter content occurs in both drill cores, from G1 to G5 . The lateral variation of mineral matter content within individual sub-seams from CPCH 57 towards CPCH 60, shows a trend in the sub-seams G 1 and G5, where the content of mineral matter increases towards the NW direction, while in G2, G3 and G4 the mineral matter content decreases in the same direction. The total mineral matter, pyrite, total sulphur, vitrinite plus exinite, and inertinite distribution is presented in Table 5.6 and illustrated in Figure 5.10. In this figure, the total mineral matter, pyrite and total sulphur contents display a similarity of trend from sub-seams G1 to G3 in drill hole CPCH 57 and from sub-seams G1 to G4 in CPCH 60. The distribution of the total mineral matter and pyrite shows an increase from sub-seams G1 to G5 in CPCH 57, and from sub-seams G2 to G5 in CPCH 60. The total sulphur content varies in both drill holes. However, an increase of total sulphur content from sub-seams G1 to G5 in drill hole CPCH 57, and G2 to G4 in CPCH 60 is recognised in this figure. Besides the relationship of the total mineral matter, pyrite and total sulphur, Figure 5.10 depicts a relationship of vitrinite plus exinite with inertinite contents. The distribution of vitrinite plus exinite is present inversely to the distribution of inertinite in CPCH 57. However in CPCH 60, the vitrinite plus exinite content distributes inversely against the total mineral matter content.

The characters of mineral matter of the Gairdner Block coal based on the petrographic investigation are summarised as follows :

- The dominant mineral matter content in the Gairdner Block coal is represented by clays, followed by pyrite. Based on the SEM observations, the clays are composed of kaolinite, illite and montmorillonite, and present as bands, pellets, cell cavities, and cleat infillings. However, the contents of each individual clay minerals in the coal are unable to calculate, because of the limited selected samples were available for SEM study. The pyrite consists of framboidal, cleat, cell - infilling, isolated - body, and fracture - infilling types. These two mineral matter are present as syngenetic and epigenetic types in the coal.
- The mineral matter is mainly associated with vitrinite B, to a lesser extent with inertinite, exinite and vitrinite A. The details of associations have not been included because only selected samples were available for SEM study.
- On the basis of the mineral matter content, the Gairdner Block coal, having a mineral range from 2.80 % to 35.60 %, is categorised as a "normal - grade coal".

CHAPTER 6. GEOCHEMISTRY

6.1. Introduction

This chapter describes proximate, ultimate, and trace elements analyses of the Hill River coal from the Mintaja and the Gairdner Blocks. The analyses for nineteen trace elements for the coal from the individual sub-seams of drill holes CPCH 1, 39 and 57 were analysed by ANALABS, and the proximate and ultimate analyses of the individual sub-seams of drill holes CPCH 1, 37, 39, 47, 57 and 60, were obtained from CRAE Pty. Ltd.

6.2. Proximate Analysis

The proximate analysis is a relatively easy and rapid method, especially for coal rank determination and general commercial assessment. It gives a measure of the relative amount of volatile to non-volatile organic compounds in the coal. The analysis includes the determination of total moisture, volatile matter, fixed carbon and ash content, as well as the calorific value of the coal. The moisture, volatile matter, fixed carbon and ash content are reported in percent, and calorific value in MJ/kg, and a brief description of these follows:

6.2.1. Moisture

The moisture content is one of the contaminants of coal. The moisture content of coal consists of the free or surface moisture that can be removed by exposure to air, and the inherent moisture which can be entrapped and is removed by heating at 220 ° F,

Merritt (1987). Commonly, moisture values are residual moisture, and is named "as determined" (AD) moisture, because these were determined on air-dried coal samples, Langenberg *et al.* (1992). The moisture content is a good indicator of rank of brown- and sub-bituminous coal stages, and it increases with increasing depth, Stach *et al.* (1982) and Diessel (1992). They also stated that porosity is the main factor controlling the degree of moisture content of coal and as a decrease of moisture content occurs, a corresponding rise in specific energy is noted. In warm temperate or hot climates, difficulties in sample preparation of coal for moisture content analysis occur, because the moisture may be released rapidly from the coal, Cook and Kantsler (1982).

6.2.2. Volatile Matter

The term volatile matter defines the amount of components of the coal other than moisture, that are removed when coal is heated in the absence of air, Merritt (1987). The volatile matter which is released from the organic compounds during heating or combustion of coal occurs as hydrocarbon and nitrogen gases, and vapour. Volatile matter yield of a whole coal sample presents very useful information particularly on coal type analysis, and thus the volatile matter concentration of whole coal samples probably is unreliable as a measure of coal rank, because it is extremely sensitive to coal type, Cook and Kantsler (1982). The type of coal rich in exinite produces more volatile matter than the exinite-poor coal.

6.2.3. Fixed Carbon

The fixed carbon is the stable solid carbon compound or char other than ash obtained upon combustion of coal in the absence of oxygen after the removal of moisture and volatile matter (oxygen, hydrogen, sulphur, and nitrogen), Merritt (1987). It

represents the decomposition residue of the organic compounds of coal, and is calculated by subtracting from 100 the sum of the percentages of moisture, volatile matter and ash, as per the Australian Standard (1975). The fixed carbon content is used as an index of the yield of coke expected from a coal on carbonisation. It may be used also as an "index" of coal rank and a parameter in coal classification, Stach *et al.* (1982). Diessel (1992) pointed out that the amount of fixed carbon in coal is inversely proportional to volatile matter.

6.2.4. Specific Energy

The specific energy of coal expressed in MJ/kg, is the quantity of the heat unit released when one kg-weight of coal is completely burned in oxygen under standard pressure or volume, Australian Standard (1975). The heating value of coal can be used as a measure of the rank of coal, and it is related to coal type, Cook and Kantsler (1982).

6.2.5. Ash

The ash is an inorganic residue consisting of the non-combustible mineral matter in coal, when coal is completely burned. It represents the bulk of the mineral matter in coal, after volatile components have been released. Ash content determined by thermal decomposition is one of the parameters invariably reported in coal analyses, because of the diluting effect of ash on properties of coal related to organic constituents. Yudovich (1978) genetically classified ash as biogenic, absorption and terrigenic types. These three types of ashes are responsible for the presence of most of the trace elements in coals. Graese *et al.* (1992) categorised ash in coal in the following categories:

. Very high : 15% - 20 %

. High : 10% - 15%

. Moderate : 5% - 10%

. Low : < 5%

other factors being equal,

Coal with very high ash content is less suitable for utilisation than the low ash coal. The amount, composition and distribution of ash in a coal are determined principally by processes within the initial peat-forming environment. The chemical composition of coal ash is directly related to the composition of minerals contained in coal.

6.3. Ultimate Analysis

The ultimate analysis of coal is the elementary analysis undertaken in terms of carbon, hydrogen, nitrogen and sulphur contents, Schlatter (1973). The results are usually corrected for moisture and mineral matter contents of coal. The ultimate analyses are dependent on the rank of coal, as well as coal composition, Stach *et al.* (1982). The carbon content in coal increases with increasing vitrinite reflectance, whilst the hydrogen content and the H/C ratio decreases with an increase in vitrinite reflectance. The carbon content in brown coals and low-rank bituminous coals, increases rapidly with increasing specific energy, Patteisky and Teichmüller (1960). The percentage of carbon in coal is a suitable rank parameter of coal, because the carbon content varies from 78 % in a sub-bituminous coal to around 95 % in high rank anthracite, Diessel (1992). In high rank coal, hydrogen content is also suitable for coal rank classification.

The amount of nitrogen is related to the vitrinite content in coal, Diessel (1992), and it has no relationship with depositional environment of coal precursor. Chaffee *et al.*

(1986) stated that high nitrogen content in coal is indicative of extensive microbial reworking within the coal-precursor-forming vegetation.

William and Keith (1963) studied pyritic sulphur formation in coal and considered that high sulphur content in coal was the results of bacterial reduction of sea-water sulphate, and this process is directly related to a marine influence during the deposition of coal. According to Cook (1975), three types of sulphur in coal are recognised:

. Sulphate sulphur occurring as small quantities of ferrous sulphate ($FeSO_4\ 7H_2O$) and as gypsum ($CaSO_4.2H_2O$).

. Organic sulphur which is associated with the carbon and nitrogen to form coal compound.

. Pyritic sulphur which is present as ferrous sulphide (FeS_2).

Casagrande *et al.* (1977) pointed out that the elemental sulphur is produced from oxidation of hydrogen sulphide coming in contact with dissolved oxygen of interstitial waters or from microbiological activity. In 1987, he studied sulphur formation and occurrence in peat and coal, and summarised his findings as:

. Low sulphur (less than 5.00 %) coals of the United States of America contained more organic compounds than pyritic sulphur.

. Australian coals with a total sulphur content in excess of 1.0 %, show a similarity in characteristics to that of USA coals. The Australian coals show a reversal in the proportion between organic and pyritic sulphur when the total sulphur content is more than 1.0 %.

. Organic sulphur is produced by the reaction of hydrogen sulphide with organic matter, whilst a reaction of hydrogen sulphide with ferrous iron results in the syngenetic precipitation or pyritic sulphur.

. High sulphur coals are associated with marine influence in coal measures.

. Sulphur concentration in coal is dependent upon the sulphate content of the aqueous

environment of peat, and the activity of sulphate reducing bacteria.

Concentration of sulphate by ponding in the distributive distal facies probably leads to the high sulphur content in coal, Hunt and Hobday (1984). Chou (1990) who studied Herrin coal in Illinois Basin, considered that sulphur in low-sulphur coals (< 1.0 % S) is related to the parent plant material, whilst in medium-sulphur (>1.0% to <3.0 % S) and high-sulphur coals (>3.0 % S) both plant material and seawater sulphates are the major source for the sulphur. The presence of sulphur is the consequence of the activity of sulphate reducing bacteria occurring in the peat depositional environment and during a marine transgression phase, sulphate-rich seawater penetrates into the surface of the peat and induces the growth of sulphate-reducing bacteria, Veld *et al.* (1991). Inorganic sulphur compounds such as pyrite, and also organic sulphur compounds are produced whereby the chemical composition of the peat can undergo considerable change. The majority of the sulphur in coal belongs to mineral matter in inorganic forms, and the small amount is present as organic compounds of coal. The inorganic sulphur is present as various types of iron sulphides, mainly pyrite which occurs as the most common iron-bearing mineral in coal.

The sulphur is the most harmful impurity of coal in industrial use and in its environmental implications. It occurs as possible sources of pollution during the combustion of coal, Swaine (1982). Brodily *et al.* (1991) considered that high sulphur coal is a major source of anthropogenic sulphur oxides emissions, which leads to the contribution of acid rain.

6.4. Trace Elements

A large number of trace elements are present in coal and these elements combine to

form organic, inorganic, and mixed organic-inorganic compounds in coal, which are related to depositional setting and parent plant material, Diessel (1992). The trace element analyses of the ten coal samples from the Mintaja Block and the five coal samples from the Gairdner Block have been carried out by ANALABS. The purpose of the trace element study in the coal is to determine the utility, behaviour and associations with organic and inorganic fractions. Trace elements in coal have geological and environmental significance, and they are important from the viewpoint of the depositional environment and seam correlation. Swaine (1971) considered that the trace elements in coal may be helpful as an indicator of marine influence on coal deposition, particularly the concentration of boron (B) which is the basis for interpreting peat depositional condition. Rimmer (1991) suggested that the trace elements distribution within coal, was expected to indicate variations in depositional environment of the peat swamp, transport and alteration of inorganic matter within the swamp, as well as coalification.

From the viewpoint of environmental considerations, certain kinds and concentrations of trace elements produce potential environmental hazards, which might affect humans, animals and plants. Gehr *et al.* (1981) concluded that trace element emissions including radioactive elements from coal combustion in power plants are generally considered as an unimportant source of trace element pollution. However, Swaine (1982) considered that the elements, which ultimately were recognised in fly-ash, bottom-ash and very-fine ash, and reached the atmosphere, led to the subsequent deposition of "dry" matter and precipitation with rain. He also suggested that trace elements should be considered during mining, preparation and storage of coal. Overburden (soil) which becomes topsoil during coalfield rehabilitation and contains a certain amount of trace elements may limit the growth of vegetation. Therefore, it is necessary to find out the concentrations of certain trace elements in coal prior to its use. The trace elements, such as As, Cd, Cr, Ni, and Pb have to be taken into consideration, because they are of primary environmental

significance. Moreover, the remainders, like Co, Cu, Mn, Mo, Th, U, V, and Zn are related to potential interest, but they could be also of "presumed" environmental significance, Swaine (1982).

Goldschmidt (1935, 1937) studied the chemical combinations of trace elements in coal and he considered that in comparison to the average trace element content in the earth's crust, high concentrations of certain trace elements are present in coal ash. Enrichment of trace elements in coal are due to concentration by plants during their life, during peat degradation, and concentration by mineralisation in peat after the burial process. Several elements, including B, Ge, As, and B have enrichment in coal of several times over their average crustal concentration. The enriched content of these elements is called "Clarke" values, Murray *et al.* (1990). In 1954, Goldschmidt introduced the concept of geochemical classification of trace elements based on their affinities and also their tendencies to be present in minerals. Furthermore, he considered that Ca, Mg, K, S, P, Mn, and B are required for the growth of plants. These elements are retained within plant tissues when the peat forms and present as organic combination in hydroxyl and carboxyl groups. The organic fraction also adsorbed other elements which were transported into the peat swamp as solutions. Three types of trace element assemblages: lithophyllic elements (V, Cr, Y and B), chalcophyllic elements (Cu and Pb), and siderophyllic elements (Co and Ni) were introduced by Goldschmidt (1935) and Rankama and Sahama (1950). Mason (1958) considered that the trace elements recognised in coal are accumulated in plants during their growth, from groundwater during the coalification processes, and in mineral matter. The majority of Ba, Cr, Co, Pb, Sr and V are associated with inorganic compounds of coal, whilst Ni, Ga, Ge, Mo and Cu are associated with either or both organic and inorganic matter in coal, Nicholls (1968). He also reported that various processes influence the trace-element assemblages in coal. An incorporation of B and small amounts of Ni and Cu in coal is due to primary biological concentration or absorption by organic matter at a very early stage of coalification. The post-burial

absorption by organic matter affected contents of Mo, absorption of clay minerals at an early stage of coal formation incorporates Ga, Cr, and W, whereas the occurrence of high contents of Cr and V, and some Ge and Mo are due to post-burial absorption by silicates. The incorporation of Cu and some Pb, Ni, Co and possibly Ga is due to the primary sulphide precipitation, whilst post-burial reaction between ground water and pre-existing sulphides leads to production of high contents of Pb, Ni, Co, As and Zn in coal. Thus, the post-burial enrichment process produces high contents of trace elements in coal. The origin, mode of occurrence and concentration of trace elements in the Australian coal were reviewed by Swaine (1975). In 1981, Gluskoter *et al.* presented summaries of detailed descriptions of elemental distribution in coal. Pareek and Bardhan (1985) studied Indian coals and they suggested that a relationship between maceral and trace elements developed during biochemical decay. Lindahl and Finkelman (1986) considered that trace element content in coal was controlled by ash content, coal rank, Eh, pH and salinity of the peat environment; and the mineralogy of the source rocks. Smith (1987) reported that B, Be, Br, Ge, and Sb are organically bound trace elements in coal, whilst As, Cd, Ce, Fe, Mn, Mo, and Zn have the lowest organic affinity, and the ones with the intermediate or variable affinities are Ga and Ni. Some trace elements, such as Co, Cr, Cu, Pb, Sb, and U are associated with both organic and inorganic compounds. The organic affinities of trace elements in coal are very useful in determining the effects of coal cleaning on their concentrations, and the ease of their removal by coal cleaning, Knott, Thompson and Ruch (1985), and they categorised trace elements of some Permian Australian coals as follows:

$$Mn > Zn > F > B > U > Ba > Sr > Th > La > Cu.$$

Davy and Wilson (1984) reported trace element composition of some Collie coals, followed by Martin (1987) who studied trace elements in the Hebe coal seam, Collie Basin, Western Australia, in terms of their distribution and origin. Preliminary study on the distribution of trace elements in the Early Jurassic coal of Western Australia are reported by Sappal and Suwarna (1993). Trace elements in coal associated with the

inorganic matter, occur either within mineral structures or adsorbed onto the surface of minerals, whilst the organic association is present as chelated ions or in ion-exchange position, Rimmer (1991). These elements were introduced into the peat swamp as water- and air-borne matter, and associated with detrital mineral.

The data on trace elements, proximate and ultimate analyses, and the rank of coal from the Mintaja and the Gairdner Blocks, are presented and discussed in this section, under two separate headings of Mintaja and the Gairdner Blocks. The ultimate analyses and their relationship with macerals are described in section 6.5.2 for both the blocks, and the ultimate analyses in Table 6.2 for the entire drill cores rather than for the individual sub-seams as in Table 6.1.

In describing the correlation or relationship between two variables of coal analysed data, the "simple-linear regression" method is used, Davis (1973), Kachigan (1986), Anderson (1989), Megeath (1989), and McPherson (1990). There is a "linear trend" in the relationship reflecting a condition in which change of values in one variable is related to change in the other. The relationship between the two variables is sub-divided into :

. Positive relationship (Figure 6.1 a), where increases in one variable tend to be associated with increases in the other variable.

. Negative relationship (Figure 6.1 b) implying that decreases of values in one variable are associated with increasing values of the other variable.

. No apparent relationship (Figure 6.1 c), shown by a trend line which runs almost parallel to one or other axis. An increase/decrease in the one variable is not accompanied by a corresponding increase/decrease in the other.

A "weak" relationship occurs if the points of values are localised less closely to the trend line (Figure 6.1 d). Conversely, the relationship tends to be stronger as the points of values are localised more closely about the trend line (Figure 6.1 e). The

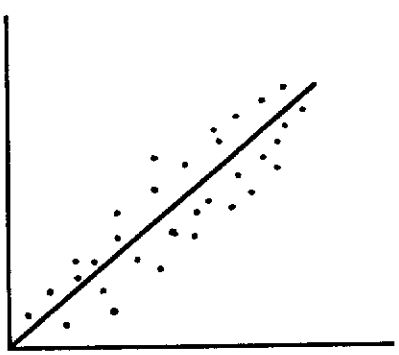

a. Positive relationship

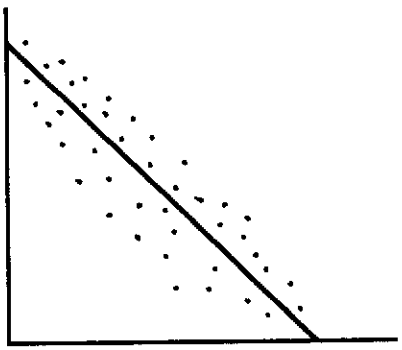

b. Negative relationship

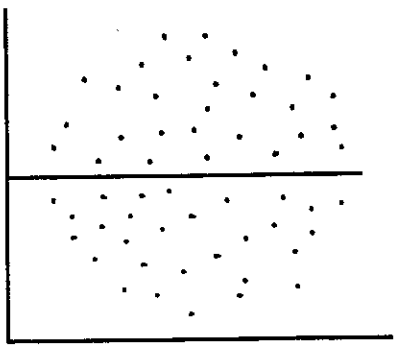

c. No apparent relationship

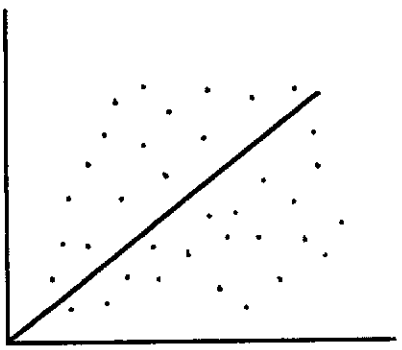

d. Weak (low) positive relationship

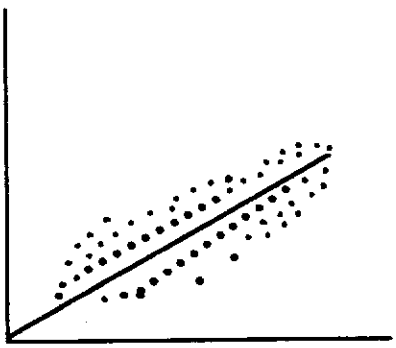

e. Strong positive relationship

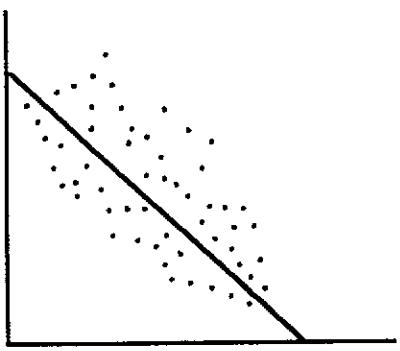

f. Moderate negative relationship

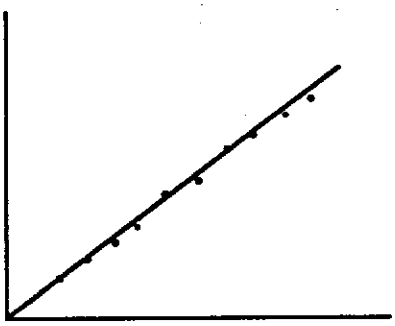

g. Perfect positive relationship

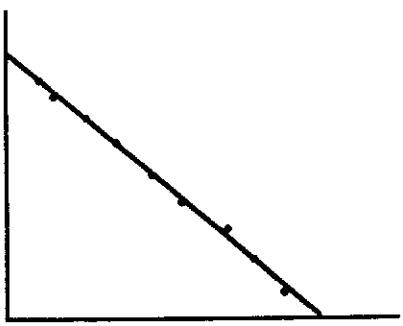

h. Perfect negative relationship

Figure 6.1. Division/types of correlation between two variables.

relationship is moderate when it shows a transition between a weak and strong relationship (Figure 6.1 f). When all the points lie on an oblique linear line, the relationship is termed perfect positive (Figure 6.1 g) or perfect negative (Figure 6.1 h).

6.5. Mintaja Block Coal

The proximate and ultimate analyses, total sulphur, trace elements distribution, and rank of coal from the drill holes CPCH 1, 37, 39 and 47 are discussed.

6.5.1. Proximate Analyses

The proximate analyses of the Mintaja Block coal is presented in Table 6.1 , which includes moisture content, volatile matter, fixed carbon, specific energy, and ash content from drill holes CPCH 1, 37, 39 and 47.

The moisture in the coal ranges between 9.10 % to 19.30 % or 11.84 % to 23.66 % (daf). The relationship between the moisture content and the reflectance of vitrinite, vitrinite+exinite and vitrinite contents of coal is weak to moderately positive (Figure 6.2. a, b, and c). However, the moisture content shows weak to moderate negative correlation with specific energy, inertinite content, and ash content in the coal (Figures 6.2.d, e and f). Thus, as the vitrinite reflectance and concentration of vitrinite and exinite contents increase, the total moisture content of coal also increases, which suggests a higher proportion of moisture in the coal is the surface moisture.

The volatile matter content of coal has a range of 24.40 % to 33.90 % or 34.38 % to 39.86 % (daf). The volatile matter of the coal has a weak to moderate positive relationship with vitrinite+exinite content, vitrinite content, inertinite content, and

Table 6.1 . Proximate and total sulphur analyses of Hill River coal from Mintaja Block.

Drill hole	Sub-seam	Ash (%)	Moisture (%)	Volatile Matter (%)	Fixed Carbon (%)	Specific Energy (MJ/kg)	Total Sulphur (%)
CPCH 1	G 1	17.20	13.41	33.00	36.39	16.08	0.92
	G 2	14.90	12.98	33.67	38.45	20.80	1.42
	G 3	17.41	13.26	32.25	37.08	19.77	1.17
	G 4	22.80	11.8	32.20	33.20	18.70	2.36
	G 5	29.84	N/A	N/A	N/A	N/A	N/A
	G 6	34.05	N/A	N/A	N/A	N/A	N/A
CPCH 37	G 1	18.90	9.60	30.90	40.60	21.99	1.18
	G 2	9.60	10.80	33.90	45.70	25.56	1.00
	G 3	13.00	10.90	32.30	43.70	23.82	1.09
	G 4	20.30	10.20	31.00	38.50	21.72	2.40
	G 5/6	31.80	9.10	25.70	33.40	17.98	1.82
CPCH 39	G 1	20.50	16.80	29.60	33.10	18.11	0.87
	G 2	9.80	18.50	31.50	40.10	22.25	1.19
	G 3	10.40	19.10	31.30	39.10	21.73	1.16
	G 4	13.90	19.30	29.60	37.20	19.76	2.35
	G 5	32.80	15.90	24.70	26.60	14.62	0.91
	G 6	24.40	16.70	26.30	32.60	17.34	1.97
CPCH 47	G 1	16.10	11.80	31.50	40.70	21.20	2.38
	G 2	11.90	12.10	33.30	42.70	22.70	1.57
	G 3	12.90	12.80	32.40	41.90	22.30	1.16
	G 4	17.20	12.20	30.90	39.70	21.18	1.95
	G 5	34.00	10.00	24.40	31.60	15.82	3.36
	G 6	29.40	11.10	25.20	34.30	17.14	3.55

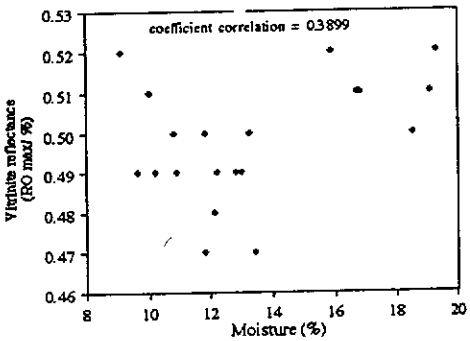

a. Moisture content versus maximum vitrinite reflectance.

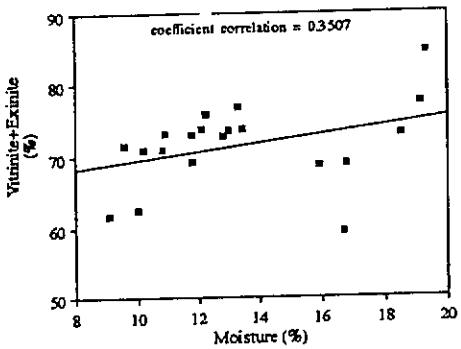

b. Moisture content versus vitrinite+exinite content.

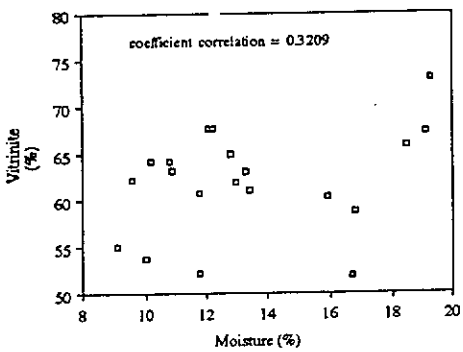

c. Moisture content versus vitrinite content.

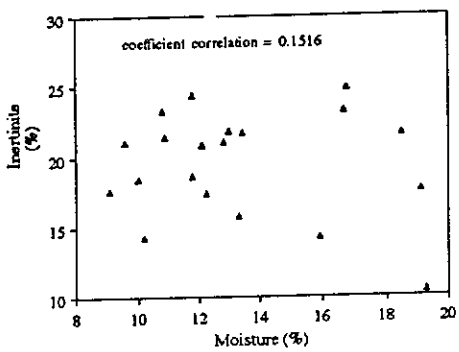

d. Moisture content versus inertinite content.

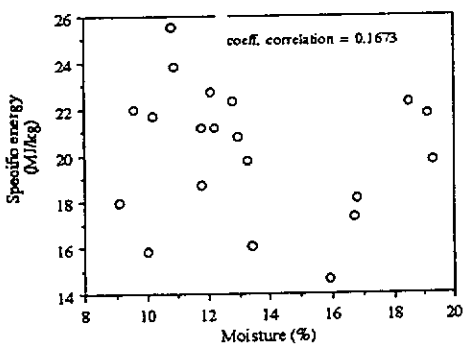

e. Moisture content versus specific energy.

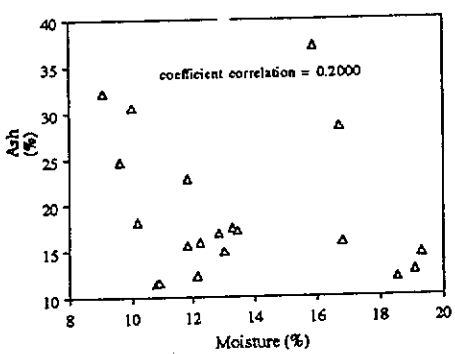

f. Moisture content versus ash content.

Figure 6.2. Relationship between moisture content and maximum vitrinite reflectance (a), vitrinite+exinite content (b), vitrinite content (c), inertinite content (d), specific energy (e) and ash content (f) of the Mintaja Block coal.

specific energy of coal (Figure 6.3. b, c, d, and e). However, a moderate to strong negative relationship is present between the volatile matter with maximum vitrinite reflectance and ash content in coal (Figure 6.3. a and f). Therefore, the volatile matter is dependant of maceral groups content, and specific energy of coal. However, as expected, it decreases slightly with increasing vitrinite reflectance and ash content in coal.

The fixed carbon content in the coal shows a range between 26.60 % and 45.70 % or 39.58 % to 50.55 % (daf). A moderate to strong positive relationships with vitrinite+exinite content, vitrinite content, inertinite content, and volatile matter content in coal are depicted in Figures 6.4 b, c, d, and e, respectively. Thus, an increase in the fixed carbon content in the coal is in agreement with increasing maceral group content, and volatile matter content of coal. Conversely, Figures 6.4 a and f, depict the moderate to strong negative correlation between fixed carbon content, with maximum vitrinite reflectance and ash contents in coal, respectively. The correlation shows that an increase in fixed carbon content is accompanied by decreasing vitrinite reflectance and ash content in coal.

The distribution of specific energy in the coal, ranges between 15.82 to 25.56 MJ/kg. The weak to moderate positive correlations occur between specific energy and vitrinite+exinite content (Figure 6.5 b), vitrinite content (Figure 6.5 c), and inertinite content (Figure 6.5 d). Figure 6.5 e depicts a strong positive relationship between specific energy and fixed carbon content in coal. Thus, the specific energy is dependent upon maceral group contents and also the fixed carbon content of coal; an increase in specific energy is concomitant with increasing maceral group content and fixed carbon content in coal. The specific energy of coal has a moderate to strong negative relationship with maximum vitrinite reflectance (Figure 6.5 a) and with ash content in coal (Figure 6.5 f). This negative correlation which reflects an increase in the specific energy value of coal leads to a decrease in vitrinite reflectance.

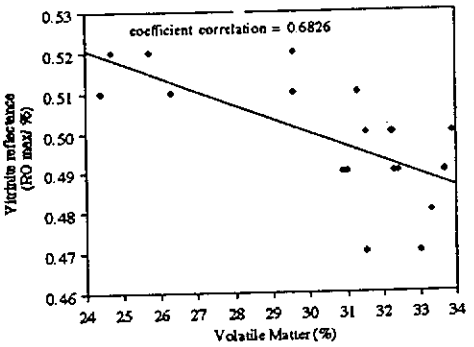

a. Volatile matter content versus maximum vitrinite reflectance.

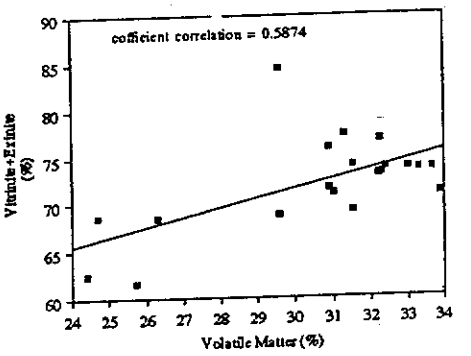

b. Volatile matter content versus vitrinite + exinite content.

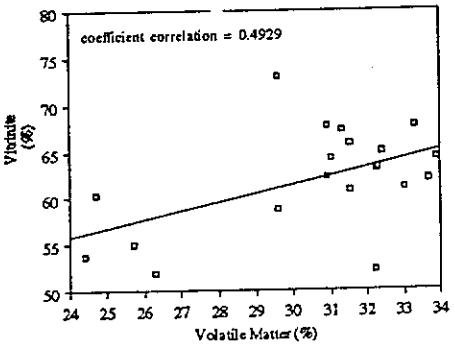

c. Volatile matter content versus vitrinite content

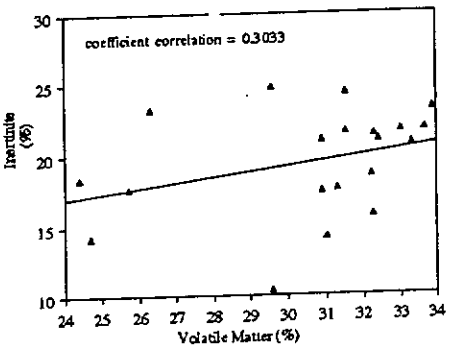

d. Volatile matter content versus inertinite content.

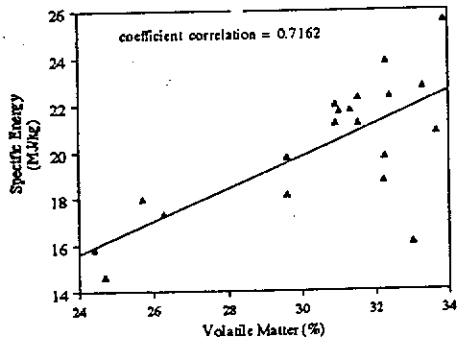

e. Volatile matter content versus specific energy.

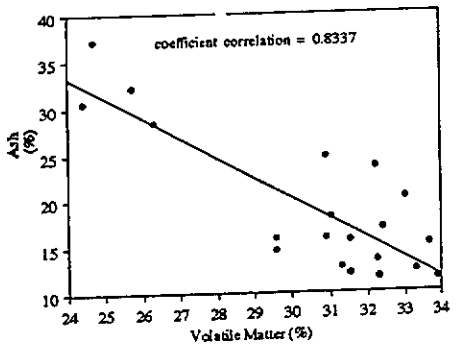

f. Volatile matter content versus ash content.

Figure 6.3. Relationship between volatile matter content and vitrinite reflectance (a), vitrinite+exinite (b), vitrinite (c), inertinite (d), specific energy (e) and ash (f) contents of the Mintaja Block coal.

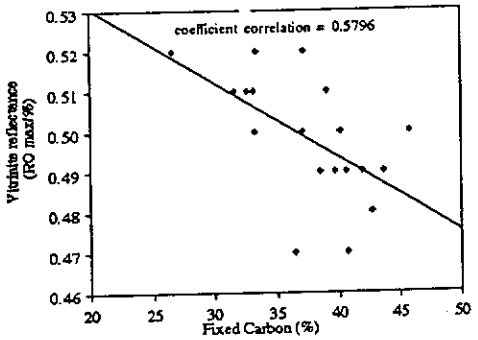

a. Fixed carbon content versus maximum vitrinite relectance.

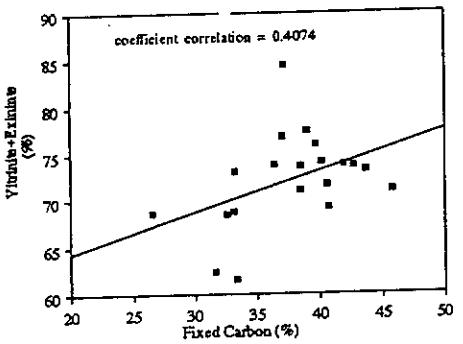

b. Fixed carbon content versus vitrinite+exinite content.

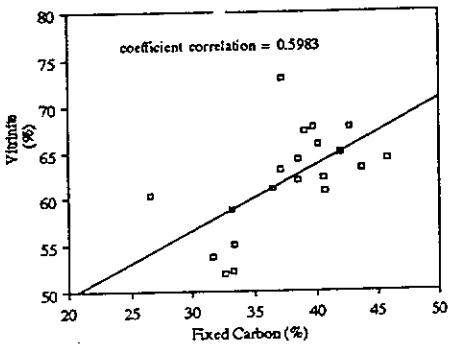

c. Fixed carbon content versus vitrinite content.

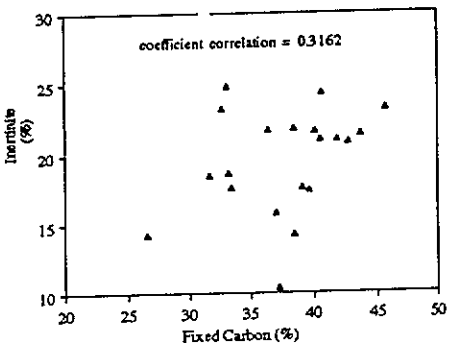

d. Fixed carbon content versus inertinite content.

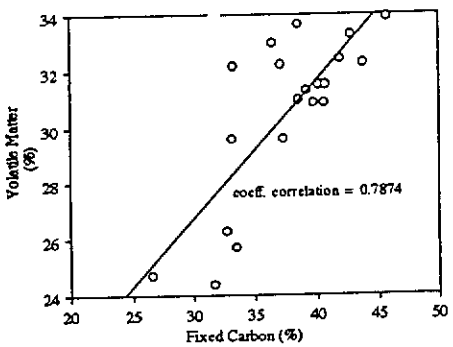

e. Fixed carbon content versus volatile matter content.

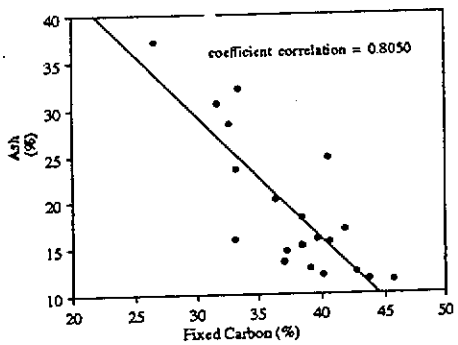

f. Fixed carbon content versus ash content.

Figure 6.4. Relationship between fixed carbon content and vitrinite reflectance (a), vitrinite+exinite (b), vitrinite (c), inertinite (d), volatile matter (e) and ash (f) contents of the Mintaja Block coal.

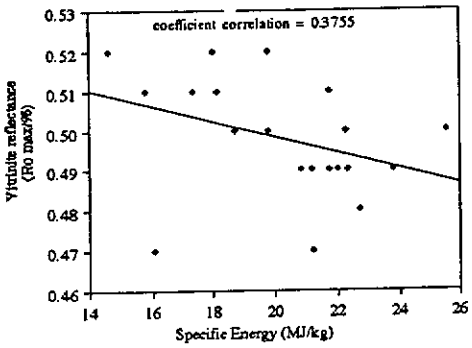

a. Specific energy versus maximum vitrinite reflectance.

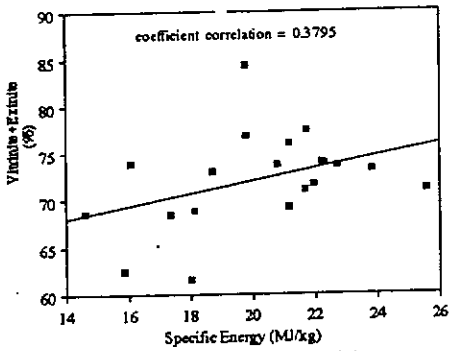

b. Specific energy versus vitrinite+exinite content.

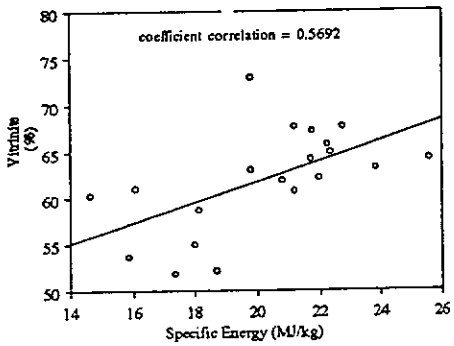

c. Specific energy versus vitrinite content.

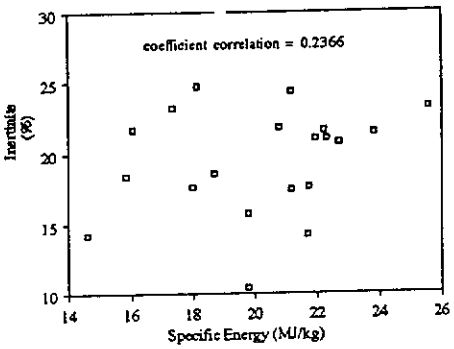

d. Specific energy versus inertinite content.

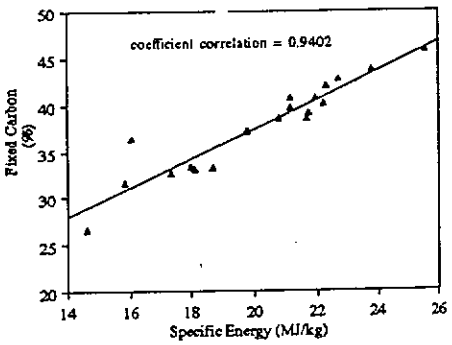

e. Specific energy versus fixed carbon content

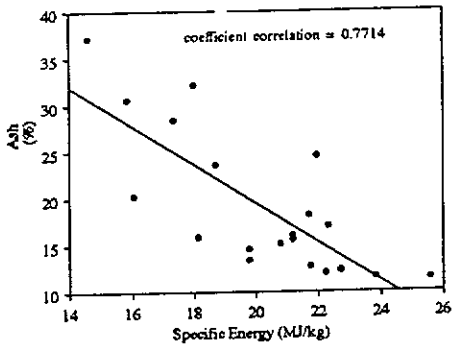

f. Specific energy versus ash content.

Figure 6.5. Relationship between specific energy and vitrinite reflectance (a), vitrinite+exinite (b), vitrinite (c), inertinite (d), fixed carbon (e) and ash (f) contents of the Mintaja Block coal.

The ash content of the coal varies from 9.60 % to 34.05 %. According to ash category proposed by Graese *et al.* (1992), it is dominated by a moderate to very high level with minor moderate degree (sub-seams G2 of CPCH 37 and 39) (Table 6.1). The relationship between ash content and moisture content, volatile matter, fixed carbon, and specific energy of the coal is depicted in Figures 6.2 f, 6.3 f, 6.4 f, and 6.5 f, respectively.

The relationships between the proximate analyses and maceral contents of coal appear to be simple, but in reality these are very complex to explain from a petrological point of view due to the complex and heterogeneous chemistry of coal.

6.5.2. Ultimate Analyses of Mintaja and the Gairdner Blocks

Table 6.2 gives ultimate analyses of whole coal seams from the drill holes CPCH 33, 35, 37, 39, 40, 41, 43, 47, 49, 50 located in and around the Mintaja Block and CPCH 60, 61, 62, and 63 from the Gairdner Block. The elements analysed in the coal consist of carbon, hydrogen, nitrogen, oxygen, and sulphur. The distribution of each individual element and a correlation between carbon and hydrogen, with ash, pyrite, vitrinite reflectance, and maceral group contents are described.

The carbon concentration (daf) varies from 72.60 % to 79.10 % in the coal. The carbon content increases with the increasing vitrinite reflectance, vitrinite content, fixed carbon content, specific energy, and the volatile matter content of the coal (Figures 6.6 a, b, e, f, and g). The nearly perfect positive relationships are present in Figures 6.6 a and f, and the strong positive relationships exist in Figures 6.6 a and g, while Figure 6.6 b shows a weak positive relationship. A strong positive to nearly no apparent correlation between carbon content and exinite content in the coal is illustrated in figure 6.6 c, which indicates that an increase in carbon content

Table 6.2 . Ultimate analyses of Hill River coal from Mintaja and Gairdner Blocks.

Block/ Area	Drill hole	Carbon (% daf)	Hydrogen (% daf)	Oxygen (% daf)	Nitrogen (% daf)	Sulphur (%)			
						Total	Pyritic	Sulphate	Organic
Mintaja	CPCH 33	75.88	5.19	15.90	1.25	1.78	0.66	0.09	1.03
	CPCH 35	78.06	5.32	13.78	1.30	1.54	0.39	0.04	1.11
	CPCH 37	77.42	5.36	13.86	1.29	2.07	0.43	0.05	1.59
	CPCH 39	74.70	4.68	17.38	1.30	1.94	0.44	0.09	1.41
	CPCH 40	76.44	5.22	15.27	1.32	1.75	0.76	0.05	0.94
	CPCH 41	73.82	5.11	17.88	1.31	1.88	0.82	0.14	0.92
	CPCH 43	73.07	4.93	18.36	1.27	2.37	0.96	0.07	1.34
	CPCH 47	72.91	5.23	18.18	1.29	2.39	1.05	0.04	1.30
	CPCH 49	72.60	5.18	18.44	1.27	2.51	0.93	0.18	1.40
	CPCH 50	75.10	5.21	16.56	1.35	1.78	0.61	0.07	1.10
Gairdner	CPCH 60	79.10	5.63	12.28	1.39	1.60	0.54	0.01	1.05
	CPCH 61	77.84	5.59	13.19	1.38	2.00	0.76	0.03	1.21
	CPCH 62	77.57	5.77	13.39	1.40	1.87	0.69	0.03	1.15
	CPCH 63	77.72	5.65	13.57	1.37	1.69	0.62	1.00	1.06

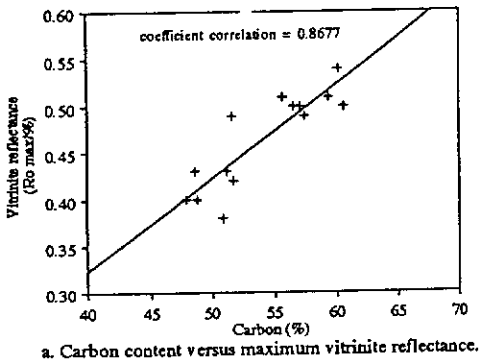

a. Carbon content versus maximum vitrinite reflectance.

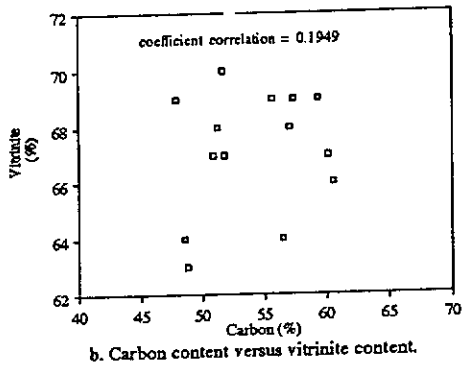

b. Carbon content versus vitrinite content.

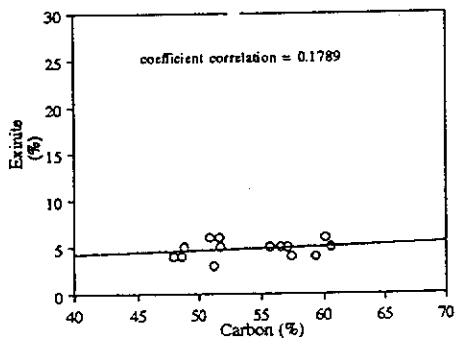

c. Carbon content versus exinite content

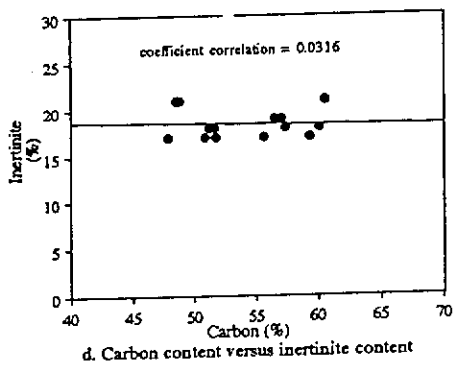

d. Carbon content versus inertinite content

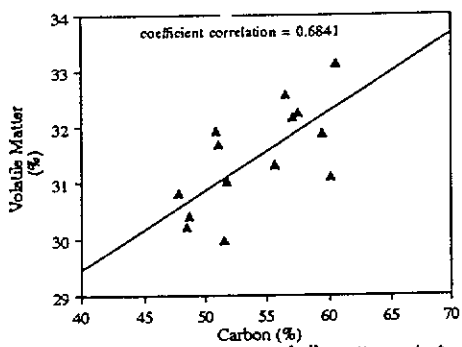

e. Carbon content versus volatile matter content.

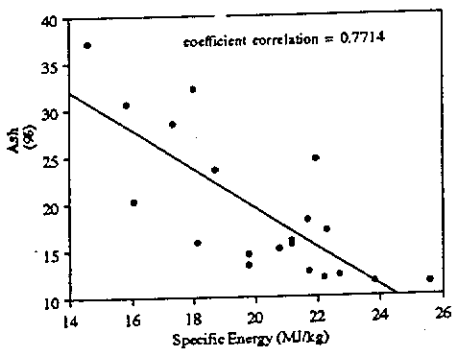

f. Specific energy versus ash content.

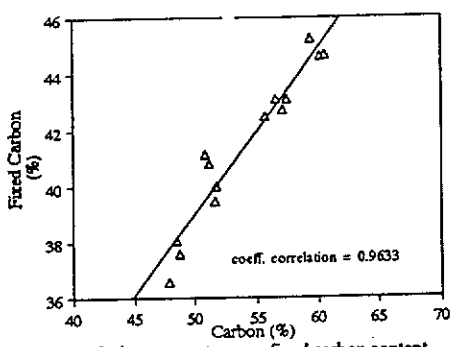

g. Carbon content versus fixed carbon content

Figure 6.6. Relationship between carbon content and vitrinite reflectance (a), vitrinite content (b), exinite content (c), inertinite content (d), fixed carbon content (e), specific energy (f), and volatile matter content (g) of the Mintaja and Gairdner Blocks coal.

is accompanied by a slight increase in the exinite content of the coal. No apparent correlation occurs between carbon content and inertinite content (Figure 6.6 d), and it represents that carbon content is independent of inertinite content in the coal, because of the association of mineral matter with inertinite group of macerals. A good correlation between carbon and fixed carbon contents reflects that the fixed carbon of the coal is largely composed of carbon with minor amounts of hydrogen, oxygen, nitrogen, and total sulphur.

The hydrogen content in the coal makes up 4.68 % to 5.77 %. The strong positive relationships between the hydrogen content and vitrinite reflectance, volatile matter content, specific energy, and fixed carbon content in the coal are illustrated in Figures 6.7 a, e, f, and g, respectively; whilst a weak positive relationship is present between the hydrogen content and vitrinite content in the coal (Figure 6.7 b). The hydrogen content increases with increasing vitrinite reflectance, vitrinite content, volatile matter content, specific energy, and fixed carbon contents in the coal. This is in agreement with the work of Stach *et al.* (1982) on hydrogen content of vitrinite in low rank coal. A negative to nearly no apparent relationship exists between the hydrogen content and inertinite content in the coal (Figure 6.7 d), which indicates that the amount of hydrogen increases with the very low decreasing inertinite content of the coal. In addition, no apparent relationship occurs between the hydrogen content and exinite content in the coal (Figure 6.7 c). Thus, the hydrogen content is independent of exinite content in the coal.

The oxygen content of the coal varies between 12.28 % to 18.44 %. A strong to moderate negative relationship with vitrinite reflectance, volatile matter content, specific energy, and fixed carbon content in the coal are illustrated in Figures 6.8 a, e, f, and g, respectively. Thus, an increase in the oxygen content in the coal coincides with decreasing vitrinite reflectance, volatile matter content, specific energy, and fixed carbon content of the coal. The Figures 6.8 b and c depict a

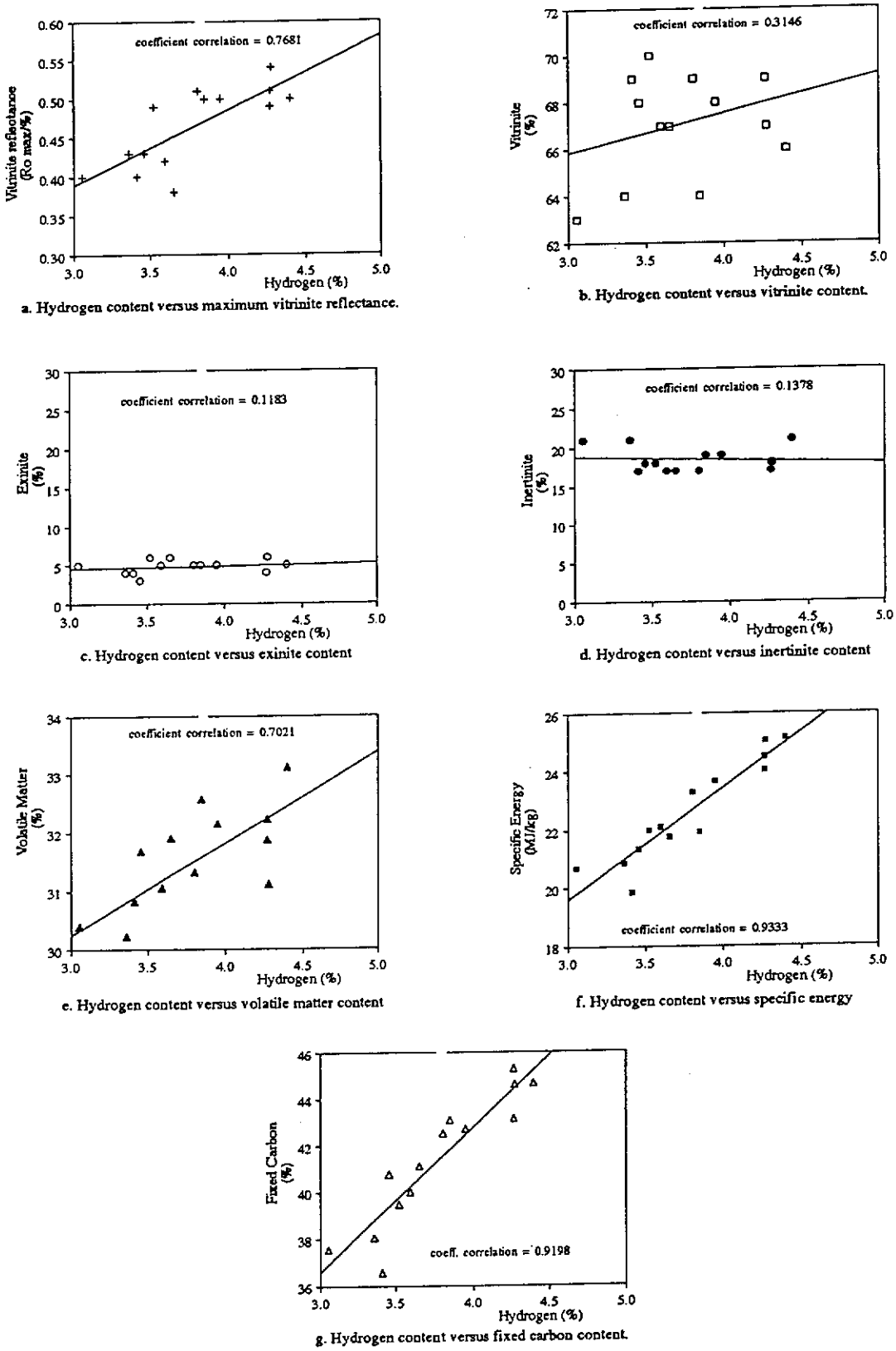

Figure 6.7. Relationship between hydrogen content and vitrinite reflectance (a), vitrinite content (b), exinite content (c), inertinite content (d), volatile matter content (e), specific energy (f), and fixed carbon content of the Mintaja and Gairdner Blocks coal.

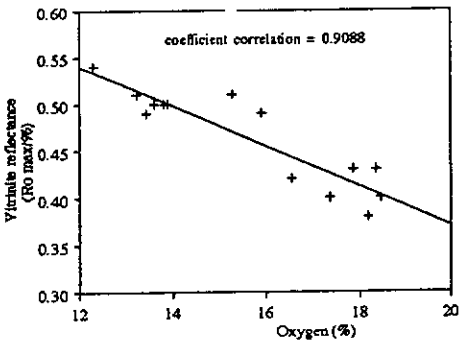

a. Oxygen content versus maximum vitrinite reflectance.

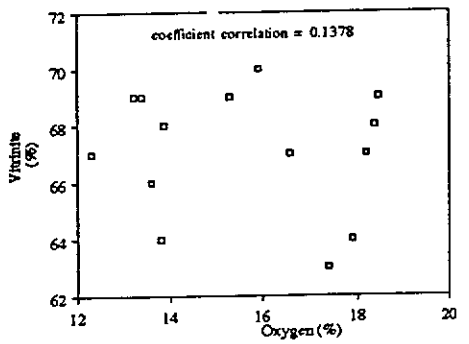

b. Oxygen content versus vitrinite content.

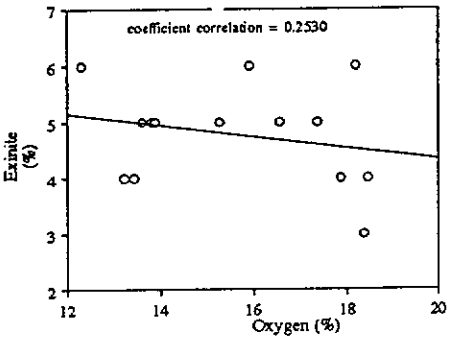

c. Oxygen content versus exinite content.

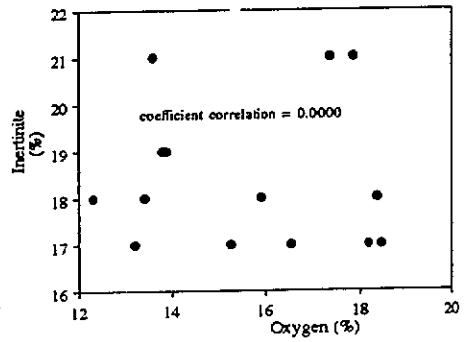

d. Oxygen content versus inertinite content.

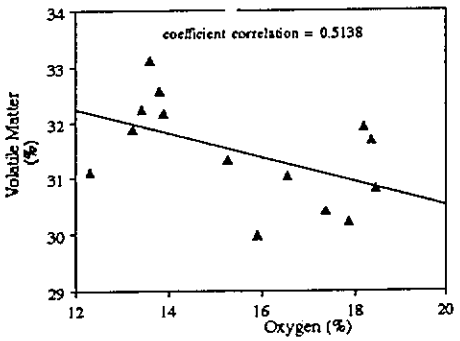

e. Oxygen content versus volatile matter content.

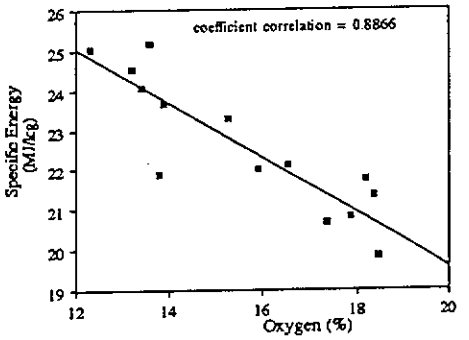

f. Oxygen content versus specific energy.

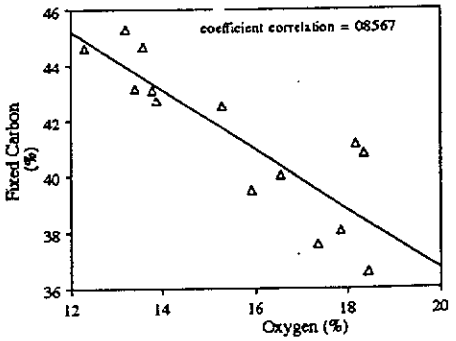

g. Oxygen content versus fixed carbon content.

Figure 6.8. Relationship between oxygen content and vitrinite reflectance (a), vitrinite content (b), exinite content (c), inertinite content (d), volatile matter (e), specific energy (f), and fixed carbon content (g) of the Mintaja and Gairdner Blocks coal.

weak negative relationship between the oxygen content and the vitrinite content and exinite content in the coal. These illustrations indicate that the oxygen content is dependent slightly upon vitrinite and exinite contents of the coal; an increase in oxygen content is accompanied by a slight decreasing vitrinite and exinite content in the coal. Additionally, no apparent correlation occurs between the oxygen content and inertinite content (Figure 6.8 d), which shows independency of the oxygen content and inertinite content in the coal.

The concentration of nitrogen content in the coal, ranges between 1.25 % to 1.40 %. The moderate to strong positive correlations occur between the nitrogen content and vitrinite reflectance, volatile matter content, specific energy, and fixed carbon content in the coal (Figures 6.9 a, e, f, and g). These indicate that an increase in the nitrogen content is moderately to strongly concomitant with increasing vitrinite reflectance, volatile matter content, specific energy, and fixed carbon content in the coal. On the other hand, Figures 6.9 b, c, and d, depict no apparent correlation between the nitrogen content and vitrinite content, exinite content, and inertinite content in the coal, respectively. Thus, the nitrogen content is independent of the maceral composition of the coal.

The total sulphur analyses of the Mintaja Block coal were carried out on sub-seams G1 to G6 from the drill holes CPCH 1, 37, 39, and 47. The total sulphur distribution of the Mintaja Block coal is presented in Table 6.1 together with proximate analysis. The different values for total sulphur content in the coal presented in Table 6.1 and 6.2 are due to the fact that the analyses on the individual sub-seams are reported in Table 6.1 and the analyses for the entire drill hole samples are given in Table 6.2. The concentration of the total sulphur content in the Mintaja Block coal is classified from medium (0.55 % - 1.00%) to high (>1.00 %) with a range between 0.92 % to

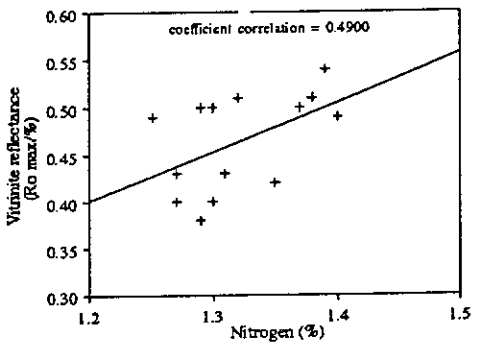

a. Nitrogen content versus vitrinite reflectance.

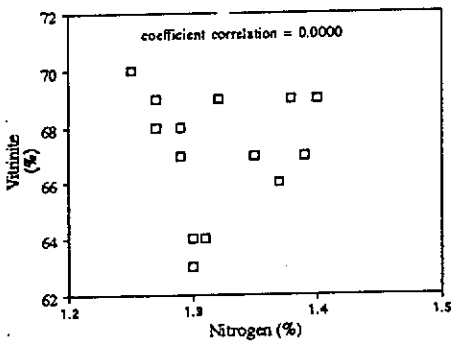

b. Nitrogen content versus vitrinite content.

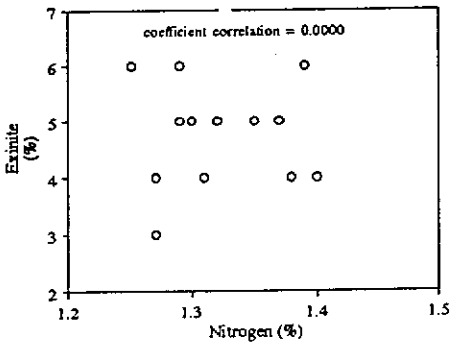

c. Nitrogen content versus exinite content.

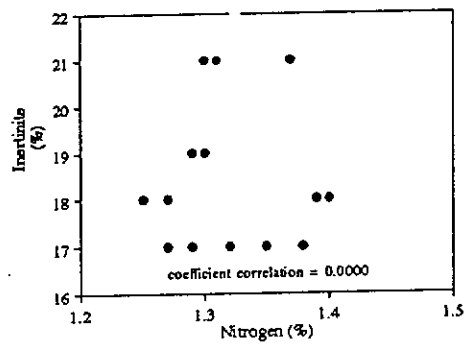

d. Nitrogen content versus inertinite content.

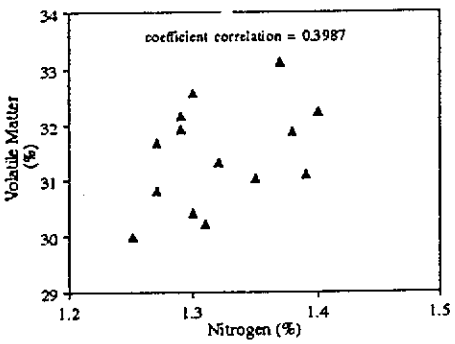

e. Nitrogen content versus volatile matter content.

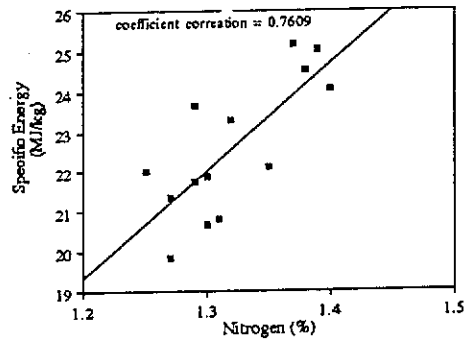

f. Nitrogen content versus specific energy.

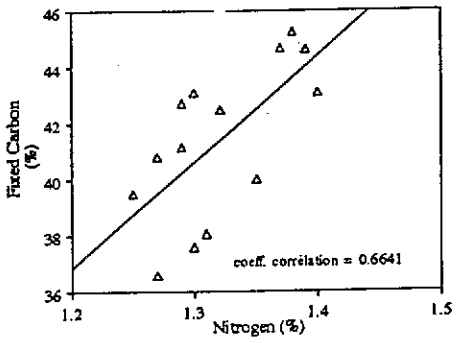

g. Nitrogen content versus fixed carbon content.

Figure 6.9. Relationship between nitrogen content and vitrinite reflectance (a), vitrinite content (b), exinite content (c), inertinite content (d), volatile matter content (e), specific energy (f) and fixed carbon content (g) of the Mintaja and Gairdner Blocks coal.

3.55 %. The correlation between the total sulphur content with ash, pyrite, and vitrinite contents of the coal is examined and illustrated in Figures 6.10, 6.11, and 6.12, respectively.

The vertical variation of the total sulphur content in each drill hole, shows a tendency to increase towards the lower sub-seams (G1 to G5/6) (Table 6.1). The increase in value of the total sulphur content from G1 to G5/6 is accompanied by an increase in total ash and also an increase in the pyrite content (Figures 6.10 and 6.11), and a decrease in the vitrinite content (Figure 6.12) . The lateral variation of the total sulphur content from SE to NW direction varies, and does not show a remarkable trend.

The relationship illustrated in Figure 6.10 between the total sulphur content and the total ash content, demonstrates a weak positive correlation. The sulphur is slightly dependent on mineral matter (ash-yield). The relationship between these two variables is not strong, because the mineral matter of coal is predominantly composed of clay minerals which probably do not contain sulphur. Figure 6.11 depicts a strong positive relationship between the total sulphur content and the pyrite content of coal. This condition reflects that variations in the total sulphur content are mainly due to the changes in the pyritic sulphur content, whereas variations in organic and sulphate sulphur are less significant. This interpretation is in agreement with the Casagrande *et al.*'(1990) who studied Australian Permian coal having a total sulphur content of more than 1.00 %. The values for the sulphur content based on ultimate analyses (Table 6.2) and the above values discussed from Table 6.1 differ because of the differences in the samples used in the two analyses. In Figure 6.12 a moderate negative relationship occurs between the vitrinite and total sulphur contents in the coal, and it reflects that a pattern of increasing vitrinite content is concomitant with a decreasing total sulphur content.

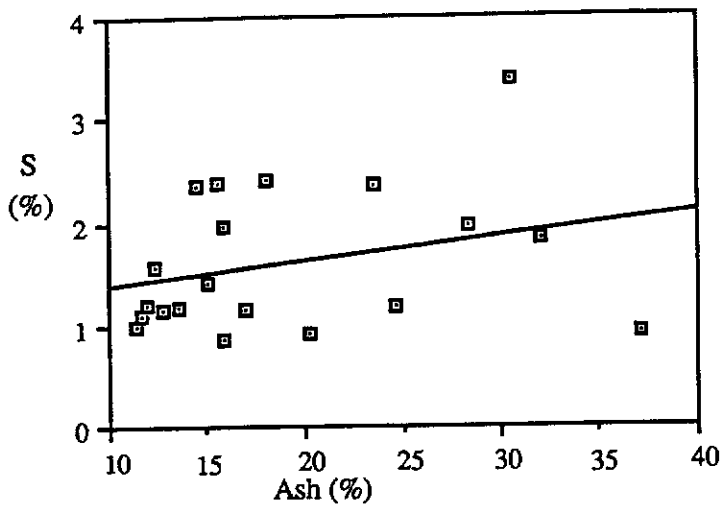

Figure 6.10. Relationship between ash and total sulphur contents of the Mintaja Block coal.

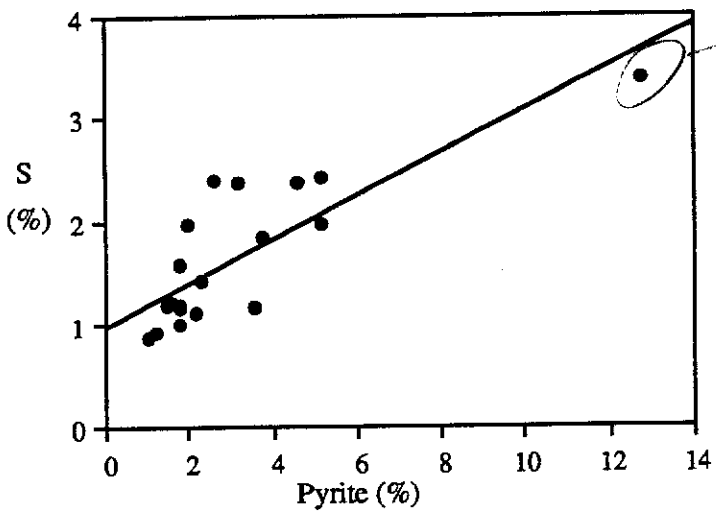

Figure 6.11. Relationship between pyrite and total sulphur contents of the Mintaja Block coal.

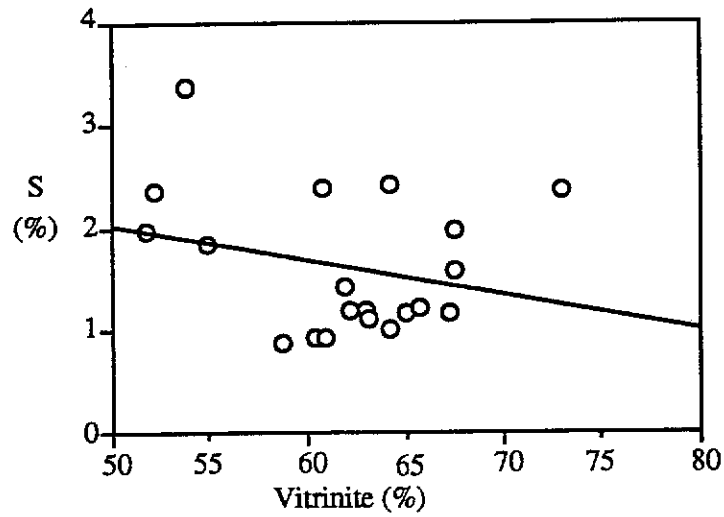

Figure 6.12. Relationship between vitrinite and total sulphur contents of the Mintaja Block coal.

6.5.3. Trace Elements Distributions

The trace elements analysis of the coal samples described in this sub-section includes the Mintaja and Gairdner Blocks. The trace element analyses for the 10 coal samples from the Mintaja Block and 5 coal samples from the Gairdner Block are presented in Table 6.3. The concentration of the trace elements in the coal varies greatly as from 0.30 ppm to 3140 ppm. The association of trace elements with inorganic or organic matter in coal are illustrated in Figures 6.13 and 6.14. Descriptions of individual trace elements and its variations in the coal are described and discussed.

Arsenic (As)

Arsenic is predominantly found in coal fractures and in micro fractures of pyrite, Finkelman *et al.* (1979). Lyons *et al.* (1989) recognised arsenic's strong inorganic affinity in most samples of Permian Australian coals. Swaine (1982) considered that some checks should be made on the arsenic contents of flyash applied to soil, and on leachates from flyash dump associated with power plants. Coal containing arsenic concentration of less than 80 ppm is usually used for power production.

The arsenic distribution in the Hill River coal varies between 5.00 ppm to 48.00 ppm. The vertical and lateral distributions of arsenic content in the coal are variable. Its correlation with ash content in the coal is almost in a "no relationship" condition, but an inorganic relationship still exists (Figure 6.13a). Therefore, it can be assumed that there is only a slight difference in proportion between inorganic and organic association of arsenic in the coal.

Boron (B)

Boron is recognised to be associated with clay minerals in coal according to Harder

Table 6.3 . Total mineral matter, pyrite, ash, and trace element concentrations of Hill River coal.

Block/ Area	Drill hole	Sub-seam	Mineral matter (%)	Pyrite (%)	Ash (%)	Trace Element (ppm)																		
						As	B	Be	Cd	Co	Cr	Cu	Ga	Mn	Mo	Ni	Pb	Sr	Th	U	V	Y	Zn	Zr
Mintaja	CPCH 1	G 1	4.50	1.20	20.26	9	163	13	1.57	28	133	148	39	274	19	76	27	342	31	5	221	56	138	256
		G 2	4.50	2.30	15.11	5	406	7	< 0.1	28	117	246	28	895	19	61	23	991	24	5	183	55	51	193
		G 3	7.50	1.50	13.50	5	409	7	< 0.1	26	132	205	28	1150	< 10	72	25	978	32	6	246	80	84	225
		G 4	8.40	4.60	23.56	24	244	8	< 0.1	26	137	141	31	619	< 10	92	39	702	32	6	258	61	240	180
		G 5/6	13.20	5.10	32.22	19	196	10	0.21	47	116	112	31	447	< 10	123	43	573	29	6	184	83	183	172
	CPCH 39	G 1	6.40	1.00	15.84	8	60	19	0.81	40	101	169	29	494	< 10	214	45	331	24	5	178	45	159	193
		G 2	5.40	1.60	11.97	9	128	4	2.01	18	113	189	29	457	< 10	75	57	771	30	5	175	46	56	193
		G 3	5.00	1.80	12.69	7	147	10	0.33	21	128	164	41	373	< 10	86	63	231	35	6	184	115	123	186
		G 4	5.20	3.20	14.54	19	141	12	0.30	32	148	166	43	292	< 10	101	48	213	35	9	266	84	106	195
		G 5	17.20	1.20	37.08	7	85	12	0.56	11	112	133	44	590	< 10	52	75	218	30	9	232	90	90	199
Gairdner	CPCH 57	G 1	4.20	1.20	17.53	7	38	8	1.12	12	125	158	38	2720	< 10	43	63	94	29	6	221	46	72	210
		G 2	3.80	1.60	13.25	9	47	5	3.63	14	117	201	31	1951	< 10	54	79	180	32	5	199	42	95	180
		G 3	7.40	2.80	16.96	48	52	11	0.56	19	130	145	35	3140	< 10	49	51	120	24	5	205	66	135	193
		G 4	7.80	1.40	20.95	12	53	11	2.44	28	131	177	34	331	< 10	70	53	128	24	7	283	61	213	225
		G 5	19.60	4.80	37.86	12	37	10	1.48	29	112	150	31	833	< 10	79	46	197	19	5	217	47	82	189

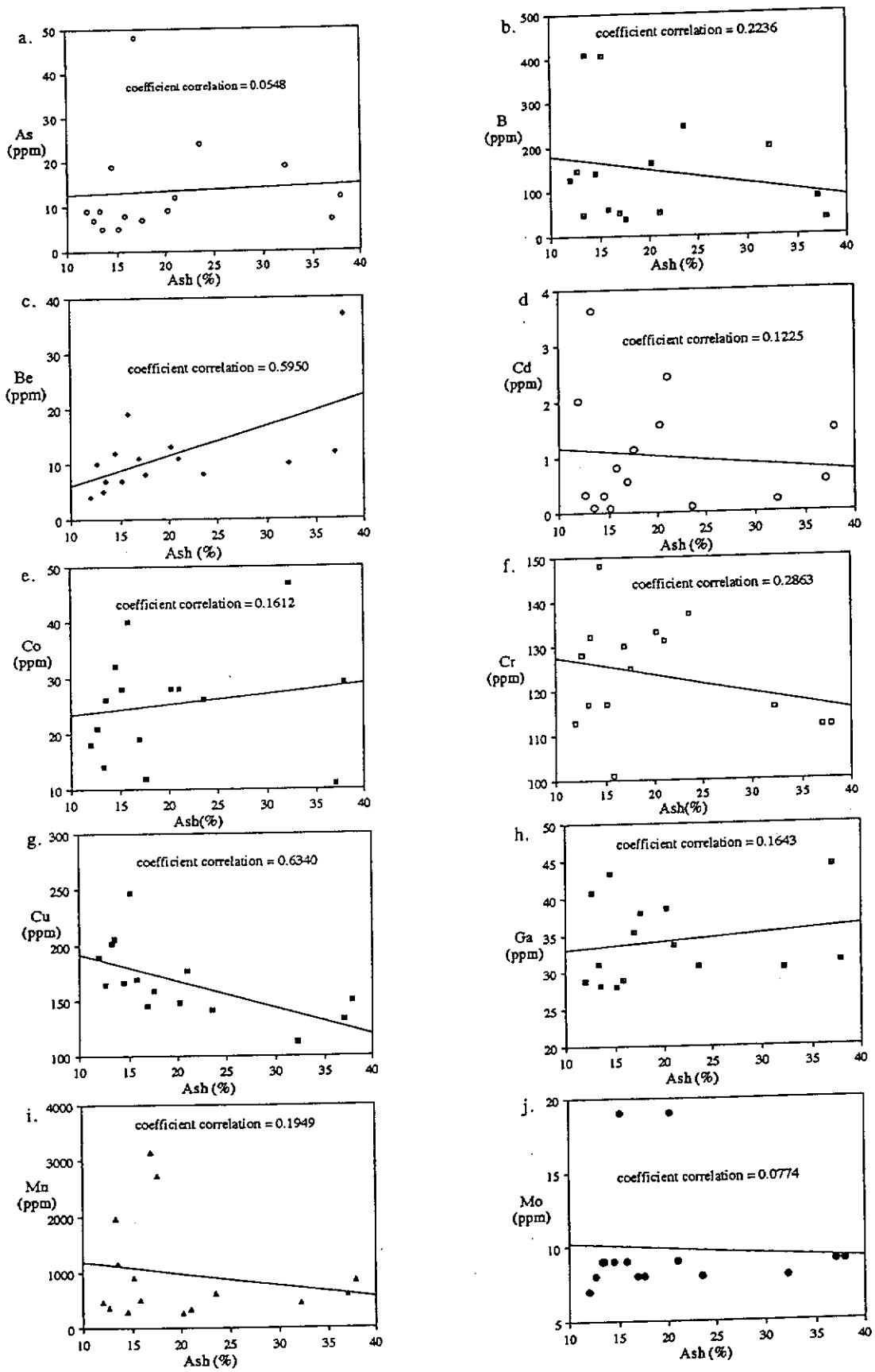

Figure 6.13. Relationship between ash and trace element contents of the Mintaja and Gairdner Blocks coal. As (a), B (b), Be (c), Cd (d), Co (e), Cr (f), Cu (g), Ga (h), Mn (i) and Mo (j).

(1961) and Couch (1971). Predominant organically bound boron in most coals was reported by Nicholls (1968), and it accumulated either biologically or during very early diagenesis of the peat. Boron is probably associated or chemically combined with the organic matter in the vitrain of Canadian coal, Bohor and Gluskoter (1973). A selective entrapment of boron from marine water leads to its formation as organic affinity in coal. However, high content of boron is also due to hydrothermal activity. Boron is the only geochemical indicator which is consistently sensitive to varying degrees of salinity, Landergreen and Manheim, (1963). Lyons *et al.* (1989) also considered that boron is an indicative of paleosalinity, and it shows a significant enrichment in sea water, Diessel (1992). Swaine (1982) stated that boron is essential for healthy plant growth, but certain plants are the most susceptible. Coal ash with boron concentration of 210 - 16210 ppm, may be useful for agricultural purposes, Michailova and Gladkaya (1980).

The boron content in the coal ranges between 37.00 ppm and 409.00 ppm. Vertical variation shows that the coal from sub-seam G3 of drill holes CPCH 1, 39 and 57 contains the highest concentration of the boron. Laterally, towards a NW direction (CPCH 1 to CPCH 57), the boron content in the individual sub-seams decreases (Table 6.3), which reflects a slight change in depositional condition that has occurred towards that direction. This element is predominantly associated with organic matter in coal, which is represented by the weak to moderate negative correlation between the boron content and ash content in coal (Figure 6.13.b). However, a minor amount of boron is probably inorganically bound in the coal.

Beryllium (Be)

Beryllium is organically associated in most coals, in variable concentrations according to Hak and Babcan (1967) and Gluskoter *et al.* (1977). According to Miller and Given (1978), the occurrence of beryllium is due to fixation by organic matter in

low-rank coal. However they suggested that it probably was associated with clay minerals. Singh, Singh and Chandra (1983) also reported that beryllium is recognised as clay and quartz affinities. When the content of beryllium in ash is more than 100 ppm, it is a comparatively high value for health problems, but no clear ill effects occur, Swaine (1982).

The beryllium concentration in the coal ranges from 4.00 ppm to 19.00 ppm. The beryllium concentration tends to increase from sub-seams G2 to G5, whereas, it decreases from sub-seams G1 to G2. The vertical variation of its content shows a decrease from sub-seams G1 to G2, an increasing value is represented from sub-seams G2 to G5. Laterally, the variation of beryllium content is not consistent, and it does not shows a remarkable trend. Its relationship with ash content in the coal is presented in Figure 6.13.c, and it displays a moderate positive relationship. This correlation reflects that largely beryllium is inorganically bound and to a lesser degree it has organic association.

Cadmium (Cd)

Kirsch, Schirmer and Schwarz (1980) recorded cadmium association with clay minerals, carbonates, and pyrite in some German coals. However, minor amounts of cadmium are organically bound in most coals. Cadmium in coal is of primary environmental significance, because it causes harmful effects in areas contaminated by industrial wastes which contain cadmium, Swaine (1982).

The cadmium content in the coal is relatively very low, with a range from < 0.10 ppm to 3.63 ppm. The vertical and lateral variations of cadmium distribution in the coal do not show a remarkable trend. Figure 6.13.d. depicts a weak negative relationship between cadmium and ash content in the coal. Therefore, the cadmium is predominantly present as an organic association in coal. However, a significant

amount of inorganic affinity probably occurs in the coal.

Cobalt (Co)

Zubovic (1960) recognised that the cobalt in coal is mainly associated with organic matter. Conversely, Nicholls (1968) considered that generally it formed as an inorganic affinity. Organometallic compounds, associations with sulphide minerals and sometimes as absorbed cations of the cobalt in coal, has been reported by Gluskoter *et al.* (1977). On the basis of his investigation, Swaine (1982) stated that cobalt is associated with mineral matter and organic matter fractions of coal. In environmental and health significance, the cobalt concentration in coal plays an important role in nutrition for grazing animals.

The cobalt concentration in the coal ranges from 11.00 ppm to 47.00 ppm. The distribution of cobalt is variable, and a random trend in the vertical and lateral variation of cobalt distribution occurs in the coal. The element in the coal has a predominant inorganic association, which is presented by a weak positive relationship between the cobalt and ash contents in coal (Figure 6.13.e). Less significant organic affinity is probably present in the coal.

Chromium (Cr)

Nicholls (1968) stated that the association of chromium with inorganic matter in coal formed as insoluble compound under reducing conditions, and it is conserved in peat during peatification and early diagenesis. High concentration of chromium is due to organic matter and inorganic matter affinities, Gluskoter *et al.* (1977), Cavallaro *et al.* (1978), and Wagner *et al.* (1980). Finkelman (1981) reported an association of chromium with clays, whereas, Mayers *et al.* (1984) stated that chromium is bound to colloidal substances. Cobalt as an essential trace element is required for normal

carbohydrate metabolism of plants and animals according to Anderson (1981). Chromium is not toxic, except in the hexavalent state, which may occur in some waste waters and industrial activities. During coal mining and usage, no environmental effects caused by chromium concentration are present.

The concentration of chromium ranges from 101.00 ppm to 148.00 ppm in the coal. The concentration decreases from sub-seams G1 to G2, and is then followed by an increase from G2 to G5 (Table 6.3). No significant lateral variation of chromium occurs in the coal. It is significantly associated with organic matter in coal, and to a lesser extent in inorganic association. There is a weak to moderate negative relationships between chromium content and ash content as shown in Figure 6.13.f.

Copper (Cu)

Copper was found to be associated intimately with vitrain and clarain in coal, Crossley (1946, 1947). However, it was commonly recognised as an inorganic affinity with sulphide and pyrite minerals. The high concentration of copper is indicative of inorganic association. The copper may be associated with either or both organic and inorganic fractions of coal, Nicholls (1968). Gluskoter *et al.* (1977) concluded that the copper was associated with sulphide minerals, although it shows an organic affinity in coal. According to Wagner *et al.* (1980), copper is mainly associated with clays, marcasite, and pyrite. Singh, Singh and Chandra (1983) recorded copper association with pyrite in the Permian Indian coal. Some environmental and health problems could occur in coal containing a high copper content, Swaine (1982). Therefore copper can be classified as of "moderate concern" in environmental and health significance.

The copper concentration has a range between 112.00 ppm to 246.00 ppm in the coal. Vertically, the content of copper has a tendency to increase from sub-seams G1 to G2,

followed by a decrease in content from sub-seams G2 to G5 (Table 6.3). It has a strong negative relationship with ash content in the coal (Figure 6.13.g). This means that copper is predominantly present as an organic association. However, a less significant inorganic affinity may occur in the coal.

Gallium (Ga)

In large concentrations, gallium is present as an organic affinity in coal, Nicholls (1968), and it has also been observed to be associated mainly with clays and sulphide minerals, and to a lesser extent with organic matter, Swaine (1982). He also stated that the gallium has a close association with the organic and inorganic matter of peat, probably through a functional group of humic acids. However, it seems to favour clay association in coal. No harmful effects are recognised caused by gallium content in coal, during coal mining and its usage.

The range of gallium content in the coal is between 28.00 ppm to 44.20 ppm. The vertical and lateral variations show an insignificant trend. A weak positive to no apparent relationship exists between gallium and ash content in the coal as depicted by Figure 6.13.h, and thus, gallium is associated with slightly dominant inorganic fractions in coal, and some amount of organic affinity.

Manganese (Mn)

Swaine (1975), Gluskoter *et al.* (1977), and Finkelman (1980) considered that manganese had been recognised in association with carbonates, including calcite and siderite. It is also present in clay affinity in coal, Miller and Given (1978) and Finkelman (1980). In 1981, Finkelman suggested that manganese might be associated with clays, when sufficient carbonates were not present. In Australian coal, mixed organic and inorganic affinities of the manganese element exist, Lyons *et al.* (1989).

Problems in environmental situations may occur, which are due to manganese concentration in coal, Swaine (1982).

The concentration of manganese in the coal varies from 274.00 ppm to 3140.00 ppm. Both vertical and lateral variations of manganese content show a random trend in the sub-seams. A weak negative relationship with ash content in the coal is depicted by Figure 6.13.i., and it represents a predominant organic association of manganese in coal, and perhaps some inorganic affinity is also present.

Molybdenum (Mo)

Molybdenum in coal is recognised as inorganic and organic affinities. Finkelman (1981) and Chou (1984) recognised an association of molybdenum with pyrite in Herrin coal from Illinois Basin. Moreover, Leventhal, Briggs and Baker (1983) indicated that molybdenum is concentrated in organic and sulphide-rich mineral matter of coal, whilst Teschner and Wehner (1991) classified molybdenum as a chalcophile element. Swaine (1975) stated that molybdenum as MoS_2 might have been precipitated under reducing conditions in coal swamps. Furthermore, Teschner and Wehner (1991) indicated that molybdenum is the best marker for lacustrine deposition. Biologically, molybdenum is essential for plant growth, but environmentally, an excess of molybdenum concentration may harm animals, Swaine (1982). Some vegetation could cause molybdenosis in sheep and cattle, Erdman, Ebens and Case (1978).

The molybdenum distribution in the coal has a range from < 10.00 ppm to 19.00 ppm. No significant trend is obtained from the vertical and lateral variations of molybdenum content in the coal. An almost "no relationship" occurs between the molybdenum content and ash content in the coal (Figure 6.13 j). However, slightly

predominant organic association of molybdenum is presumably present in the coal, mixed with a small significant amount of inorganic association .

Nickel (Ni)

Zubovic *et al.* (1961) investigated the biogenic affinity of nickel, and this affinity occupies a higher position in the organic affinitive series. The element is recognised to be associated with organic matter and sulphides, and adsorbed on clay, Nicholls (1968) and Gluskoter *et al.* (1977). Small amounts of nickel are associated with organic fraction in coal, whereas, larger fraction is present as an association with inorganic constituents. Gluskoter *et al.* (1977) has placed nickel in the intermediate category of the organic affinitive series, and it exists either as an organometallic compound or chelated species and/or absorbed cations. Its association with inorganic mineral matter was recognised in coal by Cavallaro *et al.* (1978) and Wagner *et al.* (1980). Finkelman (1978) considered that nickel was sulphide, clay, and organically bound. Underwood (1977) classified nickel as " a relatively non-toxic element" and considered it is very useful in plant nutrition. However, if it is present in excessive amounts, it causes some undesirable health effects. Under certain conditions, relatively high levels of nickel may harm certain plants, and during coal mining and usage, nickel contents did not cause any environmental and health effects, Swaine (1982).

The distribution of nickel in the coal ranges between 43.00 ppm to 214.00 ppm. No significant trend occurs in both vertical and lateral variation of nickel in the coal. This is a somewhat uniformity in the concentration of nickel with respect to the ash content in the coal as evidenced in the Figure 6.14.a, which suggests that the element has organic and inorganic affinities in similar proportions.

Lead (Pb)

Nicholls (1968), Gluskoter *et al.* (1977), and Wagner *et al.* (1980) considered that

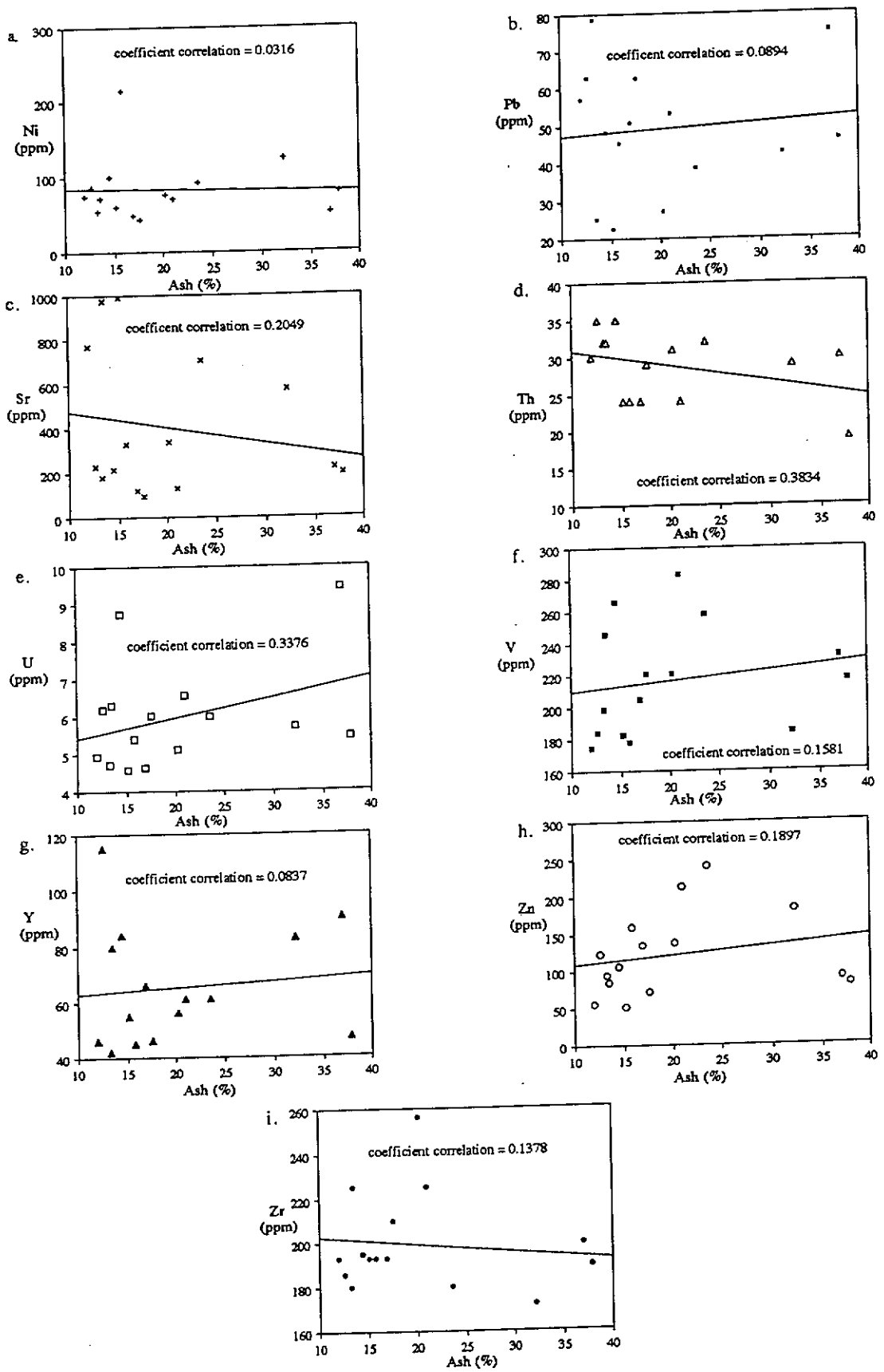

Figure 6.14. Relationship between ash and trace element contents of the Mintaja and Gairdner Blocks coal. Ni (a), Pb (b), Sr (c), Th (d), U (e), V (f), Y (g), Zn (h) and Zr (i).

lead is mainly associated with the inorganic matter of coal, especially pyrite and clay minerals. In relation to health and environment significance, certain amounts of lead in coal, gives rise to illness, Swaine (1982).

The lead concentration in the coal varies from 22.70 ppm to 75.10 ppm. The vertical variation of lead content in coal shows no significant trend. However, laterally, the content of lead in coal tends to increase towards a NW direction (CPCH 1 to CPCH 57). Figure 6.14.b. illustrates a weak positive relationship between lead and ash contents in the coal, which leads to the assumption that the association of lead is slightly dominated by inorganic affinity, with some organic affinity .

Strontium (Sr)

Strontium occurs as either organic or inorganic affinities in coal, Miller and Given (1978), Finkelman (1980), and Lindahl and Finkelman (1980). Inorganically, strontium is recognised to be associated with carbonates, Swaine (1975) and Finkelman (1980); and with clay, Miller and Given (1978) and Finkelman (1980). Permian Australian coal shows mixed organic-inorganic associations of strontium, Lyons *et al.* (1989). From the viewpoint of environmental and health implications, no deleterious effect is present from the strontium concentration in coal, Swaine (1982).

The element has a range of 94.00 ppm to 991.00 ppm in the coal. Vertically, strontium concentration in coal increases from sub-seams G1 to G2, and decreases from sub-seams G2 to G5 (Table 6.3). Lateral variation of strontium content in coal does not show a significant trend. A weak negative relationship between strontium and ash content in coal is presented in Figure 6.14.c, and this relationship reflects a slightly predominant organic affinity.

Thorium (Th)

An association of thorium with mineral matter in a United States of America coal was

found by Palmer and Filby (1984). Swaine (1984) also recognised a predominant mineral matter affinity of thorium in Permian Australian coal. The element contributes to the total radioactivity content in coal and its concentration has biological and environmental significance. However, an amount of 4.0 ppm thorium in burned coal, is probably a reasonable value for most coals.

The range of thorium content in the coal varies between 19.00 ppm and 35.00 ppm. Both vertical and lateral variations of the thorium content in coal show no significant trend. It is predominantly organically bound, which is shown by an opposite relationship to that of the ash content in the coal and the correlation showing a strong positive type (Figure 6.14.d). However, a less significant inorganic association may be present in the coal.

Uranium (U)

This element is predominantly associated with organic compounds especially in low-U coal, Breger, Deul and Rubinstein (1955). However, an affinity of uranium and clays was found in two Canadian coals, Van der Flier and Fyfe (1985). Furthermore, Asuen (1987) pointed out an association of uranium with carbonate minerals. In Australian coals, the uranium element tends to be associated with organic matter, Lyons et al. (1989). Swaine (1990) also indicated that organic bonding of uranium seems to be general, together with mineral matter affinities in coal. The element is a source of radioactivity in coal. Uranium content in coal of range 0.5 to 10.0 ppm with mean value of 2.0 ppm, is reasonable for power production, Swaine (1982).

The uranium distribution in the coal ranges between 4.56 ppm to 9.44 ppm. The variation of uranium content in the coal does not display a remarkable trend in either vertical or lateral directions. The relationship between the uranium and ash contents in

the coal shows a weak to moderate positive correlation (Figure 6.14.e), which leads to the occurrence of a predominant inorganic association in coal. However, a lesser amount of organic affinity is also present in the coal.

Vanadium (V)

Goldschmidt (1935) a pioneer of trace element investigation in coal, reported that vanadium was associated with the organic fraction as metal organic complexes. Crossley (1946, 1947) recognised that vanadium was intimately associated with vitrain and clarain compounds. Nicholls (1968) observed the association of vanadium with inorganic matter of coal. Based on their investigation on trace elements of coal, Gluskoter *et al.* (1977) and Wagner *et al* . (1980) considered that vanadium occurred especially as quartz and clay affinities. Vanadium solubility is strongly pH dependent; an increase in the solubility is due to the increasing pH of the water, Shiller and Boyle (1987). A high level of vanadium concentration (> 214 ppm) leads to possible corrosion during utilisation and also to health problems, Swaine (1982).

The vanadium content in the coal varies between 175.00 ppm to 283.00 ppm, and like beryllium, the vanadium content increases from sub-seams G2 to G5, whilst from G1 to G2, it decreases (Table 6.3). Laterally the vanadium concentration is similar in all the drill holes. The concentration shows a weak positive relationship with ash content in coal as depicted in Figure 6.14.f. Therefore, although the vanadium is dominated by inorganic affinity, organic association of significant amounts is present in the coal.

Yttrium (Y)

Mason (1958) considered that yttrium in coal was derived from inorganic matter because it displayed a lithophyllic character. Reshov (1961) found an organometallic compound of yttrium in Soviet coal, whilst Given and Miller (1987) observed yttrium in lignites to be partly associated with organic matter. Singh, Singh and Chandra (1983) stated that the yttrium was associated with inorganic substances, those are clay

and quartz. Merritt (1988) considered that yttrium in coal is of a primary environmental concern .

The yttrium content ranges between 42.00 ppm to 90.00 ppm in the coal. The concentration of yttrium shows no remarkable trend in both vertical and lateral direction of the sub-seams and the element has a predominant inorganic association in coal, mixed with probable organic affinity, which is based on the occurrence of very weak positive to almost no apparent relationship between yttrium content and the ash content in coal (Figure 6.14.g).

Zinc (Zn)

In 1977 Gluskoter *et al.* observed the association of zinc with sulphide minerals in coal whilst Miller and Given (1978) reported a relationship of zinc with clays. A strong inorganic affinity of zinc in Australian coal was investigated by Lyons *et al.* (1989). Zinc is an essential matter in plant nutrition, and it is an environmentally important element . However an excess amount may be detrimental. Deleterious effects do not arise from zinc concentration during coal mining and usage, Swaine (1982).

The concentration of zinc in the coal varies from 51.00 ppm to 240.00 ppm. Distribution of zinc content in the coal is variable, and it does not show a remarkable trend in both vertical and lateral variations. The relationship between the zinc and ash content in coal is illustrated in Figure 6.14.h, and a weak to moderate positive correlation occurs, which reflects a predominant inorganic association of zinc.

Zircon (Zr)

It is associated with detrital minerals such as clays, and its distribution exhibits a trend similar to that of clays in coal, Mackowsky (1968) and Finkelman (1980). In Australian coal, Ward (1980) observed a predominantly organic association of zircon.

Zircon concentration is less prominent in lacustrine environments in comparison to fluvial ones. The element provides the most suitable criteria for distinction between fluvial and lacustrine carbonaceous rocks, Dill *et al.* (1991). Zircon is a rather harmless element in coal and no deleterious effects occur in coal containing zircon, because of its insolubility.

The zircon content in the Mintaja and Gairdner Block coal shows a range between 172.00 ppm to 256.00 ppm. The vertical and lateral variations of zircon concentration in coal present no significant trend. The element displays a weak negative to almost no apparent relationship with ash content in coal (Figure 6.14.i). It is interpreted that zircon has a slightly dominant organic affinity, with some significant inorganic association in the coal.

The data on the distribution of trace elements in the coal as described above, show that B, Cr, Mo, Cu, Sr, Zr, Mo, Cd, and Th are present predominantly in organic association; Be, V, Co, Zn, Ga, Y, Pb, and U have inorganic affinity; whereas, Ni and As are presumed to be present as both organic and inorganic associations. According to Lyons *et al.* (1989) who studied some Australian coals, high concentrations of Cr and Zr which are not related to high ash content, are likely to be related to basinal processes and mineralisation, as well as organic association.

On the basis of proximate, ultimate, and trace element analyses mentioned above, the Mintaja Block coal has the following geochemical characteristics:

- Moisture content has a positive relationship with vitrinite reflectance, vitrinite plus exinite, and vitrinite contents, but a negative relationship with inertinite content, specific energy, and ash content in the coal.

- Volatile matter represents a positive relationship with maceral group content

and specific energy in the coal. However, a negative relationship occur with vitrinite reflectance and ash content in the coal.

- Fixed carbon content has a positive relationship with maceral groups and volatile matter contents, and a negative relationship with vitrinite reflectance and ash content in the coal.

- Specific energy and maceral groups and fixed carbon contents have a positive relationship, whilst a negative relationship exist between specific energy and vitrinite reflectance and ash content in the coal.

- Carbon content shows a positive relationship with vitrinite reflectance, vitrinite content, fixed carbon content, specific energy, and volatile matter content. On the other hand, it has no apparent to positive relationship with exinite content, and no apparent relationship with inertinite content in the coal.

- Hydrogen content has a positive relationship with vitrinite reflectance, vitrinite content, volatile matter content, specific energy, and foxed carbon content in the coal. However, a no apparent relationship and no apparent to negative relationship occur between hydrogen and exinite content, and hydrogen and inertinite content in the coal, respectively.

- Oxygen content and vitrinite reflectance, vitrinite content, exinite content, volatile matter content, specific energy, and fixed carbon content in the coal, have negative relationships, whilst no apparent relationship occurs between the hydrogen content and the inertinite content of the coal.

- Nitrogen content of the coal presents positive relationships with vitrinite reflectance, volatile matter content, specific energy, and fixed carbon content. However, no

apparent relationships appear between the nitrogen content and vitrinite, exinite, and inertinite contents in the coal.

- Total sulphur content is classified as medium to high degree, and it ranges from 0.92 % to 3.55 %. It is composed of pyritic sulphur, organic and sulphate sulphur, deposited in brackish-water swamp facies.

- The trace elements B, Cr, Mn, Cu, Sr, Zr, Mo, Cd, and Th predominantly occur as organic affinities and the Be, V, Co, Zn, Ga, Y, Pb, and U are present as inorganic affinities. The Ni and As tend to be present as both organic and inorganic associations.

6.6. Gairdner Block Coal

The proximate analyses and total sulphur content of the coal samples of the drill holes CPCH 57 and 60 from the Gairdner Block are described in this section as the ultimate analyses are already covered in the Section 6.5.2. The distribution of the trace elements in the coal samples from drill hole CPCH 57 has been included together with the Mintaja Block section , because samples from only one drill hole were available for the analyses, and these are described in the Section 6.5.3.

6.6.1. Proximate Analyses

The proximate data of the Gairdner Block coal presented in Table 6.4, include moisture, volatile matter, fixed carbon contents, and specific energy from the drill holes CPCH 57 and 60.

The moisture content of the Gairdner Block coal ranges from 5.50 % to 7.50 % or

Table 6.4 . Proximate and total sulphur analyses of Hill River coal from Gairdner Block.

Drill hole	Sub-seam	Ash (%)	Moisture (%)	Volatile Matter (%)	Fixed Carbon (%)	Specific Energy (MJ/kg)	Total Sulphur (%)
CPCH 57	G 1	19.40	5.85	31.50	43.25	23.95	0.85
	G 2	13.35	6.55	33.50	46.60	25.62	0.99
	G 3	15.25	6.95	32.30	45.50	25.06	1.63
	G 4	20.20	7.30	31.00	41.50	23.12	1.74
	G 5	38.30	5.50	24.80	31.40	16.84	2.10
CPCH 60	G 1	21.30	7.00	30.40	41.10	23.19	1.49
	G 2	13.30	7.50	31.90	47.20	26.23	1.00
	G 3	17.80	6.80	31.10	43.60	24.44	1.20
	G 4	16.80	7.00	31.70	44.50	24.86	1.92
	G 5	54.60	6.00	17.20	22.20	11.40	1.13

7.26 % to 13.21 % (daf). The moisture content shows a strong positive relationship with maximum vitrinite reflectance (Figure 6.15.a), and weak to moderate positive relationship with vitrinite+exinite content (Figure 6.15 b), vitrinite content (Figure 6.15 c), and specific energy (Figure 6.15.e) in the coal. Thus, an increase in moisture content is accompanied by decreases of those four variables. However, the moisture content of coal has a moderate to strong negative correlation with ash content (Figure 6.15.f) and a weak negative correlation with inertinite content in the coal (Figure 6.15 d). Therefore, an increase in moisture content is in agreement with decreasing ash and inertinite contents in the coal.

The volatile matter content in the coal varies between 17.20 % and 33.50 % or 36.79 % to 40.19 % (daf). The volatile matter has a moderate positive correlation with maximum vitrinite reflectance (Figure 6.16.a) and inertinite content (Figure 6.16 d), a strong positive relationship with vitrinite+exinite content (Figure 6.16.b) and vitrinite content (Figure 6.16.c), and an almost perfect positive relationship with specific energy (Figure 6.16 e). These relationships show that increasing volatile matter content in the coal is in agreement with increases in maceral groups content, vitrinite reflectance, and specific energy. On the other hand, a strong negative correlation between volatile matter content and ash content in the coal is present (Figure 6.16.f), and it reflects that increasing volatile matter is accompanied by decreasing ash content in the coal.

The fixed carbon content varies between 22.20 % to 47.20 % or 48.90 % to 54.56 % (daf), and its distribution in the coal, displays weak to moderate positive relationship with maximum vitrinite reflectance and inertinite content, a strong positive relationship with vitrinite+exinite and vitrinite contents, and an almost perfect positive relationship with volatile matter content. These relationships are depicted in Figure 6.17 a, d, b, c, and e, respectively. However, a strong to almost perfect negative correlation with ash content is present in the coal (Figure 6.17 f). From these relationships, increasing

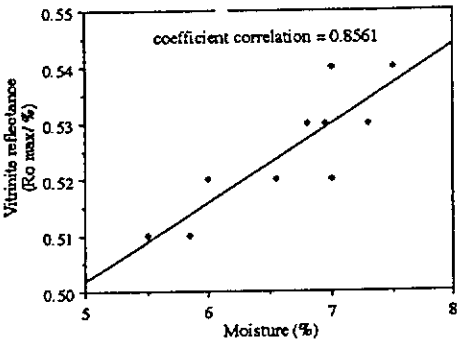

a. Moisture content versus maximum vitrinite reflectance.

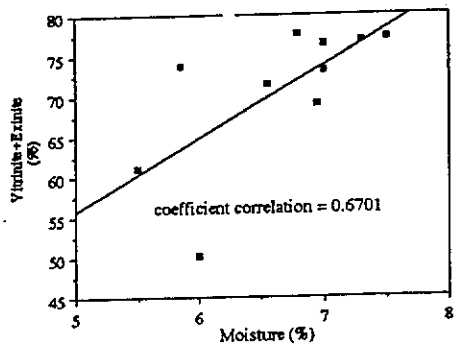

b. Moisture content versus vitrinite+exinite content.

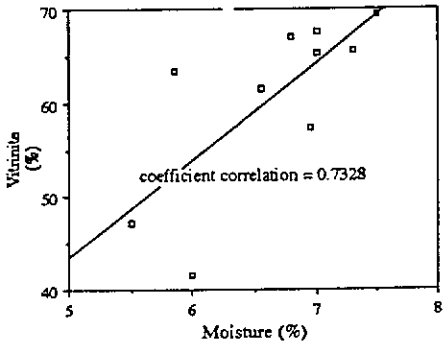

c. Moisture content versus vitrinite content.

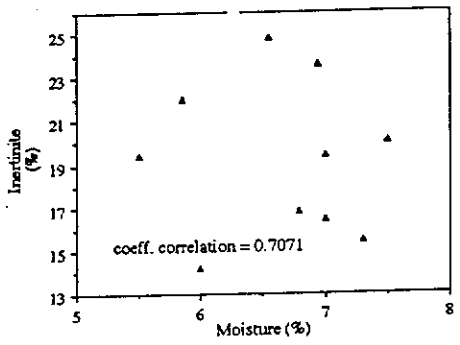

d. Moisture content versus inertinite content.

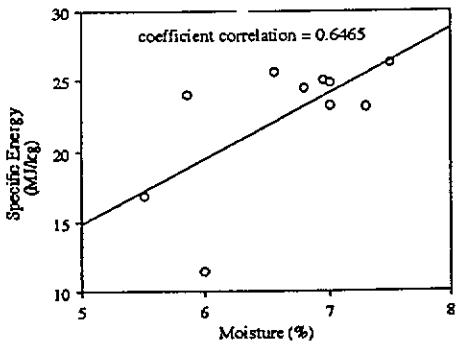

e. Moisture content versus specific energy.

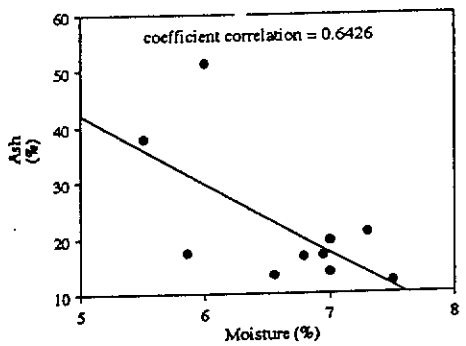

f. Moisture content versus ash content.

Figure 6.15. Relationship between moisture content and maximum vitrinite reflectance (a), vitrinite+exinite content (b), vitrinite content (c), inertinite content (d), specific energy (e), and ash content (f) of the Gairdner Block coal.

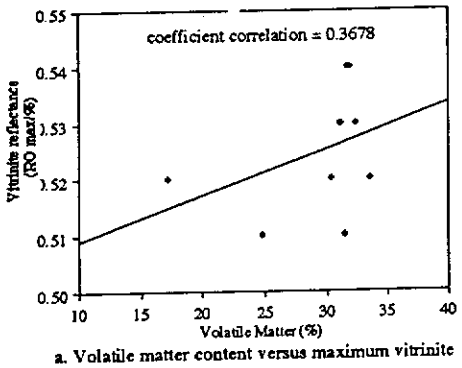

a. Volatile matter content versus maximum vitrinite reflectance

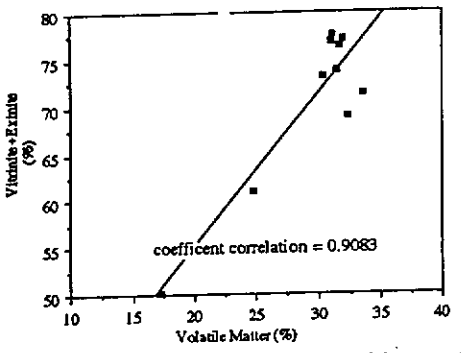

b. Volatile matter content versus vitrinite+exinite content.

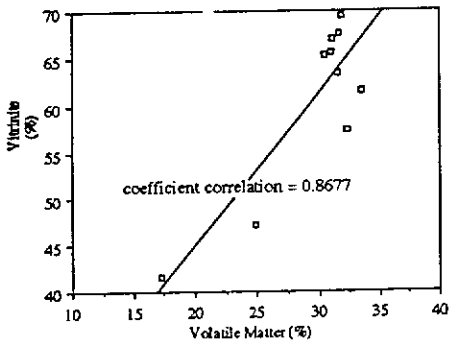

c. Volatile matter content versus vitrinite content.

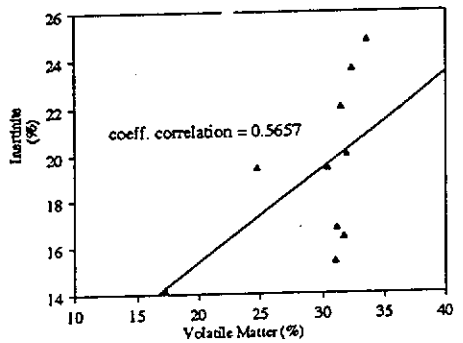

d. Volatile matter content versus inertinite content.

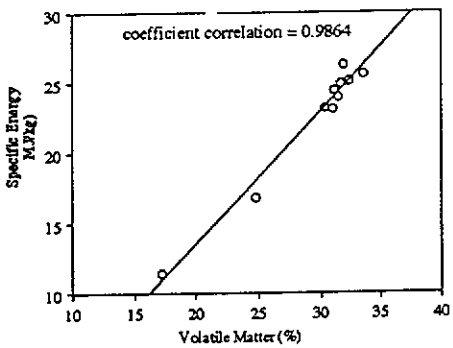

e. Volatile matter content versus specific energy.

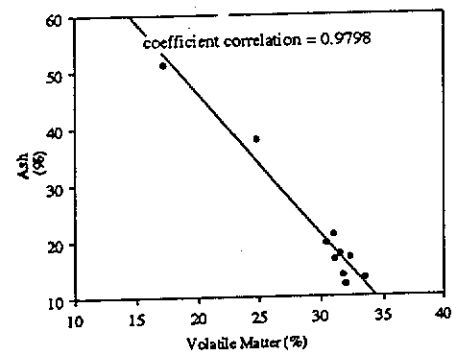

f. Volatile matter content versus ash content.

Figure 6.16. Relationship between volatile matter content and maximum vitrinite reflectance (a), vitrinite+exinite (b), vitrinite (c), inertinite (d), specific energy (e) and ash (f) contents of the Gairdner Block coal.

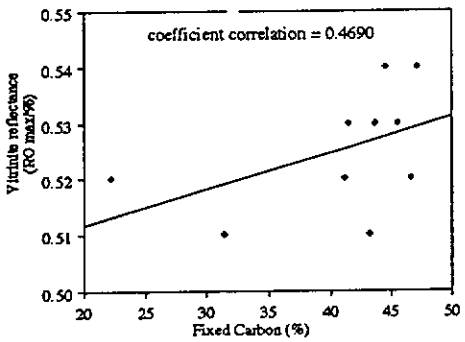

a. Fixed carbon content versus maximum vitrinite reflectance.

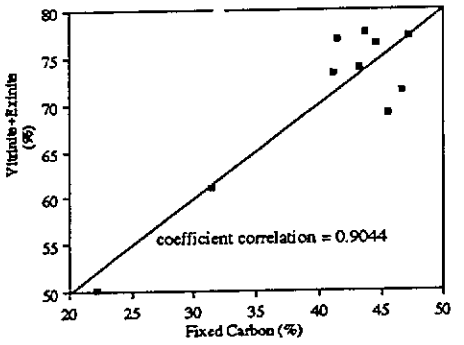

b. Fixed carbon content versus vitrinite+exinite content.

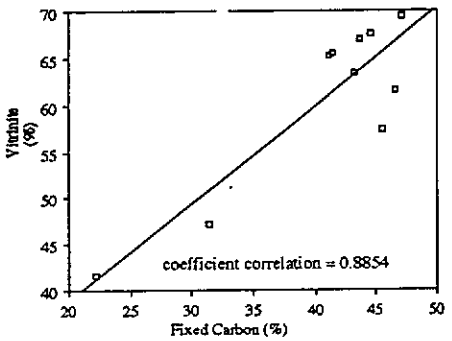

c. Fixed carbon content versus vitrinite content.

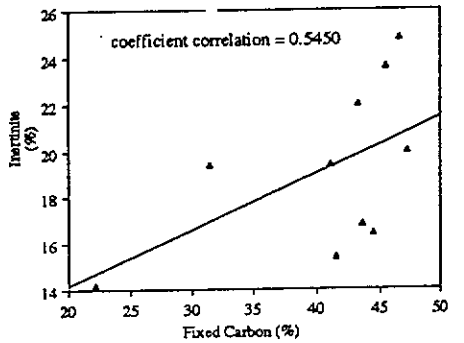

d. Fixed carbon content versus inertinite content.

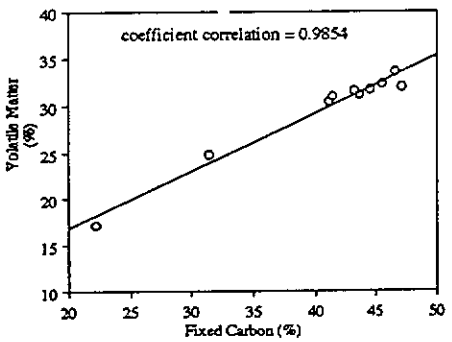

e. Fixed carbon content versus volatile matter content.

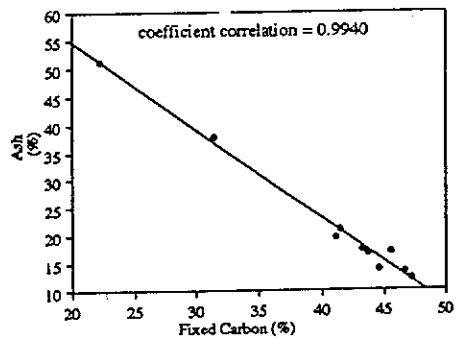

f. Fixed carbon content versus ash content.

Figure 6.17. Relationship between fixed carbon content and maximum vitrinite reflectance (a), vitrinite+exinite (b), vitrinite (c), inertinite (d), volatile matter (e) and ash (f) contents of the Gairdner Block coal.

fixed carbon content leads to increases in vitrinite reflectance, maceral groups, and volatile matter contents, and a decrease in ash content in the coal. In addition, an increase in fixed carbon content is accompanied rapidly by an increase in volatile matter, and a rapid decrease in ash content in the coal.

The specific energy of coal ranges from 11.40 MJ/kg to 26.23 MJ/kg. Figures 6.18.a and c, depict a weak to moderate positive relationship between the specific energy and maximum vitrinite reflectance, and inertinite content, whilst Figures 6.18 b and c shows a strong positive relationship between the specific energy and vitrinite+exinite and vitrinite contents. Moreover, a perfect positive relationship occurs between the specific energy and fixed carbon contents in the coal (Figure 6.18 e). Therefore, specific energy increases with increasing maximum vitrinite reflectance, maceral group content, and fixed carbon content in coal. The correlation of specific energy and ash content shows a strong to perfect negative relationship (Figure 6.18.f), and it reflects that a rapid increase of the specific energy coincides with a rapid decrease of ash content in the coal.

The ash concentration in the coal varies from 13.30 % to 54.60 %, and it can be categorised as high to very high degree, Graese *et al.* (1992). Furthermore, in accordance with ICCP (1963 and 1971), sub-seams G5 of CPCH 57 and 60 having extremely high ash (Table 6.4) are classified as clayey coal and coaly shale, respectively. The correlation between ash content and moisture content, volatile matter content, fixed carbon content, and specific energy of the coal which represent very close relationships between each other, are presented in Figures 6.15 f, 6.16 f, 6.17 f, and 6.18 f, respectively.

6.6.2. Ultimate Analyses

The analysis described in the section is the total sulphur content of the coal, because

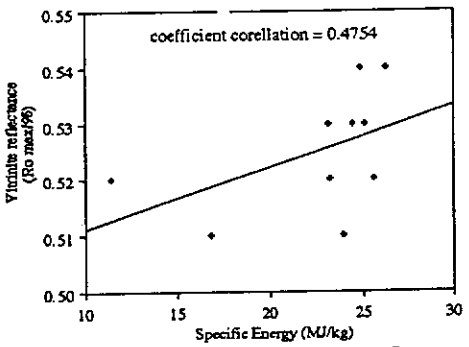

a. Specific energy versus maximum vitrinite reflectance.

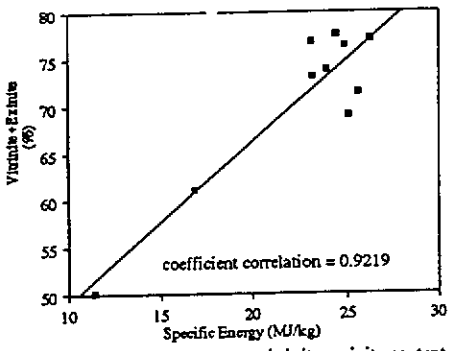

b. Specific energy versus vitrinite+exinite content.

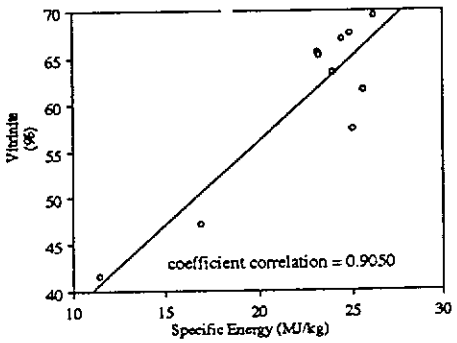

c. Specific energy versus vitrinite content.

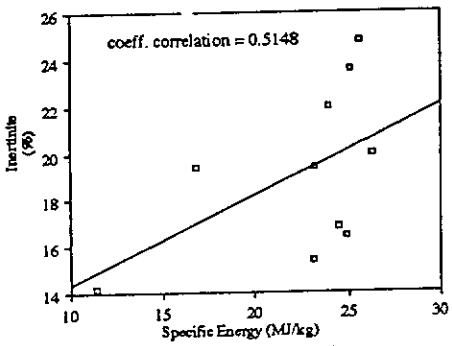

d. Specific energy versus inertinite content.

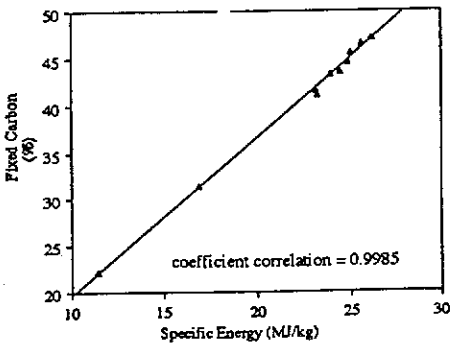

e. Specific energy versus fixed carbon content.

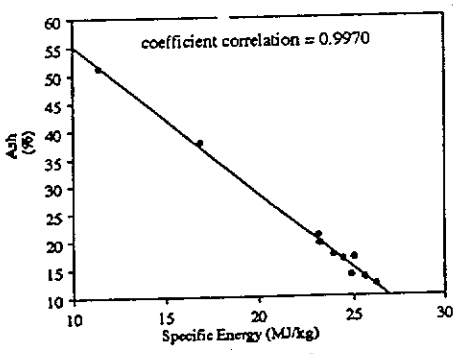

f. Specific energy versus ash content.

Figure 6.18. Relationship between specific energy and maximum vitrinite reflectance (a), vitrinite+exinite (b), vitrinite (c), inertinite (d), fixed carbon (e) and ash (f) contents of theGairdner Block coal.

carbon, hydrogen, oxygen, and nitrogen contents have been included and described in the ultimate analyses of the Mintaja Block coal (Section 6.5.2).

The total sulphur contents of the Gairdner Block coal are presented in Table 6.4. The total sulphur distribution which is categorised as moderate (0.55% - 1.00%) to high (>1.00%), varies between 0.85 % to 2.10 %. Figures 6.19, 6.20, and 6.21 depict the relationship of the total sulphur content and the ash, pyrite, and vitrinite contents in the coal, respectively. The sulphur content increases with the increases in ash and pyrite contents, but it is accompanied with a decrease of vitrinite content in the coal.

Vertically, the content of total sulphur in drill hole CPCH 57, shows a remarkable trend from sub-seams G1 to G5 reflected by increasing content of the sulphur. However, in drill hole CPCH 60, the total sulphur content in the coal is variable from sub-seams G1 towards G5, and a random trend is present. In general, increases in the total sulphur content in both drill holes coincide with increases in the total ash content and also the pyrite content of the coal. The lateral variation of the total sulphur content of each sub-seam in the SE-NW direction (CPCH 57 to CPCH 60), shows no significant trend.

A weak positive relationship between the total sulphur content and the total ash content is illustrated in Figure 6.19. It reflects that an increase in the total sulphur content is accompanied by a slight increase of mineral matter (ash-yield) which contains sulphur in the coal. However, a slightly strong positive correlation between the total sulphur and pyrite contents is depicted in Figure 6.20, which means that a rise in the total sulphur content in coal coincides with a slightly strong increase in pyritic sulphur. Based on both the figures, it can be interpreted that predominantly the total sulphur content in the coal is constituted by pyritic sulphur, and a minor amount is present as organic sulphur and sulphate sulphur. This interpretation is in accordance with Casagrande, Gronli and Sutton's consideration (1980) regarding the Australian

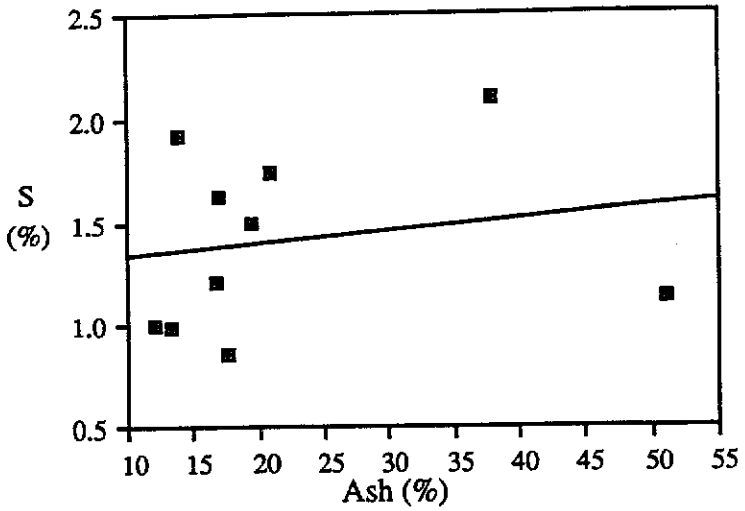

Figure 6.19. Relationship between ash and total sulphur contents of the Gairdner Block coal.

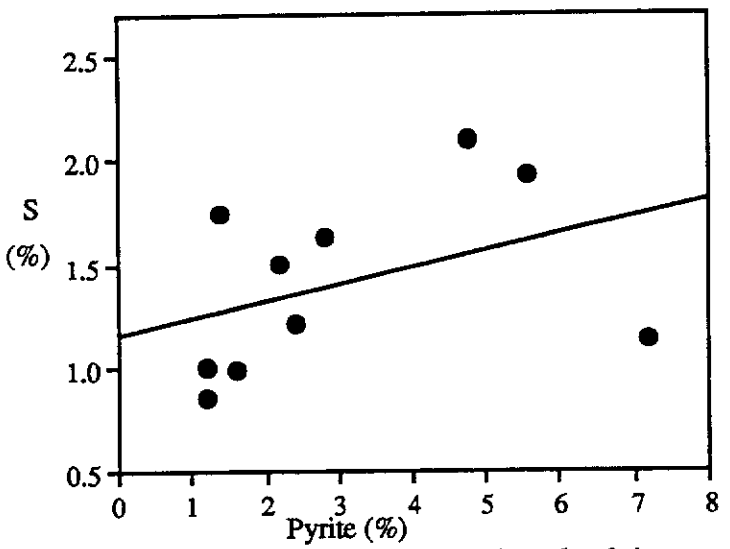

Figure 6.20. Relationship between pyrite and total sulphur contents of the Gairdner Block coal.

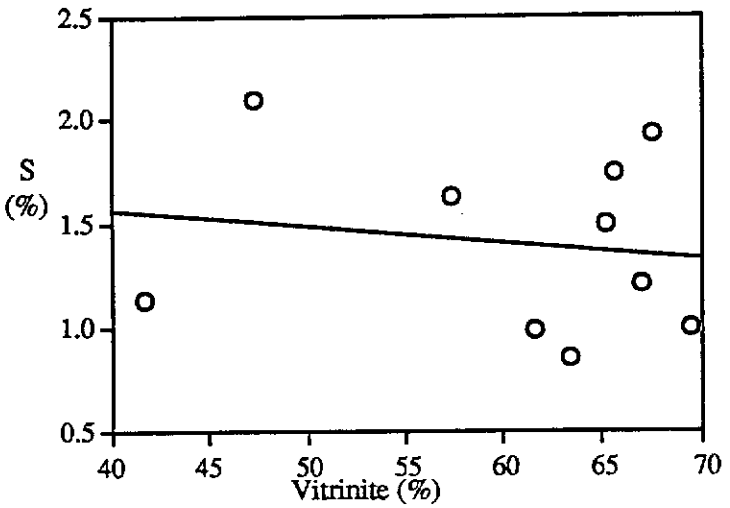

Figure 6.21. Relationship between vitrinite and total sulphur contents of the Gairdner Block coal.

coal having a total sulphur content of more than 1.00 %. The correlation between sulphur content and vitrinite content in the coal showing a weak positive relationship is depicted in Figure 6.21, and it reflects that an increase in sulphur content is compensated by a slight decrease in vitrinite content in the coal.

The geochemical characteristics of the Gairdner Block coal based on proximate and total sulphur analyses are :

- Positive relationships are present between moisture, volatile matter, fixed carbon contents, and specific energy of the coal and vitrinite reflectance, vitrinite+exinite content, and vitrinite content in the coal.

- Positive relationships exist between specific energy and moisture and volatile matter, fixed carbon content and volatile matter and specific energy.

- A negative correlation between moisture, volatile matter, and fixed carbon and ash content, and a weak negative correlation between moisture content and inertinite content, exist in the coal.

- Total moisture, volatile matter, and fixed carbon contents are dependent of specific energy in the coal, and they have a very close relationship among each other.

- The total sulphur content varies from 0.85 % to 2.10%, and is categorised as moderate to high. Predominantly the sulphur content is constituted by pyritic sulphur. However, a minor amount of organic and sulphate sulphur is present in the coal.

6.7. Coal Rank and Classification

The rank of Mintaja and the Gairdner Block coal determined on the basis of volatile matter content, moisture content, and specific energy in the coal, is depicted in Figures 6.22, 6.23, and 6.24, respectively. The coal rank determined on volatile matter content is categorised as high volatile bituminous A to C, and on the basis of specific energy it is lignite to sub-bituminous A. In this classification, volatile matter content cannot be used as a precise rank parameter of the coal, because it does not correspond to the rank based on maximum vitrinite reflectance of the coal as described in Chapter 4. The difference is probably caused by the relatively high inertinite content in the coal. The high inertinite content leads to a decrease of the amount of volatile matter, and results in a higher rank of the coal, Kroeger and Pohl (1957). Specific energy is an important rank parameter, because its values increase rapidly with increasing carbon content, Stach *et al.* (1982) and Diessel (1992). However, in the Mintaja and Gairdner Blocks coal, the specific energy content gives a lower and wide range of the coal rank (Figure 6.24). It is probably due to the high concentration of mineral matter which lowers the value of specific energy in the coal. Based on the moisture content, rank is classified as sub-bituminous A to B, which is in agreement with the one based on vitrinite reflectance described in Chapter 4. Figure 6.25 illustrates coal rank which is based on the carbon content (daf) of the coal, and the rank of the Mintaja Block coal is categorised as sub-bituminous A to B, which is in accordance with that of vitrinite reflectance and moisture content basis. Furthermore, on the basis of hydrogen and carbon contents (% dry ash free) which are plotted on Seyler's chart (Figure 6.26), the coal from Mintaja Block can be classified as a sub-hydrous to per-hydrous ortho-lignitous type, whilst the Gairdner Block coal can be classified as a transition between per-hydrous ortho-lignitous to meta-lignitous one.

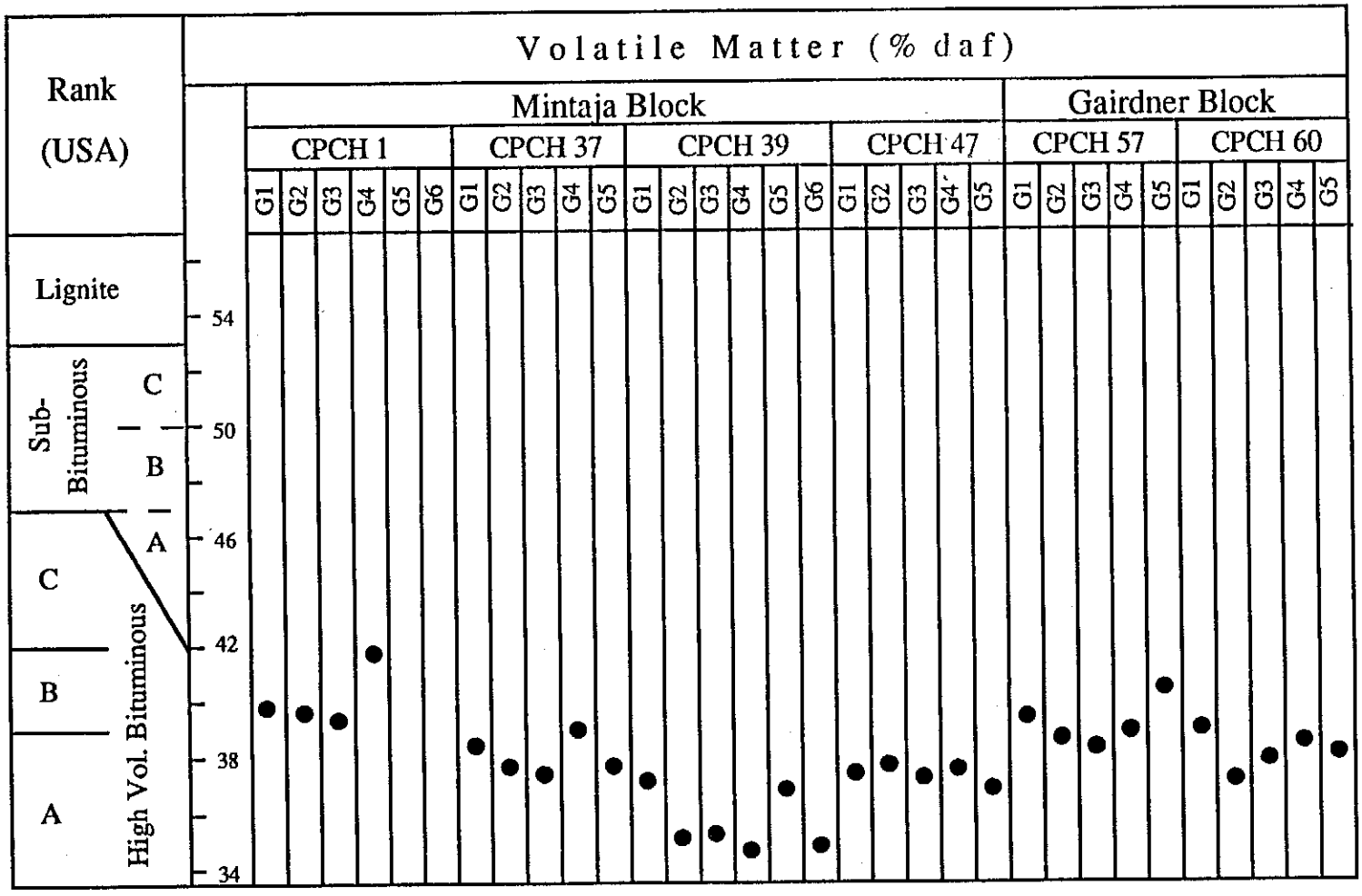

Figure 6.22. Rank and classification of Hill River coal from Mintaja and Gairdner Blocks.

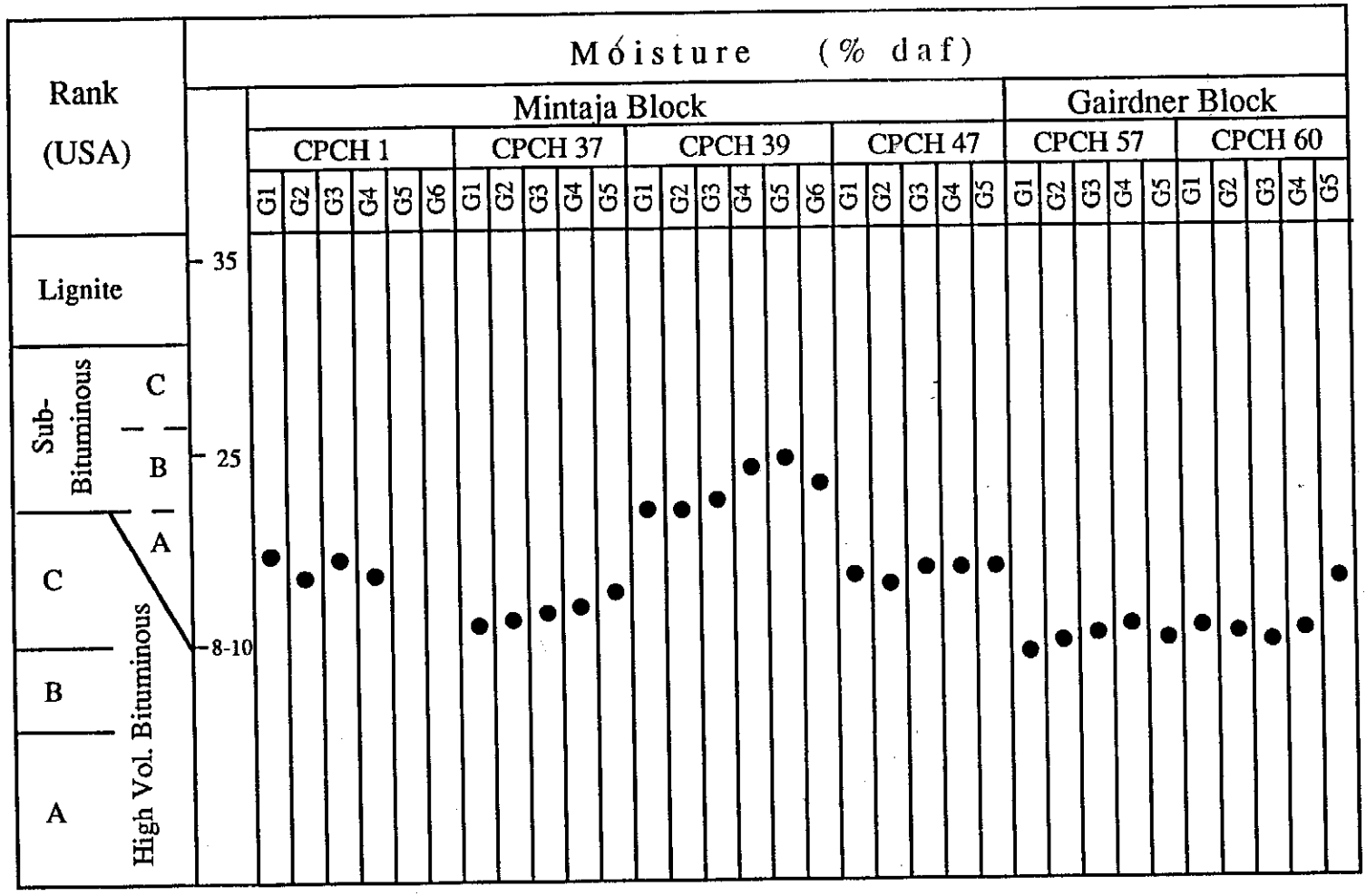

Figure 6.23. Rank and classification of Hill River coal from Mintaja and Gairdner Blocks.

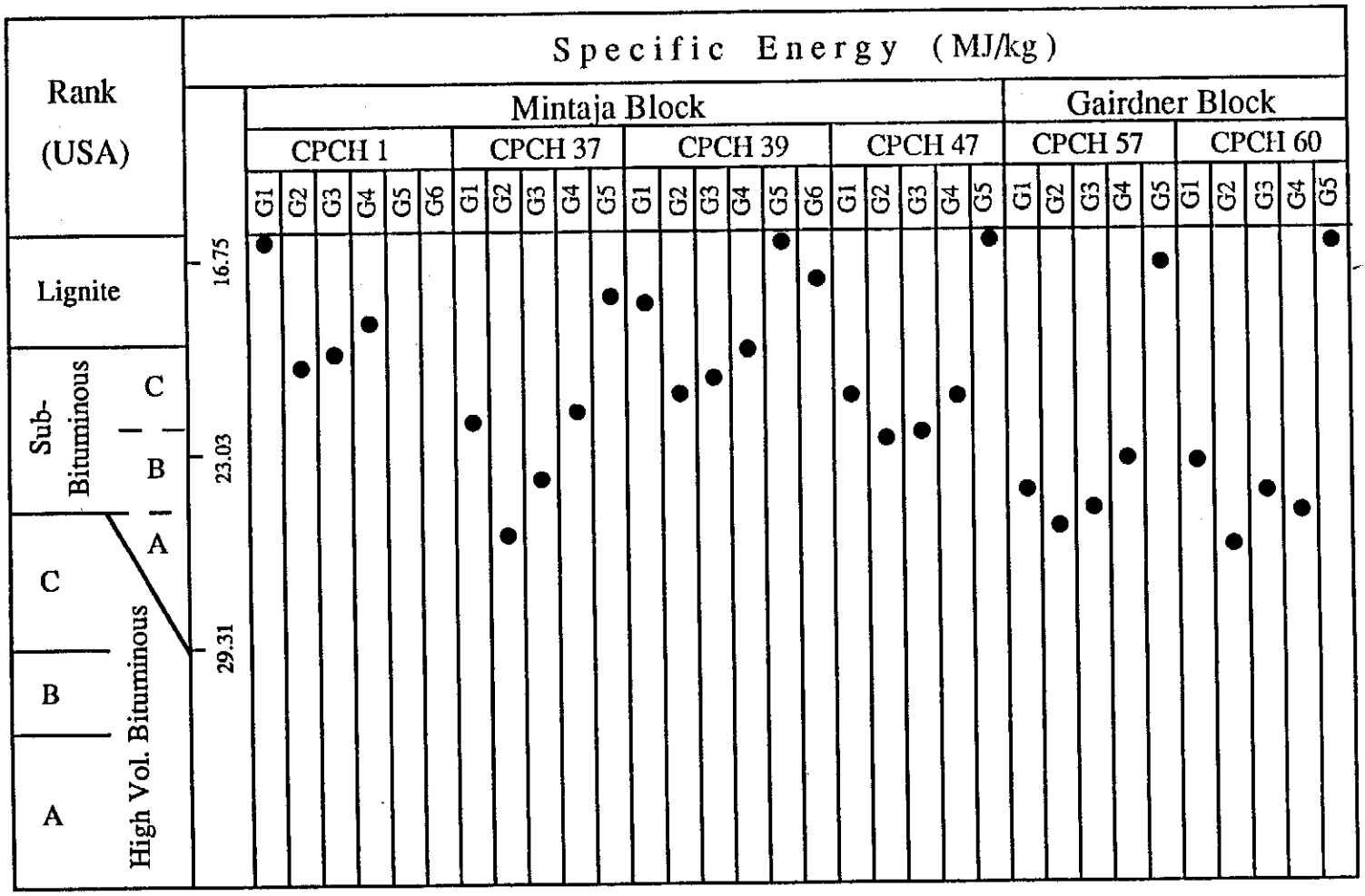

Figure 6.24. Rank and classification of Hill River coal from Mintaja and Gairdner Blocks.

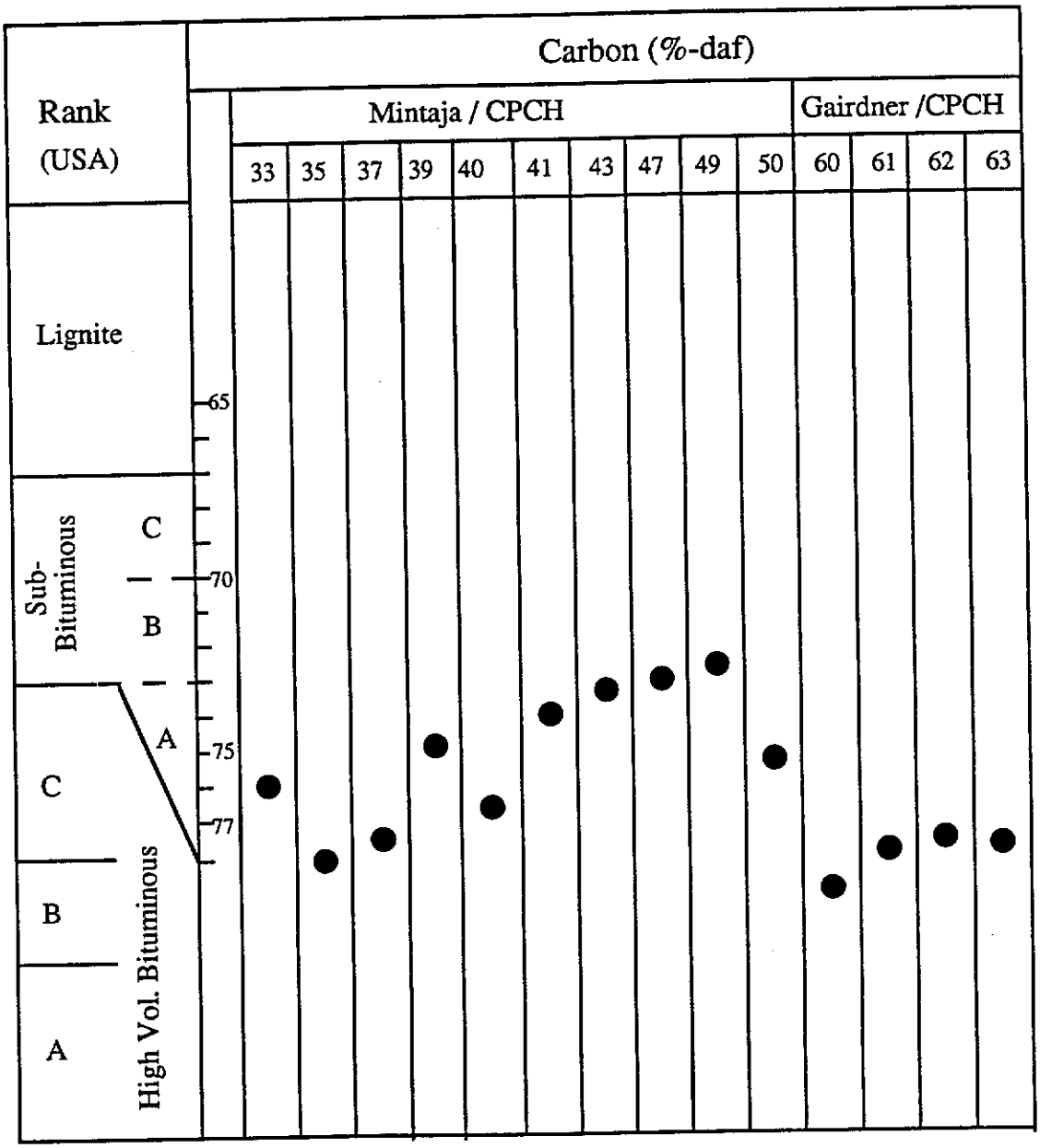

Figure 6.25. Rank and classification of Hill River coal from Mintaja and Gairdner Blocks.

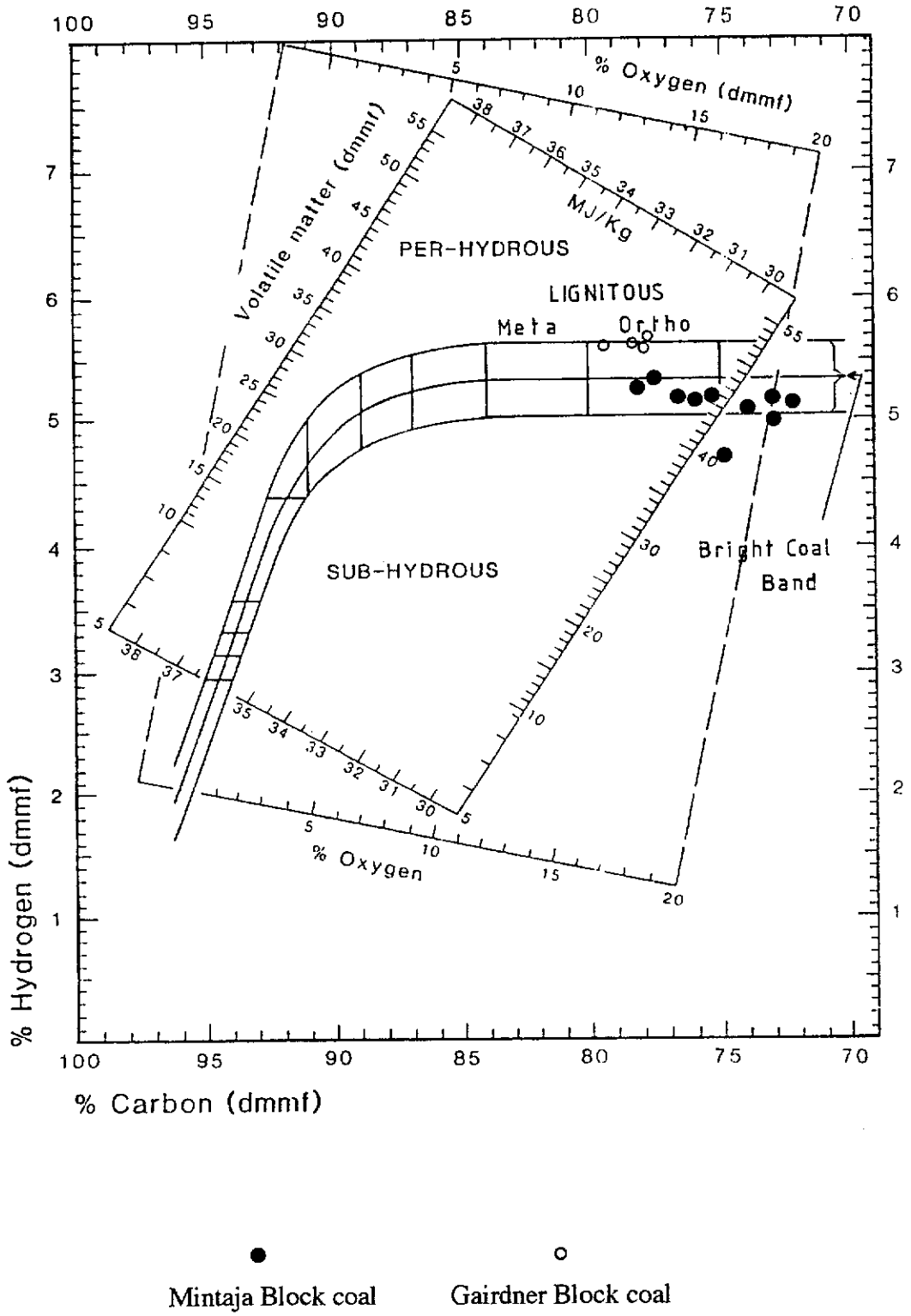

Figure 6.26. Seyler's chart showing classification of Hill River coal from Mintaja and Gairdner Block coal.

CHAPTER 7. DEPOSITIONAL ENVIRONMENT

7.1. Introduction

This chapter describes models of the depositional environment of Hill River coal from the Mintaja and the Gairdner Block . The depositional environment of the coal is constructed on the basis of models as described earlier in chapter 3 (pages 78 - 84 and 89 - 94). To establish depositional environment of the coal , petrographic analyses of the sub-seams in terms of macerals and microlithotypes are used, supported by trace elements and sulphur analyses. The sedimentary structures in the interseam sediments and earlier palynological work on Cattamarra Coal Measures by Sappal and Islam (1991, 1992) are also used in the interpretation of the environment.

The maceral data of the coal are plotted on facies diagrams of Diessel (1982 and 1986), whereas, microlithotype data are plotted on ternary facies diagrams of Marchioni (1980), Hunt and Hobday (1982), and Smyth (1979). The interpretations of the depositional environment are described separately for the coal from Mintaja and the Gairdner Blocks.

7.2. Depositional Environment and the Macerals, Mintaja Block

As described above, interpretation of the depositional environment of the Mintaja Block coal on the basis of maceral analyses, uses models proposed by Diessel (1982, 1986) for the Permian coal of eastern Australia.

The maceral compositions obtained from the sub-seams G1 to G5/6 of drill holes CPCH 1, 37, 39 and 47 are plotted onto the D-T-F ternary diagram as illustrated in

Figure 7.1. The construction of the ternary diagram is explained in chapter 3 and depicted in Figure 3.15 (page 81). All sub-seams analysed contain more than 50% of diagnostic macerals and thus all the sub-seams are localised close together in the wet forest moor of mainly telmatic to limno-telmatic environments. For sub-seams G4 and G6 of CPCH 1, and G1 of CPCH 39, a shift to an accumulation in somewhat limno-telmatic zone is present. The (T+F)/D ratios of the sub-seams range mostly between 3.5 and 4.5, except sub-seams G1 and G2 of CPCH 1, and G6 of CPCH 39, which indicate high input of woody tissues in the coal. The T/F ratios have values from 3 to 5 and reflect the wet condition of coal environment. The high value of T/F also indicates that the coal has high gelification and moisture levels with low "dispersed" maceral content, and this suggests a moderate influence of circulating water which influenced the coal mire. Figure 7.1 also depicts that coal from drill hole CPCH 1 has lower woody tissues in comparison to that of CPCH 37, 39 and 47. The depositional environment for the coal from drill holes CPCH 37, 39 and 47 is interpreted dominantly of wet forest moor condition with relatively low detrital input. Moreover, the deposition of the sub-seam G1 of the drill hole CPCH 39 developed in a very wet forest moor.

In order to assess the type of prevailing moor during deposition of coal precursor, variations in maceral content throughout the sub-seams of drill holes CPCH 1, 37, 39 and 47 are illustrated in Figure 7.2 by using Tissue Preservation and Gelification Indices (TPI and GI), Diessel (1992). On this TPI-GI diagram sub-seams G1-G5 of CPCH 1 and CPCH 37, sub-seams G2-G3 and G5-G6 of CPCH 39, and sub-seams G1-G2 and G4-G5 of CPCH 47 are located close together, and this is an evidence of a stable swamp phase. On the other hand, sub-seams G6 of CPCH 1, G1 and G4 of CPCH 39 and G3 of CPCH 47 are plotted slightly away from the others. The coal facies diagram indicates that the Mintaja Block coal mostly falls within telmatic wet forest swamp with minor limno-telmatic fen environments. It represents an intermittently to permanently flooded area of coal deposition. The sub-seams G4 of

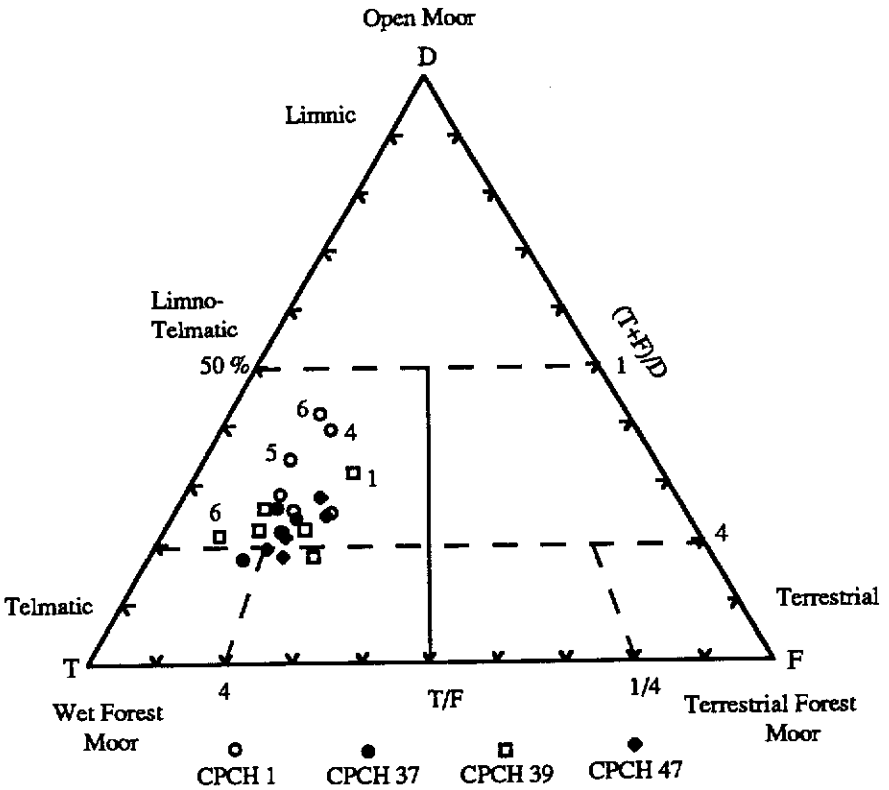

Figure 7.1. Ternary facies diagram of Hill River coal from Mintaja Block.

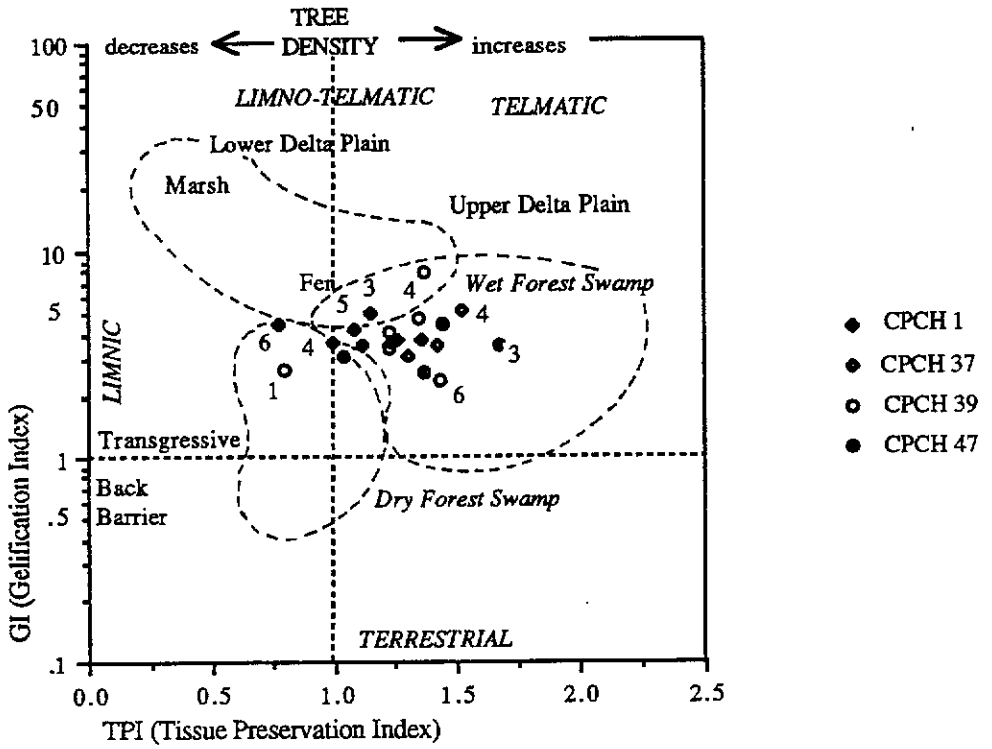

Figure 7.2 . Facies diagram of Hill River coal from Mintaja Block.

CPCH 39 plots in the zone of lower delta plain, sub-seams G3 and G5 of CPCH 1 are in a transitional zone between upper delta and lower delta plains, whilst sub-seams G4 and G6 of CPCH 1, G1 of CPCH 39 and G1 of CPCH 47 are present within a transgressive back-barrier area. The rest of the sub-seams fall in the zone of upper delta plain. The wide TPI plot ranging within 0.77 to 1.67 interval, is indicative of somewhat more frequent clastic influx during peat accumulation, and favoured preservation of structured vitrinite precursor, Kalkreuth *et al.* (1991). It also suggests a presence of cyclic development of plant communities with variables tissues in the mire, Akande, Hoffknecht and Erdtmann (1992). The low value of TPI (sub-seams G4 and G6 of CPCH 1, and G1 of CPCH 39) may indicate that a substantial degree of transportation processes took place in the coal precursor swamp prior to final deposition of peat, Kalkreuth and Leckie (1989). It also reflects a predominant occurrence of shrubs and grass in coal precursor environment. The GI values varying from 2.40 to 7.80, do not show wide fluctuation, and this indicates that all the sub-seams of the Mintaja Block coal developed in a wet area of the depositional environment. The highest GI value (7.80) shown by sub-seam G4 of CPCH 39 coinciding with the highest vitrinite content and the lowest inertinite content, indicate the wettest condition of the Mintaja Block coal. It also represents a low level of aerobic decomposition with rapid organic matter accumulation, Lamberson, Bustin and Kalkreuth (1991). On the basis of the variation of GI and TPI values, the Mintaja Block coal accumulated in forested peatland from weakly to relatively strong decomposed woody tissues, under condition of slow to moderate subsidence in telmatic and/or limno-telmatic setting, and mild to strong humification and strong gelification of plant tissues occurred in coal mire.

7.3. Depositional Environment and the Microlithotypes, Mintaja Block

The interpretation of the depositional environment of coal using microlithotype

analyses of the coal is based on ternary diagrams of Marchioni (1980), Hunt and Hobday (1982) and Smyth (1979) for the eastern Australian Permian coal.

In Figure 7.3, microlithotype composition of coal from drill holes CPCH 1, 37, 39 and 47 is plotted on B, C, and A+D ternary diagram, Marchioni (1980). The data mainly fall in telmatic forest moor zone with transition zone to reed moor, as evident by the relatively higher content of vitrinite-rich clarite (clarite-V), vitrite, cutinite-rich clarite (cuticloclarite), and vitrinite-rich vitrinertite (vitrinertite-V) in the coal related to alternating high and low ground water table conditions. However, a decrease of vitrinite-rich clarite and vitrite with increasing sporinite-rich clarite (sporoclarite) occurs in the sub-seams located in reed moor zone (sub-seams G3, G4 and G6 of CPCH 1 and G5 of CPCH 39).

In addition, the interpretation of the environment of deposition for the Mintaja Block coal is established using "bandwidth" in the Figure 7.4, Hunt and Hobday (1982). In this diagram coal samples from Mintaja Block are situated within very fine- to fine-banded zones. The finely banded nature of the Mintaja Block coal reflects that oxidation occurred in peat depositional area due to the fluctuations of tidal water in the delta plain.

The microlithotypes of the coal samples from drill holes CPCH 1, 37, 39 and 47, are plotted on the ternary diagram of Smyth (1979) as illustrated in Figure 7.5. The microlithotypes of the coal mainly fall in area C, with two sub-seams (G6 of CPCH 1 and CPCH 39) in area B, whilst, sub-seam G1 of CPCH 39 within a transition zone of C to D areas. On the basis of microlithotype interpretation, the Mintaja Block coal mainly accumulated in brackish environment with sediment influx of fluvial system. Occurrence of alginite in coal is also indicative of intermittent brackish conditions. However, sub-seam G1 of CPCH 39 is located in the transition area of the brackish

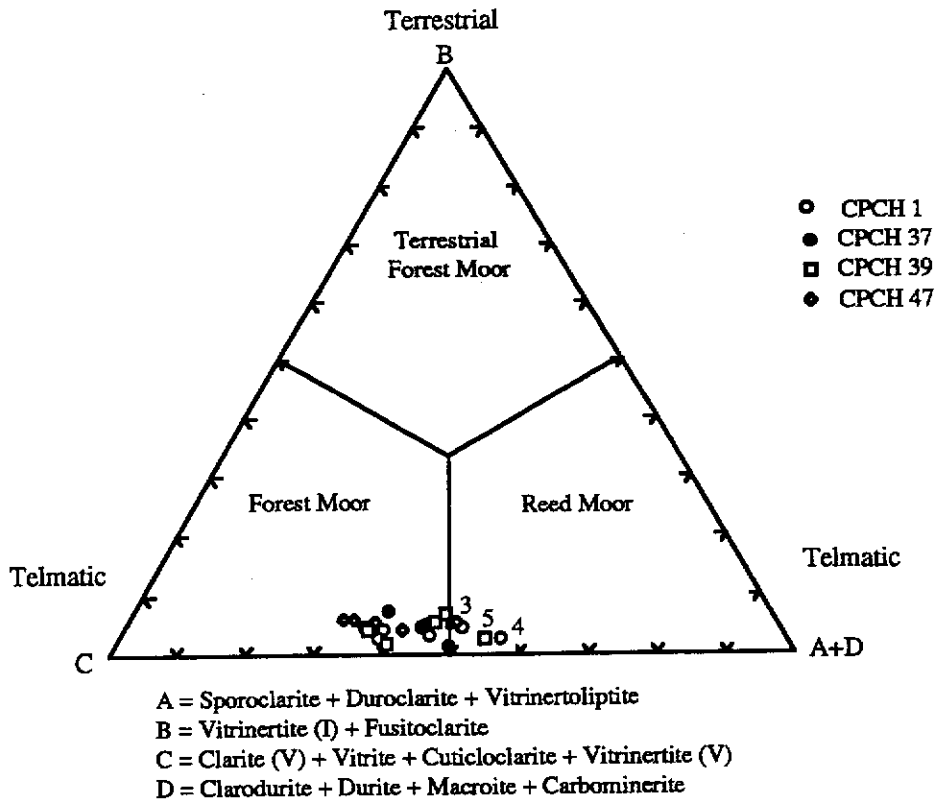

Figure 7.3. Ternary facies diagram of Hill River coal from Mintaja Block.

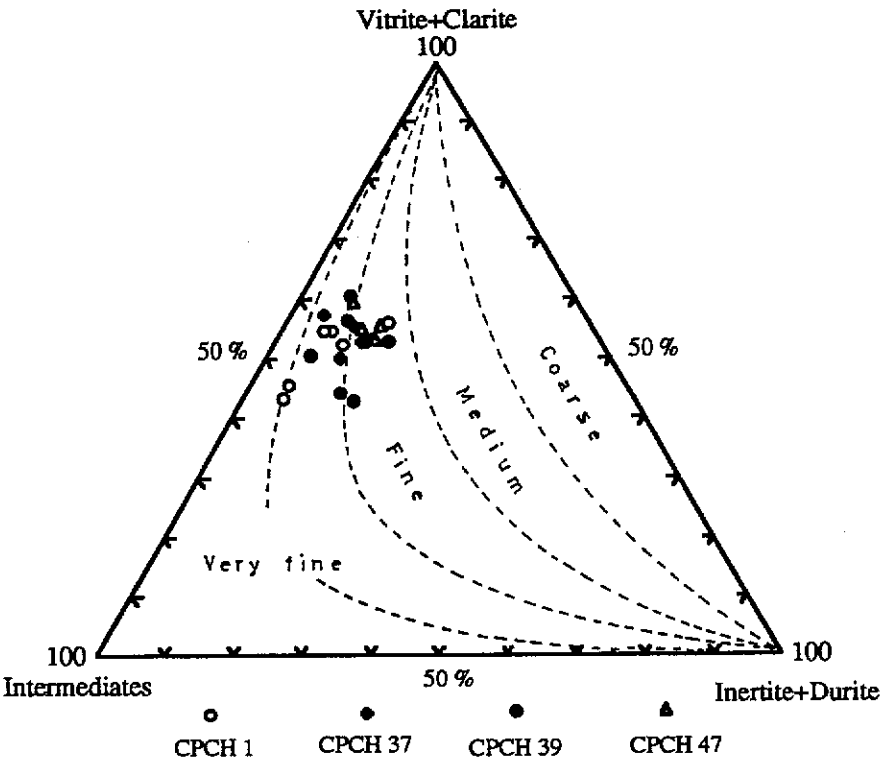

Figure 7.4. Bandwidth curves of microlithotype facies of Hill River coal from Mintaja Block.

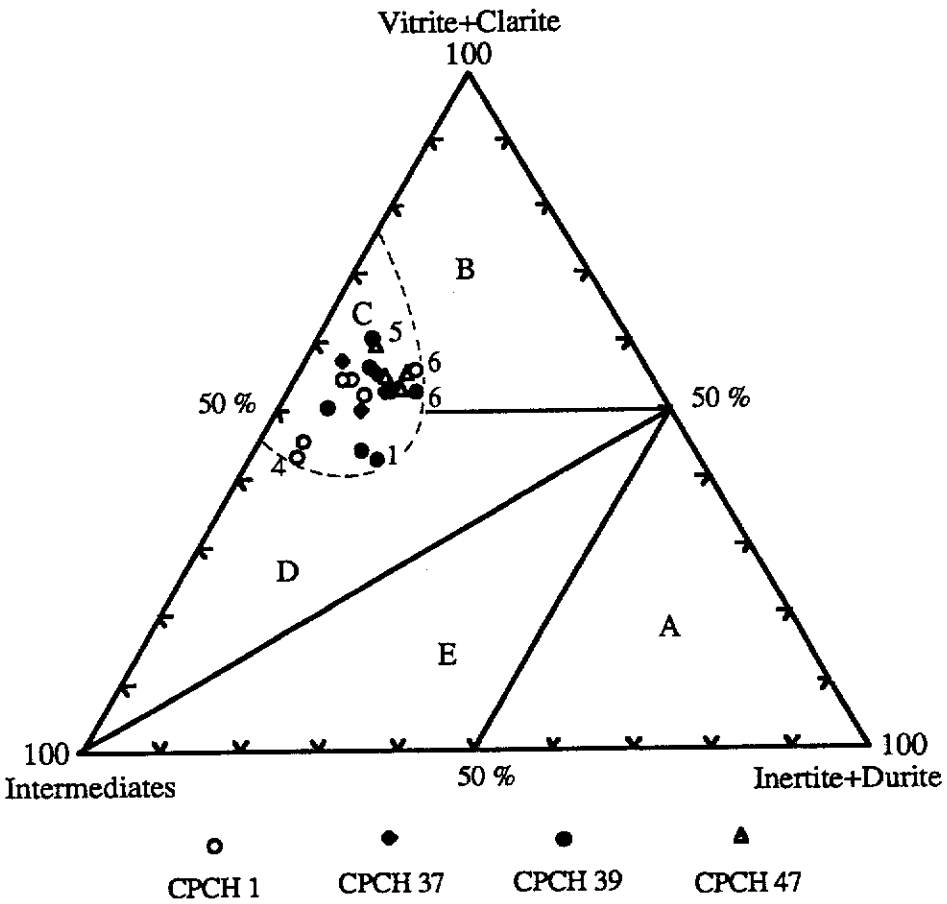

A= lacustrine; B=fluvial; C=brackish; D= upper delta-plain; E=lower delta-plain.

Figure 7.5. Ternary diagram of depositional environment of Hill River coal from Mintaja Block.

zone and upper delta plain, whilst sub-seams G6 of CPCH 1 and 39 are related to fluvial systems with high sediment influx.

7.4. Depositional Environment, Sulphur Content, Trace Elements, Palynology, and the Sedimentary Structures, Mintaja Block

Hunt and Hobday (1984) considered that sulphur content in coal is a useful guide to interpret the depositional environment of coal precursor. Based on their observations of the Permian coal of Southern Sydney Basin, they stated that coal containing a total sulphur content between 0.55 % to > 1.00 % was deposited in the lower delta plain, whilst total sulphur content less than 0.55 % reflects upper delta and fluvial facies. In addition, Horne *et al.* (1978) and Cecil *et al.* (1985) studied Late Paleozoic peat deposits in the central Appalachian Basin, USA, and reported that high sulphur-peat developed in a back-barrier zone. Therefore, the Mintaja Block coal having a total sulphur content of more than 0.55 % accumulated in lower delta plain to back-barrier environments. Furthermore, syngenetic pyrite is also important in coal facies analysis, because its precipitation within coal is contemporary with coal precursor deposition. Moderately to high sulphide and sulphate mineral, especially pyrite in coal is related to marine-influence into peat mire, Casagrande and Erchull (1976), Casagrande *et al.* (1977; 1980), Casagrande, Gronli and Sutton (1980), Teichmüller (1982) Mackowsky (1982), Davis and Raymond (1983), Styan and Bustin (1983 a and b), and Casagrande (1987). Cohen, Spackman and Dolsen (1984) reported that peat in southern Florida, USA, containing high pyrite and total sulphur content, tends to accumulate in marine to brackish conditions. Epigenetic pyrite occurring as small irregular veins is also associated with marine aqueous sulphate influx that took place after deposition of coal precursor, Lyons *et al.* (1989). On the basis of these criteria, low to moderate contents of pyrite (1.00 % to 6.00 %) in the

Mintaja Block coal indicate a marine to brackish environment (delta plain) with tidal influence.

Concentration of certain trace elements in coal, especially boron, is helpful as an indicator of the depositional environment of coal precursor. Swaine (1971, 1983) and Lyons *et al.* (1989) considered that coal having a boron content of 40 - 120 ppm tends to indicate brackish water coal, whilst a boron content varying from 120 ppm to 450 ppm in coal represents marine-influenced environment. On the basis of boron concentration between 60 and 409 ppm (Table 6.3), the Mintaja Block coal is postulated to have accumulated in brackish to marine-influenced environments.

The palynological studies on the Mintaja Block coal and its associated sediments carried out by Islam and Sappal (1991) and Sappal and Islam (1992), support the interpretation that the coal was deposited in a brackish environment, due to the presence of acanthomorphs and sphaeromorphs acritarchs in the coal measures.

The tidal influence during the deposition of coal-bearing sediments is also supported by sedimentary structures, depicted in Figures 7.6, 7.7 (a, and b), 7.8 (a, and b), 7.9 (a and b), and 7.10 (a, b, and c). The facies described here, were identified on the basis of sediment composition, grain size, sedimentary structures, and bedding type. The graphic log of core from the drill hole CPCH 1 was prepared to include lithologic characters of Mintaja Block coal-bearing sediments as depicted in Figure 7.6. Section A (179.46 m - 186.00 m deep) consists of a fining-upward sequence of predominate sandstone, siltstone, claystone, and carbonaceous claystone. Cross-bedded sandstone with carbonaceous streaks, and poorly laminated sandstone with bioturbation, are also present in this section (Figure 7.7. a, and b, respectively). The sedimentary structures in section A support the presence of sub-tidal setting in the area. Section B (174.32 m - 178.15 m in depth) is composed of interbedded fine- to medium-grained sandstone, mudstone/siltstone, and claystone. The sedimentary structures recognised

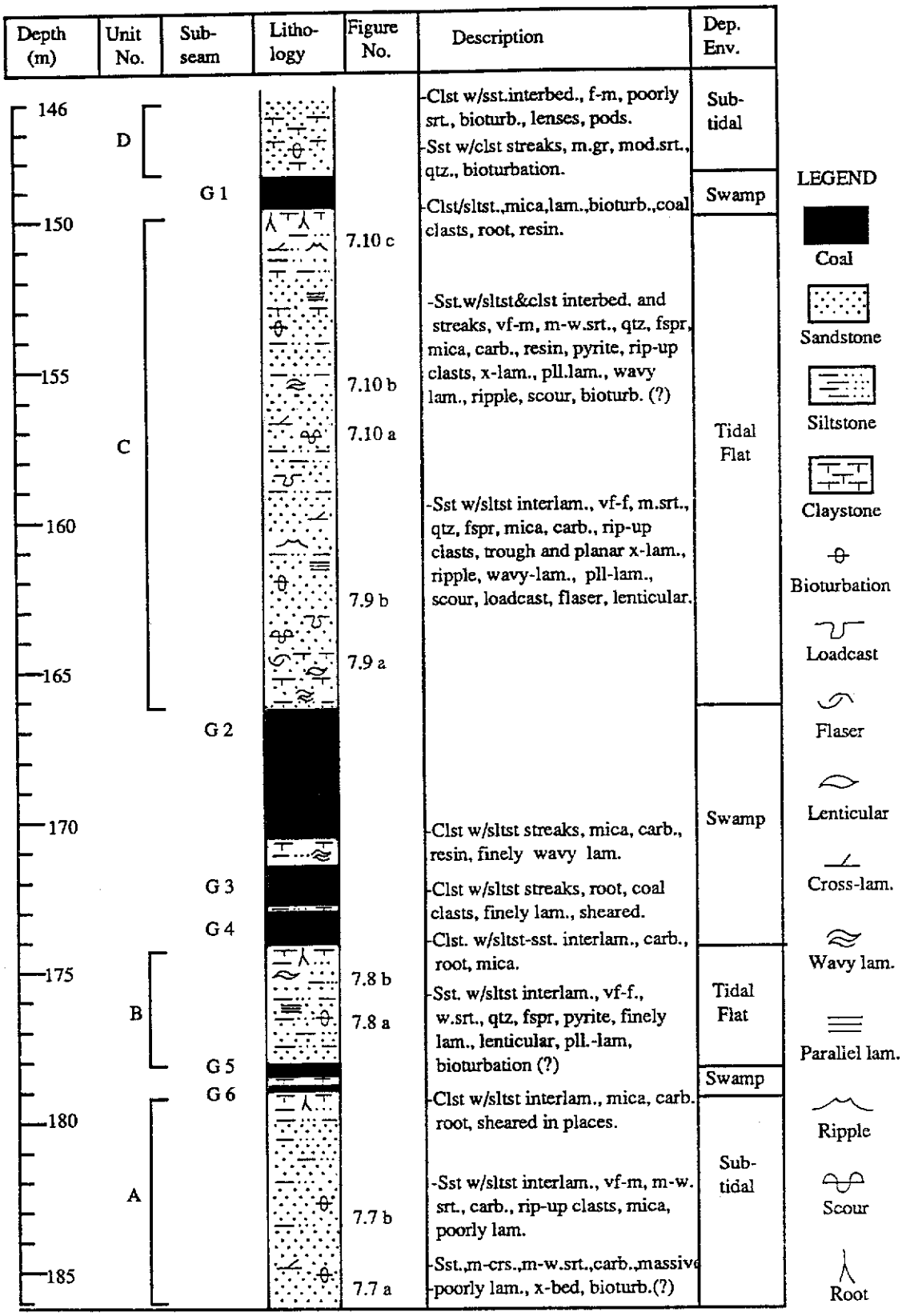

Figure 7.6 . Lithological log of drill hole CPCH 1, between 146.00 and 186.00 m in depth.

Figure 7.7. Photographs of portions of Section A (179.46 m - 186.00 m in depth).
a. Cross - bedded sandstone with very thin carbonaceous streaks (183.13 m - 185.32 m in depth).
b. Poorly laminated sandstone showing bioturbation (183.60 m - 183.84 m in depth).

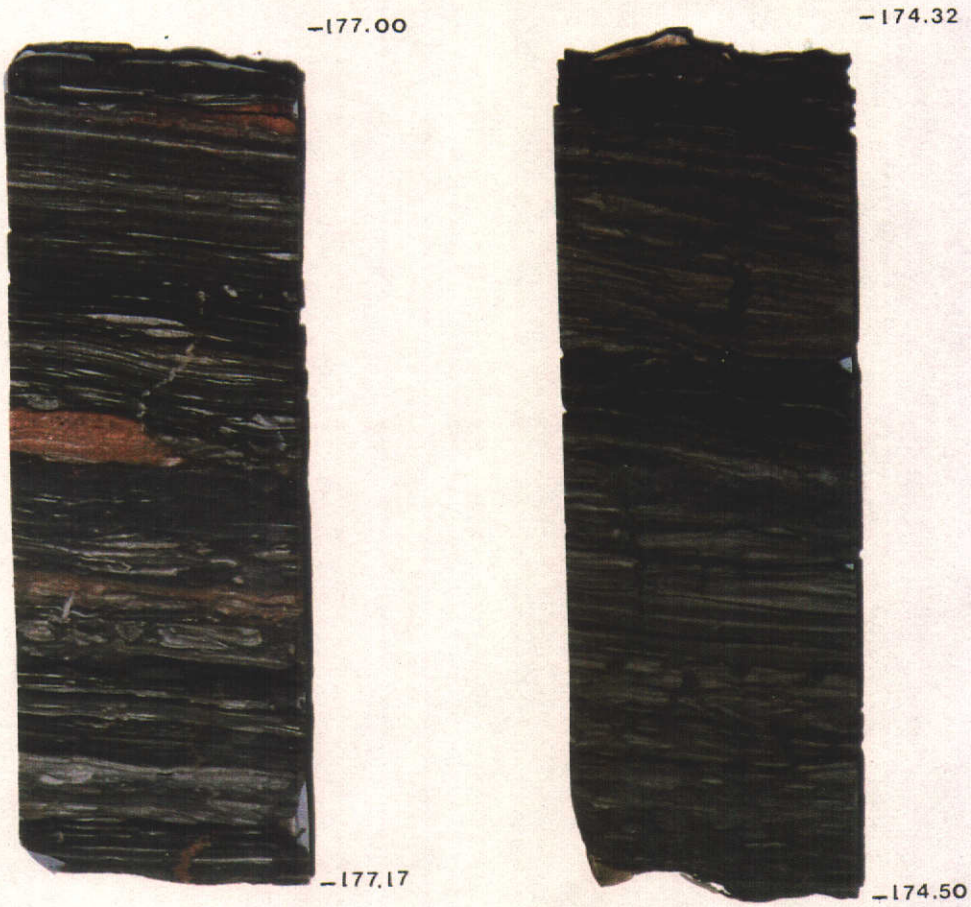

Figure 7.8. Photographs of portions of Section B (174.32 m - 178.15 m in depth).

a. Lenticular, lenses, pods, and streaks of sandstone interbedded with siltstone (177.00 m - 177.17 m in depth).

b. Regularly interlaminated siltstone and fine-grained sandstone, with bioturbations (174.32 m - 174.50 m in depth).

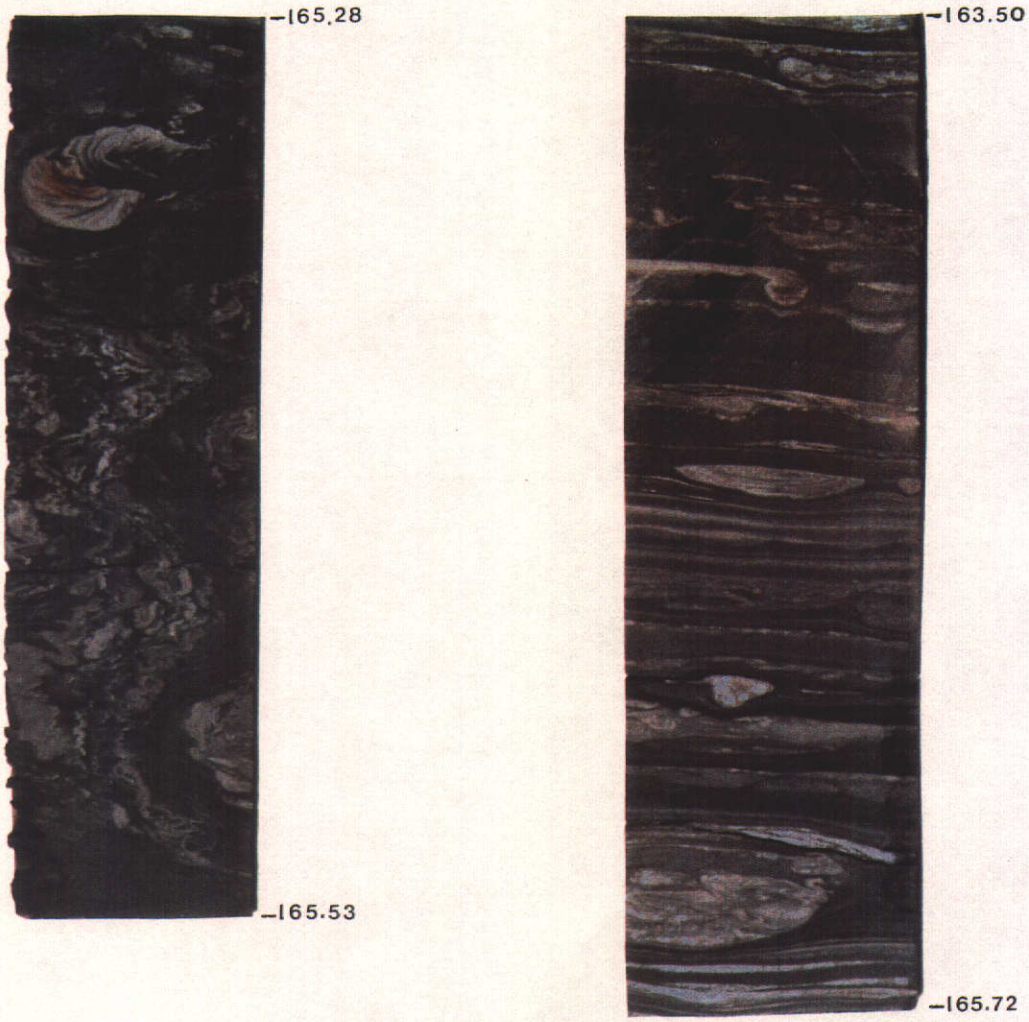

Figure 7.9. Photographs of portions of Section C (150.26 m - 167.50 m in depth).

a. High degree of bioturbation structure (165.28 m - 165.53 m in depth).

b. Flaser bedding and ripple structure, with lenses and pods of fine-grained sandstone (165.50 m - 163.72 m in depth).

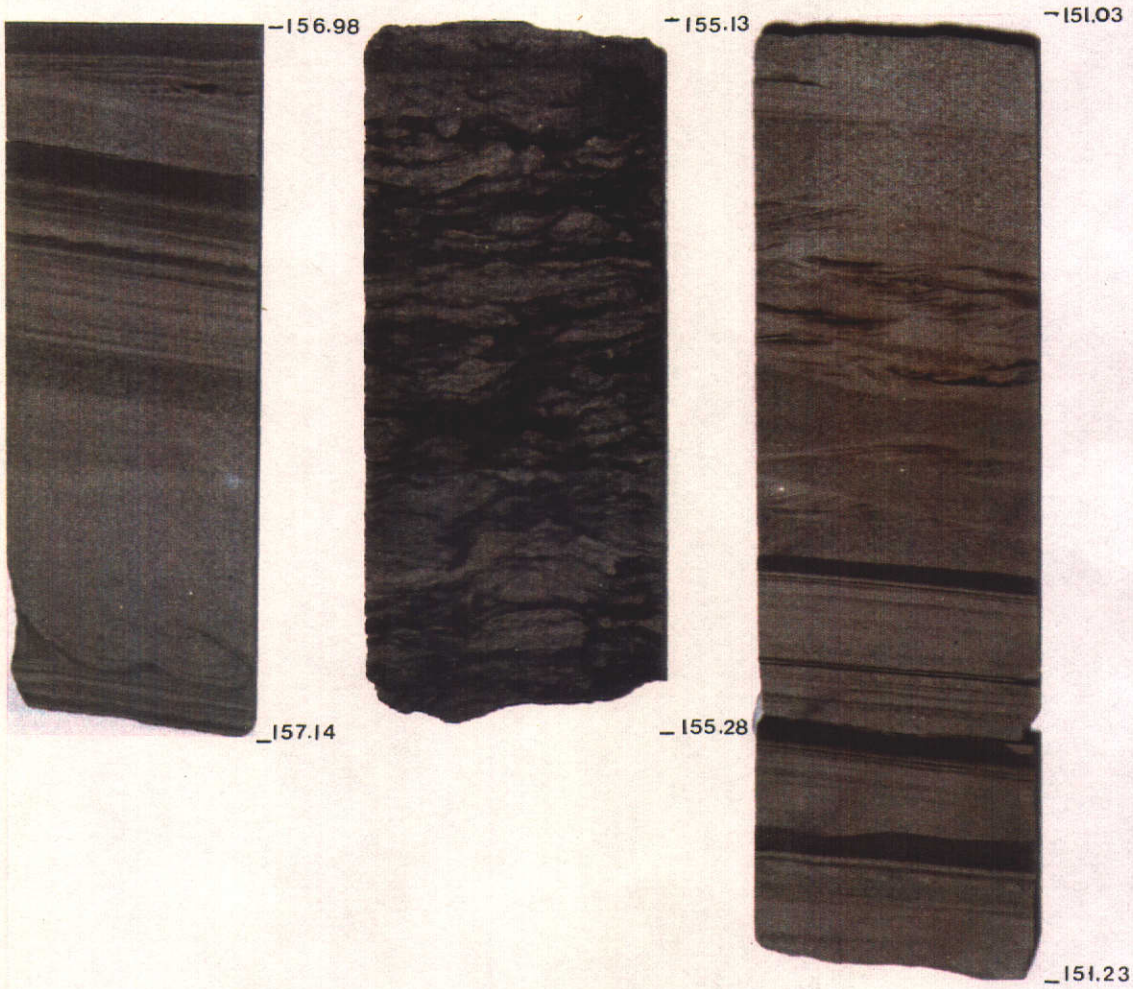

Figure 7.10. Photographs of portion of Section C (150.26 m - 167.50 m in depth).

a. Parallel and cross-bedded sandstone, scour and fill at bottom part (156.98 m -157.14 m in depth).

b. Lenses and pods of light grey sandstone interbedded with siltstone (155.13 m - 155.28 m in depth).

c. Parallel lamination, cross-bedding, and ripple lamination in sandstone (153.03 m - 153.23 m in depth).

in the section are lenses, pods, and streaks of fine-grained sandstone interbedded with finely laminated mudstone/siltstone (Figure 7.8 a), regularly interlaminated siltstone and fine-grained sandstone showing bioturbations (Figure 7.8 b) and parallel lamination. The siltstone predominates in the portions of the core showing lenticular bedding, and in the sandstone layers, pyrite is recognised. In the claystone portion, root remains are found. This section is presumed to be deposited in an intertidal to supra-tidal setting. Section C (150.26 m - 167.50 m deep) is composed of light to dark grey sandstone with interbedded siltstone and shows fining-upward sequence. The sedimentary sequence contains mica, carbonaceous streaks, and resinous material. Discrete burrows present in this section, reflect extensive bioturbation (Figure 7.9 a) which represents a marine influence setting during the coal precursor deposition. The rip-up clasts consisting of siltstone, claystone and coal fragments are present in the section, and indicate that a reworking process of earlier sediments and coal was occurring during the depositional time. This reworked activity was due to migrating interdistributary channel which was active at that time. The presence of flaser bedding (Figure 7.9 b) and lenticular bedding in the section is due to oscillatory currents which are only present in an intertidal setting of a tidal flat condition. The other sedimentary structures recognised are cross-beds, parallel lamination, and scour and fill (Figure 7.10 a), wavy lamination with lenses and pods of light grey sandstone within siltstone (Figure 7.10 b), ripples, cross-beds and parallel laminations (Figure 7.10 c). The sequence of sandstone with siltstone interbeds is capped by very fine-grained sandstone, and siltstone with interbedded claystone, and contains root remains. According to Reineck and Singh (1980), Collinson and Thompson (1982), and Einsele (1992), these bedding types and sedimentary structures are commonly present in areas that are influenced by tidal currents, such as estuaries and tidal flats. The uppermost portion is Section D (146.00 m - 148.52 m in depth) and the section shows fining-upward sequence. It consists of sandstone with claystone interbeds and streaks, and lenses and pods of grey sandstone interbedding with claystone. Bioturbation is also present in the section. On the basis of the sedimentary structures, the section D is

presumed to be deposited in sub-tidal zone. Therefore, the Mintaja Block coal-bearing sediments discussed above on the basis of lithology and sedimentary structures, are interpreted to accumulate in bodies of water that were connected to the marine zone influenced by tidal currents.

In summary, the depositional environment of the Mintaja Block coal and associated sediments based on macerals, microlithotypes, sulphur content, trace elements, and the sedimentary structures is postulated to be upper to lower delta plain influenced by tidal currents, possibly in a regressive phase of a marine transgression.

7.5. Depositional Environment and the Macerals, Gairdner Block

The interpretation of depositional environment of the coal on the basis of maceral analysis, is presented using facies diagrams of Diessel (1982, 1986, and 1992), for the drill holes CPCH 57 and 60.

Figure 7.11 is constructed by plotting maceral composition of coal for the drill holes CPCH 57 and 60 on the D-T-F triangle of Diessel's (1982). The three apices of this triangle is described in chapter 3 and illustrated in Figure 3.15. The diagnostic maceral concentrations of the coal from five sub-seams (G1 to G5) are more than 50 % and the majority of the sub-seams are plotted close together within T/F interval of 3 to 4, whilst sub-seams G2 of CPCH 57 and G3 of CPCH 60 fall in T/F area of 0.5 to 1.5. Evidently, all the sub-seams are located within telmatic wet forest moor setting. However, sub-seam G 2 of CPCH 57 represents a slightly drier condition in this wet forest moor. The value of T/F ratio also reflects that medium to high level of gelification and moisture is present in the coal. A moderate influence of circulating water in coal mire probably occurred, and is indicated by low content of "dispersed" maceral (D) in the coal. (T+F)/D ratio of the coal varies between 1.8 to 4.2, and

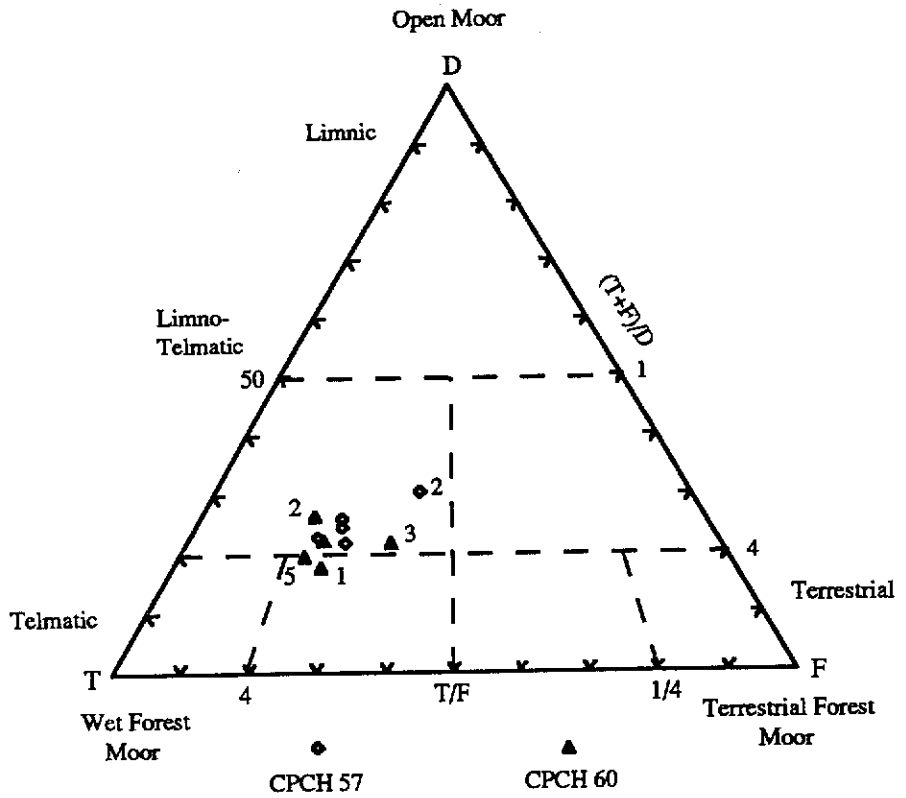

Figure 7.11. Ternary facies diagram of Hill River coal from Gairdner Block.

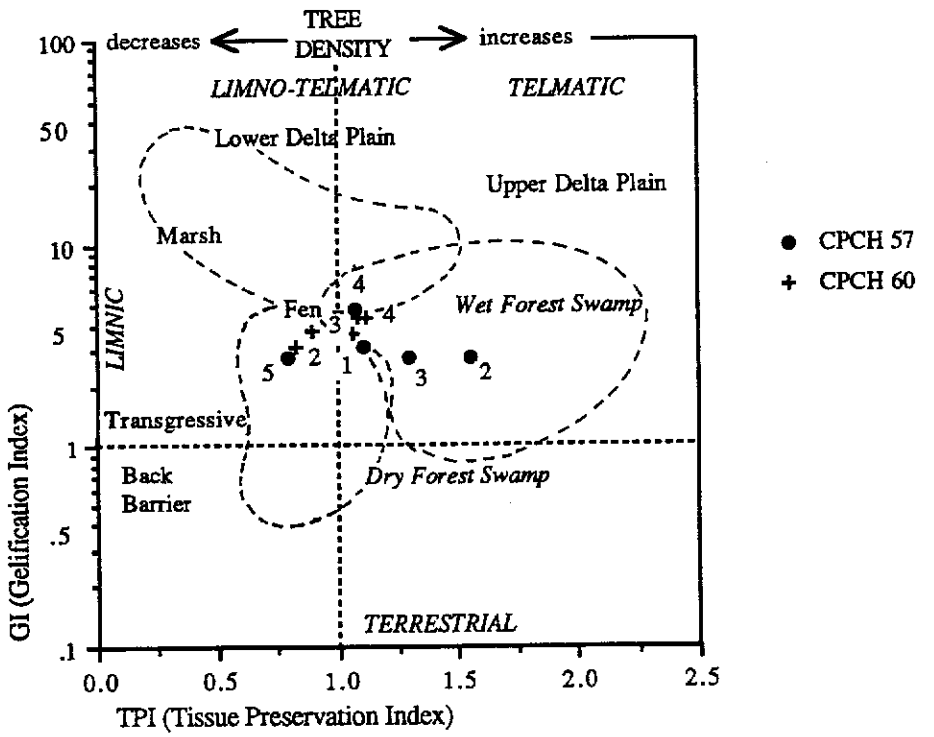

Figure 7.12 . Facies diagram of Hill River coal from Gairdner Block.

indicates a high tree density for the coal constituents.

In addition, by plotting TPI and GI data of the Gairdner Block coal on the TPI-GI facies diagram of Diessel (1986 and 1992) (Figure 7.12), it is obvious that the coal sub-seams are located randomly like the sub-seams of the Mintaja Block. The TPI shows a wide range of value (0.79 - 1.55), whilst the GI occurs in a narrow range (2.73 - 4.77). Frequent clastic input during peat accumulation was probably present, which is indicated by the wide range of the TPI value. The narrow range of GI values indicates that all of the sub-seams accumulated in a similar wet depositional environment. The facies diagram shows that the coal falls within telmatic wet forest swamp to limno-telmatic fen and marsh settings, with an influence of intermittently to permanently flooded condition in coal precursor mire. The figure illustrates that sub-seams G2 and G3 of CPCH 57, and G1, G3 and G4 of CPCH 60 accumulated in upper delta plain; sub-seam G4 of CPCH 57 in transition zone of upper to lower delta plains, whilst sub-seams G1 and G5 of CPCH 57 and G2 of CPCH 60 are located in a transgressive back-barrier zone. In summary, based on the TPI-GI diagram, the Gairdner Block coal was formed mainly in forested peatland with weakly to moderately decomposed woody tissues, in telmatic to limno-telmatic setting, experienced with marine influx.

7.6. Depositional Environment and the Microlithotypes, Gairdner Block

The discussion of depositional environment on the basis of microlithotypes is interpreted using ternary diagrams of Marchioni (1980), Hunt and Hobday (1982), and Smyth (1979), similar to the Mintaja Block.

On the basis of Marchioni's diagram, the depositional environment of the Gairdner Block coal is depicted in Figure 7.13. Microlithotype associations of the coal are

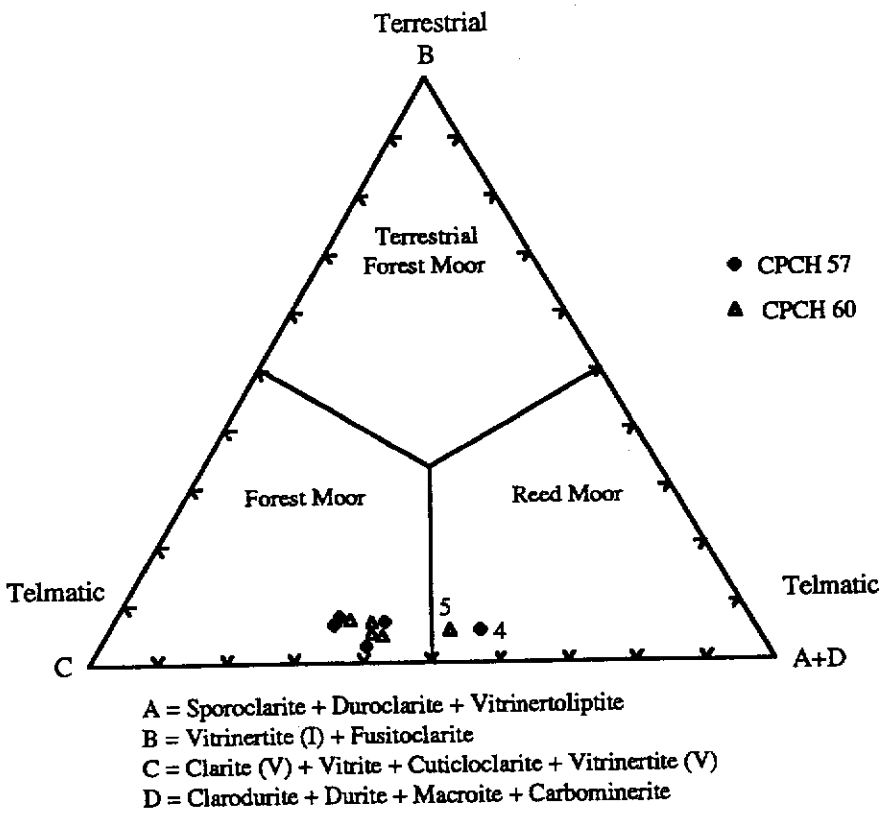

Figure 7.13. Ternary facies diagram of Hill River coal from Gairdner Block.

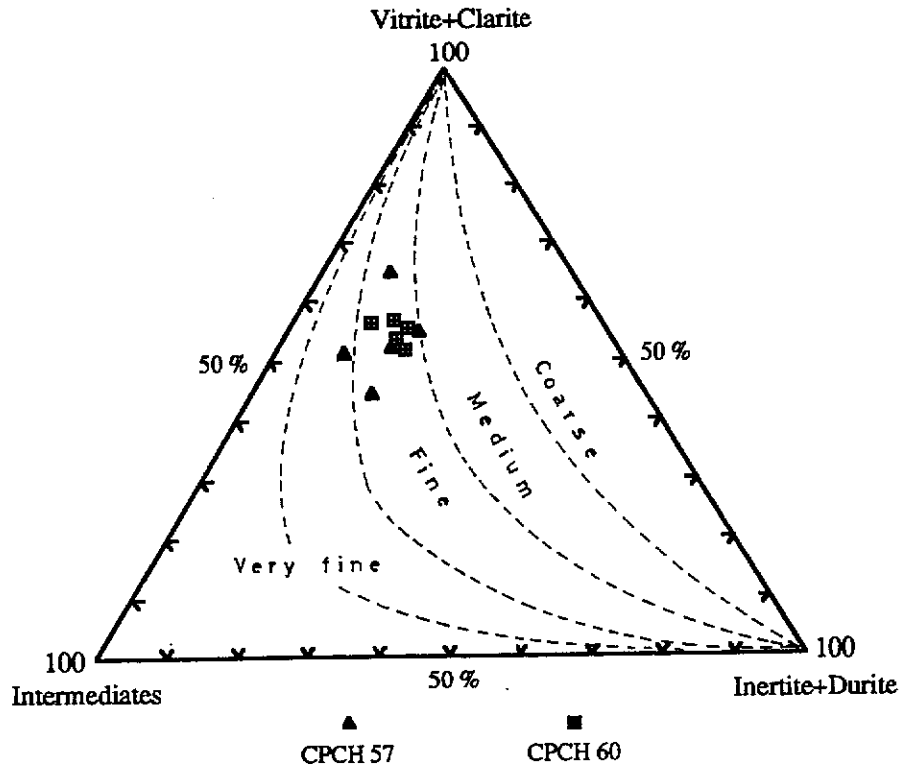

Figure 7.14. Bandwidth curves of microlithotype facies of Hill River coal from Gairdner Block.

plotted in a triangle constituted of B, C, A+D apices. The figure represents that generally the sub-seams accumulated within telmatic forest moor margin and close to reed moor zone, and the sub-seams G4 of CPCH 57 and G5 of CPCH 60 are located in the reed moor setting. This suggests the coal originated from forest peatland with minor shrubs and grass, and the relatively higher content of structured vitrinite and low to moderate semifusinite and fusinite contents in the coal are indicative of alternating high and low ground water table conditions.

Figure 7.14 illustrates microlithotype compositions of the Gairdner Block coal plotted in ternary diagram of Hunt and Hobday (1982). The coal occupies the fine-banded zone in the diagram. However, sub-seam G2 of CPCH 57 is plotted in a very fine-banded zone close to the fine-banded area of the diagram. Therefore, the Gairdner Block coal precursor, presumably accumulated in upper delta plain setting, and the tidal current fluctuation led to oxidation in peat mire.

Figure 7.15 illustrates microlithotype associations of the Gairdner Block coal plotted onto ternary facies diagram of Smyth (1979). In this diagram, the sub-seams fall in areas C and B, which represent brackish and fluvial conditions of the depositional environment, respectively, similar to the Mintaja Block. Thus, the Gairdner Block coal also accumulated in brackish to fluvial environments.

7.7. Depositional Environment, Sulphur Content, and the Trace Elements, Gairdner Block.

Total sulphur content of the Gairdner Block coal varies from 0.85 % to 2.10 % (Table 6.4), and it is categorised as moderate to high. According to Hunt and Hobday (1984), coal that contains total sulphur between 0.55 % to more than 1.00 % represents lower delta plain condition, and high sulphur-peat accumulated in back-

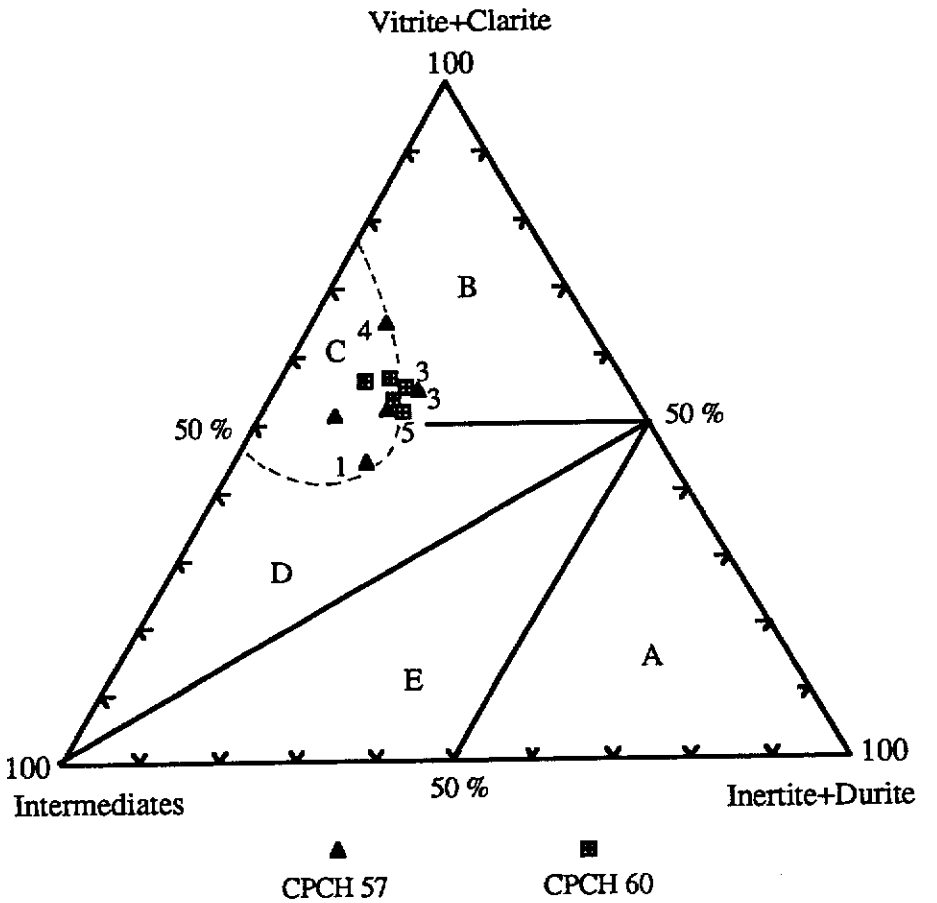

A= lacustrine; B= fluvial; C= brackish; D= upper delta-plain; E= lower delta-plain.

Figure 7.15. Ternary facies diagram of depositional environment of Hill River coal from Gairdner Block.

barrier zone, Horne *et al.* (1978) and Cecil *et al.* (1985). On the basis of these two criteria, the Gairdner Block coal is interpreted to accumulate in lower delta plain and back-barrier depositional environments. The existence of syngenetic pyrite in coal is very important, because it is formed contemporary with coal precursor accumulation, and related to marine influence into peat mire, Casagrande *et al.* (1977), Mackowsky (1982), Teichmuller and Teichmuller (1982), and Styan Bustin (1983 a and b). High pyrite and sulphur peat was formed in marine to brackish water area, Cohen, Spackman and Dolsen (1984). Therefore, the Gairdner Block coal containing significant syngenetic pyrite and high total sulphur content was presumably deposited in brackish depositional environments with some marine influence.

The boron content ranges from 37.0 ppm to 53.0 ppm in the Gairdner Block coal. According to Swaine (1971, 1982, and 1990) and Lyons *et al.* (1989), this range of boron in coal, tends to indicate a brackish water environment. Thus, the Gairdner Block coal is interpreted to have accumulated in brackish environment.

On the basis of the above interpretations, it can be concluded that the depositional environment of the Gairdner Block coal is similar to the Mintaja Block which varies from lower delta plain to upper delta plain influenced by brackish and fluvial conditions.

CHAPTER 8. CONCLUSIONS

The present study has covered aspects of the petrology of the Jurassic coal of the Hill River Area, Perth Basin, Western Australia. The conclusions drawn from this study are :

1. The coal from Mintaja and Gairdner Blocks is one of the potentially commercial coal resources in Western Australia, situated in the Hill River Shelf of the northern Perth Basin. The seam G with its six sub-seams G1 to G6 has been petrographically studied in detail for the first time in Western Australia.

The coal-bearing sediments named Cattamarra Coal Measures are Early to Middle Jurassic in age. The Cattamarra Coal Measures are also referred to as the Cattamarra Group, comprising Bitter Pool Claystone and the overlying Hill River Coal Measures, Kristensen (1989). The Hill River Coal Measures consist of cyclic sequences of sandstone fining upwards into siltstone, claystone and coal, and show tidal deposit characteristics. The cumulative thickness of the coal for the sub-seams G 1 to G 6 is 8.50 m.

2. Macroscopically the coal is finely banded of intermediate lustre. Based on Stopes' terminology, the major proportion of the coal is clarain and durain, with minor amounts of vitrain and fusain. According to to Diessel's terminology, the coal is mostly dull banded, and this lithotype represents 32.19 % of the sub-seam. The second dominant lithotype is the dull type, with a content of 25.51 %, followed by 16.38 % of banded lithotype for all the sub-seams. The bright banded and banded lithotypes are of 12.54 % and 8.76 %, respectively in the coal. The fusainous type is present to a lesser extent in the sub-seams, with a value of 5.11 % . The type variation in the coal represents a frequency of changes in the water table during the coal-precursor formation.

3. Vitrinite and inertinite are the dominant maceral groups present in the coal, whilst exinite and mineral matter form minor components. Thus, the Hill River coal can be

regarded as a vitrinite-rich coal. The vitrinite content varies from 47.2 % to 73.0 %, and it consists mainly of telocollinite and desmocollinite, followed by corpocollinite, telinite, and to a lesser extent vitrodetrinite. The lack of telinite indicates a slow burial and high pH of mire water. The inertinite in the coal consists of semifusinite, fusinite, inertodetrinite, macrinite, and very low sclerotinite and micrinite contents, and the inertinite content ranges between 10.4 % to 24.8 %. These low values reflect that the coal has undergone a low degree of oxidation. The exinite content varies between 7.2 % and 20.8 %, and it is represented by sporinite, cutinite, alginite, resinite and liptodetrinite. The association of cutinite with corpocollinite suggests a leaf source for the peat. The abundance of resinite-rich leaf remains in the coal may indicate a dense shrubby of vegetation. The maximum reflectance of vitrinite varies from 0.47 % to 0.53 %, which represents the coalification stage of sub-bituminous level based on the Australian rank values, and corresponds to the sub-bituminous A and B of the ASTM classification. On the basis of the Pareek classification (1987), the coal is categorised as a metalignitous type.

4. In terms of microlithotypes, vitrite plus clarite content dominates the coal, which is due to the increased level of standing water and water table, with concomitant change in floral type and preservation of organic accumulation from oxidation processes in the basin. The vitrite plus clarite concentration, ranging between 42.5 % and 64.8 % in the coal, followed by the intermediates having a range of 25.4 % to 50.7 % represents an occurrence of forest in the mire. The inertite plus durite content varies between 4.8 % and 18.5 %, whilst carbominerite content varies from 5.5 % to 33.6 %.

5. The mineral matter in the coal is dominated by clays and pyrite, followed by quartz and carbonates. It is mainly associated with vitrinite B and to a lesser extent with inertinite, exinite and vitrinite A. The clay minerals range from 1 % to 27.0 %, and are most dominant in the coal. The second dominant mineral in the coal is pyrite, which varies in content from 1.0 % to 7.2 %. The carbonates and quartz in the coal have a range between

traces to 3.6 % and traces to 0.6 %, respectively. Distribution in size fractions shows that the mineral matter contents are lower in coarser size fractions in comparison to the finer ones. On the basis of the mineral matter content, the Hill River coal is classified as a "normal - grade" coal.

6. The ash contents range between 12.0 % to 51.0 % inclusive of total sulphur content which varies from 0.85 % to 3.55 % and is classified as medium to high. The volatile matter in the coal shows a range from 17.2 % to 33.9 %, fixed carbon varies between 26.6 % and 47.2 %, specific energy ranges between 11.40 MJ/kg to 26.23 MJ/kg, and moisture content varies from 5.50 % to 19.30 % in the coal. The moisture, volatile matter, and fixed carbon contents are dependent of specific energy in the coal. On the basis of proximate analysis, the coal is classified as high-volatile bituminous A to sub-bituminous A , sub-bituminous A to B, and sub-bituminous A to lignite. On the basis of ultimate analysis, the Hill River coal is classified as per-hydrous meta-lignitous to ortho-lignitous type. The concentration of trace elements in the coal varies greatly from 0.30 ppm to 3140 ppm. The boron content in the coal is used in ascertaining the presence of marine influence during peat deposition, and has a range between 37.0 ppm and 409 ppm. The trace elements B, Cr, Mn, Cu, Sr, Zr, Mo, Cd, and Th predominantly occur as organic affinities, while the Be, V, Co, Zn, Ga, Y, Pb, and U are present as inorganic affinities. The Ni and As tend to be present as both organic and inorganic associations.

7. On the basis of maceral content, the coal was deposited in the wet forest moor, under condition of slow to moderate subsidence, in mainly telmatic to limno-telmatic fen environments with weakly to relatively strong input of decomposed woody tissues and relatively low detrital input, representing an intermittently to permanently flooded area of coal deposition. Furthermore, it was experienced with marine influx. Microlithotype composition of the coal indicates that generally the Hill River coal accumulated within telmatic forest moor margin and close to reed moor zone, presumably in upper delta plain setting with minor shrubs and grass. The microlithotype compositions also reflect a

transition area of the brackish zone to fluvial setting. Based on the sulphur content, pyrite content and boron content, the coal is postulated to have accumulated in brackish to marine-influenced environments with tidal influx. The tidal influence during the deposition of coal-bearing sediments is also supported by sedimentary structures identified in them. The presence of acanthomorphs and sphaeromorphs acritarchs in the coal measures supports the interpretation that the coal accumulated in a brackish conditions. In summary, the depositional environment for the Hill River coal and the coal measures is fluvial to brackish in an upper to lower delta plain influenced by tidal currents during a regressive phase of a marine transgression.

Finally, in future, the experience gained by the author during this study will be useful and applicable to the petrological characterisation of Indonesian coal in its utilisation at home and for export .

Akande, S.O., Hoffknecht, A. and Erdtmann, B.D. (1992). Rank and petrographic composition of selected Upper Cretaceous and Tertiary coals of Southern Nigeria. *International Journal of Coal Geology,* 20 pp209 - 224.

Alpern, B. (1954). Sur quelques proprietes chimiques et cokefiantes des constituents petrographiques elementaires du charbon. *Congress Chemica Indica* , 2 (7) pp9 - 13.

Alpern, B., Durand, B., Espitalie, J. and Tissot, B. (1972). Localisation, characterisation et classification petrographiques des substances organiques sedimentaires fossiles. *Advances in Organic Geochemistry*, Pergamon Press, Oxford-Braunschweig : pp1 - 28.

Alpern, B. (1979). Essai de classification des combustibles fossils solides. *Publication Technics,* 3 pp195 - 210.

Alpern, B. (1981). Draft proposal for Universal Classification of solid fossil fuels. *International Committee of Coal Petrology.*

Alpern, B, Nahuys, J., Lemos da Sousa, M.J., Pinheiro, H.J., Marques, M.M., Flores, D., Moreira, V. and Jorge, A. (1988). The application of the Alpern - ICCP , scientific classification of solid fossil fuels to qualify Gondwana coals from different basins. *Abstracts, 7th Gondwana Symposium*, Sao Paulo, Brazil, p 127.

Alpern, B., Lemos da Sousa, M.J. and Flores, D. (1989). A progress report on the Alpern coal classification, in Lyons, P.C. and Alpern, B. (Editors) *Coal:*

Classification, Coalification, Mineralogy, Trace-element Chemistry, and Oil and Gas Potential. International Journal of Coal Geology, 13 pp1 - 9.

Altschuler, Z.S., Schnepfe, K.K., Silber, C.C. and Simon, F.O. (1983). Sulfur diagenesis in Everglades peat and origin of pyrite in coal. *Science*, 221 pp221-227.

Ammosov, I.I. (1956). New methods of coal petrography. *Studies of the Laboratory of Coal Geology*, 6, Moskwa (Russian).

Anderson, R.A. (1981). Nutritional role of chromium. *Science Total Environments*, 17 pp 13-39.

Anderson, T.W. and Sclove, S.L. (1984). *Introductory Statistical Analysis.* Houghton Mifflin Company, Boston.

Andrews, E.C. (1938). The structural history of Australia during the Palaeozoic. *Royal Society of New South Wales, Proceedings*, 71 pp 118-187.

Asuen, G.O. (1987). Assessment of major and minor elements in the Northumberland coalfield, England. *International Journal of Coal Geology*, 9 pp 171-186.

Balme, B.E. (1964). The palynological record of Australian pre-Tertiary floras, in Cranwell, L. (Editor) *Ancient Pacific floras, Honolulu University Hawaii Press*, pp. 49-80.

Balme, B.E. (1969). The Triassic System in Western Australia. *Australia Petroleum Exploration Association Journal*, 9 pp 67-78.

Bell, J.A., Diessel, C.F.K., and Ng., N. (1970). Various interpretations of coal petrographic nomenclature and their effects on maceral analysis. *Proceeding of Australasian Institute of Mining and Metallurgy,* 234 pp27-36.

Bennet, A.J.R. and Taylor, G.H. (1970). A petrographic basis for classifying Australian coals. *Proceeding of Australasian Institute of Mining and Metallurgy,* 233 pp1-5.

Berner, R.A. (1971). *Principal of chemical sedimentology.* Mc Graw-Hill, New York.

Birk, D. 1990. Quantitative coal mineralogy of the Sydney Coalfield, Nova Scotia, Canada, by scanning electron microscopy, computerised image analysis, and energy-dispersive X-ray spectrometry. *Canadian Journal of Earth Sciences,* 27 pp163-179.

Bohor, B.F. and Gluskoter, H.J. (1973). Boron in illite as an indicator of paleosalinity of Illinois coals. *Journal of Sedimentary Petrology,* 43 (40) pp945-956.

Botz, R.W., Hunt, J.W. and Smyth, J.W. (1986). Isotope geochemistry of minerals in Australian bituminous coal. *Journal of Sedimentary Petrology,* 56 pp99-111.

Bouska, V. (1981). *Geochemistry of coal.* Amsterdam, Elsevier Science Publication Company.

Breger, I.A., Deul, M. and Rubinstein, S. (1955). Geochemistry and mineralogy of a uraniferous lignite. *Economic Geology,* 50 pp206-226.

Brodily, D.M., Wann, J.P., Chen, W., Zhu, X., Hu., W. and Wadsworth, M.E. (1991).Characterisation of mineral and coal pyrite. *International Conference on Coal Science Proceedings*, 973 pp973-976.

Brown, H.R., Cook. A.C and Taylor, G.H. (1964). Variations in the properties of vitrinite in isometamorphic coal. *Fuel*, 43 pp111-124.

Burbridge, A.A., Hopper, S.D. and van Leeuwen, S. (eds.) (1990).Nature conservation and recreation values of the Lesueur area. A Report to the Environmental Protection Authority from the Department of Conservation and Land Management. *Environmental Protection Authority Perth, Western Australia, Bulletin* 424.

Bustin, R.M., Hills, L.V., and Gunther, P.R. (1977). Implications of coalification levels, Eureka Sound Formation, northeastern Arctic Canada. *Canadian Journal of Earth Sciences*, 14 pp1588-1597.

Bustin, R.M., Cameron, A.R., Grieve, D.A. and Kalkreuth, W.D. (1983). Coal Petrology: its principles, methods and applications. *Geological Association of Canada, Short Course Notes*, 3. 2nd ed.

Cameron, A.R. (1978). Megascopic description of coal with particular reference to seams in southern Illinois, in Dutcher, R.R. (Editor) Field description of coal. *ASTM Special Technical Publication*, 661 pp33- 40.

Capes, C.E., Mc Ilhenney, A.E., Russel, D.S. and Sirianni, A.F. (1974). Rejection of trace metals from coal during beneficiation by agglomeration. *Environmental Science Technology*, 8 pp35-38.

Casagrande, D.J. and Erchul, L.D. (1976). Metals in Okefenokee peat-forming environments: Relation to constituents found in coal. *Geochimica et Cosmochimica Acta,* 40 pp387-393.

Casagrande, D.J., Gronli, K. and Sutton, N. (1980). The distribution of sulphur and organic matter in various fractions of peat : origins of sulphur in coal. *Geochimica et Cosmochimica Acta,* 44 pp25-32.

Casagrande, D.J., Idowu, G., Friedman, A., Ricket, P., Siefert, K. and Schlenz, D. (1979). H2S incorporation in coal precursors: origins of organic sulphur in coal. *Nature,* 82 pp599-560.

Casagrande, D.J., Siefert, K., Berschinki, C. and Sutton, N. (1977), Sulfur in peat forming systems of the Okefenokee swamp and Florida Everglades : origin of sulfur in coal. *Geochimica et Cosmochimica Acta,* 41 pp161-167.

Casagrande, D.J. (1987). Sulphur in peat and coal, in Scott, A.C. (ed.) *Coal and Coal-Bearing Strata, : Recent Advances,* pp87-105. United Kingdom Geological Society Special Publication, 32. Blackwell, Oxford.

Castano, J.R. and Sparks, D.M. (1974). Interpretation of vitrinite reflectance measurements in sedimentary rocks and determination of burial history using vitrinite reflectance and authigenic minerals. *Geological Society of America, Special Paper,* 153 pp31-52.

Cavallaro, J.A., Deurbrouck, A.W., Gibbon, G.A., Hattman, E.A. and Schultz, H. (1978). A washability and analytical evaluation of potential pollution from trace elements in coal, in Karr, C. (ed.) *Analytical Methods for Coal and Coal Products.* New York, Academic Press, , I pp435-463.

Cecil, C.B., Stanton, R.W., Neuzil, S.G., Dulong, F.T., Rupert, L.F. and Pierce, B.S. (1985). Paleoclimate controls on late Paleozoic sedimentation and peat formation in the central Appalachian Basin (U.S.A.), in Phillips, T.L. and Cecil, C.B. (Editors) *Paleoclimatic Controls on Coal resources of the Pennsylvanian System of north America. International Journal of Coal Geology,* 5 pp195-230.

Chaffee, A.L., Johns, R.B., Baerken, M.J., Leeuw, J.W., Schenck, P.A. and Boon, J.J. (1984). Chemical effects in gelification processes and lithotype formation in Victorian brown coals. *Advanced Organic Geochemistry*, 6 pp409-416.

Chaffee, A.L. and Johns, R.B. (1985). Aliphatic components of Vistorian brown coal lithotypes. *Organic Geochemistry,* 8 pp349-365.

Chandra, D., Samsuddin, A.K. and Bannerjee, K.C. (1981). An approach to the selection of coals for the production of fertilixers by powdered coal gasification process.*Quarterly Journal of Geology and Mineralogy, Metalliferous Society of India,* 20 pp40-43.

Chao, E.C.T., Minkin, J.A. and Thompson, C.L. (1982). Recommended procedures and techniques for the petrographic description of bituminous coals. *International Journal of Coal Geology,* 2 pp151-180.

Chou, C.L. (1984). Relationship between geochemistry of coal and the nature of strata overlying the Herrin coal in the Illinois Basin, USA. *Geological Society of China, Memoir 6,* pp269-280.

Chou, C.L. (1990). Geochemistry of sulfur in coal, in Orr, W.L. and White, C.M. (editors) *Geochemistry of sulfur in fossil fuels, American Chemical Society Symposium Series,* 429 pp30-52.

Cockbain, A.E. (1990). Perth Basin, in Geology and Mineral Resources of Western Australia : *Western Australia Geological Survey, Memoir 3*, pp495-524.

Cohen, A.D. and Spackman, W. (1972). Methods of peat petrology and their application to reconstruction of paleo-environments. *Geological Society of America, Bulletin,* 83 pp129-142.

Cohen, A.D. (1973). Petrology of some Holocene peat sediments from the Okefenokee swamp-marsh complex of southern Georgia. *Geological Society of America, Bulletin,* 84 pp3867-3878.

Cohen, A.D., Spackman, W. and Dolsen, P. (1984). Occurrence and distribution of sulfur in peat-forming environments of southern Florida. *International Journal of Coal Geology,* 4 pp73-96.

Cook, A.C. (ed.) (1975). Australian Black Coal - its occurrence, mining and preparation, and use. *Australasian Institute of Mining and Metallurgy,* Illawarra Branch, pp72-83.

Cook, A.C., Hutton, A.C, and Sherwood, N.R. (1981). Classification of oil shales. *Bulletin des centres de Reserches Exploration - Production Elf - Aquitaine,* 5 pp353-381.

Cook, A.C. and Kantsler, A.J. (1982). *The origin and petrology of organic matter in coals, oil shales and petroleum source-rocks.* The University of Wollongong,

Wollongong, New South Wales, 35 pp.

Cook, A.C. and Sherwood, N.R. (1986). *Proposal for the definition of the terms Telalginite and Lamalginite for submission to the ICCP meeting*, 16 pp.

Corvinus, D.A. and Cohen, A.D. (1984). Micropetrographic characteristics of peats from the Okefenokee Swamp: the origin of macerals, in Cohen, A.D., Casagrande, D.J., Andrejko, M.J. and Best, G.R. (editors) *The Okefenokee Swamp: its natural history, geology and geochemistry.* Wetland Surveys, Los Alamos, New Mexico, pp651-667.

Couch, E.L. (1971). Calculation of paleosalinities from boron and clay mineral data. *American Association of Petroleum Geologists Bulletin*, 55 (10) pp1929-1837.

CRAE (1989). Ultimate and proximate analyses of Hill River Coal. *Unpublished Report.*

Creelman, R.A., Greenwood-Smith, R. and Paulson, C.J. (1986). QEM*SEM : A new tool for the investigation and characterisation of the mineral matter in coal and the products of coal combustion. *Australian Institute of Energy, Australian Coal Sciences Conference 2, Proceedings,* 1 pp215-221.

Crossley, H.E. (1946). The inorganic constituents of coal. *Institute of Fuel, London, Bulletin,* 67 pp57-60.

Davies, T.D. and Raymond, R.Jr. (1983). Sulfur as a reflection of depositional environments in peats and coals, in Raymond, R.Jr. and Andrejko, M.J. (editors) *Proceedings of Workshop on Mineral matter in Peat : Its occurrence, Form and*

Distribution, Los Alamos National Laboratory Report, LA - 9977 - OBES, pp123-139.

Davis, J.C. (1986). *Statistics and Data Analysis in Geology.* Kansas Geological Survey. John Willey & Sons, Inc., New York.

Davy, R. and Wilson, A.C. (1984). An orientation study of the trace and other element composition of some Collie coals. Western Australia Department of Mines, *Geological Survey Records*, 3 p48.

Demchuk, T.D. (1992). Epigenetic pyrite in a low-sulphur, sub-bituminous coal from the central Alberta Plain. *International Journal of Coal Geology,* 21 pp187-196.

Diessel. C.F.K. (1965). Correlation of macro- and micropetrography of some New South Wales coals, in Woodcock, J.T., Madigan, R.T. and Thomas, R.G. (editors), *Proceedings - General, Volume 6, 8th Commonwealth Mineral and Metallurgy Congress,* Melbourne, pp669-677.

Diessel, C.F.K. (1982). An appraisal of coal facies based on maceral characteristics. *Australian Coal Geology,* 4(2) pp474-484.

Diessel, C.F.K. (1986). On the correlation between coal facies and depositional environments. *Proceeding 20th Symposium of Department Geology, University of New Castle, New South Wales,* pp19-22.

Diessel, C.F.K. (1992). *Coal-bearing Depositional System.* Springer-Verlag, berlin, Heidelberg.

Dill, H., Teschner, M. and Wehner, H. (1991). Geochemistry and lithofacies of Permo-Carboniferous carbonaceous rocks from the southwestern edge of the Bohemian Massif (Germany). A contribution to facies analysis of continental anoxic environments. *International Journal of Coal Geology,* 18 pp251-291.

Einsele, G. (1992). *Sedimentary Basins : Evolution, Facies, and Sedimentary Budget.* Springer-Verlag, Berlin, Heidelberg.

Erdman, J.A., Ebens, R.J. and Case. A.A. (1978). Molybdenosis : a potential problem in ruminant grazing on coal mine spoils. *Journal of Range Management,* 31 pp34-36.

Esterle, J.S. and Ferm, J.C. (1986). Relationship between petrographic and chemical properties of coal seam geometry, Hance seam, Breathitt Formation, southeastern Kentucky. *International Journal of Coal Geology,* 6 pp99-124.

Exon, N.F. (1980). The stratigraphy of the Surat basin, with special reference to coal deposits. *Coal Geology,* 1(1) pp57-69.

Falcon, R.M.S. and Snyman, C.P. (eds.) (1986). An introduction to coal petrography: Atlas of petrographic constituents in the bituminous coals of southern Africa. *The Geological Society of South Africa.*

Fielding, C.R. (1985), Coal depositional models and the distinction between alluvial and delta plain environments. *Sedimentary Geology,* 42 pp41-48.

Fielding, C.R. (1987). Coal depositional models for deltaic and alluvial plain sequences. *Geology,* 15 pp661-664.

Fielding, C.R. (1993). The Middle Jurassic Walloon Coal Measures in the type area, the Rosewood-Walloon Coalfield, Southeastern Queensland. *Australian Coal Geology,* 9 pp4-16.

Finkelman, R.B. (1978). Determination of trace element sites in the Wynesburg coal by SEM analysis of accessory minerals. *Scanning Electron Microscopy,* 1 pp143-148.

Finkelman, R.B. and Stanton, R.W. (1978). Identification and significance of accessory minerals from a bituminous coal. *Fuel,* 57 pp763-768.

Finkelman, R.B., Stanton, R.W., Cecil, C.B. and Minkin, J.A. (1979). Modes of occurrence of selected trace elements in several Appalachian coals. *American Chemical Society Division, Fuel Chemistry Preparation,* 24 (1) pp236-241.

Finkelman, R.B. (1980). Modes of occurence of trace elements in coal. *US Geological Survey Open-File Report,* No. OFR 81-99, 301 pp.

Finkl, C.W. (1979). Stripped (etched) landsurfaces in southern Western Australia. *Australian Geographical Studies,* 17 pp33-52.

Flood, P.G. (1985). Facies studies of the Callide seam, Central Queensland: Implications for mine design. *Australian Coal Geology,* 5 pp13-24.

Francis, W. (1961). *Coal, its formation and composition.*; Edward Arnold, Ltd., London, 806 pp.

Franki, K.A. and Hower, J.C. (1987). Variations in pyrite size, form and micro-lithotype associations in the Springfield (No. 9) and Herrin (No. 11) coals, western Kentucky. *International Journal of Coal Geology,* 7 pp349-364.

Gehr, C.W., Shriver, D.S., Herbes, S.E,, Salmon, E.J. and Perry, H. (1981). Environmental, health and safety implications of increased coal utilisation, in Elliott, M.A. (ed.) *Chemistry of Coal Utilisation: Second Supplementary Volume.* New York, Willey, pp2159-2223.

Ghosh, R. (1987). A study of trace elements in lithotypes of some selected Indian coals. *International Journal of Coal Geology,* 8(3) pp269-278.

Given, P.H. and Miller, R.N. (1985). Distribution of forms of sulfur in peats from saline environments in the Florida Everglades. *International Journal of Coal Geology,* 5 pp397-409.

Glikson, M. and Fielding, C. (1991). The Late Triassic Callide Coal Measures, Queensland, Australia: Coal petrology and depositional environment. *International Journal of Coal Geology,* 17 pp313-332.

Gluskoter, H.J. (1975). Mineral matter and trace elements in coal, in Babu, S.P. (ed.) *Trace Elements in Fuel. American Chemical Society Special Publication,* 14 pp1-22.

Gluskoter, H.J., Ruch, R.R., Miller, W.G., Cahill, R.A., Dreher, G.B. and Kuhn, J.K. (1977). Trace elements in coal: occurrence and distribution. *Illinois State Geological Survey Circular,* 499 pp1-54.

Goldschmidt, V.M (1935). Rare elements in coal ashes. *Industrial and Engineering Chemistry,* 27 pp1100-1102.

Goldschmidt, V.M (1937). The principals of distribution of chemical elements in minerals and rocks. *Journal of the Chemical Society,* 52 pp655-673.

Goodarzi, F., Foscolos, A.E. and Cameron, A.R. (1985). Mineral matter and elemental concentrations in selected western Canadian coals. *Fuels,* 64 pp1599-1605.

Gould, K.W. and Smith, J.W. (1979). The genesis and isotopic composition of carbonate associated with some Permian Australian coals. *Chemical Geology,* 24 pp137-150.

Gould, K.W. and Shibaoka, M. (1980). Some aspects of the formation and petrographic features of coal members in Australia, with special reference to the Tasman Orogenic Zone. *Coal Geology,* 2 (1/2) pp1-29.

Graese, A.M., Baynard, D.N., Hower, J.C., Fern, J.C. and Liu, Y. (1992). Stratigraphic and regional variation of the petrographic and chemical properties of the Tradewater Formation coals. *International Journal of Coal Geology,* 21 pp237-259.

Hacquebard, P.A. and Donaldson, J.R. (1969). Carboniferous coal deposition associated with floodplain and limnic environments in Nova Scotia, in Dapples, E.C. and Hopkins, M.E. Editors) *Environments of Coal Deposition. Geological Society of America, Special Paper,* 114 pp143-191.

Hak, J. and Babcan, J. (1967). Geochemistry of germanium and beryllium in coal of the Sokolov Basin. *Geochem Czechoslovakia Trans 1st Conference on Geochemistry,* Ostrava, C.A., 70 pp163-170.

Hamilton, L.H. and Salehy, M.R. (1986). Use of SEM for coal petrology. *Australian Coal Geology,* 6 pp77-85.

Harder, H. (1961). Incorporation of boron into detrital clay minerals. *Geochimica et Cosmochimica Acta*, 21 pp284-294.

Harris, L.A., Rose, T., Derose, L. and Greene, J. (1977). Quantitative analysis of pyrite in coal by optical image techniques. *Economic Geology*, 72 pp695-697.

Harvey, R.D. and Dillon, J.W. (1985). Maceral distributions in Illinois coals and their palaeoenvironmental implications. *International Journal of Coal Geology*, 5 pp141-165.

Hatch, J.R., Gluskoter, H.J. and Lindahl, P.C. (1976). Sphalerite in coals from the Illinois Basin. *Economic Geology*, 71 pp613-624.

Horne, J.C., Ferm, J.C., Carucci, F.T. and Baganz, B.P. (1978). Depositional models in coal exploration and mine planning in Appalachian region. *American Association of Petroleum Geologists Bulletin*, 62 pp2379-2411.

Hower, J.C. and Davis, A. (1981). Application of vitrinite reflectance anisotropy in the evaluation of coal metamorphism. *Bulletin of Geological Sosiety of America, Part 1*, 92 pp350-366.

Hunt, J.W. (1982). Relationship between microlithotype and maceral composition of coals and geological setting of coal measures in the Permian Basin of eastern Australia. *Australian Coal Geology*, 4 pp 484-502.

Hunt, J.W., Brakel, A.T. and Smyth, M. (1985). Origin and distribution of the Bayswater seam and correlatives in the Permian Sydney and Gunnedah Basins, Australia. *Australian Journal of Coal Geology*, 6 pp59-75.

Hunt, J.W. and Hobday, D.K. (1984). Petrographic composition and sulphur content of coals associated with alluvial fans in the Permian Sydney and Gunnedah Basins, Eastern Australia, in Rahmani, R.A and Flores, R.M. (Editors) Sedimentology of coal and coal-bearing sequence. *International Association of Sedimentologists, Special Publication,* 7 pp43-60.

Hunt, J.W., Brakel, A.T. and Smyth, M. (1985). Origin and distribution of the Bayswater Seam and correlatives in the Permian Sydney and Gunnedah Basins, Australia. *Australian Journal of Coal Geology*, 6 pp.59-75.

Hunt, J.W. and Smyth, M. (1989). Origin of inertinite-rich Gondwana coals in Australian cratonic basins. *International Journal of Coal Geology,* 1 pp23-46.

Hutton, A.C. and Cook, A.C. (1980). Influence of alginite in the reflectance of vitrinite from Joadja, New South Wales and some other coals and oil shales containing alginite. *Fuel,* 59 pp711-716.

Hutton, A.C., Kantsler, A.J., Cook, A.J. and McKirdy, D.M. (1980). Organic matter in oil shales. *APEA Journal,* 20 pp44-67.

Hutton, A.C.(1987). Petrographic classification of oil shales. *International Journal of Coal Geology,* 8 pp203-231.

ICCP, International Committee for Coal Petrology (1963). *Handbook,* 2nd Edition, Centre National de la Recherche Scientifique, Paris, France.

ICCP, International Committee for Coal Petrology (1971). *International Handbook of Coal Petrology, 1st supplement to 2nd edition.* Centre National de la Recherche Scientifique, Paris, France.

ICCP, International Committee for Coal Petrology (1975). Analysis subcommission, fluorescence microscopy and fluorescence photometry and subcommission nomenclature, in *International Handbook of Coal Petrography, 2nd supplement to 2nd edition.* Centre National de la Recherche Scientifique, Paris, France.

Islam, A. and Sappal, K.K. (1991). Palynological analyses of part of the Cattamarra Coal Measures, Borehole No. CPCH 1, Hill River Area, Perth Basin, Western Australia. *Curtin University of Technology, School of Applied Geology, SAG Report*, No.1/1991, 10 pp.

Johnstone, M.N. (1964). A preliminary investigation of the Jurassic coals of the Perth Basin. *Proceeding of Australasian Institute of Mining and Metallurgy,* 211 pp61-73.

Jones, D.K. and Pearson, G.R. (1972). The tectonic elements of the Perth Basin. *APEA Journal,* 12 pp17-22.

Jones, J.M., Murchison, D.G. and Saleh, S.A. (1972). Variation of vitrinite reflectivity in relation to lithology, in Gaertner, H.W. and Wehner, H. (editors) *Advances in Organic Geochemistry,* Pergamon, New York, pp602-612.

Jones, J.M., Davis, A., Cook, A.C., Murchison, D.G. and Scott, E. (1984). Provincialism and correlations between some properties of vitrinites. *International Journal of Coal Geology,* 3 pp315-331.

Kachigan, S.K. (1986). *Statistical Analysis: an interdisciplinary introduction to univariate and multivariate methods.* Radius Press, New York.

Kalkreuth, W.D. and Leckie, D.A. (1989). Sedimentological and pterological characteristics of Cretaceous strandplain coals - a model for coal accumulation from the North American Western Interior Seaway, in Lyons, P.C. and Alpern, B. (editors), Peat and Coal : Origin, Facies and Depositional Models. *International Journal of Coal Geology,* 12 pp382-424.

Kalkreuth, W.D., Marchioni, D.L, Calder, J.H., Lamberson, M.N., Naylor, R.D. and Paul, J. (1991). The relationship between coal petrography and depositional environments from selected coal basins in Canada, in Kalkreuth, W., Bustin, R.M. and Cameron, A.R (Editors) *Recent Advances in Organic Petrology and Geochemistry : a Symposium Honouring Dr.P. Hacquebard. International Journal of Coal Geology,* 19 pp21-76.

Kantsler, A.J. and Cook, A.C. (1979). Maturation patterns in the Perth Basin. *Journal of Australian Petroleum Exploration Association,* 19 (1) pp94-107.

Khorasani, G.K. (1987). Oil-prone coals of the Walloon Coal Measures, Surat Basin, Australia, in Scott, A.C. (ed.) *Coal and Coal-bearing Strata, Recent Advances, Geological Society Special Publication,* 32 pp303-310.

Kirsch, H., Schirmer, U. and Schwarz, G. (1980). The origin of the trace elements zinc, cadmium and vanadium in bituminous coals and their behaviour during combustion. *VGB Kraftwerktechnik,* 60 pp734-744.

Knott, A.C., Thompson, S.C. and Ruch, R.R. (1985). The effects of coal cleaning procedurs on inorganic and trace elements in coal products. *Part 2 of Report NERDDP*, No.EG/85/433, 51 pp.

Kosina, M. (1987). Scientific classification of bituminous coals. *International Journal of Coal Geology,* 8(3) pp233-246.

Kristensen, S.E. and Wilson, A.C. (1986). A review of the coal and lignite resources of Western Australia. *Proceeding of 13th CMMI Congress,* Singapore, 2 pp87-97.

Kristensen, S.E. (1989). *Hill River Coal Project, Regional Geology.* Unpublished CRAE Report.

Kröger, C. and Pohl, A. (1957). Die physikalischen und chemischen Eigenschaften der Steinkohlengefügebestandteile (Macerale), III. *Das Entgasungsverhalten : Brennstoffe-Chemie,* 38 pp102-107.

Lamberson, M.N., Bustin, R.M. and Kalkreuth, W.D. (1991). Lithotype (maceral) composition and variation as correlated with paleo-wetland environments, Gates Formation, northeastern British Columbia, Canada. *International Journal of Coal Geology,* 18 pp87-124.

Landergreen, S. and Manheim, F.T. (1963). On the dependence of the distribution of heavy metals on facies. *Fortschrift Geologische Rheinl. Westfalen,* 10 pp173-192.

Langenberg, W., Macdonald, D. and Kalkreuth, W. (1992). Sedimentologic and tectonic controls on coal quality of a thick coastal plain coal in the Foothills of Alberta, Canada, in McCabe, P.J. and Parrish, J.T. (Editors) *Controls on the Distribution and Quality of Cretaceous Coals* : Boulder, Colorado. *Geological Society of America, Special Paper,* 267 pp101-116.

Le Blanc Smith, G. (1990). Coal, in *Geology and Mineral Resources of Western Australia: Western Australia Geological Survey, Memoir 3* , pp628-629.

Leblang, G.M., Rayment, P.A. and Smyth, M. (1981). The Austinvale coal deposit-Wandoan. A palaeoenvironmental analysis. *Coal Geology,* 1 pp185-195.

Leventahl, J.S., Briggs, P.H. and Baker, J.W. (1983). Geochemistry of the Chattanooga shale, Dekalb County, Central Tennessee. *Southeastern Geology,* 24 pp101-116.

Lindahl, P.C. and Finkelman, R.B. (1984). Factors influencing trace elements in coal by and oxygen bomb combustion/atomic absorption spectrophotometric method. *Fuel,* 61 pp658-662.

Love, L.G., Coleman, M.L. and Curtis, C.D. (1983). Diagenetic pyrite formation and sulfur isotope fractionation associated with a Westfalian marine incursion, northern England. *Transcript of Royal Society, Edinburgh Earth Sciences,* 74 pp165-182.

Lowry, D.C. (1974). *Dongara-Hill River, Western Australia,1:250 000 Geological Series - Explanatory Notes.* Australian Government Publishing Service, Canberra.

Lyons, P.C., Palmer, C.A., Bostick, N.H., Fletcher, J.D., Dulong, F.T., Brown, F.W., Brown, Z.A., Krasnow, M.R. and Romankiw, L.A. (1989). Chemistry and origin of minor and trace elements in vitrinite concentrates from a rank series from the eastern United States, England and Australia, in Lyons, P.C. and Alpern, B. (Editors) Coal : Classification, Mineralogy, Trace - element, Chemistry, and Oil and Gas Potential. *International Journal of Coal Petrology,* 13 pp481-527.

Mackowsky, M.Th. (1968). Mineral matter in coal, in Murchison, D.G. and Westoll, T.S. (Editors) *Coal and Coal - bearing Strata.* Oliver and Boyd, Edinburg, pp105-123.

Mackowsky, M.Th. (1982). Minerals and trace elements occurring in coal, in Stach, E., Mackowsky, M.Th., Teichmüller, M., Taylor, G.H., Chandra, D. and Teichmüller, R. (Editors) *Stach's Textbook of Coal Petrology,* Berlin, 3rd edition, pp.153-171.

Maitland, A.G. (1907). Recent advances in the knowledge of the geology of Western Australia. *Western Australia Geological Survey Bulletin,* 26 pp37-66.

Marchioni, D.L. (1980). Petrography and depositional environment of the Liddell seam, Upper Hunter Valley, New South Wales. *International Journal of Coal Geology,* 1 pp35-61.

Marchioni, D.L. and Kalkreuth, W.D. (1991). Coal facies interpretation based on lithotype and maceral variations in Lower Cretaceous (Gates Formation) coals of Western Canada. *International Journal of Coal Geology,* 18 pp125-162.

Martin, D.J. (1987). Trace elements in coal, Collie Basin, Western Australia. Master of Applied Science Thesis. *Curtin University of Technology,* 189 pp.

Mason, B. (1958). *Principles of Geochemistry.* Willey, New York, N.Y.

Mayer, L.M., Schick, L.L., and Chany, C.A. (1984). Incorporation of trivalent chromium into riverine and estuarine colloidal material. *Geochimica et Cosmochimica Acta,* 48 pp1717-1722.

McCabe, P.J. (1984). Depositional environments of coal and coal-bearing strata, in Rahmani, R.A. and Flores, R.M. (Editors) depositional models for coal and associated strata. *International Association of Sedimentologists, Special Publication,* 7 pp1-30.

MacCartney, J.T. and Teichmuller, M. (1972). Classification of coals according to degree of coalification by reflectance of the vitrinite component. *Fuel,* 51 pp64-68.

McPherson, G. (1990). *Statistics in Scientific Investigation : Its Basis, Application, and Interpretation.* Springer-Verlag, New York.

McLean-Hodgson, J. and Kempton, N.H. (1981). The Oaky-Dalby Region, darling Downs coalfield : stratigraphy and depositional environments. *Coal Geology,* 1 pp165-177.

Megeath, J.D. (1975). *How to use statistics.* Canfield Press, San Francisco.

Merritt, R.D. (Ed.) (1987). Dictionary of coal science and technology. *Alaska Division of Mining and Geology.* Noyes Publications, Park Ridge, New Jersey, U.S.A.

Miao, F., Qian, L. and Zhang, X. (1989). Peat-forming materials and evolution of swamp sequences - case analysis of Jurassic inland coal basin in China, in Lyons, P.C. and Alpern, B. (Editors) *Peat and Coal : Origin, Facies, and Depositional Models. International Journal of Coal Geology,* 12 pp733-765.

Mikhailova, A.I. and Gladkaya, G.G. (1980). Boron in the coals of Eastern Siberia. *Solid Fuel Chemistry,* 14 (3) pp119-120.

Miller, R.N. and Given, P.H. (1978). A geochemical study of inorganic constituents in some low-rank coals. *Technical Reports 1, Unites States Department of Energy Report,* FE - 2494 - TR 1.

Mishra, H.K., Chandra, T.K. and Verna, R.P. (1990). Petrology of some Permian coals of India. *International Journal of Coal Geology,* 16 pp47-71.

Murray, H.H., Harter, T.A., Merkl, R.S. and Taylor, R.E. (1990). Mineralogy, petrography, and trace elements of the Danville Coal Member (VII) in Indiana, in Chy, L.L. and Chou, C.L. (Editors) *Recent Advances in Geochemistry : Geological Society of America, Special Paper,* 248 pp35-39.

Nankervis, J.C. and Furlong, R.B. (1980). Phases changes in mineral matter of North Dakota lignites caused by heating to 1200° C. *Fuel,* 59 pp425-430.

Nicholls, G.D. (1968). The geochemistry of coal-bearing strata, in Murchison, D. and Wertoll, T.S. (Editors) *Coal and coal-bearing strata.* pp266-307. Elsevier, New York.

Northcote, K.H., Bettenay, E.M. Churchward, H.M. and McArthur, W.M. (1967). *Atlas of Australia Soils. Sheet 5, Perth - Albany - Esperance Area, with explanatory data,* CSIRO - Melbourne University Press, Melbourne.

Palmer, C.A. and Filby, R.H. (1984). Distribution of trace elements in coal from the Powhatan No. 6 Mine, Ohio. *Fuel,* 63 pp318-328.

Pareek, H.S. and Bardhan, B. (1985). Trace elements and their variation along seam profiles of certain coal seams of middle and upper Barakar Formations

(Lower Permian) in East Bokaro Coalfield, District Hazaribagh, Bihar, India. *International Journal of Coal Geology,* 5 pp281-314.

Pareek, H.S. (1987). Petrographic, chemical and trace elemental composition of the coal of Sohagpur coalfield, Madhya Pradesh, India. *International Journal of Coal Geology,* 9 pp187-207.

Patteisky, K. and Teichmüller, M. (1960). *Inkohlungs - Verlauf, Inkohlungs - Maßstäbe und Klassifikation der Kohlen auf Grund von Vitrit - Analysen* - Brennst. Chemie, 41 pp79-84, 97-104, 133-137.

Peterson, H.I. (1993). Petrographic facies analysis of lower and Middle Jurassic coal seams on the island of Bornholm, Denmark. *International Journal of Coal Geology,* 2 pp189-216.

Playford, P.E., Cockbain, A.E. and Low, G.H. (1976). Geology of the Perth Basin, Western Australia. *Western Australia Geological Survey, Bulletin* 124.

Potonié, R. (1924). *Einführung in die Kohlenpetrographie.* Borntraeger, Berlin.

Potter, P.E., Shimp, N.F. and Witter, J. (1963). Trace elements in marine and fresh-water argillaceous sediments. *Geochimica et Cosmochimica Acta,* 27 p669.

Rankama, K. and Sahama, T.B. (1950). *Geochemistry.* The University of Chicago Press, 912 pp, Chicago.

Raymond, R. Jr., Cameron, C.C. and Cohen, A.D. (1987). Relationship between peat geochemistry and depositional environments, Cranberry Island, Maine. *International Journal of Coal Geology,* 8 (1/2) pp175-188.

Reineck, H.E. and Singh, I.B. (1980). *Depositional sedimentary environments, 2nd edition.* Springer, Berlin Heidelberg, New York.

Renton, J.J. and Cecil, C.B. (1979). The origin of mineral matter in coal, in Donaldson, A.C., Presley, M.W. and Renton, J.J. (Editors) Carboniferous Coal Guidebook, Volume 1. *West VA Geological Economy Survey Bulletin, B,* 37 (1) pp206-223.

Renton, J.J. (1982). Mineral matter in coal, in Meyers, R.A. (editor) *Coal Structure.* pp283-324. Academic Press, New York.

Rimmer, S.M. and Davis, A. (1986). Geologic controls on the inorganic composition of the Lower Kittaning coal, in Vorres, K.S. (Editor) Mineral matter and ash in coal. *American Chemical Society Symposium Series,* 301 pp41-52.

Rimmer, S.M. and Davis, A. (1988). The influence of depositional environments on coal petrographic composition of the Lower Kittaning seam, Western Pennsylvania. *Organic Geochemistry,* 12 (4) pp375-387.

Rimmer, S.M. and Davis, A. (1990). Relations between ash-fusion characteristics and depositional environment for an Appalachian Basin coal seam, in Chyi, L. and Chou, C.L. (Editors) *Recent advances in coal geochemistry : Geological Society of America, Special Paper,* 248 pp63-72.

Rimmer, S.M. (1991). Distributions and associations of selected trace elements in Lower Kittaning seam, Western Pennsylvania, USA. *International Journal of Coal Geology,* 17 pp189-212.

Robert, P. (1981). Classifcation of organic matter by means of fluorescence :

Application to hydrocarbon source rocks. *International Journal of Coal Geology,* 1 pp101-137.

Robert, P. (1988). *Organic metamorphism and geothermal history. Microscopic study of organic matter and thermal evolution of sedimentary basins.* ELF-Aquitaine Reidel, Dordrecht.

Salehy, M.R. (1986). Determination of rank and petrographic composition of Jurassic coals from eastern Surat Basin, Australia.. *International Journal of Coal Geology,* 6 pp149-162.

Sappal, K.K. (1986). Petrography of Collie Coal, Collie Basin, Western Australia. *WAMPRI,* 26, 202 pp.

Sappal, K.K. and Islam, A. (1992). Petrology and palynology of Cattamarra Coal, Perth Basin, Western Australia. *Geological Society of Australia, Abstracts,* 32, p132.

Sappal, K.K. and Suwarna, N. (1993). Petrography and geochemistry of early Jurassic coal, Western Australia. *International Conference on Coal Science, Conference Proceedings,* pp611-614.

Schlatter, L.E. (1973). *Coal petrology.* 76 pp.

Schopf, J.M. (1956). A definition of coal. *Economic Geology,* 51 pp521-528.

Schopf, J.M. (1960). Field description and sampling of coal beds. *U.S. Geological Survey Bulletin, 1111 - B,* 70 pp.

Sen, S. (1992). Usefulness of petrographic classification in defining national coal resources. *International Journal of Coal Geology,* 20 pp263-275.

Seyler, C.A. (1938). Petrology and the classification of coal I and II. *Proceeding South Wales Inst Eng.* 53 pp254-327.

Seyler, C.A. (1954). *Letter to the nomenclature Sub-Committee of the International Committee for Coal Petrology.* Unpublished.

Sherwood, N.R. and Cook, A.C. (1986). Organic matter in the Toolebuc Formation, in Grave stock, D.I., Moore, P.S. and Pitt, G.M. (Editors) Contribution to the Geology and Hydrocarbon Potential of the Eromanga Basin. *Geological Society of Australia, Special Publication,* 12 pp255-265.

Shibaoka, M. (1972). Silica/alumina ratio of the ashes from some Australian coals. *Fuel,* 51 pp278-383.

Shibaoka, M. and Smyth, M. (1975). Coal petrology and the formation of coal seams in some Australian sedimentary basins. *Economic Geology,* 70 pp1463-1473.

Singh, R.M., Singh, M.P. and Chandra, D. (1983). Occurrence, distribution, and probable source of the trace elements in Ghugus coals, Wardha valley, districts Chandrapur and Yeotmal, Maharshtra, India. *International Journal of Coal Geology,* 2 pp372-381.

Slansky, J.M. (1985). Geochemistry of high-temperature coal ashes and the sedimentary environment of the New South Wales coals, Australia. *International Journal of Coal Geology,* 5 pp339-376.

Smith, A.H.V. (1968). Seam profiles and seam characters, in Murchison, D.G. and Westroll, T.S. (Editors) *Coal and Coal-bearing strata*, Oliver & Boyd: Edinburgh, pp31-40.

Smith, M.J. (1987). *Trace-elements from coal combustion : emission.* IEA Coal Research, London.

Smyth, M. (1974). The relationship between coal macerals and microlithotypes. *Australian CSIRO Mineral Research Laboratory, Investigation Report,* 105, 26 pp.

Smyth, M. (1979). Hydrocarbon generation in the Fly Lake-Brolga area of the Cooper Basin. *Journal of Australian Petroleum Exploration Association,* 19 pp108-114.

Smyth, M. and Cameron, M. (1982). Organic petrology and source rock potential of sediments in the Eromanga Basin, South Australia. *International Journal of Coal Geology,* 1 pp263-281.

Smyth, M. (1984). Coal microlithotypes related to sedimentary environments in Cooper Basin, Australia. *International Association of Sedimentologists, Special Publication,* 7 pp333-347.

Smyth, M. (1989). Organic petrology and clastic depositional environments with special reference to Australian coal basins, in Lyons, P.C. and Alpern, B. (Editors) Peat and Coal : Origin, Facies, and Depositional Models. *International Journal of Coal Geology,* 12 pp635-656.

Smyth, M. (1990). Coal petrology, in Paterson, L. (Editor) *Methane Drainage from Coal, CSIRO Division of Geomechanics,* pp12-18.

Spears, D.A. and Caswell, S.A. (1986). Mineral matter in coals ; cleat minerals and their origin in some coals from the English Midlands. *International Journal of Coal Geology,* 6 pp107-125.

Spears, D.A. (1987). Mineral matter in coals, with special reference to the Pennine coalfields, in Scott, A.C. (Editor) *Coal and Coal-bearing Strata - Recent Advances in Geological Society, Special Paper,* 32 pp171-185.

Stach, E. and Alpern, B. (1966). Inertodetrinit, Makrinit und Mikrinit. *Fortschr Geol Rheinld w Westf,* 13 pp 969-980.

Stach, E., Mackowsky, M-T., Teichmüller, M., Taylor, G.H., Chandra, A.D. and Teichmüller, R. (1982). *Stach's Textbook of Coal Petrology,* 3rd edition. Borntraeger, Berlin.

Standard Association of Australia (1966). *Glossary of terms for coal and coke.* ASK 149.

Standard Association of Australia (1970). *Graphical representation for coal seams.* ASK 183.

Standard Association of Australia (1971). *Methods for the analysis and testing of coal and coke. Part 6 - Ultimate analysis of coal.* AS 1038.

Standard Association of Australia (1975). *Methods for the sampling of hard coal.* AS 1676.

Standard Association of Australia (1977). *Code of practice for preparation of hard coal samples for microscopical examination by reflected lights.* AS 2061.

Standard Association of Australia (1979). *Methods for the analysis and testing of coal and coke. Part 3 - Proximate analysis of hard coal.* AS 1038.

Standard Association of Australia (1981). *Microscopical detremination of the reflectance of coal macerals.* AS 2486.

Standard Association of Australia (1981). *Determination of the maceral group composition of bituminous coal and anthracite (hard coal).* AS 2515.

Standard Association of Australia (1982). *Terms relating to the petrographic analysis of bituminous coal and anthracite (hard coal).* AS 2418 (5).

Standard Association of Australia (1983). *Guide for the taking of samples from hard coal seams in-situ.* AS 2617.

Stanton, R.W. and Finkelman, R.B. (1979). Petrographic analysis of bituminous coal : optical and SEM identification of constituents. *Scanning Electron Microscopy*, I pp645-471.

Stanton, R.W., Cecil, C.B., Pierce, B.S., Ruppert, L.F. and Dulong, F.T. (1986). Geologic processes affecting the quality of the Upper Freeport coal bed, west-central Pennsylvania. *US Geological Survey Open-File Report*, No. 86-173, 22 pp.

Stavrakis, N. and Smyth, M. (1991). Clastic sedimentary environments and organic petrology of coals in the Orange Free State, South Africa. *International Journal of Coal Geology*, 18 pp1-16.

Stopes, M.C. (1919). On the four visible ingredients in banded bituminous coal.

Proceeding of Royal Society, London, B, 90 pp478-487.

Stopes, M.C. (1935). On the petrology of banded bituminous coals. *Fuel,* 14 pp4-13.

Strauss, P.G., Russell, N.J., Bennet, A.J.R. and Atkinson, C.M. (1976). Coal petrography as an exploration aid in the west Circum-Pacific, in Muir, W.L.G (Editor) *Coal Exploration,* pp401-443. Miller Freeman Publications Incorporation, San Francisco, California.

Struckmeyer, H.I.M. and Felton, E.A. (1990). The use of organic facies for refining palaeoenvironmental interpretations. A case study from the Otway Basin, Australia. *Australian Journal of Earth Sciences,* 37 pp351-364.

Styan, W.B. and Bustin, R.M. (1983 a). Petrography of some Fraser River Delta peat deposits : coal maceral and microlithotype precursors in temperate-climate peats. *International Journal of Coal Geology,* 2 pp321-370.

Styan, W.B. and Bustin, R.M. (1983 b). Sedimentology of some Fraser River Delta peat deposits: a modern analogues for some deltaic coals. *International Journal of Coal Geology,* 3 pp101-143.

Suwarna, N. and Sappal, K.K. (1992). Organic petrology of Hill River Coal, Perth Basin, Western Australia. *Geological Society of Australia, Abstracts,* 32 p132.

Swaine, D.J. (1971). Boron in coals of the Bowen Basin as an environmental indicator. *Proceedings Second Bowen Basin Symposium, Geological Survey Queensland Report,* 62 pp41-48.

Swaine, D.J. (1975). Trace elements in coal, in Tugarinov, A.I. (Editor) *Recent contributions to Geochemistry and Analytical Chemistry.* Halsted Press, New York, N.Y., p539-550.

Swaine, D.J. (1982). The importance of trace elements in Australian coals. *ert Energy News Journal,* 4 (3) pp18-22.

Swaine, D.J. (1985). Modern methods in bituminous coal analysis; Trace elements. *CRC Critical Reviews in Analytical Chemistry,* 15 (4) pp1273-1285.

Swaine, D.J. (1990). *Trace elements in coal.* Butterworth and Company Ltd., London.

Sweeney, R.E. and Kaplan, I.R (1973). Pyrite framboid formation : laboratory synthesis and marine sediments. *Economic Geology,* 68 (5) pp618-634.

Tasch, K.H. (1960). Die Möglichkeiten der Flözgleichstellung unter Zuhilfenahme von Floszbildungdiagrammen. *Bergbau Rdsch.,* 1 pp150-157.

Taylor, G.H. (1967). Coals of the Bowen Basin, Eastern Queensland. *CSIRO Division Mineral and Chemistry Technics Communication,* 50, 51 pp.

Teichmüller, M. (1962). Die Genese der Kohle ; *Compte Rendu 4th Congress Stratigraphy Geology Carbonaceous,* Heerlen, 3 pp699-722.

Teichmüller,M. and Thomson, P.W. (1958). Vergleichende mikroskopische und chemische Untersuchungen der wichtigsten Fazies-Typen in Hauptflosz der niederrheinischen Braunkohle. *Fortschrift Geologischen Rheindl Westfalen,* 2 pp323-355.

Teichmüller, M. and Teichmüller, R. (1979). Diagenesis of coal (coalification), in Larsen, G. and Chilingar, G.V. (Editors) *Diagenesis in sediments and sedimentary rocks,* pp218-243. Elsevier, Amsterdam.

Teichmüller, M. (1982). The geological basis of coal formation, in Stach, E., Mackowsky, M-Th, Teichmüller, M., Taylor, G.H., Chandra, D. and Teichmüller, R. (Editors) *Coal Petrology,* 3rd edition, pp5-86. Gebruder, Borntraeger, Berlin-Stuttgart.

Teichmüller, M. (1989). The genesis of coal from the viewpoint of coal petrology, in Lyons, P.C. and Alpern, B. (Editors) *Peat and Coal : Origin, Facies, and Depositional Models,* pp1-87. Elsevier, Amsterdam.

Thiessen, R. (1920). Structure in Paleozoic bituminous coals. *US Bureau of Mines Bulletin,* 117, 296 pp.

Thomas, B.M. (1979). Geochemical analysis of hydrocarbon occurrence in northern Perth Basin, Australia. *American Association of Petroleum Geologists Bulletin,* 63 (7) pp1092-1107.

Thompson, D.B. and Collinson, J.D. (1982). *Sedimentary structures.* George Allen and Unwinn, London.

Ting, F.T.C. (1978). Petrographic techniques in coal analysis, in Karr, C. Jr. (Editor) *Analytical Methods for Coal and Coal Products,* 1 pp3-26. Academic Press, New York.

Thiessen, R. (1920). Structure in Paleozoic bituminous coals. *Bureau of Mines Bulletin,* 117.

Underwood, E.J. (1977). *Trace elements in human and animal nutrition.* New York, Academic Press.

Uribe, C.A. and Perez, F.H. (1985). Proposal for coal classification. *Fuel,* 64 pp147-150.

Van der Flier, E. and Fyfe, W.S. (1985). Uranium-thorium systematics of two Canadian coals. *International Journal of Coal Geology,* 4 pp335-353.

Van Krevelen, D.W. (1954). Representation of the quantitative petrographical analysis by means of a decimal code (proposal). *Proceeding of International Committee for Coal Petrology,* 1 pp59-60.

Veld, H., Fermont, W.J.J., de Leeuw, J.W. and Sinninghe Damste, J.S. (1991). The effects of early diagenetic bacterial sulphate reduction upon the petrology and chemistry of coal. *International Conference on Coal Science Proceeding,* pp.143-146.

Wagner, P., Williams, J.M., Wewerka, E.M., Bertino, J.P., Wanger, L.W. and Wanek, P.L. (1980). Trace element contamination of drainage from coal cleaning wastes. *American Institute of Chemical Engineering,* 21 pp79-86.

Ward, C.R. (1978). Mineral matter in Australian bituminous coals. *Proceeding of Australasian Institute of Mining and Metallurgy,* 267 pp7-25.

Ward, C.R. (1980). Mode of occurrence of trace elements in some Australian coals. *Coal Geology,* 2 (2) pp77-98.

Ward, C.R. (Editor) (1985). Coal Geology and Coal Technology. Oxford, Blackwell, 352pp.

Ward, C.R. (1986). Review of mineral matter in coal. *Australian Coal Geology,* 6 pp87-110.

Ward, C.R. (1989). Minerals in bituminous coals of the Sydney Basin (Australia) and the Illinois Basin (U.S.A.). *International Journal of Coal Geology*, 13 pp455-479.

Ward, C.R. (1992). Mineral matter in Triassic and Tertiary low-rank coals from South Australia. *International Journal of Coal Geology,* 20 pp185-208.

White, D. (1909). The effect of oxygen in coal. *US Geological Society Bulletin,* 382.

Wiese, R.G. and Fyfe, W.S (1986). Occurrences of iron sulphides in Ohio coals. *International Journal of Coal Geology,* 6 pp251-276.

Williams, E.G. and Keith, M.L. (1963). Relationship between sulphur in coals and the occurrence of marine roof beds. *Economic Geology,* 58 pp720-729.

Willmott, S.P. (1964). Revisions to the Mesozoic stratigraphy of the Perth Basin. *Australia Bureau of Mineral Resources, Petroleum Search Subsidy Acts Publications,* 54, App 1, p 11.

Yudovich, Y.E. (1978). *Geochemistry of coals (Inorganic components).* Leningrad, Nauka.

Zubovic, P., Stadnichenko, T. and Sheffrey, N.B. (1961). Chemical basis of minor-element associations in coal and other carbonaceous sediments. *United States Geological Survey Professional Papers*, 424-D pp345-352.

APPENDIX 1. LITHOLOGY LOG OF THE SEAM G, DRILL CORE CPCH 1, MINTAJA BLOCK, HILL RIVER AREA.

Rock Type	Depth Range (m)	Estimated Thickness (m)	Depth To Base (m)	Description
CLASTICS	146.00 - 147.50	0.50	Roof	Claystone with sandstone interbedded, dirty grey. Sandstone, fine to medium-grained, poorly sorted, bioturbation, lenses, pods.
	147.50 - 148.52	1.02	Roof	Sandstone with claystone streaks, dirty (greenish) grey, medium-grained, subangular - subrounded, well sorted, brittle, well porosity, carbonaceous material at the bottom.
COAL	148.52 - 148.54	0.02	0.02	D (dull) containing small sandstone lenses and ash.
	148.54 - 148.64	0.10	0.12	D (dull), black.
	148.64 - 148.66	0.02	0.14	DB (dull banded), black.
	148.66 - 148.68	0.02	0.16	B (bright), conchoidal fracture.
	148.68 - 148.71	0.03	0.19	BD (banded), sandstone lamination at the upper part
	148.71 - 148.72	0.01	0.20	Fusain, fibrous, soft, friable.
	148.72 - 148.94	0.22	0.42	DB (dull banded) contains thin layers of fusain.
	148.94 - 149.11	0.17	0.59	BD (banded), black.
	149.11 - 149.31	0.20	0.79	B (bright), black.
	149.31 - 149.40	0.09	0.88	BB (bright banded), black.
	149.40 - 149.41	0.01	0.89	Fusain, fibrous, soft, friable, black.
	149.41 - 149.46	0.05	0.94	BB (bright banded), black.
	149.46 - 149.69	0.23	1.17	DB (dull banded), thin layers and lenses of fusain.
	149.69 - 149.71	0.02	1.19	B (bright), black.
	149.71 - 149.73	0.02	1.21	D (dull), with broken resin.
CLASTICS, dip of 14°	149.73 - 150.26	0.53	1.74	Interlamination siltstone with sandstone, brownish grey, rootlets, coal streaks, resinous fragments.
	150.26 - 150.63	0.37	2.11	Sandstone, greenish grey, feldspathic, very fine to fine-grained, subangular - subrounded, well sorted, carbonaceous material (5.0 %), mica, load cast, convolute lamination.

150.63 - 151.10	0.47	2.58	Sandstone, grey, very fine-grained, coal pellets and carbonaceous material laminations (10.0 %), feldspar, mica, cross-lamination, parallel-lamination.
151.10 - 152.13	1.03	3.61	Interlamination sandstone with siltstone. Sandstone (60.0 %) greenish to brownish grey, very fine-grained, feldspar, carbonaceous material (10.0 %), mica, parallel lamination, cross-lamination, scour and fill, climbing ripples, flaser-structure, rip-up clasts. Siltstone (30.0 %), brownish grey.
152.13 - 153.00	0.87	4.48	Sandstone, greenish to brownish grey, fine to medium-grained, subangular- rounded, moderately sorted, a small amount of carbonaceous material, rip-up clasts, some calcite veinlets at lower part, scour and fill.
153.00 - 153.33	0.33	4.81	Sandstone, greenish to brownish grey, fine to medium-grained, subangular to rounded, moderately to well sorted, carbonaceous material, mica, rip-up clasts pellets, scour and fill.
153.33 - 153.39	0.06	4.87	Interbedded sandstone with claystone. Sandstone (50.0 %), grey, fine-grained, subrounded to rounded, well sorted, lenses of carbonaceous material/coal pellets (10.0 %), mica, flaser structure, cross-lamination. Claystone (40.0 %), greyish brown.
153.39 - 154.12	0.73	5.60	Sandstone, grey, fine-grained, subangular to rounded, well sorted, feldspar, mica, small amount of carbonaceous material, massive.
154.12 - 154.18	0.06	5.66	Interlamination sandstone with siltstone, brownish to dark grey, oval to rounded rip-up clasts.
154.18 - 154.51	0.33	5.99	Sandstone, grey, fine-grained, subangular to rounded, well sorted, feldspar, carbonaceous material, mica, massive.
154.51 - 154.55	0.04	6.03	Sandstone, greyish black, coaly (plenty of carbonaceous material), fine to medium-grained, moderately sorted, subangular to rounded, fining upwards, top part is eroded.
154.55 - 154.90	0.35	6.38	Sandstone, grey, fine to medium-grained, subangular to rounded, moderately to well sorted, feldspar, rip-up clasts, massive.
154.90 - 155.00	0.10	6.48	Sandstone (20.0 %), dark grey, very fine-grained, subangular to rounded, plenty of carbonaceous material layers (80.0 %), mica, parallel lamination, cross-lamination.

155.00 155.06	0.06	6.54	Sandstone, grey, fine to medium-grained, subangular to rounded, moderately to well-sorted, feldspar, mica, carbonaceous material, plenty rip-up clasts, massive.
155.06 - 155.11	0.05	6.59	Sandstone, greenish to brownish grey, very fine-grained, well sorted, feldspar, mica.
155.11 - 155.14	0.03	6.62	Siltstone, brownish to greenish dark grey, scoured at top part.
155.14 - 155.46	0.32	6.94	Sandstone, grey, very fine to fine-grained, subangular to subrounded, moderately sorted, mica, a little bit of carbonaceous material, scour and fill, parallel lamination.
155.46 - 155.50	0.04	6.98	Sandstone, brownish to light grey, very fine to fine-grained, subrounded, moderately sorted, massive.
155.50 - 157.38	1.88	8.86	Sandstone, brownish to light grey, fine to medium-grained, subangular to rounded, moderately sorted, feldspar, mica, a little bit of carbonaceous material, rip-up clasts, scour at top part, parallel lamination, wavy lamination, convolute (?) lamination, ripples, trough cross-lamination, load casts.
157.38 - 157.45	0.07	8.93	Sandstone, grey, fine-grained, subangular to rounded, moderately sorted, carbonaceous layers, scour.
157.45 - 157.75	0.30	9.23	Interlaminated sandstone with siltstone. Sandstone (70.0 %), grey, very fine-grained, mica, feldspar, carbonaceous material. Siltstone (30.0 %), brownish grey, scoured at top part.
157.75 - 163.08	5.33	14.56	Interbedded sandstone with siltstone, carbonaceous matter (5.0 %) throughout core portion, rip-up clasts. Sandstone (50.0 %), grey, very fine to fine-grained, subangular to rounded, moderately sorted, mica, cross-bedding (mainly trough type). Siltstone (45.0 %), greyish brown, wavy (rippled) lamination.
163.08 - 163.99	0.91	15.47	Interbedded sandstone with siltstone, carbonaceous layers and scattered carbonaceous material (2.0 %), rip-up clasts, load casts, parallel lamination, trough and planar cross-bedding. Sandstone (40.0 %), grey, very fine-grained. Siltstone (58.0 %), brownish grey.
163.99 - 164.16	0.17	15.64	Gap (no core).

	164.16 - 164.90	0.74	16.38	Interbedded siltstone with sandstone. Siltstone (85.0 %), brownish grey, loadcasts, scour, ripples, bioturbation. Sandstone (15.0 %), grey, very fine to fine-grained, subangular to rounded, moderately sorted, rip-up clasts, parallel bedding.
	164.90 - 165.57	0.67	17.05	Claystone (80.0 %), silty, dark brown, bioturbation (burrow). Sandstone (18.0 %), grey, very fine-grained, feldspar, mica, carbonaceous material (2.0 %).
	165.57 - 166.24	0.67	17.72	Alternated sandstone with claystone, coal pellets and streaks (15.0 %). Sandstone (45.0 %), light to brownish grey, very fine-grained, feldspar, mica, carbonaceous material, cross-lamination, flaser structure, rip-up clasts. Siltstone (40.0 %), clayey, greyish brown, climbing ripples, flaser structure, rip-up clasts.
COAL	166.24 - 166.36	0.12	17.84	D (dull), brownish black.
	166.36 - 166.38	0.02	17.86	BB (bright banded).
	166.38 - 166.48	0.10	17.96	DB (dull banded).
	166.48 - 166.64	0.16	18.12	BD (banded).
	166.64 - 166.85	0.21	18.33	D (dull).
	166.85 - 167.04	0.19	18.52	BD (banded).
	167.04 - 167.06	0.02	18.54	DB (dull banded).
	167.06 - 167.16	0.10	18.64	D (dull).
	167.16 - 167.18	0.02	18.66	D (dull), ash.
	167.18 - 167.36	0.18	18.84	DB (dull banded).
	167.36 - 167.52	0.16	19.00	BD (banded).
	167.52 - 168.00	0.48	19.48	D (dull), ash.
	168.00 - 168.10	0.10	19.58	BD (banded).
	168.10 - 168.38	0.28	19.86	DB (dull banded).
	168.38 - 168.44	0.06	19.92	BB (bright banded).
	168.44 - 168.54	0.10	20.02	DB (dull banded).
	168.54 - 168.72	0.18	20.20	D (dull), ash at lower part.
	168.72 - 168.77	0.05	20.25	B (bright).
	168.77 - 168.92	0.15	20.40	BB (bright banded).
	168.92 - 169.03	0.11	20.51	D (dull), ash, fusain.
	169.03 - 169.50	0.47	20.98	DB (dull banded), ash.

	169.50 - 169.74	0.24	21.22	BD (banded).
	169.74 - 169.89	0.15	21.37	B (bright).
	169.89 - 169.90	0.01	21.38	D (dull), ash.
	169.90 - 170.05	0.15	21.53	DB (dull banded).
	170.05 - 170.10	0.05	21.58	B (bright).
	170.10 - 170.24	0.14	21.72	BD (banded).
	170.24 - 170.25	0.01	21.73	BB (bright banded).
	170.25 - 170.30	0.05	21.78	D (dull), ash at lower part.
	170.30 - 170.38	0.08	21.86	BB (bright banded).
	170.38 - 170.40	0.02	21.88	B (bright).
	170.40 - 170.51	0.11	21.99	DB (dull banded).
	170.51 - 170.54	0.03	22.02	BB (bright banded).
	170.54 - 170.66	0.12	22.14	DB (dull banded), sheared at lower part.
CLASTICS	170.66 - 170.89	0.23	22.37	Claystone (98.0 %), brownish grey, mica, carbonaceous material (2.0 %), sheared (main sheared plane is 30° to the axis of the core).
	170.89 - 171.16	0.27	22.64	Claystone (95.0 %), silty, brownish grey, mica, carbonaceous material (5.0 %), wavy and flaser structures.
	171.16 - 171.21	0.05	22.69	Gap (no core).
	171.21 - 171.40	0.19	22.88	Claystone (95.0 %), silty, brownish grey, mica, carbonaceous material (coal fragments and resins/ 5.0 %).
	171.40 - 171. 42	0.02	22.90	Claystone (90.0 %), greyish brown, mica, coal fragments (5.0 %), wavy lamination.
	171.42 - 171.65	0.23	23.13	Gap (no core).
COAL	171.65 - 171.90	0.25	23.38	DB (dull banded).
CLASTICS	171.90 - 171.98	0.08	23.46	Claystone, greenish to brownish grey, mica, carbonaceous material (2.0 %).
COAL	171.98 - 172.03	0.05	23.51	Fusain (fibrous coal).
	172.03 - 172.07	0.04	23.55	D (dull).
	172.07 - 172.08	0.01	23.56	Fusain.
	172.08 - 172.18	0.10	23.66	DB (dull banded).
	172.18 - 172.22	0.04	23.70	BD (banded).
	172.22 - 172.23	0.01	23.71	Fusain.
	172.23 - 172.26	0.03	23.74	DB (dull banded).

	172.26 - 172.27	0.01	23.75	Fusain.
	172.27 - 172.70	0.43	24.18	BB (bright banded).
	172.70 - 172.80	0.10	24.28	BD (banded).
	172.80 - 172.98	0.18	24.46	D (dull).
CLASTICS	172.98 - 173.09	0.11	24.57	Claystone, silty, brownish to dark grey, carbonaceous material, rootlets, sheared at the bottom part.
COAL	173.09 - 173.19	0.10	24.67	DB (dull banded).
	173.19 - 173.21	0.02	24.69	Fusain, ash, fragmental.
	173.21 - 173.32	0.11	24.80	D (dull), brownish black.
	173.32 - 173.35	0.03	24.83	D (dull), non-banded, fragmental, ash.
	173.35 - 173.53	0.18	25.01	D (dull).
	173.53 - 173.64	0.11	25.12	DB (dull banded).
	173.64 - 173.77	0.13	25.25	Fusain, fibrous.
	173.77 - 173.80	0.03	25.28	D (dull).
	173.80 - 174.00	0.20	25.48	DB (dull banded), ash.
	174.00 - 174.14	0.14	25.62	BB (bright banded).
	174.14 - 174.18	0.04	25.66	BD (banded).
	174.18 - 174.22	0.04	25.70	B (bright).
	174.22 - 174.28	0.06	25.76	Gap (no core).
	174.28 - 174.32	0.04	25.80	Siltstone, greenish dark grey, carbonaceous material and coal streaks (10.0 %).
	174.32 - 175.97	0.65	27.45	Interlaminated siltstone with sandstone and mudstone. Siltstone (45.0 %), greyish brown, brittle, carbonaceous material, rootlets, flaser structure. Sandstone (45.0 %),greenish to brownish dark grey, very fine-grained, brittle, carbonaceous material and rootlets. Mudstone (10.0 %), carbonaceous, dark grey, flaser structure, sheared at the bottom part.
	175.97 - 176.97	1.00	28.45	Claystone (86.0 %), silty, dark brown, carbonaceous material. Sandstone (4.0 %), brownish dark grey, very fine-grained, carbonaceous material. Mudstone (10.0 %), carbonaceous.
	176.97 - 177.01	0.04	28.49	Interlaminated sandstone with claystone. Sandstone (70.0 %), grey, fine-grained, angular to subangular, well sorted, feldspar, pyrite, carbonaceous material, mica. Claystone (30.0 %), silty, brownish grey.

	177.01 - 177.42	0.41	28.90	Interlaminated sandstone with silty claystone; flaser structure. Sandstone (45.0 %), greenish to greyish brown, very fine-grained, carbonaceous material (5.0 %), mica. Claystone (45.0 %), silty, greyish brown, carbonaceous material (5.0 %), mica.
	177.42 - 177.76	0.34	29.24	Claystone, dark brown, intercalations of laminated siltstone, sheared (fractured).
	177.76 - 178.15	0.39	29.63	Interlaminated claystone with siltstone. Claystone (80.0 %), brown to brownish grey, carbonaceous material increases downwards. Siltstone (20.0 %), brownish grey, parallel lamination.
COAL	178.15 - 178.46	0.31	29.94	D (dull) contains fusain.
	178.46 - 178.50	0.04	29.98	BD (banded).
	178.50 - 178.52	0.02	30.00	BB (bright banded).
CLASTICS	178.52 - 178.71	0.19	30.19	Interlaminated claystone with siltstone. Claystone, greenish dark brown, sheared, fractured. Siltstone, dark brown, sheared, carbonaceous material.
	178.71 - 178.84	0.13	30.32	Claystone (95.0 %), brownish dark grey, sheared, intercalations of finely laminated siltstone, carbonaceous material (5.0 %) increases downwards.
COAL	178.84 - 178.91	0.07	30.39	D (dull), broken/fragmental, non-banded.
CLASTICS	178.91 - 179.42	0.51	30.90	Interlaminated claystone (60.0 %) with siltstone (40.0 %), greenish to brownish dark grey, sheared, carbonaceous material increases downwards, rootlets.
	179.42 - 179.97	0.55	31.45	Interlaminated very fine-grained sandstone with siltstone, brownish grey, mica, rip-up clasts, carbonaceous material decreases upwards, bioturbation.
	179.97 - 180.01	0.04	31.49	Sandstone, grey, medium-grained, subangular to rounded, well sorted, mica, carbonaceous material, poorly laminated to massive.
	180.01 - 186.00	6.99	38.58	Interlaminated very fine to coarse-grained sandstone with claystone, silty, greenish to brownish grey, carbonaceous material (3.0 %), bioturbation, poorly laminated to massive, .